GEOCHEMISTRY AND PETROLOGY OF THE LOON LAKE PLUTON, ONTARIO

GEOCHEMISTRY AND PETROLOGY OF THE LOON LAKE PLUTON, ONTARIO

By

JAROSLAV DOSTAL

A Thesis
Submitted to the School of Graduate Studies
in Partial Fulfilment of the Requirements
for the Degree
Doctor of Philosophy

McMaster University
November 1973

© Jaroslav Dostal 1974

DOCTOR OF PHILOSOPHY (1973)
(Geology)

McMASTER UNIVERSITY
Hamilton, Ontario

TITLE: Geochemistry and Petrology of the Loon Lake Pluton, Ontario

AUTHOR: Jaroslav Dostal

SUPERVISOR: Professor Denis M. Shaw

NUMBER OF PAGES: i-xix; 1-328

SCOPE AND CONTENTS:

A geochemical, petrographical and geological study of the Precambrian Loon Lake pluton (Ontario) and its surrounding rocks is presented. Emphasis is placed on the geochemistry of several "incompatible" elements (K, Rb, Tl, Sr, Ba and rare-earths).

The intrusion of this zoned composite body caused partial melting of rocks in the contact aureole. The two main zones of the pluton - quartz monzonitic and monzonitic - are believed to be related to a single magma which was probably formed by partial melting of lower crustal/upper mantle rocks or by fractional crystallization of a basic deep-seated magma.

ABSTRACT

The Precambrian Loon Lake pluton, Ontario, is a circular zoned body emplaced in metamorphosed rocks of the Grenville Province about 1075±75 m.y. ago. The intrusion of this post-tectonic pluton superimposed on country rocks, already regionally metamorphosed to amphibolite facies, a contact metamorphism of K-feldspar-cordierite hornfels facies. Various parameters indicate a maximum contact temperature range of 750-820°C and total pressure range of 2.5-4 kb, producing anatexis of rocks in the contact aureole. Garnet-sillimanite-cordierite gneisses, abundant in this aureole, are probably a residuum after partial melting of the Apsley biotite gneiss. These residual rocks contain high Al, Fe and Mg, low alkalies and also heavy REE enrichment with negative Eu anomalies, compared to the Apsley gneiss. Leucogranites associated with garnet-sillimanite-cordierite gneisses may represent anatectic material subtracted from the Apsley gneiss.

The pluton consists of two main concentric zones, a monzonitic core and outer younger quartz monzonite. Several isolated bodies of older diorite and syenodiorite occur within the pluton, mostly in the core. Intrusions of the

felsic rocks probably followed in rapid succession. The pluton is also zoned with respect to the structural state of potassium feldspar, which is mostly microcline, although some central monzonites contain orthoclase: this variation was probably controlled by water distribution.

Large variations in chemical and mineralogical composition of the basic rocks are due to (a) magmatic differentiation and (b) interaction with felsic magma. These rocks may not be genetically related to the pluton.

The variations of major elements, Rb, Sr, Ba, Tl and REE in monzonite are consistent with fractional crystallization (mainly of feldspars) and probably involved flowage differentiation. Most chemical variations in quartz monzonite are also compatible with fractional crystallization. The behaviour of REE, however, is not readily consistent with this process.

Monzonite and quartz monzonite were both formed from a single magma, which was generated either by partial melting of lower crustal/upper mantle rocks, or by fractional crystallization of basic deep-seated magma. This magma in part intruded (monzonite) and in part evolved further (quartz monzonite) and subsequently intruded. Quartz monzonite was generated by fractional crystallization of monzonitic magma and by "mixing" of monzonitic magma with anatectic granitic melt.

The composition of biotite from the felsic rocks suggests oxygen fugacities slightly higher than those in equilibrium with a Ni-NiO buffer.

ACKNOWLEDGEMENTS

I am greatly indebted to Dr. D.M. Shaw, who initiated and supervised this work, for his guidance and assistance. Many thanks are also extended to the other members of my supervisory committee, Drs. J.H. Crocket, R.H. McNutt and O.E. Hileman.

I am grateful to Drs. L.A. Haskin, P.A. Helmke, K. Fritze, Y.N. Shieh, H.D. Grundy, and Messrs. J.R. Muysson, J. Griep and H.Y. Kuo for their valuable assistance and critical discussions. The assistance of Mrs. H. Elliott and Mr. J. Whorwood in the final preparation of the manuscript is appreciated. I am also indebted to my wife Deborah for her assistance throughout the work.

Finally, I wish to acknowledge the financial aid of the National Research Council of Canada, The Department of Energy, Mines and Resources and other Departmental grants.

TABLE OF CONTENTS

Page

CHAPTER 1 INTRODUCTION 1

1.1 Purpose of the Study 1
1.2 Description of the area 2
  1.2.1 Location and Access 2
  1.2.2 Physiography 3
1.3 Method of Investigation 3

CHAPTER 2 REGIONAL GEOLOGY 5

2.1 Introduction 5
2.2 Metasedimentary and Metavolcanic Rocks 7
2.3 Metamorphism 8
2.4 Structure 10
2.5 Plutonic Rocks 12

CHAPTER 3 PREVIOUS WORK 16

CHAPTER 4 GEOLOGY AND PETROLOGY OF METAMORPHOSED COUNTRY ROCKS 20

4.1 Introduction 20
4.2 Regional Metamorphosed Rocks 22
  4.2.1 Gneisses 22
    4.2.1.1 Biotite Gneiss 23
    4.2.1.2 Calcareous Gneiss 25
    4.2.1.3 Aluminous Gneiss 28
  4.2.2 Amphibolites 29
  4.2.3 Carbonate Metasediments 30
  4.2.4 Conditions of Regional Metamorphism 33
4.3 Contact Metamorphosed Rocks 43
  4.3.1 Aluminous Hornfelses 44
  4.3.2 Mafic Hornfelses 59
  4.3.3 Contact Metamorphosed Marbles 63
  4.3.4 Conditions of Contact Metamorphism 64

Page

4.4 Retrogressive Metamorphism 74
4.5 Structure 74
4.6 Summary 77

CHAPTER 5 GEOLOGY AND PETROGRAPHY OF THE PLUTON 80

5.1 General Features of the Pluton 80
5.2 Structure 81
5.3 Contact Relations 83
5.4 Age of the Pluton 86
5.5 Petrography 87
  5.5.1 Introduction 87
  5.5.2 Quartz Monzonite 88
  5.5.3 Monzonite 91
  5.5.4 Basic Rocks 93
  5.5.5 Granodioritic Gneiss 95
  5.5.6 Inclusions 96
5.6 Compositional Variations 97
5.7 Potassium Feldspars 98
  5.7.1 Obliquity 99
  5.7.2 Unit-Cell Parameters 102
  5.7.3 Three-Peak Method 102
  5.7.4 Composition of the Potassium Feldspars 104
  5.7.5 Variation in the Structural State 104
5.8 Some Considerations on the Emplacement of the Pluton 108
5.9 Summary 111

CHAPTER 6 GEOCHEMISTRY OF THE LOON LAKE PLUTON 113

6.1 Chemistry of the Rocks 113
  6.1.1 Major Elements 113
  6.1.2 Trace Elements 133
    6.1.2.1 Rubidium 133
    6.1.2.2 Strontium 139
    6.1.2.3 Barium 146
    6.1.2.4 Thallium 151
    6.1.2.5 Rare-earth Elements 154

Page

6.1.3 Dunite 166

6.2 Chemistry of Minerals 170

6.2.1 Amphibole 170
6.2.2 Biotite 175
6.2.3 Feldspars 182

6.2.3.1 Plagioclase 182
6.2.3.2 Potassium Feldspar 187

6.2.4 Coexisting Biotites and K-feldspars 189
6.2.5 Rare-earth Elements in Minerals 193

6.2.5.1 Dioritic Rocks 193
6.2.5.2 Monzonite 196
6.2.5.3 Quartz Monzonite 202

6.3 Summary 205

CHAPTER 7 PETROGENESIS 209

7.1 Introduction 209
7.2 Dioritic Rocks 211
7.3 Monzonite 214

7.3.1 Fractionation Within the Monzonite 214
7.3.2 The Origin of Monzonitic Melt 216

7.3.2.1 Partial Melting of Crustal Rocks 216
7.3.2.2 Contamination of Basic Magma 223
7.3.2.3 Contamination of Acid Magma 224
7.3.2.4 Derivation from More Basic Magma 225
7.3.2.5 Other Considerations 226

7.4 Quartz Monzonite 231
7.5 Summary 239

CHAPTER 8 EVOLUTION OF THE PLUTON 241

Page

CHAPTER 9 CONCLUSIONS 246

REFERENCES 249

APPENDIX 1 275

A.1.1 Modal Analyses 275
A.1.2 Sampling and Chemical Analyses 282
A.1.3 Mineral Separation 288
A.1.4 Determinative Techniques for Potassium Feldspars 289

APPENDIX 2 DETERMINATION OF RARE-EARTH ELEMENTS 293

A.2.1 Introduction 293
A.2.2 Sample Preparation and Irradiation 294
A.2.3 Standards and Carriers 295
A.2.4 Chemical Separation of the Rare-earth Element Group 298
A.2.5 Counting Equipment 299
A.2.6 Counting Conditions 300
A.2.7 Peak Integration 303
A.2.8 Determination of Chemical Yields 303
A.2.9 Calculations 305
A.2.10 Evaluation of Results for REE 306
A.2.11 Chemical Treatment of Rock Samples 315
A.2.12 Chemical Treatment of Some Minerals 322
A.2.13 Treatment of the Standards 327

LIST OF TABLES

Table		Page
4.2.1	Modal composition of gneisses	26
4.2.2	Modal compositions of amphibolites and marbles	31
4.2.3	Composition of coexisting feldspars from regional metamorphosed gneiss	40
4.2.4	Composition of Mg-calcite from regional metamorphosed marble and estimated temperature from the calcite-dolomite solvus	40
4.3.1	Least square solution for bulk chemical relations between Apsley gneiss, aluminous hornfels and leucogranite	53
4.3.2	Modal compositions of mafic hornfelses and contact metamorphosed marbles	62
4.3.3	Composition of Mg-calcites from contact metamorphosed marbles and estimated temperature from the calcite-dolomite solvus	72
5.1	Obliquity and composition of potassium feldspar; composition of coexisting plagioclase	101
6.1.1	Comparison of average composition of granitic rock types	116
6.1.2	Comparison of average composition of monzonitic and syenitic rocks	117
6.2.1	Chemical compositions and structural formulae of hornblende and biotites	172-174
6.2.2	Chemical compositions and structural formulae of feldspars	184-185
6.2.3	Some trace element abundances in feldspars and their host monzonites	201
A.1.1	Modal analyses of rocks from the quartz monzonitic zone of the pluton	277-278

Table Page

A.1.2 Modal analyses of rocks from the monzonitic core of the pluton 279

A.1.3 Modal analyses of basic rocks 280

A.1.4 Modal analyses of granodioritic gneisses 280

A.1.5 Modal analyses of aluminous gneisses 281

A.1.6 Chemical analyses of quartz monzonites 283

A.1.7 Chemical analyses of monzonites 284

A.1.8 Chemical analyses of basic rocks and dunite 285

A.1.9 Chemical analyses of aluminous hornfelses and Apsley biotite gneisses 286

A.1.10 REE contents of minerals 287

A.1.11 Unit-cell parameters of potassic phases of perthitic K-feldspars 290

A.2.1 Concentrations of REE in the standard monitor and carrier solutions 297

A.2.2 Summary of information pertaining to radioassay 301

A.2.3 Precision of REE determinations 309

A.2.4 Comparison of reported REE abundances in standard rock BCR-1 310

A.2.5 Comparison of reported REE abundances in standard rock W-1 311

A.2.6 Comparison of reported REE abundances in standard rock G-2 312

LIST OF MAPS

Map		
1	Geological map of the Loon Lake pluton	in pocket
2	Sample locations	in pocket
3	Generalized geological map of the Bancroft-Madoc area	in pocket

LIST OF FIGURES

Figure		Page
1.1	Remnant surficial rocks in the Grenville Province	6
2.1	Section showing the hypothetical relationship of the Mayo and Hermon Groups	9
2.2	Approximate disposition of the regional metamorphic isograds in the Bancroft-Madoc area	11
2.3	Summary of tectonic events in the Bancroft-Madoc area	14
4.2.1	ACKF diagram for biotite gneisses	24
4.2.2	ACKF diagram for hornblende-biotite gneisses	24
4.2.3	ACKF diagram for calcomagnesian gneisses	24
4.2.4	ACKF diagram for amphibolites	24
4.2.5	$CaO-MgO-SiO_2$ diagram for regionally metamorphosed marbles	32
4.2.6	P-T graph of experimental data pertaining to the conditions of regional metamorphism	36
4.2.7	Distribution of albite between coexisting feldspars	41
4.3.1	Variations of ($FeO+Fe_2O_3$) and Al_2O_3 as a function of norm. (Q+Ab+An+Or) in aluminous hornfelses relative to the average Apsley gneiss	49
4.3.2	Variations of Na_2O, norm. composition of plagioclase and $FeO_{total}/(FeO_{total}+MgO)$ as a function of norm. (Q+Ab+An+Or) in aluminous hornfelses relative to the average Apsley gneiss	50
4.3.3	Triangular diagram $(Na_2O+K_2O)-Al_2O_3-(FeO+Fe_2O_3+MnO+MgO)$ showing the variation of these oxides in biotite gneisses, aluminous hornfelses and leucogranite 259	51

Figure		Page
4.3.4	REE distribution in Apsley biotite gneisses and the averages of North American shales	57
4.3.5	REE distribution in aluminous hornfelses, garnet 67 and the averages of North American shales	58
4.3.6	REE distribution in Apsley biotite gneisses, aluminous hornfelses and leucogranite 259	58
4.3.7	ACKF diagram for mafic (hornblende) hornfelses	61
4.3.8	ACKF diagram for mafic (pyroxene) hornfelses	61
4.3.9	CaO-MgO-SiO_2 diagram for contact metamorphosed marbles	65
4.3.10	P-T graph of experimental data pertaining to the conditions of contact metamorphism	68
4.5.1	Structural features of Chandos Township	75
5.1	Distribution of modal analyses of the rocks from the pluton relative to the classification scheme	89
5.2	Unit-cell parameters of potassic phases of perthites plotted on a b-c graph of Wright and Stewart (1968)	103
5.3	Potassic phases of perthites plotted on a 060-$\bar{2}04$ graph of Wright (1968)	103
6.1.1	Histograms of SiO_2 and Al_2O_3 distributions in the felsic rocks	114
6.1.2	Normative composition of felsic rocks in relation to the Q-Ab-Or ternary system	120
6.1.3	Normative composition of felsic rocks in relation to the An-Ab-Or ternary system	122
6.1.4	An-Ab-Or diagram showing the composition of coexisting feldspar pairs from the felsic rocks	123
6.1.5	Variation of SiO_2 as a function of D.I.	125

Figure		Page
6.1.6	Variation of Al_2O_3 as a function of D.I.	125
6.1.7	Variation of K_2O as a function of D.I.	125
6.1.8	Variation of Na_2O as a function of D.I.	126
6.1.9	Variation of CaO as a function of D.I.	126
6.1.10	Variation of MgO as a function of D.I.	126
6.1.11	Variation of TiO_2 as a function of D.I.	127
6.1.12	Variation of FeO_{total} as a function of D.I.	127
6.1.13	Variation of $FeO_{total}/(FeO_{total}+MgO)$ as a function of D.I.	127
6.1.14	Variation of $Na_2O/(Na_2O+K_2O)$ as a function of D.I.	128
6.1.15	Relation between FeO_{total} and MgO	128
6.1.16	Na_2O-K_2O-CaO diagram	131
6.1.17	AFM diagram	132
6.1.18	Variation of Rb as a function of D.I.	134
6.1.19	Variation of the K/Rb ratio as a function of D.I.	134
6.1.20	Relation between the K/Rb ratio and modal content of biotite	134
6.1.21	Variation of the K/Rb ratio as a function of Rb in the rocks from the pluton	138
6.1.22	Variation of the K/Rb ratio as a function of Rb in some well-known rock series	138
6.1.23	Relation between Ca and Sr	141
6.1.24	Variation of Sr as a function of D.I.	142
6.1.25	Variation of the Ca/Sr ratio as a function of D.I.	142

Figure		Page
6.1.26	Relation between Rb and Sr	144
6.1.27	Variation of the Ca/Sr ratio as a function of Sr in the rocks from the pluton	145
6.1.28	Variation of the Ca/Sr ratio as a function of Sr in some well-known rock series	145
6.1.29	Relation between K and Ba	147
6.1.30	Variation of Ba as a function of D.I.	149
6.1.31	Variation of the K/Ba ratio as a function of D.I.	149
6.1.32	Variation of the 100xBa/(Ca+K) ratio as a function of D.I.	150
6.1.33	Variation of the Ba/Sr ratio as a function of D.I.	150
6.1.34	Relation between Rb and Tl	153
6.1.35	Relation between K and Tl	153
6.1.36	Variation of La as a function of D.I.	157
6.1.37	Variation of the La/Yb ratio as a function of D.I.	157
6.1.38	REE distribution in dioritic rocks from the pluton	159
6.1.39	REE distribution in continental basic rocks	159
6.1.40	REE distribution in monzonites from the pluton	163
6.1.41	REE distribution in quartz monzonites from the pluton.	165
6.1.42	REE distribution in granitic composites	165
6.1.43	REE distribution in dunite 130 and some ultrabasic rocks	168

Figure Page

6.2.1 $MgO-FeO_{total}-Al_2O_3$ diagram showing composition fields of hornblendes from Caledonian plutonic rocks and composition of hornblende from diorite of the pluton 171

6.2.2 Relation between octahedral cations of biotites from the felsic rocks of the pluton 179

6.2.3 $Fe^{3+}-Fe^{2+}-Mg$ diagram of biotites from the felsic rocks of the pluton 179

6.2.4 Stability of biotite as a function of oxygen fugacity and temperature 180

6.2.5 Calculated stability curve for biotite from monzonite 251 180

6.2.6 Distribution of K/Rb in coexisting biotite and K-feldspar

6.2.7 REE distribution in biotite, hornblende, plagioclase and their host diorite 70 194

6.2.8 REE distribution in clinopyroxene, plagioclase and their host diorite 321 194

6.2.9 REE distribution in hornblende, biotite, K-feldspar, plagioclase and their host monzonite 94 198

6.2.10 REE distribution in biotite, K-feldspar, plagioclase and their host monzonite 207 198

6.2.11 REE distribution in sphene, biotite, K-feldspar, plagioclase and their host monzonite 251 199

6.2.12 REE distribution in biotite, K-feldspar, plagioclase and their host quartz monzonite 26 203

6.2.13 REE distribution in biotite, K-feldspar, plagioclase and their host quartz monzonite 115 204

6.2.14 REE distribution in biotite, K-feldspar, plagioclase and their host quartz monzonite 27 204

Figure		Page
7.1	REE distribution in monzonites, aluminous hornfelses and the averages of North American shales	218
A.2.1	REE distribution in standard rocks BCR-1 and G-2	314

CHAPTER 1

INTRODUCTION

1.1 Purpose of the Study

The Grenville Province of the Canadian Shield, which "is traditionally thought of as a sea of granite" (Wynne-Edwards, 1972, p.314), contains many small plutons of monzonitic or syenitic composition which are important to an understanding of the Grenville geology (Lumbers, 1967a; Wynne-Edwards, 1972). Although a number of theories has been invoked to explain the evolution of these plutons, their origin has been disputed for many years.

In order to contribute to the elucidation of the origin of these Precambrian plutons and to the discussions on the genesis and the geochemistry of granites and syenites, this study of the Loon Lake pluton, a small body, representative of a number of similar monzonitic plutons found in the Grenville Province, was undertaken.

The aim of this investigation is to review some geochemical, petrological and geological data related to the pluton and its contact aureole with an ultimate objective to evaluate the origin and evolution of the pluton. The emphasis is put on geochemistry, particularly of trace elements.

1.2 Description of the Area

1.2.1 Location and Acess

The Loon Lake pluton is situated in Chandos Township, Peterborough County, about 36 miles NNE of Peterborough, Ontario. From a geological point of view, the area is in the southwestern part of the Ottawa River Remnant (Lumbers, 1967a) of the Grenville Province of the Canadian Shield (Figure 1.1). The pluton appears in the southeastern part of the Chandos Township map sheet (Map 2019 - Ontario Department of Mines).

The village of Lasswade, at the southern part of the pluton, the settlements of Owenbrook near the northeastern margin of the body and several hundred summer cottages along the shores of Chandos Lake (formerly Loon Lake) are easily accessible from the major highway system. Lasswade and Owenbrook lie along highway no. 504, which makes a semicircuit around the southern and eastern side of Chandos Lake. The northern and northwestern lake shores are accessible via highway no. 620 or by gravel roads from highway no. 28, respectively. The dense network of access roads to the shores of Chandos Lake, built for the convenience of cottage residents, are connected with the highways. Most of them are fit for travel by car. There are also numerous logging and concession roads, some already abandoned, which crosscut the bush and fields around Chandos Lake.

1.2.2 Physiography

The Loon Lake pluton lies within the Cashel peneplain of the Lake Ontario homocline (Kay, 1942a,b). The peneplain has a low relief which gently slopes to the south on an average of about 7 feet per mile (Lumbers, 1967a). In Chandos Township, the maximum elevations are about 1100-1200 feet with about 200 feet relief.

The region consists mainly of numerous low ridges and hills with relatively good exposure and valleys between them. Some valleys are covered by Chandos Lake, which occupies an area of nearly ten square miles. One section of the lake, 4 miles long, trends at about N 30° W, while two roughly parallel elongated bays (West Bay and South Bay) trend at about N 45° E. Several small lakes and ponds occurring in this area mostly drain into Chandos Lake. On the east side of Chandos Township, the Crowe River, which flows southward into the Trent River drainage system, meanders throughout a large swamp, which covers the east part of the Loon Lake pluton. Generally, exposure in this region is not very good. Shaw (1972) has estimated that outcrops make up no more than 1% of the area's surface.

1.3 Methods of Investigation

The Loon Lake pluton and its surroundings were mapped during the summers of 1970 and 1971, at a scale of 4 inches to 1 mile using air photographs for locations (Map 1). A grid sampling was not possible because of inadequate exposure, especially where the area is covered by Chandos Lake.

In addition to more than 250 specimens routinely collected for petrographic purposes, 30 large representative samples were collected for chemical studies. Apart from samples obtained during field work, specimens from D.M. Shaw's collection were used in the course of this study. The locations of the samples referred to in the text are given in Map 2. A description of the laboratory work, which included chemical analyses of whole-rocks and mineral separates and X-ray diffraction studies is given in Appendices 1 and 2.

CHAPTER 2

REGIONAL GEOLOGY

2.1 Introduction

The Precambrian rocks of Chandos Township are part of the Ottawa River Remnant which is one of the largest and thickest surface rock remnants known in the Grenville Province of the Canadian Shield (Lumbers, 1967a). The remnant trends northeasterly from the Paleozoic cover in southeastern Ontario to southwestern Quebec, where it contains the type area of the Grenville series (Figure 1.1). The remnant is formed by the metavolcano-metasedimentary rock series, which were invaded by intrusions of younger plutonic rocks. This sequence, which is probably Proterozoic in age, unconformingly overlays an older basement. The Ottawa River Remnant displays a complex Proterozoic history. It has not only great lithological variability, but also a wide range of metamorphic grade. The metamorphic zones range from the greenschist facies to upper amphibolite and in places to granulite facies rocks.

The oldest dated surficial rocks of this remnant in the Bancroft-Madoc area - the Tudor metavolcanics - are about 1310±15 million years old (Silver and Lumbers, 1965). Wynne-Edwards

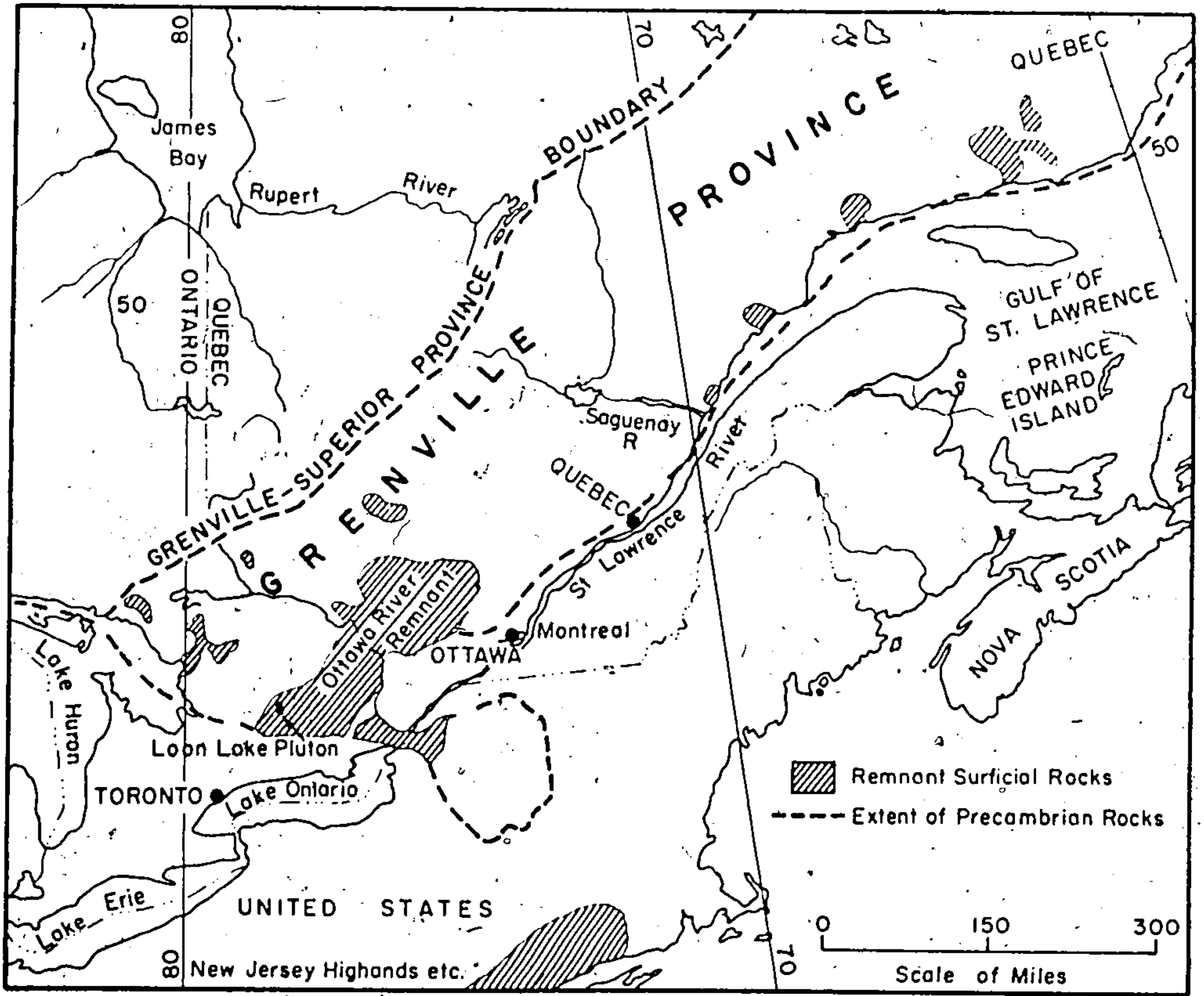
James Bay
Rupert River
BOUNDARY
PROVINCE
QUEBEC
GULF OF ST. LAWRENCE
PRINCE EDWARD ISLAND
NOVA SCOTIA
GRENVILLE-SUPERIOR PROVINCE
GRENVILLE
ONTARIO
QUEBEC
50
80
70
Saguenay R
QUEBEC
River
St Lawrence
Montreal
OTTAWA
Ottawa River Remnant
Loon Lake Pluton
TORONTO
Lake Ontario
Lake Huron
Lake Erie
UNITED STATES
New Jersey Highands etc.
Remnant Surficial Rocks
Extent of Precambrian Rocks
0
150
300
Scale of Miles

after LUMBERS (1967a)

FIGURE 1.1 Remnant Surficial Rocks in the Grenville Province

(1972), however, has suggested that this date may more accurately reflect metamorphism than the age of extrusion.

The volcanic activity was accompanied by an accumulation of carbonate and clastic sediments. A sedimentary-volcanic sequence in the Bancroft-Madoc area accumulated to a thickness of at least 27,000 feet (Lumbers, 1967a). The base of this sequence is not exposed. The rock series was affected by complex Precambrian tectonic, metamorphic and plutonic events. The abundant younger plutonic rocks are usually represented by small felsic and mafic intrusive stocks and plutons and granitic batholiths. Structural trends in the Bancroft-Madoc area are predominantly northeasterly.

The geology and stratigraphy of the Hastings Lowlands within the northwestern part of which the Loon Lake pluton lies, have been recently studied by Lumbers (1967a) who presented an integrated model of the evolution of this part of the Ottawa River Remnant. For an outline of the geology of this area on a regional scale, his model is briefly reviewed below.

2.2 Metasedimentary and Metavolcanic Rocks

The metasedimentary-metavolcanic surficial rock sequence of the Ottawa River Remnant in the Hastings Lowlands (in the sense of Best, 1966) has been subdivided by Lumbers (1967a) into two groups - the Hermon group dominated by metavolcanics and the Mayo group dominated by carbonate metasediments. The middle and upper parts of the Hermon group interfinger with, or are equivalent to, the lower part of the Mayo group suggesting sedimentation and volcanism to be contemporaneous during the accumulation of this sequence (Figure 2.1). Each of these groups has been further subdivided into several formations with distinct lithology and relatively large area extent (Map 3). But the detailed correlation of the stratigraphic units in the individual townships of this portion of the Ottawa River Remnant and the whole problem of the stratigraphic succession, however, are not yet adequately resolved (c.f. Shaw, 1972).

2.3 Metamorphism

Silver and Lumbers (1965) and Lumbers (1967a) have defined two major metamorphic culminations of the regional metamorphism in the Bancroft-Madoc area. The first culmination, producing three plagioclase isograds and the greenschist and lower amphibolite facies terrains in this region, reached a maximum at about 1250±25 million years ago. The second and most intense stage of metamorphism has an age of about 1125±25 million years. It developed the sillimanite isograd and the upper amphibolite facies terrains which lie beside but do not substantially affect the previously formed lower grade of metamorphism in the central part of the Bancroft-Madoc region dominated by metavolcanics.

Except for a few pegmatitic and hydrothermal veins, all Precambrian rocks in this region were affected by a metamorphic

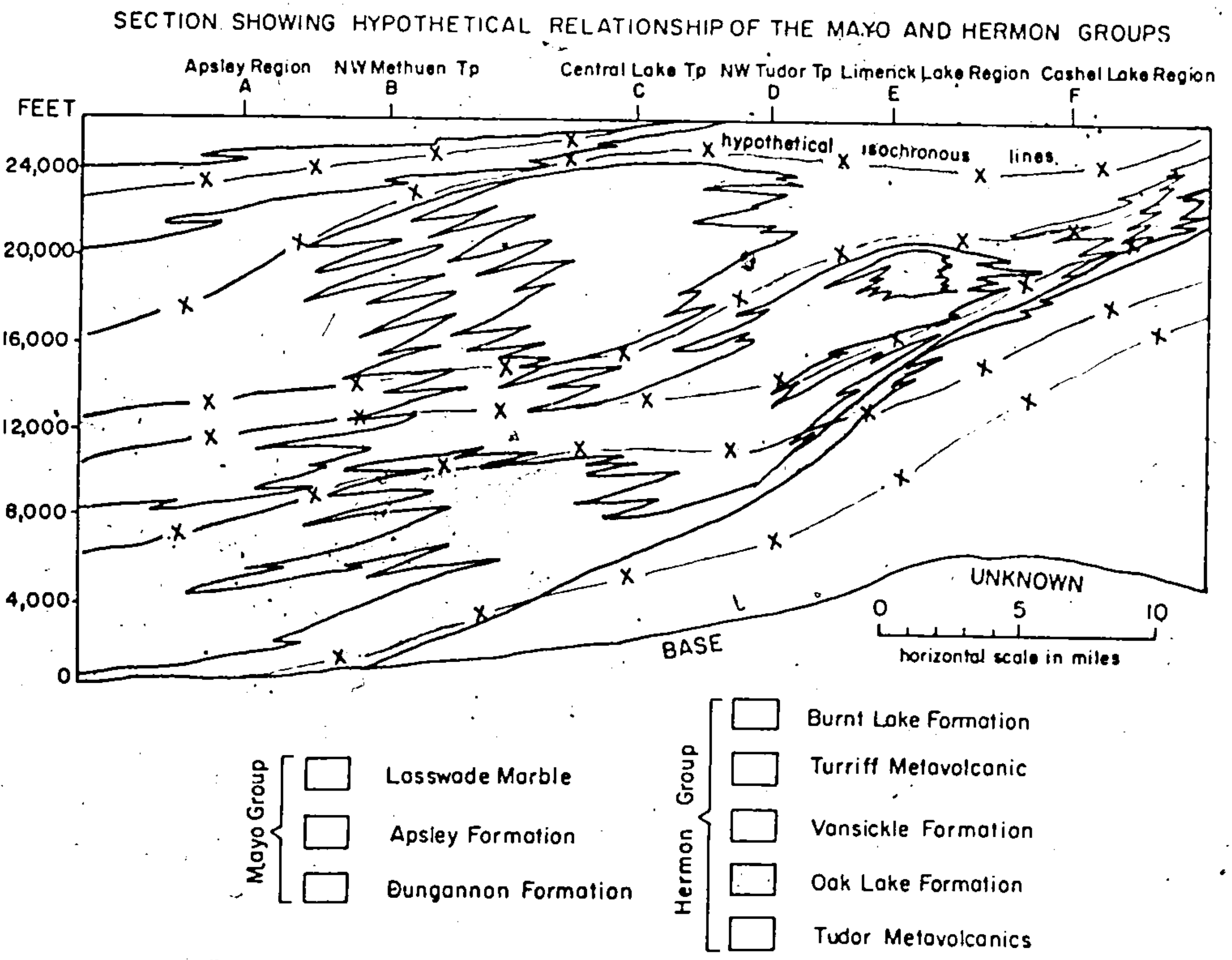
SECTION SHOWING HYPOTHETICAL RELATIONSHIP OF THE MAYO AND HERMON GROUPS
Apsley Region A
NW Methuen Tp B
Central Lake Tp C
NW Tudor Tp D
Limerick Lake Region E
Cashel Lake Region F
FEET
24,000
20,000
16,000
12,000
8,000
4,000
0
hypothetical isochronous lines.
UNKNOWN
BASE
0
5
10
horizontal scale in miles
Mayo Group
Lasswade Marble
Apsley Formation
Dungannon Formation
Hermon Group
Burnt Lake Formation
Turriff Metavolcanic
Vansickle Formation
Oak Lake Formation
Tudor Metavolcanics

FIGURE 2.1

After Lumbers (1967a)

event which culminated between 880 and 1010 million years ago as determined by K/Ar dating on micas (Stockwell, 1964). The meaning of the rather uniform K/Ar dates with prevailing ages of 950±150 million years for the Grenville Province as a whole (e.g. Harper, 1967; MacIntyre et al., 1967; Wanless et al., 1967) is still under discussion. Wynne-Edwards (1972) has pointed out that in the Grenville Province "U/Pb measurements of zircon and whole-rock Rb/Sr isochron studies have revealed dates of metamorphism or intrusion consistently about 250 m.y. older than the corresponding K/Ar values " (p.264). He has concluded that U/Pb and Rb/Sr dates are "generally considered to be a more reliable index of the actual age of the culmination of metamorphism, the K/Ar dates being interpreted as the time at which the rocks cooled through a critical isotherm of the order of 200°C so that their constituent minerals could retain radiogenic argon" (p.264).

The regional distribution of the metamorphic isograds in the Bancroft-Madoc area is shown in Figure 2.2. The facies series in the Bancroft-Madoc area is intermediate between the Barrovian type and the Abukuma type facies series (Lumbers, 1967a).

2.4 Structure

The structure of the Precambrian rocks of the Bancroft-Madoc area is very complex and considerably more data are needed to develop a regional synthesis of the tectonic evolution of this part of the Grenville Province.

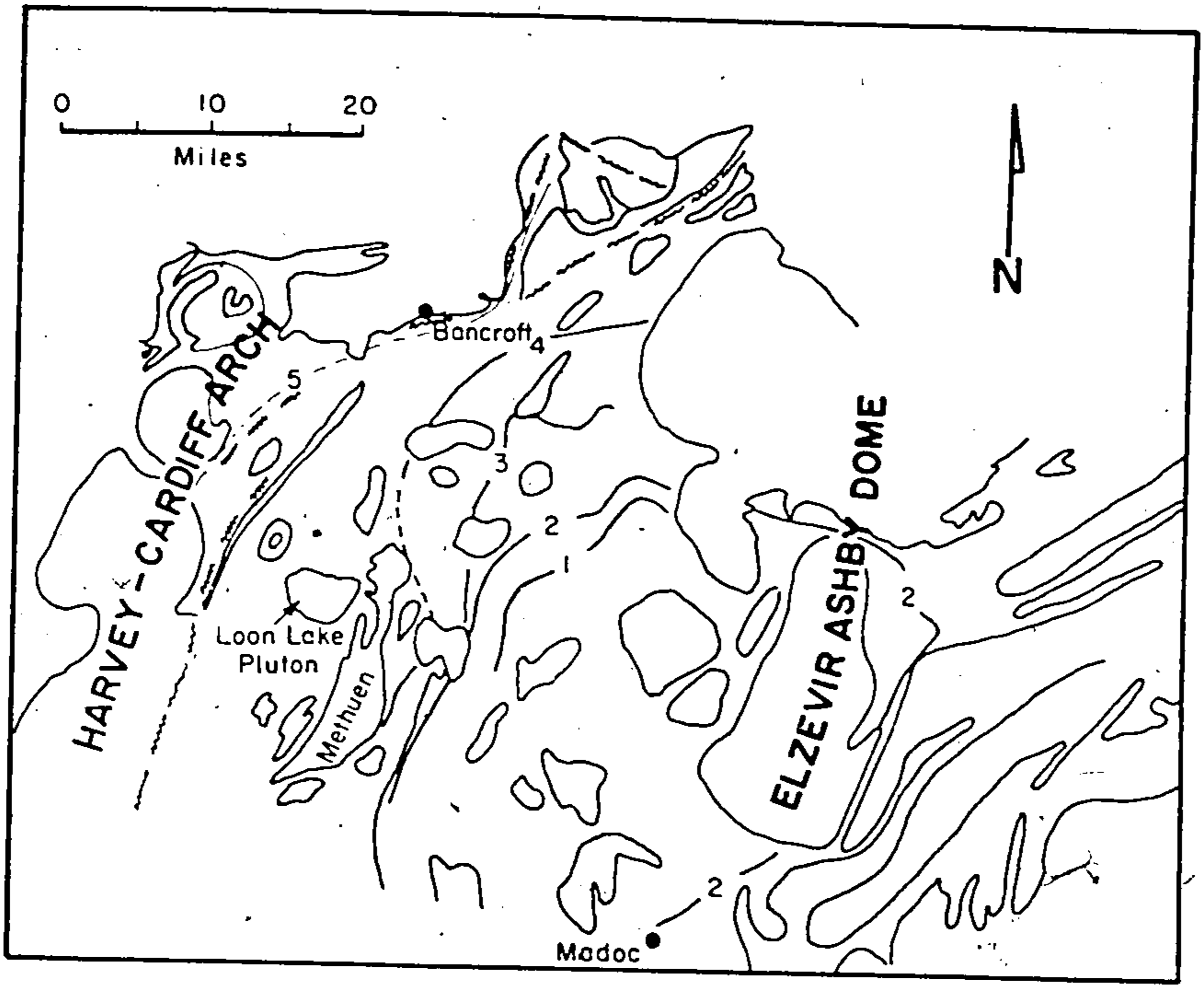
0
10
20
Miles
N
Bancroft
4
5
3
2
1
2
2
HARVEY-CARDIFF ARCH
ELZEVIR ASHBY DOME
Loon Lake Pluton
Methuen
Madoc

(after Lumbers, 1967a & Jennings, 1969)

EXPLANATION

Isograds

(1) Zoned albite / garnet

(2) Oligoclase / staurolite

(3) Andesine/andalusite / diopside

(4) Sillimanite / cordierite

(5) Orthopyroxene / forsterite–chondrodite[1] / and disappearance of muscovite

1 = isograd

= shear zone

Lithologies

☐ Granitic intrusive rocks

☐ Basic intrusive rocks

☐ Supracrustal rocks

FIGURE 2.2 Approximate disposition of regional metamorphic isograds in the Bancroft–Madoc area

Lumbers (1967a) has recognized in the Bancroft-Madoc area five dominant structural highs - the Harvey-Cardiff arch, the Hastings Highlands, the Kasshabog arch, the Ormsby dome and the Elzevir-Ashby dome - and two major synclinoria (Map 3). The Bancroft-Madoc area is bounded on the north and northwest by the Hastings Highlands and the Harvey-Cardiff arch and on the east by the Elzevir-Ashby dome. Two major synclinoria have their axes trending to the north or northeast and converging in Mayo Township (Map 3). They are dominated by marble-rich supracrustal[1] rock sequences while most of the plutonic rocks of this region occur in the structural domes and arches. The principal fold patterns generally trend northeasterly, while secondary cross-folding has usually west to northwest trending.

In the Bancroft-Madoc area, there are two main systems of major faults. The first one has a west to northwest trending and the second one has a north to east-northeast trending.

2.5 Plutonic Rocks

The plutonic activity in the Bancroft-Madoc area was closely related to the major culminations in the regional metamorphism (Silver and Lumbers, 1965; Lumbers, 1967a). During these periods, numerous felsic and mafic stocks and plutons, mafic and pegmatitic sills and dikes and also several granitic batholiths invaded the surficial rocks in the area. On the basis of petrological and geochronological studies, Lumbers (1967a) has divided the plutonic rocks into several main groups (Figure 2.3).

---

[1] "...the term 'supracrustal' is applied to metamorphic rocks of metasedimentary or metavolcanic origin which comprise the bulk of the Ottawa River Remnant." (Jennings, 1969, p.7).

The plutons of this region form two principal age series: the first has an age of about 1250±25 million years; the second is about 1125±25 million years old (Silver and Lumbers, 1965; Lumbers, 1967a). The first series - Lumbers' biotite-diorite series - is characterized by the trondhjemite-sodic granite differentiation trends. Lumbers subdivided this series into: (a) an albite granite and syenite group; (b) a diorite group and (c) a trondhjemite and sodic granite group. The plutonic rocks of the second series are represented by the quartz monzonite group, which was emplaced over a relatively long period of time, mostly before the culmination of the second stage of regional metamorphism dated at about 1125±25 million years ago. Regionally, the quartz monzonite plutons are generally restricted to the upper amphibolite facies terrain, near the margins of the remnant, while they are practically absent in the central low-grade metamorphosed part of the area.

Apart from these two main series, Lumbers (1967a) recognizes three other minor groups of plutonic rocks: (1) the late gabbro and diorite group; (2) the nepheline syenite group and (3) the potassic syenite and monzonite group. The first two groups were emplaced prior to the culmination of the upper

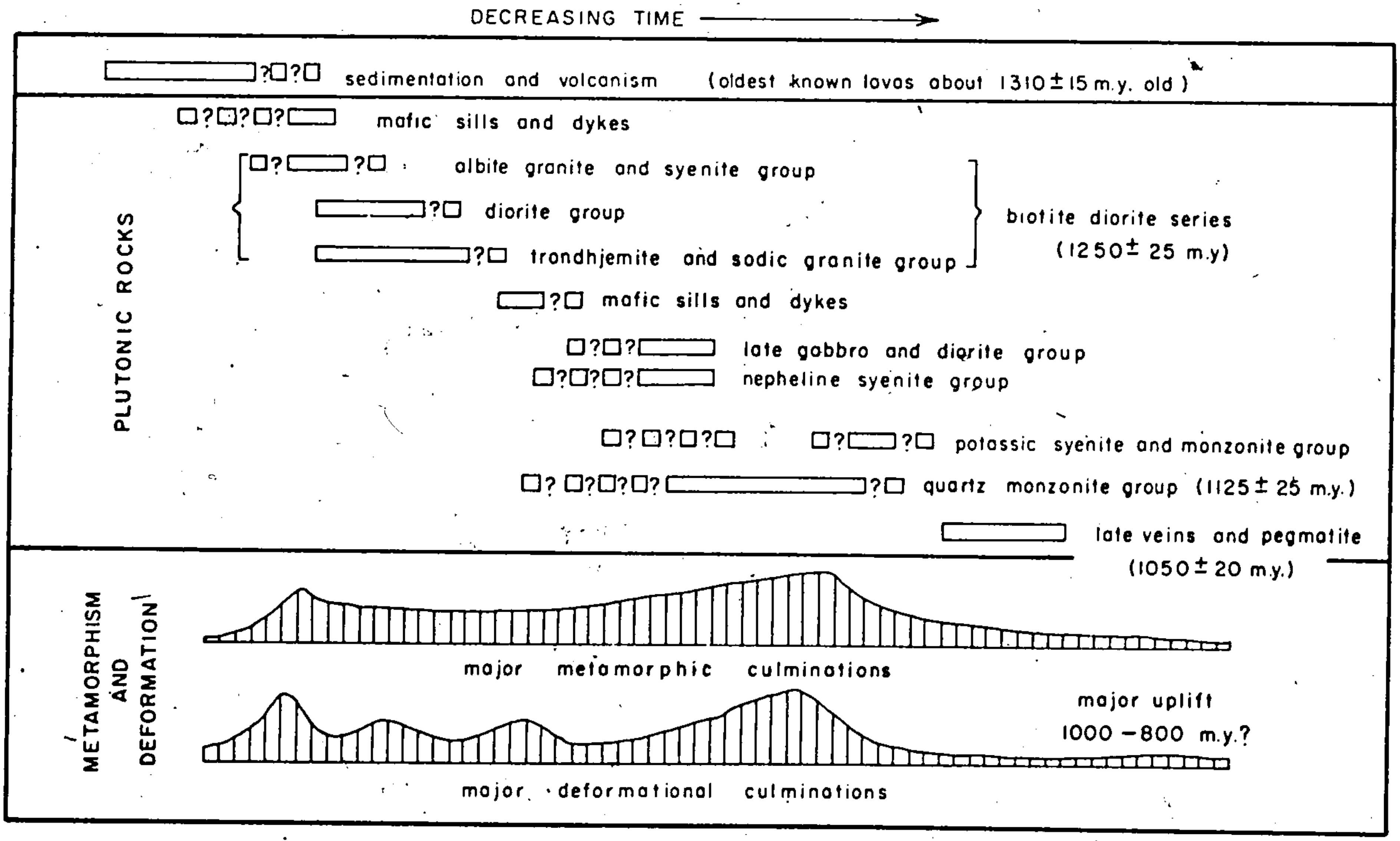

(After Lumbers, 1967a)

FIGURE 2.3 Summary of Tectonic Events in the Bancroft - Madoc Area

amphibolite facies metamorphism which then caused the recrystallization and the deformation of the nepheline syenite group, some bodies of the late gabbro-diorite groups and also some plutonic rocks of the biotite-diorite series. The intrusions of the potassic syenite and monzonite group, to which Lumbers also consigned the Loon Lake pluton, are younger than the regional metamorphism of their country rocks.

The late generation of the hydrothermal calcite-fluorite-apatite veins and dikes of pegmatitic rocks, locally abundant in the northern and western parts of the area, were emplaced about 1050±20 million years ago (Silver and Lumbers, 1965). This age is in relatively good agreement with the Rb/Sr, U/Pb, Pb/Pb and Th/Pb ages (Rb/Sr age = 1006±16 m.y., the mean of U/Pb, Pb/Pb and Th/Pb ages is 1022±56 m.y.) of pegmatites from the Bancroft area as determined by Shafiqullah et al (1973). It is possible, however, that some of these late-stage rocks, as indicated by large variations in the K/Ar ages (c.f. Lumbers, 1967a, p.207), are significantly younger.

CHAPTER 3

PREVIOUS WORK

By the end of the Nineteenth Century, this region had been subjected to geological mapping and reconnaissances of mineral occurrences and deposits (for summaries of these works see for example Hewitt, 1956; Lumbers, 1967a).

The first detailed geological maps and reports of the area which also included observations on the structure, composition and mode of emplacement of plutonic rocks, were given by Adams and Barlow (1910). In their classical study, Adams and Barlow suggested that the granitic bodies in the Haliburton-Bancroft area represent the projections of a large batholith underlying the country rocks. They also pointed out that while along the borders of most granitic bodies in this region, the country rocks dip away from the granite, the opposite is true for the Loon Lake pluton and the Methuen pluton, where host rocks "are found in almost all cases to dip inwards toward the invading granite-gneiss" (p.15).

In a brief structural study of the Loon Lake pluton, Cloos (1934) considered the pluton as funnel-shaped with inward dipping contacts. In disagreement with Adams and Barlow (1910), he noted that "the granite-filled funnel is not part of a batholith underneath but one of the many openings through which the magma has reached higher levels" (p.399).

Satterly (1943), while compiling a geological map of the Haliburton area which also includes the Loon Lake pluton, made some revisions to the original maps of Adams and Barlow. Later Hewitt presented a revised compilation geological map of the Haliburton-Bancroft region, also covering the area studied (Hewitt and Satterly, 1957), and a revised interpretation of the geology of this area (Hewitt, 1956). He did not, however, pay any special attention to the Loon Lake pluton. Hewitt's (1956, 1957, 1962a) concepts of the regional geology of the Bancroft-Madoc area became more or less widely accepted until the comprehensive study of Lumbers (1967a) who strongly refuted many of Hewitt's claims.

On the basis of this information, Buddington (1959) in his classical study of granite emplacement, mentioned the Loon Lake pluton as an example of a pluton emplaced in the transition zone between mesozone and catazone.

Saha (1957, 1959) carried out a detailed petrographic and structural study of the Loon Lake pluton in order to evaluate its manner and history of emplacement. He concluded that the composite Loon Lake pluton crystallized from the magma at a fairly deep level. The older syenite-monzonite intrusion formed the central part of the pluton while the outer granitic zone was produced by a second intrusion shortly after consolidation of the syenite-monzonite core.

Chandos Township was mapped by Shaw (1962) who devoted much attention to the Loon Lake pluton. Shaw confirmed most of Saha's findings.

Extensive geochemical study of Chandos Township has been done recently by Shaw and associates. Kudo (1962) and Shaw and Kudo (1965) investigated a few samples from the basic inclusions of the Loon Lake pluton in their test of discriminant functions to distinguish between amphibolites derived from igneous and from sedimentary rocks. The southern and eastern margins of the Loon Lake pluton have been mapped by Chiang (1965) who studied the element partition between hornblende and biotite in the contact metamorphosed rocks from the aureole of the pluton. A geochemical study of several rocks from the pluton has been carried out by McCammon (1968).

The Loon Lake pluton is also covered by aeromagnetic sheets which were produced from surveys made in 1948 and 1949 and revised in 1957 by the Geophysical Section of the Geological Survey of Canada (Coe Hill aeromagnetic sheet - G.S.C., 1950). A report describing magnetic anomalies in the area was compiled by Abraham (1951). Recently, the Geophysical Section of the G.S.C. has carried out detailed gravimetric measurements in the Bancroft-Madoc area. A compilation and interpretation of these results is given by Jacoby (1971). A detailed oxygen isotope study of the pluton and the Apsley gneiss formation was carried out by

Shieh et al. (1972, 1973). Additional information on specific problems relevant to the Loon Lake pluton are available in studies of Grant (1959), Simony (1960), Shaw (1972) and some others.

CHAPTER 4

GEOLOGY AND PETROLOGY OF METAMORPHOSED COUNTRY ROCKS

4.1 Introduction

The stratigraphy of Chandos Township and surrounding area has been discussed by Hewitt and James (1956), Hewitt (1961, 1962b), Shaw (1962, 1972), Lumbers (1967a,b) and Jennings (1969). But the stratigraphic correlation of individual lithologic units is still controversial (c.f. Shaw, 1972) and it would require detailed tectonic and stratigraphic studies before a correlation of stratigraphic units could be reliably clarified.

According to Lumbers (1967a,b), the area surrounding the Loon Lake pluton is composed of two formations - the Apsley formation and Lasswade marble.

The Apsley formation (Simony, 1960; Shaw, 1962, 1972) consists mainly of biotite gneisses, which are underlain and overlain by thin, more calcic members especially hornblende-bearing gneisses and amphibolites (Lumbers, 1967a). These more calcic members occur particularly in the northeastern and southern parts of Chandos Township (Map 1).

The Apsley formation has been recently studied by Simony (1960) and particularly by Shaw (1972), who has concluded that biotite gneisses are probably a series of interstratified silicic volcanics (about 60%) and sandstone. Lumbers (1967a) and Shaw (1972) have estimated that the thickness of the Apsley formation is about 1500 meters.

The Lasswade marble, occurring typically in the south central part of Chandos Township, overlies and locally interfingers with the upper part of the Apsley formation (Map 1, Figure 2.1). The marble formation probably continues from the vicinity of the village of Lasswade to the eastern side of Chandos Lake (Owenbrook marble - Shaw, 1962) and then further into northern and northeastern Chandos, Wollaston and southern Faraday Townships (Map 3). The Lasswade formation is composed predominantly of marble which is frequently interbedded with biotite and/or hornblende gneiss. Lumbers (1967a) has suggested that the formation probably does not exceed about 600 m in thickness.

This metasedimentary-metavolcanic sequence was subjected to complex Proterozoic metamorphic events. The main progressive regional metamorphism, which probably can be correlated with a metamorphic event, dated at 1125±25 million years (Silver and Lumbers, 1965; Lumbers, 1967a; Jennings, 1969) was followed in the study area by an intensive contact metamorphism produced by the forcible intrusion of the Loon Lake pluton. The third metamorphism was regressive in character and produced mineral assemblages of the greenschist facies. The retrograde metamorphic effects, however, are only minor and localized.

4.2 Regional Metamorphosed Rocks

Three main lithological types comprise the regionally metamorphosed supracrustal sequence in the study area. They are:

(a) gneisses

(b) amphibolites

(c) carbonate metasediments

The regional distribution of these rock types is shown on Map 1.

4.2.1 Gneisses

Gneisses include a wide range of rocks with a composition varying from aluminous through leucocratic quartz-feldspathic to basic. On the basis of the mineralogical composition, Shaw (1972) divided these rocks into four groups:

(a) biotite gneiss

(b) hornblende-biotite gneiss

(c) calcomagnesian gneiss

(d) aluminous gneiss

In the field, however, hornblende-biotite and calcomagnesian gneisses can not be mapped separately on the scale of the present investigation (Map 1) and they were considered as one map unit (unit 3). On the other hand, the group of biotite gneisses has been subdivided in the field into two units - biotite gneiss s.s. (map unit 1) and quartzitic biotite gneiss (map unit 2). These two rock types are readily distinguishable in typical localities (e.g. 90 and 211 for quartzitic biotite gneiss), but in places where the transition between these types occurs, their distinction is not so apparent.

In general, the gneisses are well stratified with relatively pronounced banding. Migmatites are very rare or lacking in this gneiss complex except in the aureole of the pluton. The gneisses in the map area have been recently studied in some detail by Shaw (1972) and therefore only a brief description is given below.

4.2.1.1 Biotite Gneiss

The biotite gneiss usually has a pronounced foliation, fine to medium grain size and lepidogranoblastic texture. The major constituents are quartz, biotite and two feldspars. The composition of plagioclase varies in the range An 10 to An 30, with the commonest between An 12 and An 18. Minor and accessory minerals include garnet, muscovite, sphene, magnetite, ilmenite, pyrite, pyrrhotite, tourmaline, apatite and zircon. The ACKF diagram for the typical prograde mineral assemblages of biotite gneisses is shown in Figure 4.2.1.

Simony (1960) recognized two types of the Apsley biotite gneiss - sodic and potassic. Shaw (1972) confirms the existence of potassic and sodic facies of biotite gneiss

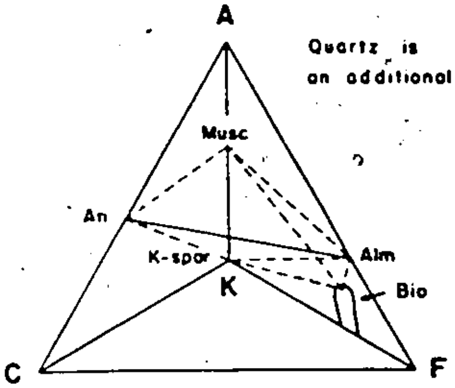
A
Quartz is
an additional phase
Musc
An
K-spar
Alm
K
Bio
C
F

Fig 4. 2.1. ACKF Diagram for Biotite Gneisses

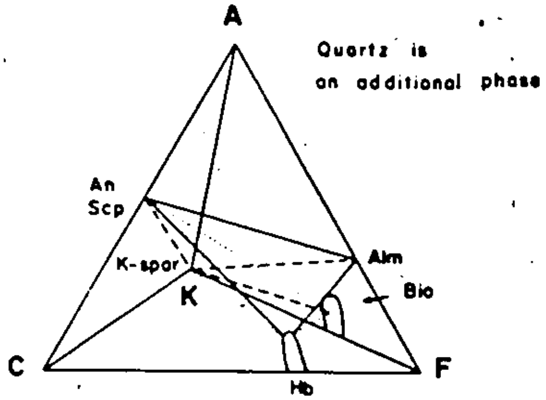
A
Quartz is
an additional phase
An
Scp
K-spar
Alm
K
Bio
C
F
Hb

Fig 4. 2.2. ACKF Diagram for Hornblende-Biotite Gneisses

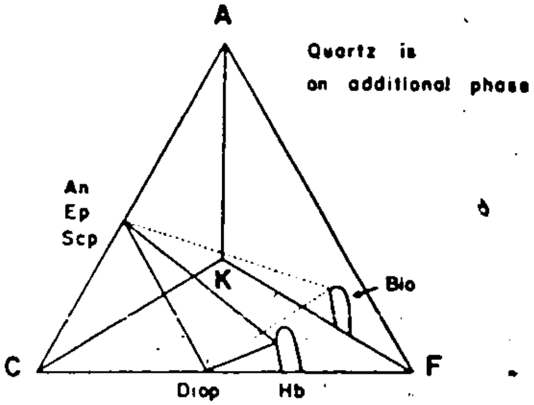
A
Quartz is
an additional phase
An
Ep
Scp
K
Bio
C
F
Diop
Hb

Fig. 4. 2. 3. ACKF Diagram for Calcomagnesian Gneisses

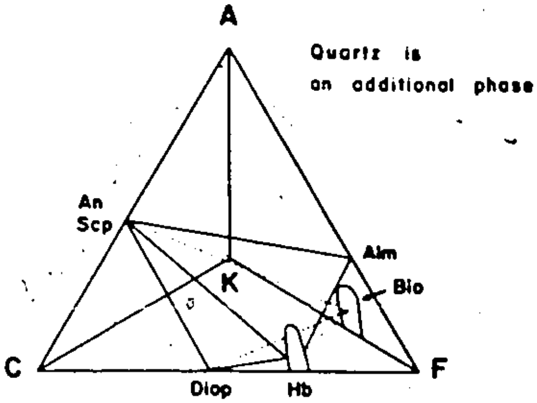
A
Quartz is
an additional phase
An
Scp
Alm
K
Bio
C
F
Diop
Hb

Fig. 4. 2. 4. ACKF Diagram for Amphibolites

Tie lines on the front face of the tetrahedron are shown by solid lines, those on the three back faces by dashed lines, and those within the volume by dotted lines.

(c.f. Table 4.2.1) but he points out that the population is not strictly bimodal. There are also wide variations in quartz content. In places, the quartz content markedly increases and biotite gneiss s.s. passes to the quartzitic biotite gneiss. The quartzitic biotite gneiss is fine-grained, rather massive with foliation and banding much less pronounced than in biotite gneiss s.s. This rock type forms the concordant horizons of varying thickness in typical biotite gneiss. In the northeastern part of the study area these horizons are large enough to show on Map 1. Qualitatively the mineral composition of quartzitic biotite gneiss is practically the same as in biotite gneiss s.s. but from a quantitative point of view, the content of quartz is higher, exceeding 40% and the content of biotite is generally lower in quartzitic biotite gneiss. The modal analyses of quartzitic biotite gneiss together with the approximate averages of biotite gneiss (Shaw, 1972) are given in Table 4.2.1.

4.2.1.2 Calcareous Gneiss

This map unit (unit 3) consists essentially of the hornblende-biotite and calcomagnesian gneiss groups of Shaw (1972). The unit is represented by a variety of rock types, which are frequently intimately interbanded. The mineral assemblages and texture of these rocks vary frequently even in individual outcrops. In places, they also grade or are interbedded with amphibolites, biotite gneiss or carbonate metasediments.

The rocks of this map unit are generally greenish-

Table 4.2.1 Modal composition of gneisses

	1	2	3	4	5	6	7	8
Quartz	30	26	25	20	25	35	45.6	45.2
Plagioclase	47	33	50	35	10	30	23.1	37.7
K-feldspar	2	19		20			22.5	3.6
Biotite	20	20	10	10		15	8.6	12.1
Muscovite								0.4
Garnet	tr	tr	tr	tr		10	tr	tr
Hornblende			15	15	10			
Sillimanite						5		
Cordierite						5		
Diopside					20			
Scapolite					30			
Epidote					3			
Calcite					2			
Opaque							tr	0.6
Apatite								tr

1. Approximate average composition of the sodic type of biotite gneiss (Shaw, 1972)
2. Approximate average composition of the potassic type of biotite gneiss (Shaw, 1972)
3. Approximate average composition of the sodic type of hornblende-biotite gneiss (Shaw, 1972)
4. Approximate average composition of the potassic type of hornblende-biotite gneiss (Shaw, 1972)
5. Approximate average composition of calcomagnesian gneiss (Shaw, 1972)
6. Approximate average composition of aluminous gneiss (Shaw, 1972)
7. Quartzitic biotite gneiss - 211
8. Quartzitic biotite gneiss - 90

gray to dark green, fine to medium-grained, mostly well foliated with hornblende and biotite preferentially aligned parallel to foliation. In places, however, the rocks have poor foliation and frequently prismatic crystals of hornblende have a "feather" arrangement.

In accordance with the classification of Shaw (1972), this map unit can be subdivided petrographically into two groups:

(a) hornblende-biotite gneiss
(b) calcomagnesian gneiss characterized by the presence of clinopyroxene and/or epidote.

Hornblende-biotite gneisses are more abundant than calcomagnesian ones. Shaw (1972) has estimated their relative abundances at the ratio 2:1.

Hornblende-biotite gneisses are composed of hornblende, biotite, plagioclase, quartz and in places also K-feldspar and scapolite. Calcite, garnet, sphene, magnetite and ilmenite frequently occur in minor to accessory amounts. The ACKF diagram for the typical prograde mineral assemblages of hornblende-biotite gneisses is shown in Figure 4.2.2.

As in the biotite gneiss group, Shaw (1972) recognizes two facies of hornblende-biotite gneisses - sodic and potassic. Geographically, the sodic facies strongly predominates over the potassic type of hornblende-biotite gneiss, which is relatively rare in the map area. The approximate mean modal composition of these two facies is given in Table 4.2.1. In the map area, the amounts of felsic minerals appear generally to be lower than their average contents in the hornblende-biotite gneisses of the Apsley formation given by Shaw (1972) and also the plagioclase composition on the average is more basic, usually An 20-40.

Calcomagnesian gneisses contain in addition to hornblende also diopsidic clinopyroxene and/or epidote in significant amounts. Apart from these, other major components are quartz and plagioclase (usually from An 25 to An 48). Minor amounts of calcite, biotite and occasionally scapolite are also present. The accessory minerals include sphene, magnetite, ilmenite, tourmaline and apatite. The ACKF compatibility diagram of characteristic mineral assemblages of calcomagnesian gneisses is shown in Figure 4.2.3. The average mode of calcomagnesian gneiss is given in Table 4.2.1.

4.2.1.3 Aluminous Gneiss

Aluminous gneisses occur only very sparsely in the Apsley formation except in the contact aureole of the Loon Lake pluton where they are thought to be contact metamorphosed rocks. (They will be described in a later section.) In order to better evaluate the degree of regional metamorphism for which these rocks are most important, the mineral assemblages of the aluminous gneisses of the Apsley formation further from the pluton (from outside the map area) which are thought to be regionally metamorphosed, will be considered for an evaluation of the grade of metamorphism. A possibility that the areas adjacent to the map region could have a different degree of metamorphism, however, does not appear to be very great as Shaw (1962) also pointed out that "there is little variation in metamorphic grade throughout the township" (p.24).

4.2.2 Amphibolites

In the map area, amphibolites (map unit 4) usually form layers or bodies ranging from less than one to several tens of meters thick, with only minor compositional banding. Thin bodies of amphibolite, often not mapable on the scale of the present investigation, are abundant in gneisses especially in the calcareous ones where they occur as conformable bands. In places, amphibolites have poikilitic crystals of hornblende arranged in a criss-cross fashion ("feather" amphibolites of Adams and Barlow, 1910).

The principal mineral assemblage of amphibolites is hornblende (X - pale yellow-green to light brownish-green; Y - olive-green to dark green; Z - dark brownish-green to blue-green, with an extinction angle generally $c \wedge Z = 16-27°$) and plagioclase whose composition mostly corresponds to andesine. In places, they contain variable minor amounts of biotite, quartz, clinopyroxene, scapolite and garnet. The texture of amphibolites is nematoblastic or nematogranoblastic.

The ACKF diagram for the typical prograde mineral assemblages is shown in Figure 4.2.4 and the modal analyses of some representative samples are given in Table 4.2.2.

4.2.3 Carbonate Metasediments

Carbonate metasediments are represented in the map area by the Lasswade marble, which occurs south of the Loon Lake pluton and probably continues on the eastern side of Chandos Lake as the Owenbrook marble (Map 1). Apart from these two units, marble also occurs in calcareous gneisses and amphibolites as parallel bands and as bands and lenses in biotite gneisses, especially north of the pluton. This latter occurrence probably represents a connection between Lasswade and Owenbrook marbles which are believed to be the same stratigraphic horizon. Marble also occurs rarely as inclusions in the Loon Lake pluton.

Carbonate metasediments consist of calcic marble, occasionally interbedded with thin bands of gneisses, amphibolites and calcsilicate pods and bands. In places, with decreasing contents of carbonates and increasing amounts of silicates, carbonate metasediments pass to calcareous gneisses and amphibolites. In the field, rocks which contain more than 50% carbonates have been mapped as marbles (map unit 5, Map 1).

Marble is usually white to gray, granular, coarse to medium-grained and poorly jointed. Calcite is the major component of marbles, comprising mostly 80-95% and in exceptional cases up to about 97% of the rocks. By a staining (c.f. Appendix 1) and X-ray method (Weber and Smith, 1961), dolomite has been

Table 4.2.2 Modal composition of amphibolites and marbles

	1	2	3	4	5	6	7	8
Clinoamphibole	52.3	54.2		0.8	4.6	3.2		tr
Biotite/phlogopite		8.6	3.0	0.6	2.0	9.7	4.8	5.6
Plagioclase	46.2	34.2	1.6	tr	2.1	2.9	12.2	0.8
Quartz	0.4	2.4						
Calcite			93.3	96.9	88.9	82.9	79.8	90.7
Scapolite					1.5			
Sphene	tr		tr		tr		tr	tr
Opaque	0.8	0.6	2.1	1.4	0.7	1.2	2.9	2.5
Tourmaline						tr		tr
% An in plagioclase	34	33						

1. Amphibolite 196-3
2. Amphibolite 196-1
3. Owenbrook marble 111
4. Owenbrook marble 145-3
5. Lasswade marble 198-3
6. Lasswade marble 198-4
7. Lasswade marble 110-3
8. Lasswade marble 198-5

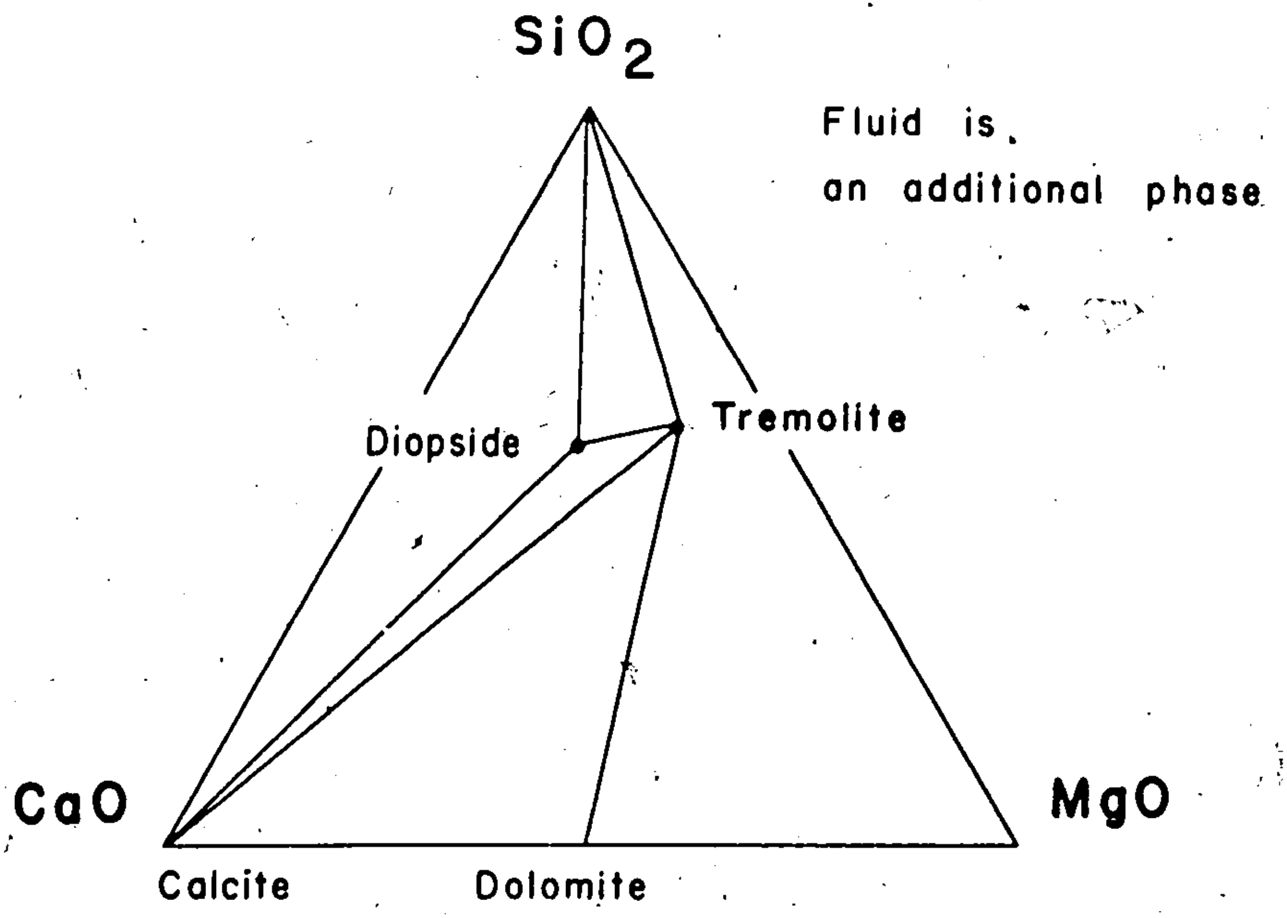
SiO2
Fluid is.
an additional phase
Diopside
Tremolite
CaO
MgO
Calcite
Dolomite

Fig. 4.2.5. $CaO-MgO-SiO_2$ Diagram for Regionally Metamorphosed Marbles identified in some marbles (in two of the twenty samples examined). The most frequent non-carbonate minerals are phlogopite, diopsidic clinopyroxene, and tremolitic or actinolitic amphibole. Other constituents present in subordinate amounts include quartz, plagioclase with a composition of oligoclase to sodic andesine, microcline, scapolite, magnetite and pyrite. Sphene, graphite, apatite and tourmaline often occur as accessories. The texture of marbles is a granoblastic mosaic commonly with lamination.

The CaO-MgO-SiO_2 diagram for the typical prograde mineral assemblages of carbonate metasediments is shown in Figure 4.2.5 and the modal analyses of some representative samples are given in Table 4.2.2.

4.2.4 Conditions of Regional Metamorphism

The detailed petrological studies of Shaw (1962), Lumbers (1967a), Chesworth (1967, 1971), Carmichael (1968, 1969, 1970) and Jennings (1969) have shown that the regional metamorphism in the Bancroft-Madoc area is intermediate between Barrovian and Abakuma facies series. In particular, the metamorphic grade in Chandos Township corresponds to amphibolite facies and more specifically lies about the first sillimanite isograd (Shaw, 1962; Lumbers, 1967a; Jennings, 1969; c.f. Figure 2.2).

Some of the characteristic features of high-grade metamorphism in the Bancroft-Madoc region which have been found to be valid in the Chandos area are: (a) staurolite persists above the first sillimanite isograd (Shaw, 1962; Carmichael, 1968; Jennings, 1969) and (b) sillimanite, muscovite and quartz coexist throughout most of the sillimanite zone (Shaw, 1962; Lumbers, 1967a; Carmichael, 1968; Jennings, 1969).

All the prograde mineral associations described earlier are compatible with amphibolite facies metamorphism. For an evaluation of the conditions of regional metamorphism, the following mineral associations appear to be characteristic of the Chandos area:

(a) muscovite-quartz-sillimanite
(b) staurolite-garnet-cordierite-biotite
(c) staurolite-sillimanite-garnet-biotite
(d) sillimanite-cordierite-garnet-biotite
(e) biotite-muscovite-plagioclase-K-feldspar-quartz
(f) epidote-quartz

Comparable mineral associations have been described from an adjacent area by Jennings (1969). The assemblages (b) and (c), which seem to indicate disequilibrium, probably represent the partial breakdown of staurolite as he suggested. The conditions of regional metamorphism can be tentatively estimated by comparing the natural assemblages with experimentally determined mineral equilibria. There is a large degree of uncertainty, however, in applying experimental conditions to natural mineral assemblages and thus these reactions can serve only as general limits of possible metamorphic conditions. A compilation of relevant experimental data is given in Figure 4.2.6. For the sake of simplicity, the reactions are drawn as lines. But "when minerals of the solid solution type are involved, as staurolite, cordierite, etc. the equilibrium of the reaction cannot be merely univariant, it must be at least divariant; this means that in the plane with P_{H_2O} and T as coordinates the univariant equilibrium line must be replaced by a divariant band" (Winkler, 1970, p.212). The same holds true for the limits of experimental error.

Also a critical problem for an estimation of metamorphic conditions is the choice of experimental curves. Even in the case of the extensively studied aluminum silicate triple point and stability fields of these polymorphs "almost an embarrassment of choice exists" (Chesworth, 1971, p.226). To partly overcome this problem, only the generally accepted reaction curves have been used (Winkler, 1970; Ganguly, 1972).

With regard to the sillimanite, kyanite and andalusite phase boundaries and their triple point, Winkler (1970) has concluded that "of all experiments made in this respect, those of Richardson et al. (1968, 1969) and those of Althaus (1967, 1969) seem to be the most reliable" (p.237). Their results are shown in Figure 4.2.6 as curves 1 and 2 respectively. The reaction curves for the stability of sillimanite thus represent the estimate of minimum temperature.

The breakdown of muscovite in the presence of quartz

Figure 4.2.6 P-T graph of experimental data pertaining to the conditions of regional metamorphism

Curve 1. Stability fields of the polymorphs of Al_2SiO_5 (Richardson et al., 1969)

2. Stability fields of the polymorphs of Al_2SiO_5 (Althaus, 1967, 1969)

3. Muscovite + quartz ⇌ K-feldspar + Al_2SiO_5 + vapour (Althaus et al., 1970)

4. Eutectic melting curve in the system K-feldspar-quartz-H_2O (Shaw, 1963; Winkler, 1970)

5. The three curves limit the field of coexistence of staurolite and cordierite (inside the angles) (Ganguly, 1972)

6. The two curves limit (within the angle) the field in which almandine, biotite, Al_2SiO_5 and cordierite are stable (Hirschberg and Winkler, 1968)

7. Fe-staurolite + quartz ⇌ almandine + sillimanite + vapour (Richardson, 1968)

8. Zoisite + quartz ⇌ anorthite + grossularite + vapour (Boettcher, 1970)

9. Beginning of anatexis in plagioclase-bearing gneiss (An 0) (Winkler, 1970)

10. Beginning of anatexis in plagioclase-bearing gneiss (An 26) (Winkler, 1970)

11. Almandine + sillimanite + quartz ⇌ Fe-cordierite (Richardson, 1968)

12. Fe-staurolite + almandine + quartz ⇌ cordierite + vapour (Richardson, 1968)

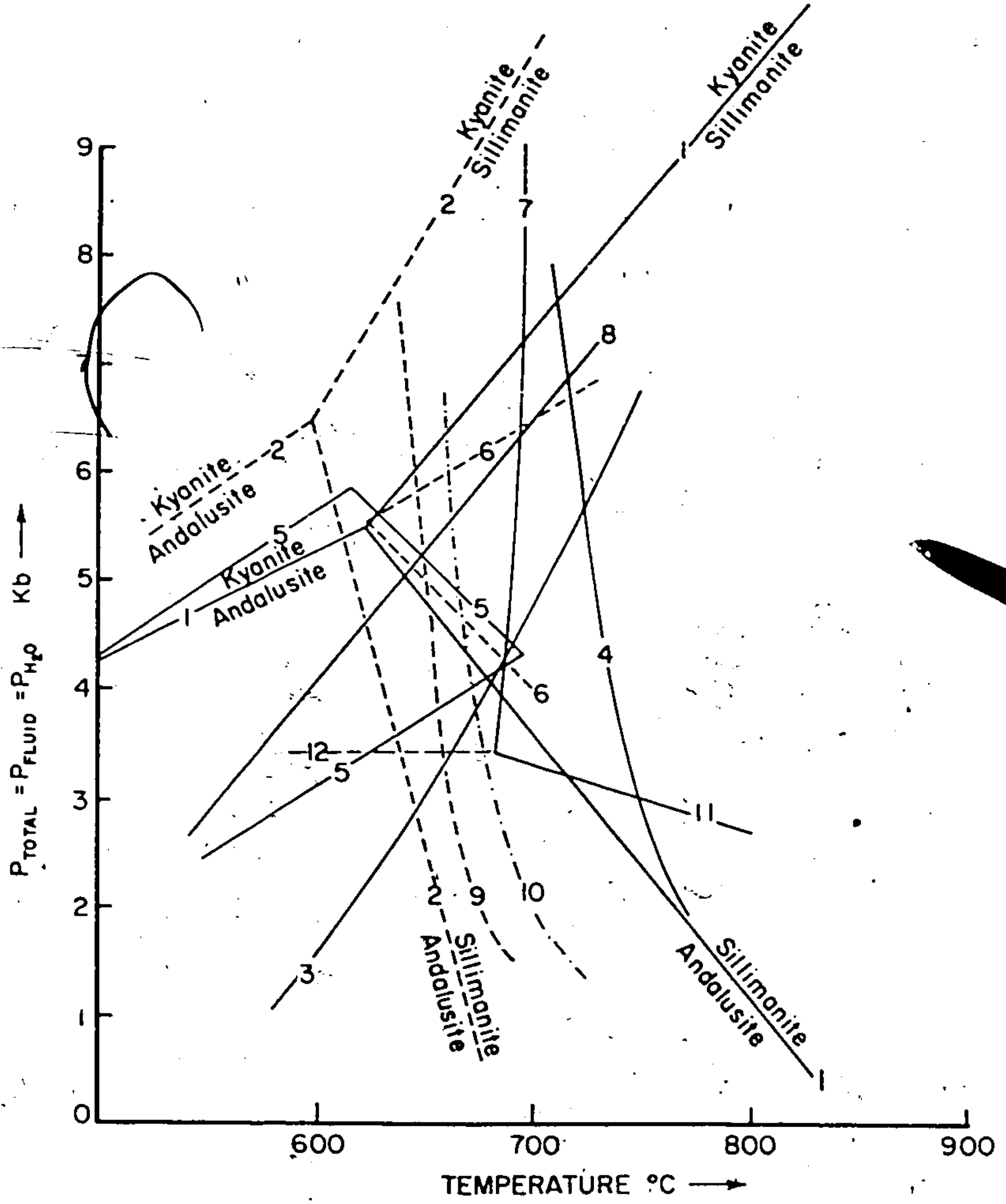
Kyanite
Sillimanite
Kyanite
Sillimanite
Kyanite
Andalusite
Kyanite
Andalusite
Sillimanite
Andalusite
Sillimanite
Andalusite
1
2
3
4
5
6
7
8
9
10
11
12
0
1
2
3
4
5
6
7
8
9
600
700
800
900
TEMPERATURE °C →
P_{TOTAL} = P_{FLUID} = P_{H2O} Kb →

provides an estimate of the maximum metamorphic temperatures at the lower pressure side (curve 3, in Figure 4.2.6). This reaction has been confirmed experimentally by Evans (1965), Althaus et al. (1970), Day (1970) and Haack (in Winkler, 1970). At the pressure in question, there is reasonably good agreement among their data. At a higher pressure, the maximum temperature is probably given by curve 4 (Figure 4.2.6) which represents the conditions of eutectic melting of quartz and potassium feldspar (Shaw, 1963). The intersection of these two curves is at about 5 kb water pressure and temperature 725°C (Winkler, 1970).

Within this general P-T framework, a more precise estimation may be inferred due to the presence of cordierite, staurolite and garnet. Ganguly (1972) has deduced the limits over which staurolite and cordierite may coexist in natural assemblages (curves 5, in Figure 4.2.6). Curves 6 (within the angle) limit the field in which coexisting almandine, biotite, sillimanite and cordierite are stable (Hirschberg and Winkler, 1968; Chakrovorthy and Ghosh, 1972).

Thus it appears that the probable range of pressure-temperature conditions for the study area is bounded by curves 3, 5 and 6 (Figure 4.2.6). This would be true, however, only if the staurolite decomposition reaction took place in the staurolite-cordierite stability field. If this assumption is not valid, then the upper temperature limit would be defined either by curve 7, representing the breakdown of coexisting staurolite and quartz (Richardson, 1968) or the breakdown of muscovite and quartz (curve 3) or the curve of eutectic melting of potassic feldspar and quartz (curve 4).

This field may be further somewhat diminished due to the presence of the association of quartz and epidote in regionally metamorphosed rocks in the Chandos area. Zoisite or clinozoisite has been usually used as a model for epidote minerals in the experimental determinations of the reaction epidote+quartz⇌anorthite+grossularite+vapour (Merrin, 1962, 1963; Winkler and Nitsch, 1962; Holdaway, 1966; Newton, 1966; Boettcher, 1970). There is, however, little agreement on the location of this reaction curve. The most widely accepted curve is that of Boettcher (curve 8, Figure 4.2.6) which is in general agreement with those of Newton (1966) and Strens (1965, 1968).

Curves 9 and 10 (Figure 4.2.6) define the temperatures of the beginning of anatexis for rocks with plagioclase composition An 0 and An 26; this is the range within which lie the plagioclase compositions of most gneisses encountered in the area studied. These curves are located very close to, but lie somewhat above the area representing the approximate limits of metamorphic conditions in the Chandos region. This may explain why migmatization in the Apsley region is very rare or lacking (except in the immediate vicinity of the granitic contacts). Thus, Figure 4.2.6 suggests that the conditions of metamorphism roughly fell within a temperature range of about 620-700°C and a pressure range (assuming $P_{total} = P_{fluid} = P_{H_2O}$) of about 4.5-6.0 kb.

In conclusion, it appears that the prograde regional metamorphism in the Chandos region corresponds to "the low-pressure intermediate type amphibolite facies" of Miyashiro (1961) or "medium stage of metamorphism" of Winkler (1970).

In order to refine the above temperature estimates, the composition of coexisting alkali feldspar pairs (Barth, 1956, 1968) and Mg-calcite-dolomite pairs (Graf and Goldsmith, 1955, 1958; Harker and Tuttle, 1955) have been determined. A similar geothermometric attempt has been made in the Chandos area by Jennings (1969) using carbonate pairs.

The present attempt was not completely successful. The data for the feldspar pair are given in Table 4.2.3. There are great uncertainties in the calibration of the two feldspar geothermometer. "Evidently, attempts at laboratory calibration of the feldspar geothermometer have not produced a consistent picture" (Fox and Moore, 1969, p.1207). Comparison of the data from Table 4.2.3 with calibrated distribution isotherms (Figure 4.2.7) indicates a temperature well under 600°C for the study sample, i.e. lower than the temperature inferred on the above petrological grounds. The distribution of albite between coexisting feldspars from the study area, however, is comparable with the natural feldspar pairs, particularly with the distribution curves of Smith (1966) constructed mainly on the basis of

Table 4.2.3 Composition of coexisting feldspars from regional metamorphosed gneiss

Sample	Mol % Ab in alkali feldspar	Mol % Ab in plagioclase	K
Hornblende-biotite gneiss, 659	11	72	0.153

Plagioclase composition determined optically; that of potash feldspar by X-ray (Orville, 1960, 1967)

K = mol. % albite in potash feldspar/mol. % albite in plagioclase

Table 4.2.4 Composition of Mg-calcite from regional metamorphosed marble and estimated temperature from the calcite-dolomite solvus

Sample	Mol % $MgCO_3$	Temp. °C
Marble, 245	3.38	420

Determination carried out according to the method of Jennings and Mitchell (1968)

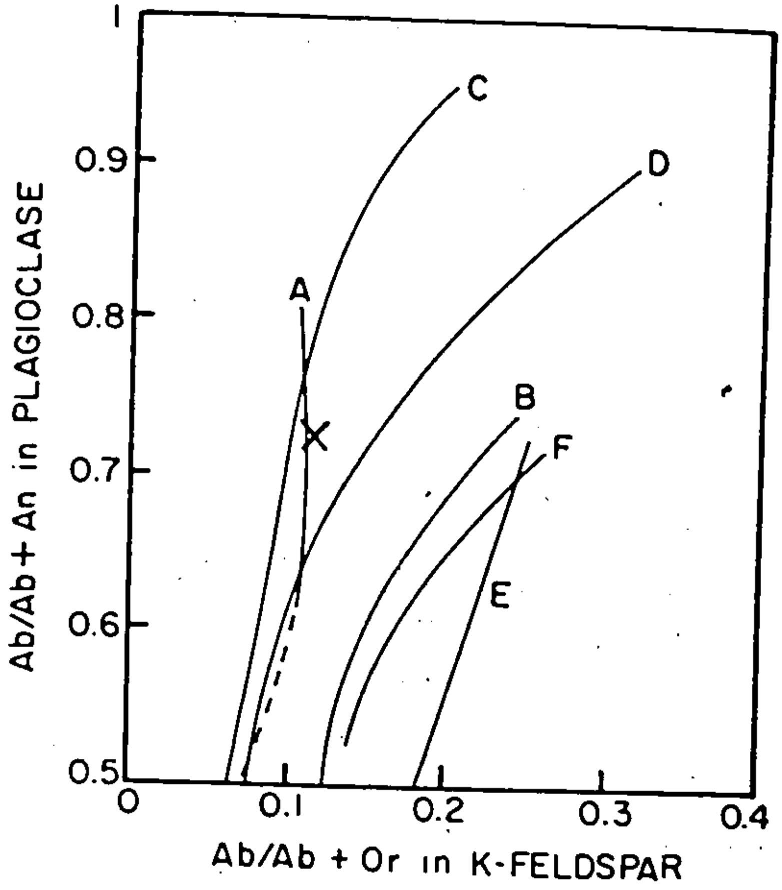

Figure 4.2.7

Distribution of albite between coexisting feldspars. A and B distribution curves for natural feldspars of middle almandine amphibolite and granulite facies, respectively, from the Clare River and Westport areas, Ontario (Smith, 1966); C and D 500° and 600°C isotherms, respectively (Orville, 1962); E and F 600°C isotherms of Barth (1962) and Perchuk and Ryabchikov (1968), respectively.

x = hornblende-biotite gneiss 659

feldspars from gneisses of the middle almandine amphibolite and granulite facies from the Clare River and Westport areas, Ontario (Figure 4.2.7). The sample from the study area lies very close to the middle almandine amphibolite isotherm of Smith (1966). Unfortunately, Smith's distribution curves are not calibrated. It is of interest that feldspar distribution coefficients from gneisses of the nearby Oak Lake and Whetstone Lake areas with a similar grade of regional metamorphism, also fall close to Smith's middle almandine amphibolite isotherm (Rambaldi, 1973).

The data for Mg-calcite from the Lasswade marble are given in Table 4.2.4. The temperature obtained is too low to represent the maximum temperature reached during metamorphism. The low recorded temperature of the carbonate geothermometer contrasts with the temperatures obtained by Jennings (1969) and those from the contact aureole of the pluton (see section 4.3.4) which are not far removed from those estimated for the metamorphic events. A probable explanation for the low-temperature estimate is a re-equilibration of carbonates during the cooling period after the metamorphic events. Such re-equilibration can be reached in laboratory conditions within days (Harker and Tuttle, 1955). Another possible cause for the low recorded temperature might be retrograde metamorphism (Jennings, 1969) or disequilibrium effects.

4.3 Contact Metamorphosed Rocks

The Loon Lake pluton is surrounded by the contact aureole, the maximal extent of which ranges between 300 and 500 m from the contact (c.f. Map 1). The contact metamorphosed rocks occur not only around the margin, but are also rather abundant as inclusions throughout the pluton. As Shaw (1962) pointed out, some inclusions "are large enough to suggest that they might be roof pendants or large stoped blocks" (p.14). It is also possible that some inclusions were brought up by the pluton and they might perhaps represent deeper-lying rocks.

The contact metamorphism was superimposed on rocks which were already regionally metamorphosed to the amphibolite grade. The aureole is not always clearly distinguishable, its geographical extent is frequently uncertain and also "there is no clear sequence of contact metamorphic zones" (Shaw, 1962, p.25). This is probably because of the metamorphic overlap, locally strong migmatization, abundant pegmatitic and aplitic veins in the vicinity of the pluton and also possibly tectonic movements. The contact metamorphosed rocks have been mapped in the field only around the southern edge of the pluton and in some inclusions throughout the pluton. Because of the absence of typical hornfelsic texture, particularly at the northeastern side of the pluton, the contact metamorphosed rocks have not been separated there from regional metamorphosed ones on Map 1.

Since the contact aureole has been extensively studied by Shaw (1962), Chiang (1965), Hinton (1972) and Shieh (1972, 1973), only certain aspects of some metamorphosed rocks will be described. The rocks under consideration include:

(1) aluminous hornfelses - comprising aluminous gneisses of Shaw (1972). (The term aluminous hornfels is occasionally used instead of the petrographically more precise name - aluminous gneiss - in order to stress the relation between the pluton and this rock type.);

(2) mafic hornfelses - which characteristically contain significant amounts of hornblende and/or pyroxene;

(3) contact metamorphosed marble.

4.3.1 Aluminous Hornfelses

In the northern and northwestern part of the contact aureole, there is a zone up to 500 m wide, comprised partially of gneissic rocks, which Shaw (1972) included in his aluminous gneiss type of the Apsley formation. The gneisses are interspersed there with granitic rocks. In comparison with the Apsley biotite gneiss, these aluminous rocks are rich in Al_2O_3, MgO and FeO and poor in alkalies and silica (c.f. Table 4.3.1). They are characterized by the presence of garnet and sillimanite and/or cordierite, which are even the major constituents in places (Table A.1.5). In general, the amount of these aluminosilicates increases toward the contact and is greatest in the xenoliths, which range in size from about a meter to a few hundres meters. The transition from aluminous hornfels to biotite gneiss appears to be continuous. (The aluminous hornfelses and biotite gneisses cannot be mapped separately in the field on the scale of the present investigation. But it should be noted that a significant portion of the migmatized biotite gneiss map unit - Map 1 - is comprised of aluminous hornfelses.)

The petrography of these rocks has been described by Shaw (1962, 1972). His estimation of their average modal composition is given in Table 4.2.1, while the modal compositions of some representative samples are presented in Appendix 1 (Table A.1.5). The common prograde minerals are:

(1) garnet-sillimanite-cordierite-biotite-plagioclase-quartz
(2) garnet-sillimanite-biotite-plagioclase-quartz
(3) sillimanite-cordierite-biotite-plagioclase-quartz
(4) garnet-biotite-plagioclase-quartz
(5) sillimanite-biotite-plagioclase-quartz

Garnet usually forms sieved porphyroblasts, sometimes up to 1 cm in diameter. The unit-cell and refractive index measurements indicate that garnet is almandine-rich (in rock 67, garnet has $n \cong 1.835$ and $a_o = 11.61$ Å suggesting about 80% of almandine component).

Cordierite occurs as anhedral grains which vary in size from about 0.2 to 2 mm. Plagioclase is typically more calcic (usually andesine) than in biotite gneiss. It appears that the basicity of plagioclase increases with the increase of the contents of aluminous minerals though not in a simple manner. Potassic feldspar is virtually absent from these rocks. Magnetite, rutile, apatite, tourmaline and zircon are frequently present as accessories.

The unusual chemical composition of the aluminous gneisses in comparison with the other members of the Apsley formation poses problems related to the cause of the high Al, Fe and Mg and low alkalies and silica contents and to the original nature of these rocks. Shaw (1962) and Lal and Moorhouse (1969) have summarized several hypotheses for the origin of the cordierite-garnet bearing rocks. Some of these theories which appear to be pertinent to the genesis of the aluminous gneisses are:

(1) Metasomatic introduction of MgO and FeO and simultaneous removal of alkalies either by the penetration of hydrothermal fluids from the pluton (Eskola, 1914, 1915; Geijer, 1917, 1963) or by formation of a "basic front" (Reynolds, 1947; Holmes and Reynolds, 1947; Ramberg, 1952; Read, 1957).

(2) Aluminous gneisses are the residuum after the extraction of minimum melting material (Eskola, 1933; Barth, 1933).

(3) Gneisses represent chemically unaltered metamorphosed shales.

As far as the metasomatic hypothesis is concerned, no evidence for this mode of origin has been found. The indication that at least some mineral assemblages of aluminous gneisses are in equilibrium (Jennings, 1969), the general lack of correlation between the composition of wall-rocks and adjacent rocks of the pluton and also geochemical data (see below) are not consistent with this theory. Likewise, experimental studies suggest that the late-stage solutions could hardly produce such an enrichment of Mg, Fe and Al (c.f. Johannes and Winkler, 1965).

The anatectic hypothesis can envisage the aluminous gneisses as the residuum after partial melting of the Apsley biotite gneiss and consequent subtraction of the granitic portion. The extensive occurrences of the aluminous gneisses in the contact aureole of the pluton, while similar rocks are very rare in the surrounding areas, may suggest that the partial melting was induced by the intrusion of the pluton, which supplied the heat required for anatexis. The feasibility of this model can be evaluated on the basis of petrological and chemical data. The estimation of pressure and temperature conditions of contact metamorphism imposed on the surrounding rocks by the pluton indicate that anatectic melting might have taken place (c.f. Figure 4.3.10 and section 4.3.4).

With regard to the chemical composition of these rocks, their chemical constituents together with the average composition of the Apsley biotite gneiss (Shaw, 1972) are plotted graphically against the sum of normative quartz-orthoclase-albite-anorthite in Figures 4.3.1-2, since this hypothesis assumes that the main difference between biotite and aluminous gneisses is subtracted quartz-feldspathic material. (The chemical analyses of aluminous gneisses are given in Appendix 1.) It should be pointed out, however, that the use of this parameter introduces a constant item-sum bias into the trends and also a prior correlation bias (Chayes, 1960; Evans, 1964).

The relatively smooth trends on the variation diagram for iron, aluminum and sodium (Figures 4.3.1-2) are in agreement with the gradual subtraction of the minimum melting fraction. The overall progressive increase of normative (Figure 4.3.2) and also modal basicity of plagioclase toward the more altered hornfelses is consistent with the experimental studies of Winkler and Von Platen (1960) which have shown that partial melting produces plagioclase fractionation with calcic enrichment in residual rocks.

Figure 4.3.2 shows that the ratio Fe/Fe+Mg in the hornfelses and the Apsley biotite gneiss is practically the same in spite of a large enrichment of these elements in hornfelses. It seems unlikely that the metasomatic process would enrich both these elements in the same proportions. But it suggests that the removal of other constituents (alkalies and silica) resulted in the relative enrichment of femics. Likewise, Figure 4.3.3 suggests that the subtraction of the

Figure 4.3.1 Variations of ($FeO+Fe_2O_3$) (top) and Al_2O_3 (below) as a function of norm. (Q+Ab+An+Or) in aluminous hornfelses relative to the average Apsley gneiss

● - aluminous hornfels

△ - average Apsley gneiss (Shaw, 1972)

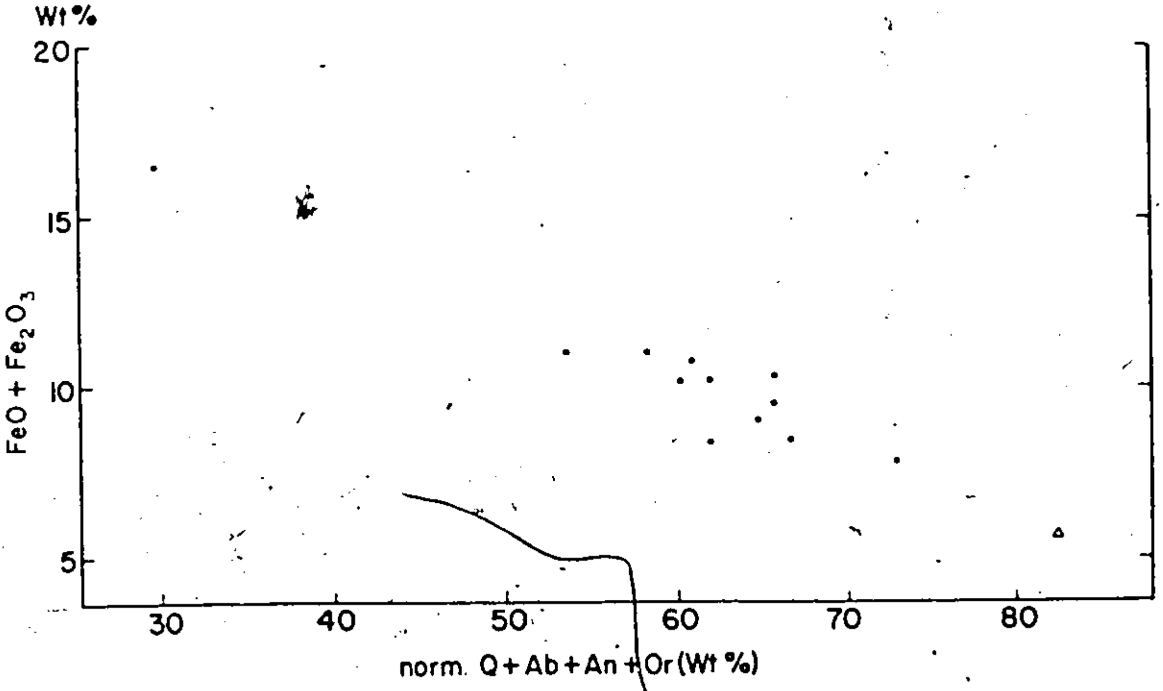
Wt%
20
15
10
5
FeO + Fe$_2$O$_3$
30
40
50
60
70
80
norm. Q+Ab+An+Or(Wt%)

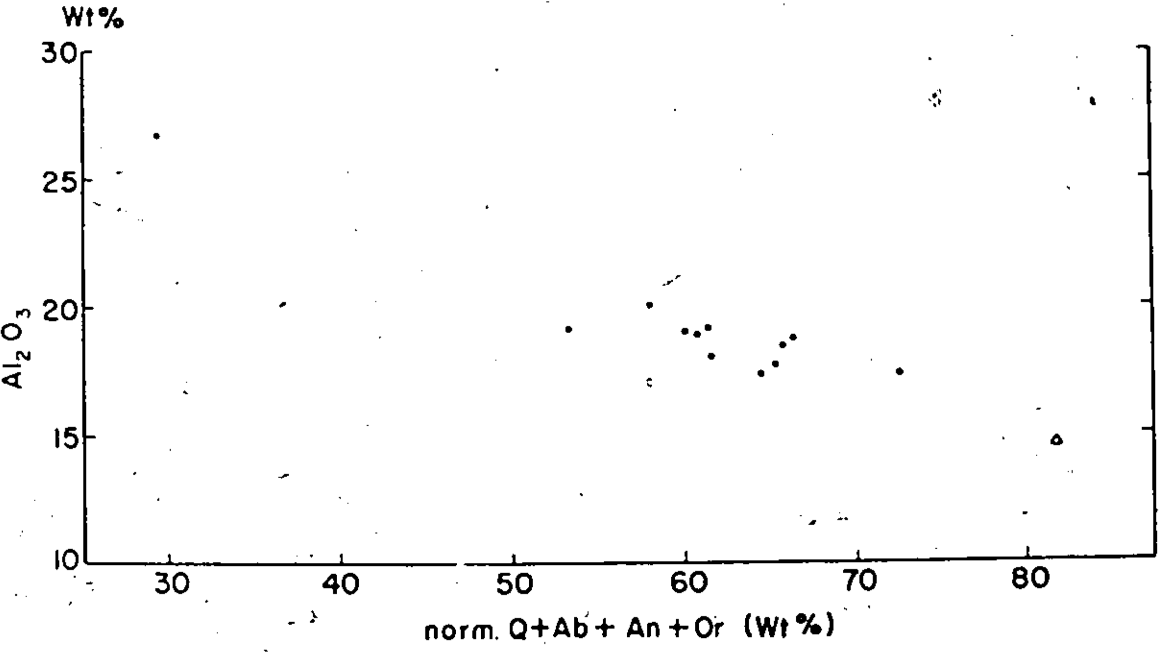
Wt%
30
25
20
15
10
Al$_2$O$_3$
30
40
50
60
70
80
norm. Q+Ab+An+Or (Wt%)

Figure 4.3.1

Figure 4.3.2 Variations of Na_2O (top), norm. (An/An+Ab) of plagioclase (centre) and ($FeO_{total}/FeO_{total}+MgO$) (bottom) as a function of norm. (Q+Ab+An+Or) in aluminous hornfelses relative to the average Apsley gneiss

● - aluminous hornfels

△ - average Apsley gneiss (Shaw, 1972)

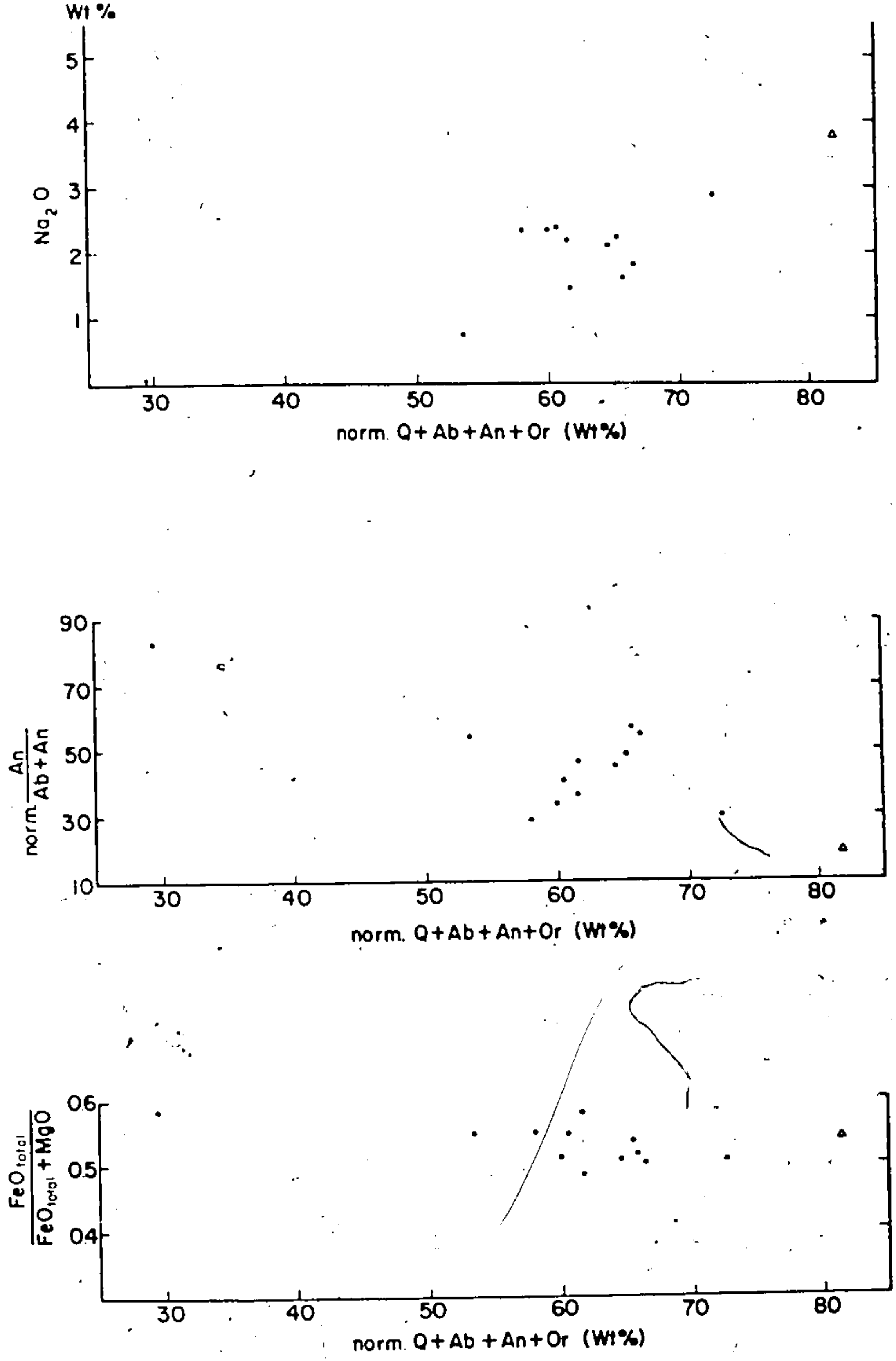
Wt %
5
4
3
2
1
Na_2O
30
40
50
60
70
80
norm. Q+Ab+An+Or (Wt%)
90
70
50
30
10
norm $\frac{An}{Ab+An}$
30
40
50
60
70
80
norm. Q+Ab+An+Or (Wt%)
0.6
0.5
0.4
$\frac{FeO_{total}}{FeO_{total}+MgO}$
30
40
50
60
70
80
norm. Q+Ab+An+Or (Wt%)

Figure 4.3.2

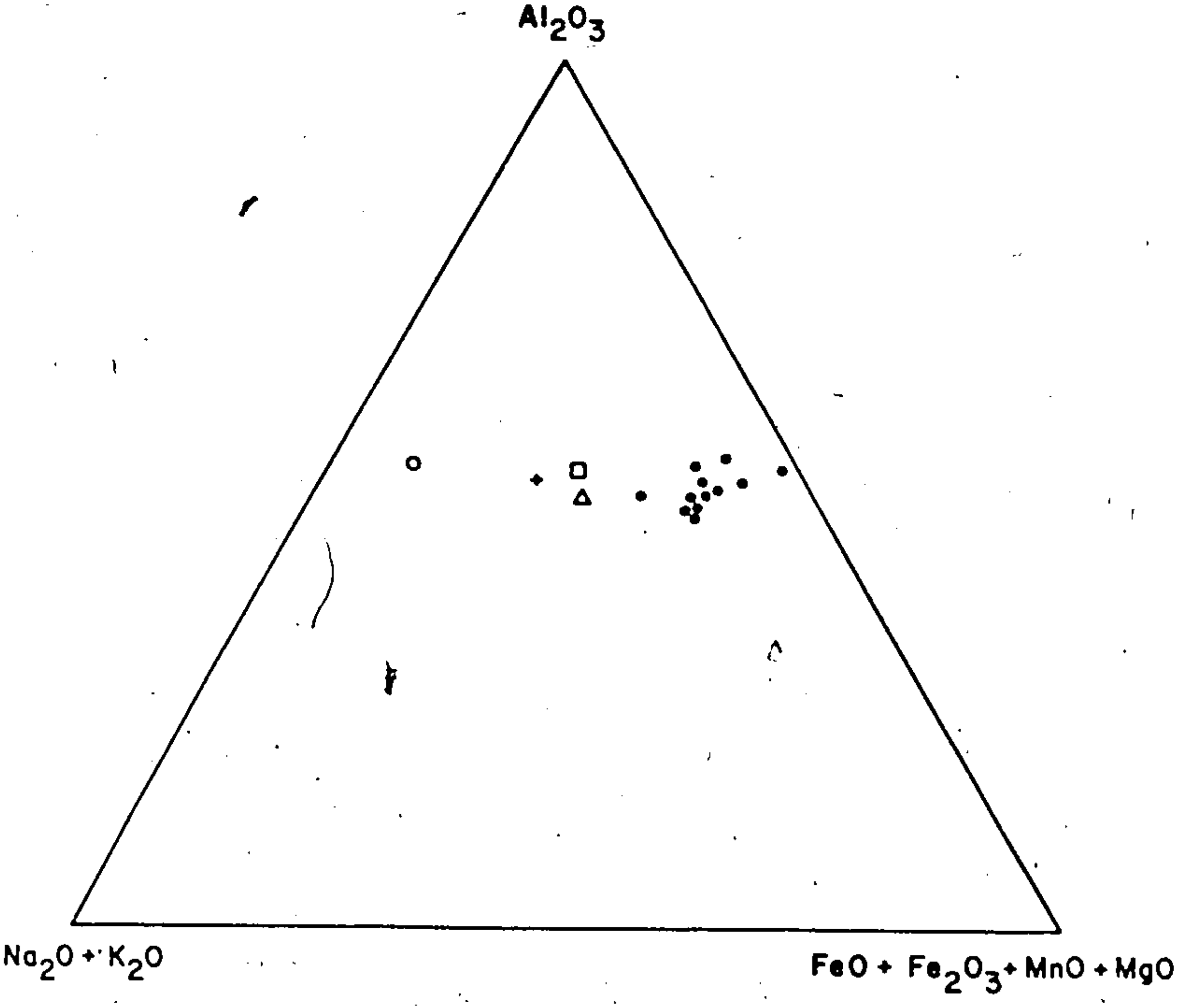

Figure 4.3.3

Triangular diagram $(Na_2O + K_2O)$-Al_2O_3-$(FeO + Fe_2O_3 + MnO + MgO)$ showing the variation of these oxides in biotite gneisses, aluminous hornfelses and leucogranite 259.

△ - average Apsley gneiss (Shaw, 1972)

□ - Na-type of Apsley gneiss (Simony, 1960)

+ - K-type of Apsley gneiss (Simony, 1960)

● - aluminous hornfels

○ - leucogranite 259

granitic portion from a parent rock such as the Apsley gneiss would leave a residue corresponding to aluminous gneisses.

To evaluate this model quantitatively and to estimate the amount of removed material, a petrological least-squares mixing computer program developed by Bryan et al. (1969) was used. The possibility that the Apsley biotite gneiss and aluminous hornfelses are parent-residuum pairs with granitic rocks representing the extracted material is tested in Table 4.3.1. The composition of aluminous hornfels 711-18 (assumed residuum) and leucogranite 259 (assumed extracted material) from the close vicinity of hornfels 711-18 were "mixed" together (taken as independent variables) while Shaw's (1972) average composition of the Apsley gneiss (assumed parent) was treated as the material to be synthesized. Rock compositions used for this least-square "mixing" and the computer generated composition compared to the actual composition of the Apsley gneiss are given in Table 4.3.1 together with the standard deviations for the average of the Apsley gneiss given by Shaw (1972), weight fractions of the "mixed" components and the sum of the squares of oxide residuals. Except for sodium, the calculated composition of the gneiss is close to the average composition given by Shaw (1972). But the content of sodium in the Apsley gneiss is variable (c.f. Simony, 1960 - Na-type and ~~K~~-type of Apsley gneiss) and its calculated content is not very different from the average sodium concentration of the K-type of gneiss (Na_2O = 2.80 wt.%) given by Simony (1960).

Table 4.3.1 Least-square solution for bulk chemical relations between Apsley gneiss, aluminous hornfels and leucogranite

	1	2	3	4	5	6
SiO_2	77.79	57.90	66.50	66.50	6.0	0.00
TiO_2	0.15	0.70	0.42	0.64	0.25	0.22
Al_2O_3	11.59	18.70	14.92	14.60	1.8	-0.32
FeO total	1.64	8.26	4.90	5.45	2.0	0.55
MnO	0.01	0.13	0.07	0.10	0.059	0.03
MgO	0.06	4.17	2.10	2.20	1.3	0.10
CaO	0.21	4.01	2.10	1.90	1.0	-0.20
Na_2O	3.36	1.81	2.53	3.80	1.2	-1.27
K_2O	5.00	1.85	3.34	3.10	1.6	-0.24
P_2O_5	0.00	0.21	0.10	0.17	0.08	0.07

Column 1 gives the chemical composition of leucogranite (259)

Column 2 is the composition of aluminous hornfels (711-18).

Column 3 represents computer generated oxide weight percentages of gneiss obtained from "mixing" of granite (column 1) and aluminous hornfels (column 2) in proportions given below[1].

Column 4 gives the actual average composition of the Apsley biotite gneiss. (Shaw, 1972).

Column 5 lists the standard deviation for column 4. (Shaw, 1972).

Column 6 is the difference between the actual composition of the Apsley gneiss (column 4) and the calculated composition (column 3).

[1] Weight fractions of granite (259) and aluminous gneiss (711-18) needed to generate the oxide weight percentages in column 3

leucogranite (259)	0.485
aluminous gneiss (711-18)	0.497
Sum of squares of oxide residuals	2.18

These data confirm that the aluminous gneisses could have been generated by a simple subtraction of granitic material from the biotite gneiss.

Regarding leucogranite 259, its position in the low temperature regions of the synthetic granitic system (Figures 6.1.2-3) is also compatible with a partial melting origin of this rock. It is of interest that on a Q-Ab-Or diagram (Figure 6.1.2), leucogranite 259 plots close to the "ternary minimum" but outside the cluster of quartz monzonitic rocks from the pluton. The position of the normative composition of leucogranite 259 in the system Ab-An-Or-Q-H_2O is, however, also, consistent with the process of fractional crystallization of a more basic magma. But there is some evidence that a partial melting process has taken place in the formation of leucocratic veins closely associated with aluminous gneisses. In a few places, plagioclase from migmatites shows inverse zoning suggesting partial melting, in situ, during which the progressively more anorthite-rich material was available (Mehnert, 1963, 1968). Even if this petrographic feature was not observed in granite 259, its close association with migmatites and aluminous gneisses further indicates that this rock was formed by partial melting of the Apsley gneiss.

It appears, however, that apart from the leucocratic granitic veins, which are interspersed with aluminous gneisses, the majority of granitic rocks in the pluton were not generated by a partial melting of the Apsley gneiss or at least not from the type which is now exposed in the wider vicinity of the pluton (see below).

The hypothesis that the aluminous gneisses in the contact aureole represent an isochemically metamorphosed shale is possible but not very probable. Sedimentary rocks with very similar major element compositions certainly can be found. But the extensive occurrences of these gneisses in the contact aureole, while similar rocks are very seldom encountered in the Apsley region, argue against this origin, as do the chemical and mineralogical variations of these rocks which indicate that the residual character is most pronounced in the xenoliths and rocks close to the contact.

This hypothesis can also be evaluated by the distribution of the rare-earth elements (REE) in these rocks. Figures 4.3.4-6 show the REE distributions of aluminous and biotite gneisses represented by means of Coryell-Masuda plots (Coryell et al., 1963), in which REE concentrations of samples are divided element by element by the chondrite average of Frey et al. (1968) and plotted against REE atomic numbers. (The REE abundances are listed in Appendix 1, while the precision and accuracy of the REE analyses are given together with an outline of analytical procedure for their determination in Appendix 2. The precision of REE analyses is also shown graphically in the Coryell-Masuda plot by error-bars in Figure A.2.1).

Haskin et al. (1966, 1968a) have shown that sedimentary and metasedimentary rocks have REE patterns similar to the average North American shale. The REE distribution patterns of the Apsley gneisses resemble that of North American shale although their absolute contents of the light rare-earths are slightly lower (Figure 4.3.4). On the other hand, the aluminous gneisses are depleted in the light REE with respect to heavy ones, and have variable negative Eu anomalies (Figure 4.3.5). Both these features of aluminous gneisses suggest that these rocks do not represent isochemically metamorphosed shale.

With regard to the aluminous gneisses, it is of interest that the depletion of light REE and the size of the negative Eu anomaly is most pronounced in the inclusion of aluminous hornfels (67) from the monzonitic core of the pluton, which virtually lacks any feldspars. Also, garnet which appears to dominate REE patterns of the aluminous rocks has a pronounced negative Eu anomaly (Figure 4.3.5) contrary to reported REE distributions for garnet (Haskin et al., 1966; Masuda, 1967; Herrmann, 1970). This indicates that garnet was formed from a source material which was already depleted not only in light REE but also in Eu. Since the only common minerals with positive Eu anomalies are feldspars, which also have REE patterns progressively decreasing toward the heavy REE (i.e. complementary to garnet), the Eu depletion suggests that the aluminous gneisses are residuum after the extraction of feldspar-rich fractions.

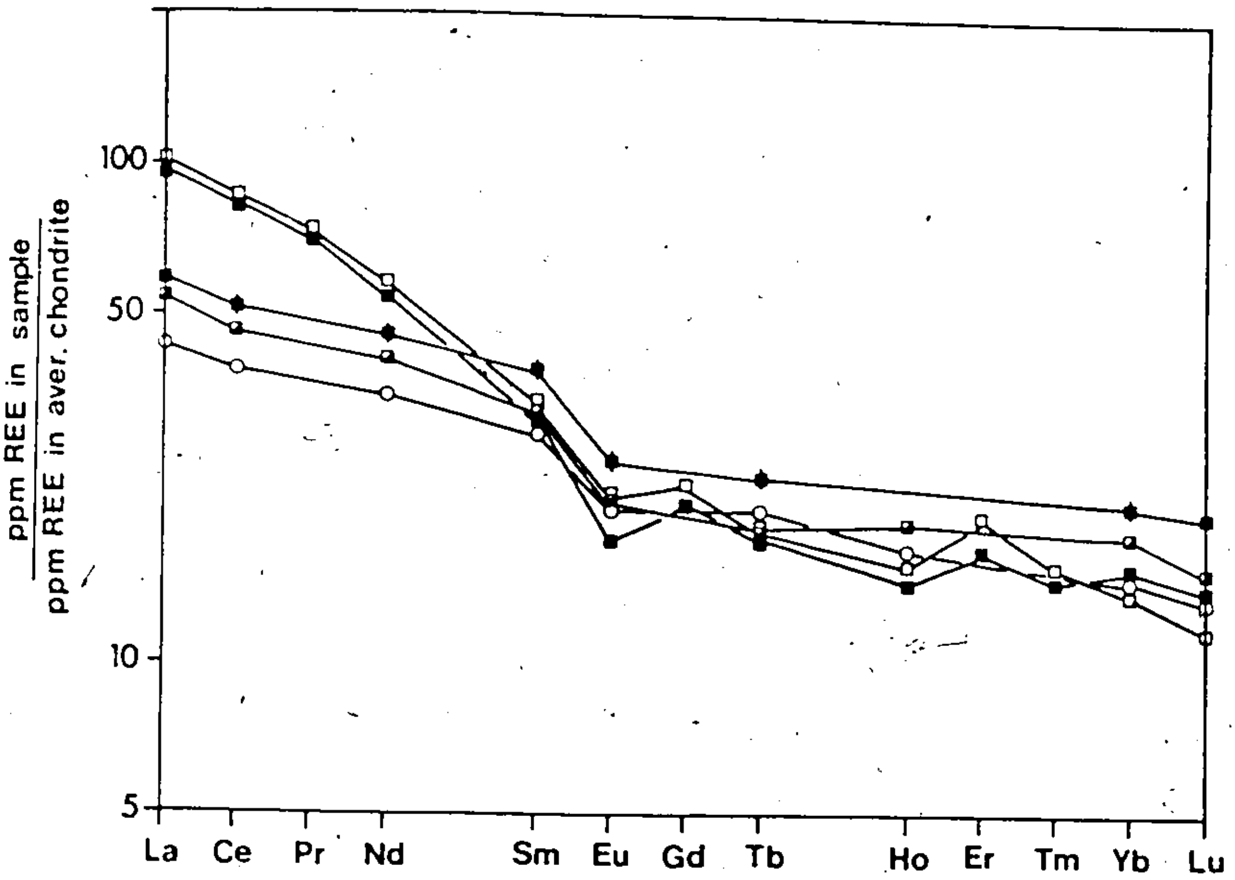

Figure 4.3.4 REE distribution in Apsley biotite gneisses and the averages of North American shales

○ - biotite gneiss 711-2

◪ - biotite gneiss 712-1

▮ - biotite gneiss 173

■ - composite of North American shale (Haskin et al., 1968a)

□ - composite of metamorphosed North American shales (Haskin et al., 1968a)

Figure 4.3.5 REE distribution in aluminous hornfelses, garnet 67 and the averages of North American shales

○ - aluminous hornfels 712-4
● - aluminous hornfels 711-8
◪ - aluminous hornfels 67
⧯ - garnet from aluminous hornfels 67
■ - composite of North American shales (Haskin et al., 1968a)
□ - composite of metamorphosed North American shales (Haskin et al., 1968a)

Figure 4.3.6 REE distribution in Apsley biotite gneisses, aluminous hornfelses and leucogranite 259

▲ - biotite gneiss 173
□ - biotite gneiss 711-2
○ - biotite gneiss 712-1
■ - aluminous hornfels 712-4
◇ - aluminous hornfels 711-18
⧯ - leucogranite 259

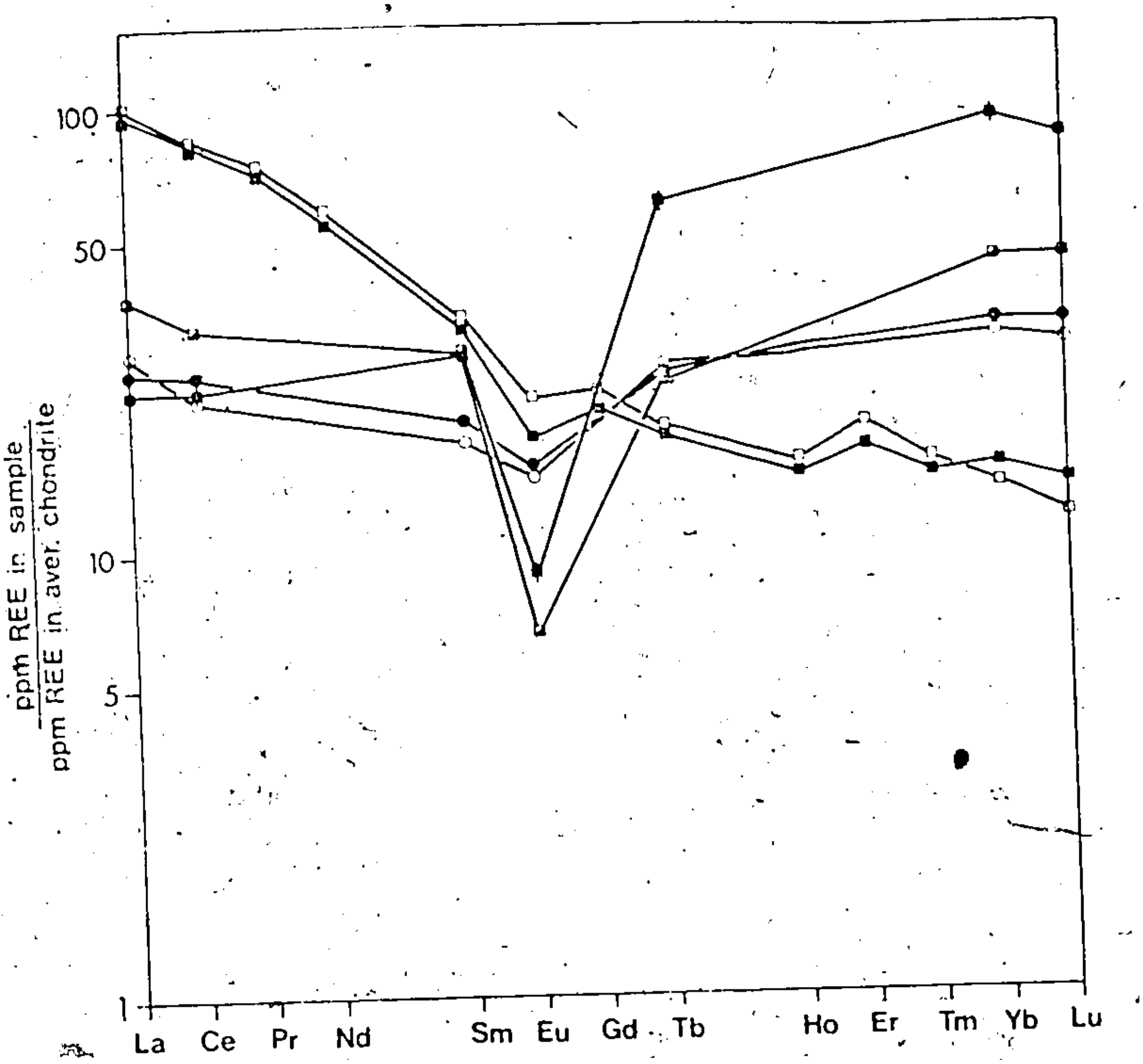
ppm REE in sample / ppm REE in aver. chondrite
100
50
10
5
1
La
Ce
Pr
Nd
Sm
Eu
Gd
Tb
Ho
Er
Tm
Yb
Lu

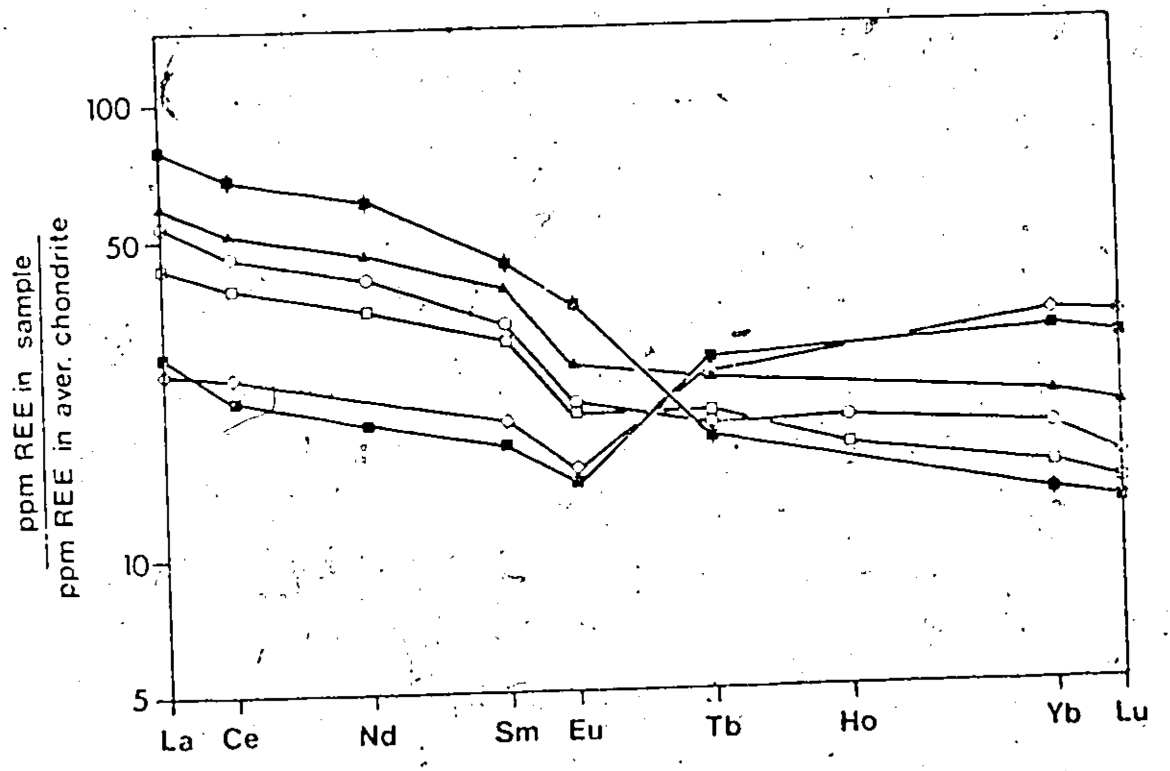
ppm REE in sample / ppm REE in aver. chondrite
100
50
10
5
La
Ce
Nd
Sm
Eu
Tb
Ho
Yb
Lu

Figure 4.3.6 shows the REE patterns of the Apsley biotite gneiss together with those of aluminous gneisses and leucogranite 259. The latter two rock types were considered above as products of anatexis. The pattern of granite is complementary to that of aluminous gneiss with respect to the Apsley gneiss, once again suggesting that aluminous gneisses may indeed represent the residuum after partial melting of the Apsley gneiss.

The REE distribution pattern of leucogranite 259 without any negative Eu anomaly does not indicate the extensive crystal fractionation, which would be expected if this rock was produced by differentiation of a more basic magma. As will be shown later, the REE pattern of granite 259 is less fractionated than those of quartz monzonite, which forms the outer zone of the pluton. It is also of interest that the REE distribution of leucogranite markedly differs from those of aplites (Balashov, 1963; Condie and Lo, 1971) which either show enrichment in the heavy REE as observed in the Susamyr batholith (Balashov, 1963) or large absolute depletion of REE as reported from the Louis Lake batholith (Condie and Lo, 1971).

4.3.2 Mafic Hornfelses

These rocks occur particularly along the southern margin of the pluton and also frequently as isolated inclusions within it. The mafic hornfelses are massive, laminated in places, usually dark gray and fine to medium-grained with hornfelsic granoblastic texture. On the geological map (Map 1) the outer contact of the aureole (map unit 6a) was drawn where calcareous gneisses and amphibolites give way to fine to medium-grained recrystallized massive hornfels with a distinct granoblastic texture (i.e. the outer contact represents textural changes). The border between regional metamorphic rocks and the contact aureole is not sharp; the gradational transition can be traced over a distance of several tens of meters. Toward the outside of the aureole, the hornfelses become slightly schistose with biotite and hornblende preferentially oriented.

Shaw (1962) and Chiang (1965) have subdivided the mafic hornfelses into two groups - hornblende and pyroxene hornfelses. Hornblende hornfelses (map unit 6a) embrace the large majority of mafic hornfelses. Their typical prograde mineral assemblages are: hornblende-biotite-plagioclase-quartz, and diopsidic clinopyroxene-hornblende-biotite-plagioclase-quartz. In places, the hornblende hornfels contains varying, sometimes even major amounts of scapolite, K-feldspar and carbonate. Plagioclase in the form of small equidimensional grains, has a composition of mostly andesine or calcic oligoclase (An 25-40). The common accessory minerals are sphene, magnetite and apatite. The ACKF diagram for some typical prograde assemblages is shown in Figure 4.3.7 and modal analyses of some representative samples are given in Table 4.3.2. The mineral assemblages of these hornfelses resemble those of

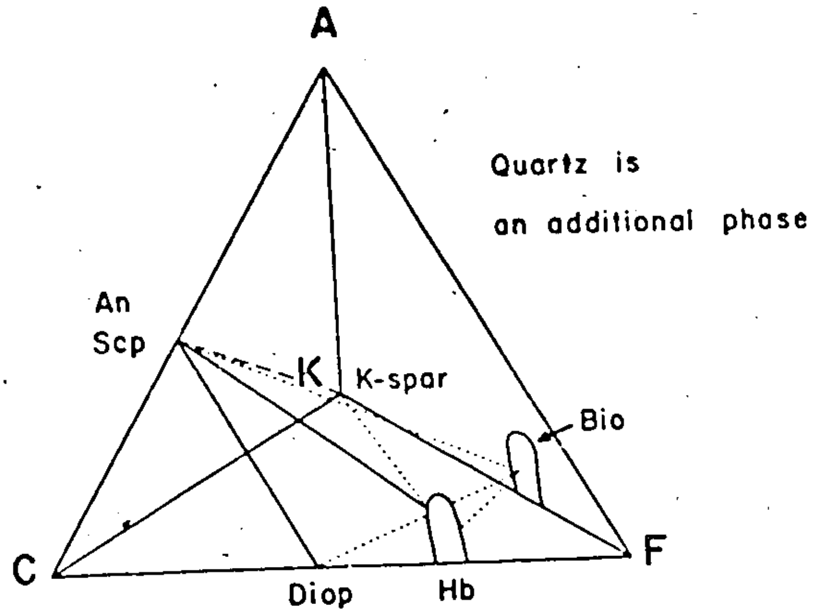
A
Quartz is
an additional phase
An
Scp
K
K-spar
Bio
C
F
Diop
Hb

Fig. 4.3.7. ACKF Diagram for Mafic (Hornblende) Hornfelses

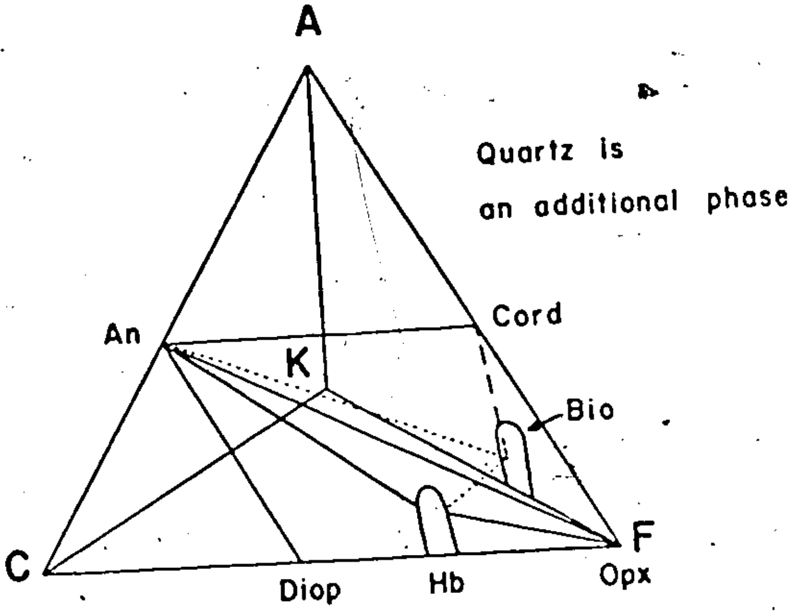
A
Quartz is
an additional phase
Cord
An
K
Bio
C
F
Diop
Hb
Opx

Fig. 4.3.8. ACKF Diagram for Mafic (Pyroxene) Hornfelses

Tie lines on the front face of the tetrahedron are shown by solid lines, those on the three back faces by dashed lines, and those within the volume by dotted lines.

Table 4.3.2 Modal composition of mafic hornfelses and contact metamorphosed marbles

	1	2	3	4	5	6	7
Quartz	9.0	24.2	9.6				
Plagioclase	35.8	39.2	48.6				
Biotite/phlogopite	20.8	2.7	7.0	9.3	5.0	9.8	
Clinoamphibolite	33.5	31.3	34.3	0.5	tr	4.0	
Clinopyroxene					0.5		
Calcite				89.0	92.1	78.1	83.5
Dolomite						5.2	
Chondrite							13.7
Forsterite							tr
Serpentine							tr
Spinel							1.2
Sphene	0.4	0.6	tr		tr	tr	
Apatite	tr					tr	
Epidote		0.9	tr				
Opaque	tr	1.2	tr	1.2	2.0	2.5	1.5
% An in plagioclase	30	38	38				

1.	Hornblende hornfels	145
2.	Hornblende hornfels	786
3.	Hornblende hornfels	121
4.	Contact metamorphosed marble	143-9
5.	Contact metamorphosed marble	86
6.	Contact metamorphosed marble	181-4
7.	Contact metamorphosed marble	233

regionally metamorphosed amphibolites and calcareous gneisses. As noted earlier, the main difference between them is the texture.

Pyroxene hornfelses, which have been mapped at the appearance of hypersthene in the mafic hornfelses, occur in the study area only as inclusions in the pluton (map unit 6b). These are composed mainly of hypersthenic orthopyroxene, diopsidic clinopyroxene, hornblende, biotite, quartz and plagioclase with a composition corresponding to andesine or labradorite (An 35-55). Cordierite is also occasionally present. Magnetite and sphene are frequent accessories. The ACKF diagram for these rocks is given in Figure 4.3.8. As Chiang (1965) has already pointed out, hornblende is present both as a prograde and as a retrograde phase. In places, orthopyroxene and occasionally also clinopyroxene have been altered to uralitic hornblende with some magnetite. Prograde hornblende differs not only texturally but also optically from retrograde hornblende. It has a typical greenish-tan colour and does not show any reaction relations with the coexisting hypersthene and diopside.

4.3.3 Contact Metamorphosed Marble

In the contact aureole, marble occurs only rarely as inclusions in the pluton and as isolated lenses in the gneisses, particularly along the northern margin of the pluton. The southernmost part of the Owenbrook marble formation also lies within the aureole (c.f. Shaw, 1962). Because of the difficulties in distinguishing between regional and contact metamorphosed marble in the field, these two rock types were not mapped separately (cf. Map 1).

Marbles are usually white, medium to coarse-grained with poor foliation, occasionally intercalated with calc-silicate rocks. Two metamorphic zones have been recognized. The first "outer" zone comprises the marble lenses in the aureole, several inclusions close to the margin of the pluton and the forementioned section of the Owenbrook marble. The second "inner" zone is represented by the inclusions occurring well inside the pluton. The mineral assemblages of marble in the first "outer" zone are very similar to those of the regional metamorphosed ones. The assemblages diopside-calcite and clinoamphibole (usually pargasite)-calcite are common and phlogopite is generally present. The marble of the second "inner" zone contains apart from calcite, dolomite, phlogopite, diopside and pargasite, also chondrodite and spinel. In places, forsterite, partially altered to serpentine is also present.

The CaO-MgO-SiO_2 compatibility diagram for these rocks from the "inner" zone is shown in Figure 4.3.9. The modal composition of some representative samples of contact metamorphosed marble is given in Table 4.3.2.

4.3.4 Conditions of Contact Metamorphism

In the aureole of the pluton were recognized two

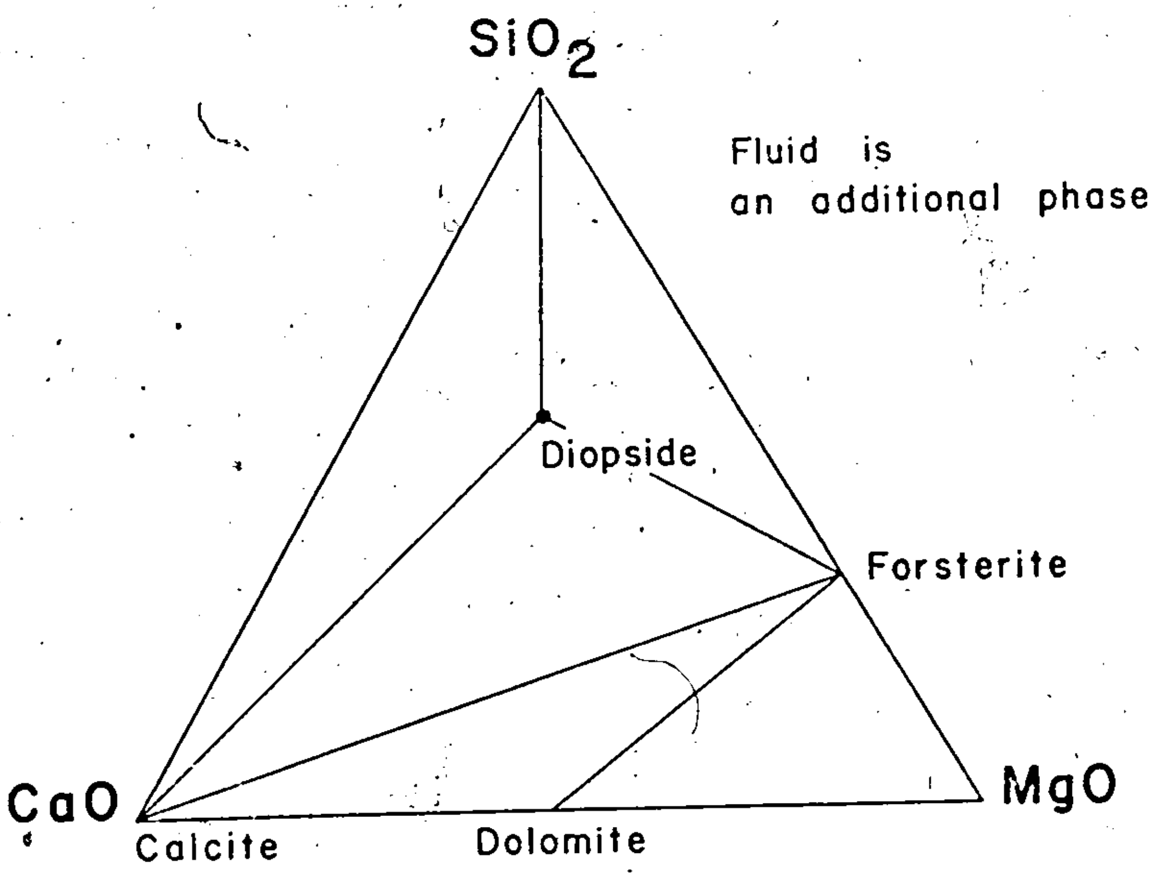
SiO_2
Fluid is
an additional phase
Diopside
Forsterite
CaO
Calcite
Dolomite
MgO

Fig. 4.3.9. $CaO-MgO-SiO_2$ Diagram for Contact Metamorphosed Marbles (Inner Zone) contact metamorphic facies - pyroxene hornfels and hornblende hornfels (Shaw, 1962; Chiang, 1965). The pyroxene hornfels facies rocks include mafic (pyroxene) hornfelses, some of the aluminous hornfelses and probably also marbles from the "inner" zone. These rocks have been encountered mainly as inclusions in the pluton, particularly at the monzonitic core. The characteristic prograde mineral assemblages of pyroxene hornfels facies rocks are:

orthopyroxene-biotite-plagioclase-quartz;
orthopyroxene-hornblende-biotite-plagioclase-quartz;
orthopyroxene-hornblende-biotite-cordierite-plagioclase-quartz;
orthopyroxene-clinopyroxene-plagioclase-quartz;
garnet-sillimanite-cordierite-biotite-plagioclase-quartz.

The hornblende hornfels facies rocks comprise mafic (hornblende) hornfelses, marbles from the "outer" zone and some aluminous hornfelses. These rocks occur mainly around the margin of the pluton.

Because of the complicated nature of the contact aureole, the sole purpose here is to estimate the physical conditions of contact metamorphism.

All major mineral phases in contact metamorphosed rocks appear to represent the prograde assemblages. As in the regional metamorphosed rocks, however, the retrograde phases (chlorite, epidote, clinozoisite, sericite, uralitic hornblende, carbonate etc.) are present in places, indicating a later retrogressive metamorphism of the greenschist facies. But these retrograde phases do not obliterate the prograde assemblages in spite of the fact that they developed from them. Disregarding the retrograde phases, however, the petrography, adherence of mineral assemblages to the phase rule and the distribution of elements among phases (Chiang, 1965) suggest that an approach to at least local equilibrium was achieved during the contact metamorphism in most samples studied. If it is assumed that the prograde mineral assemblages of contact metamorphosed rocks were formed at equilibrium, then the physical conditions of metamorphism can be tentatively estimated. The relevant experimental data are plotted in Figure 4.3.10.

The absence of prograde muscovite indicates a temperature above the second sillimanite isograd (curve 1, Figure 4.3.10 representing the breakdown of muscovite in the presence of quartz). This reaction would probably provide the minimum temperature estimate for contact metamorphism. An upper temperature limit is defined by the assemblage biotite-quartz. Luth (1967) has reported that the association phlogopite-quartz is not stable above about 815°C (curve 2). The addition of iron to the system will only lower the temperature (Wones, 1963) and thus this curve probably represents the maximum limit.

Considering the pyroxene hornfels facies, the lower temperature limit for these rocks is given by the reactions

Figure 4.3.10. P-T graph of experimental data pertaining to the conditions of contact metamorphism

Curve 1. Muscovite + quartz $\rightleftharpoons$ K-feldspar + Al_2O_5 + vapour
(Althaus et al., 1970)

2. Maximum stability of assemblage phlogopite + quartz
(Luth, 1967)

3. Gedrite + quartz $\rightleftharpoons$ hypersthene + cordierite + vapour
(Akella and Winkler, 1966)

4. Anthophyllite + hornblende$_{(1)}$ $\rightleftharpoons$ orthopyroxene +
anorthite + hornblende$_{(2)}$ + vapour
(Choudhuri and Winkler, 1967)

5. Calculated lower stability limit of assemblage
hypersthene + cordierite.
(Hess, 1969)

6. Almandine + sillimanite + quartz $\rightleftharpoons$ Fe-cordierite
(Richardson, 1968)

7. Beginning of anatexis in plagioclase-bearing
gneisses (An 0)
(Winkler, 1970)

8. Beginning of anatexis in plagioclase-bearing
gneisses (An 26)
(Winkler, 1970)

9. Eutectic melting curve in the system K-feldspar-
quartz-H_2O
(Shaw, 1963; Winkler, 1970)

10. Fe-staurolite + quartz $\rightleftharpoons$ almandine + sillimanite
+ vapour
(Richardson, 1968)

11. Re-staurolite + almandine + quartz $\rightleftharpoons$ cordierite
+ vapour
(Richardson, 1968)

12. Fe-staurolite + quartz $\rightleftharpoons$ Fe-cordierite + sillimanite
+ vapour
(Richardson, 1968)

13. Stability fields of the polymorphs of Al_2SiO_5
(Richardson et al., 1969)

14. Stability fields of the polymorphs of Al_2SiO_5
(Althaus, 1967, 1969)

15. Upper stability limit of hornblende in orthopyroxene
subfacies
(Choudhuri and Winkler, 1967; Winkler, 1967)

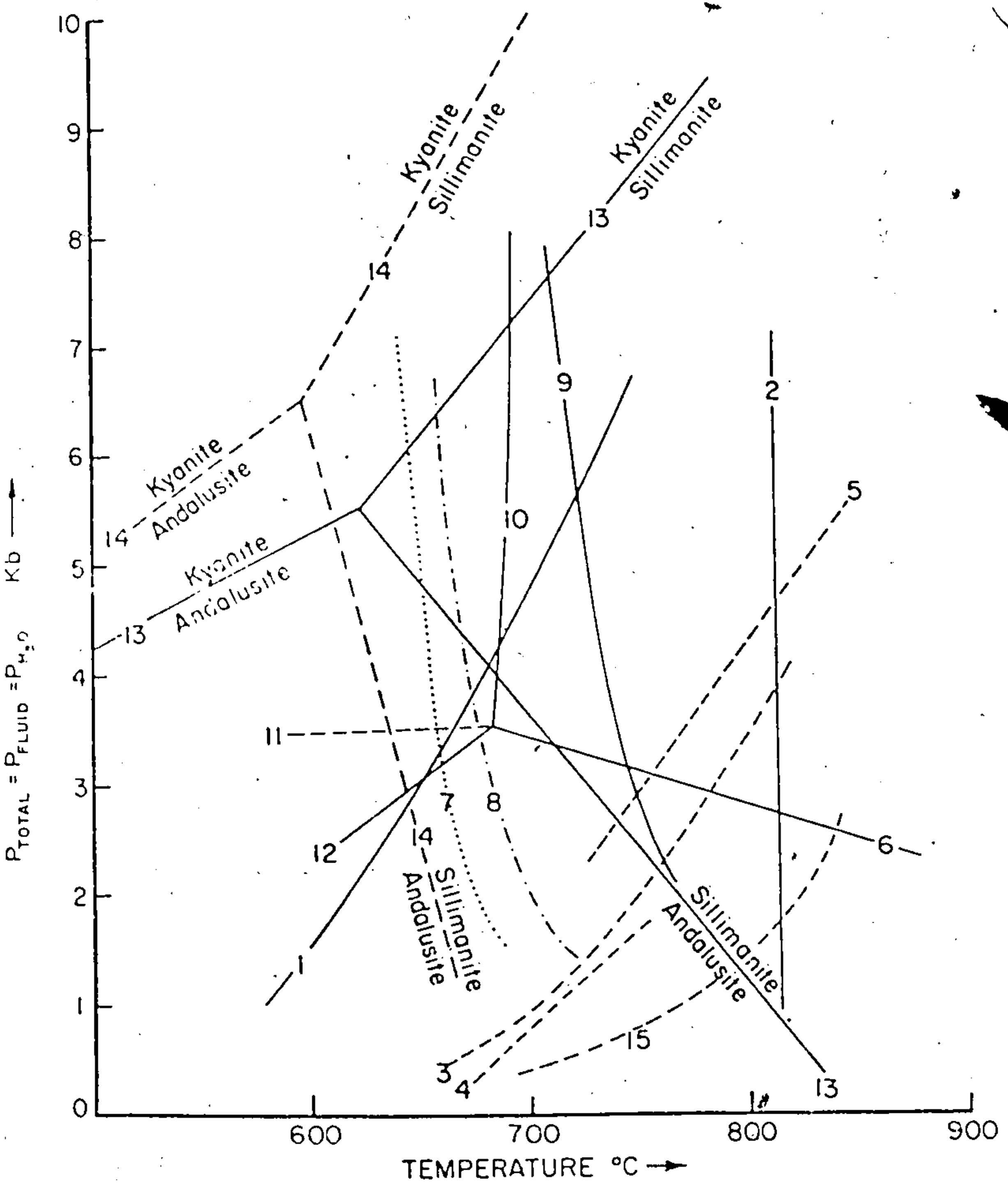
Kyanite
Sillimanite
14
Kyanite
Sillimanite
13
Kyanite
Andalusite
14
Kyanite
Andalusite
13
9
2
10
5
11
12
7
8
14
Sillimanite
Andalusite
1
6
Sillimanite
Andalusite
15
3
4
13
P_TOTAL = P_FLUID = P_H2O   Kb
0
1
2
3
4
5
6
7
8
9
10
600
700
800
900
TEMPERATURE °C

leading to the formation of orthopyroxene. Because of the incomplete thermal aureole, it is difficult to ascertain the orthopyroxene-generating reaction. Up to now, two reactions by which orthopyroxene is formed have been experimentally investigated. Akella and Winkler (1966) have studied the reaction {gedrite + quartz} $\rightleftharpoons$ {hypersthene + cordierite + H_2O} (curve 3, Figure 4.3.10), and Choudhuri and Winkler (1967) have investigated the reaction {anthophyllite + hornblende$_{(1)}$} $\rightleftharpoons$ {orthopyroxene + anorthite + hornblende$_{(2)}$ + H_2O} (curve 4). The breakdown of pure Mg-anthophyllite to enstatite, quartz and H_2O takes place at a higher temperature as determined by Greenwood (1963). Hess (1969) located a theoretically calculated curve (curve 5) for the stability of the association hypersthene-cordierite in natural assemblages at a somewhat higher pressure and lower temperature.

The assemblage cordierite-sillimanite-garnet-quartz provides an estimate of the lower pressure limit. Richardson (1968) has shown that this association is not stable below the reaction curve 6 in Figure 4.3.10 (Fe-cordierite $\rightleftharpoons$ {almandine + sillimanite + quartz}). The quartz-fayalite-magnetite buffer used by Richardson (1968) probably represents the lower limits of oxygen fugacity encountered in the common metamorphic rocks. However, the addition of magnesium to the system raises the curve with respect to pressure (Richardson, 1968). Therefore, the location of this reaction curve is probably ~~a~~ reasonable estimate of the lower pressure limit. Hence, Figure 4.3.10 suggests that the contact metamorphic conditions for the pyroxene hornfels facies rocks fall within a temperature range of about 750° to 820°C and a pressure range of about 2.5 to 4 kb (assuming $P_{total} = P_{H_2O}$ and that the experimentally determined equilibrium curves are pertinent - e.g. Mueller, 1966 - and are not grossly in error).

For hornblende hornfels facies rocks, as noted earlier, the lower temperature limit is probably given by the reaction curve for the breakdown of muscovite and quartz (curve 1 in Figure 4.3.10) and the lower pressure estimate by the stability of the almandine-sillimanite-cordierite-quartz assemblage (curve 6).

All these estimates, however, probably represent the upper limits since if $P_{H_2O} < P_{total}$, it may be expected to lower the estimated temperature. Thus, according to Winkler's (1967) classification of contact metamorphism, the aureole of the Loon Lake pluton belongs to the K-feldspar-cordierite-hornfels facies of which the lower temperature limit is given by the instability of the association muscovite-quartz.

Figure 4.3.10 shows that a large portion of the field of estimated physical conditions of contact metamorphism lies well above the curves for the beginning of anatexis in rocks with plagioclase composition corresponding to those of the Apsley biotite gneiss (curves 7 and 8). If this is so, then it suggests that the contact metamorphism was accompanied by partial melting of at least some rocks of appropriate composition. This fact further supports the hypotheses that aluminous gneisses in the contact aureole of the pluton represent the residue after partial melting of biotite gneiss, as discussed earlier.

If the estimation of the conditions of contact metamorphism is correct, then water pressure as high as 2.5-4 kb would correspond to a depth of about 10 km and more, which is rather deep compared with a normal shallow-seated contact aureole. There are several other indications, however, which support this pressure estimation. The coexistence of prograde hornblende with orthopyroxene suggests a higher pressure. Winkler has pointed out that "the hornblende-free orthopyroxene subfacies results at low and the orthopyroxene-hornblende subfacies at relatively high H_2O pressure, even though the temperature is approximately the same in both cases" (1967, p.124). He has estimated the water pressure for the orthopyroxene-hornblende subfacies to be around 3-3.5 kb.

Several attempts have been made recently to estimate the pressure conditions of metamorphism by the partitioning of iron and magnesium between garnet and cordierite pairs (e.g. Okrush, 1971; Currie, 1971; Hensen and Green, 1971). The diagram of Okrush (1971) and the experimentally determined graph of Hensen and Green (1971) have been used for a rough estimation of the pressure. Both these estimates indicate pressure well above 3 kb water pressure.

For an independent estimation of the temperature, the composition of Mg-Calcite coexisting with dolomite from two marble inclusions has been determined. The calcites have been analyzed by the method of Jennings and Mitchell (1969) and the temperature was estimated from the data of Goldsmith and Newton (1969). The results are given in Table 4.3.3. The temperature obtained is relatively close to those estimated from Figure 4.3.10, considering that the carbonate geothermometer represents only the minimum quench temperature (Jennings, 1969). Likewise, if the aluminous hornfelses were indeed desilicated and dealkalized by

Table 4.3.3 Composition of Mg-calcite from contact metamorphosed marbles and estimated temperature from the calcite-dolomite solvus

Sample	Mol. % $MgCO_3$	Temp. °C
199	12.02	730
233	9.11	660

Determinations carried out according to the method of Jennings and Mitchell (1969). Both samples are from inclusions from the monzonite core of the pluton.

a partial melting process, then the estimated temperature of about 700-820°C seems reasonable.

The inferred physical conditions of contact metamorphism, particularly the pressures, are rather high. According to Turner (1968), these rocks already represent a transition to granulite facies rocks, and according to Hietanen (1967) they correspond to cordierite-granulite facies. Indeed, the mineral assemblages of the contact aureole resemble those above Lumbers' (1967a,b) orthopyroxene-forsterite-chondrodite isograd of regional metamorphism in the northwestern part of the Bancroft-Madoc area, which are characterized by the presence of hypersthene in mafic rocks, forsterite and chondrodite in marbles and the disappearance of muscovite in sillimanite-bearing rocks (c.f. Figure 2.2). These regional metamorphosed rocks have been assigned by Lumbers (1967a,b) to the highest part of the amphibolite facies or to the transition between the upper amphibolite and granulite facies. Keeping in mind that the regional metamorphism in the Bancroft-Madoc area is thought to correspond to the low-pressure intermediate type metamorphism of Miyashiro (1961) then "a low-pressure regional dynamothermal metamorphism may as well represent a contact metamorphic facies series that has come into existence at a greater depth than the classical shallow contact metamorphic hornfels facies series" (Winkler, 1967, p.123).

4.4 Retrogressive Metamorphism

In the study area, the regional and contact metamorphosed rocks have locally undergone the retrogressive metamorphism which produced minerals of the greenschist facies. The mineralogical changes of the regression include chloritization of ferromagnesian minerals, probably recrystallization of some mineral assemblages in a manner described by Jennings (1969) from the adjacent area, etc.

4.5 Structure

The structure of the Chandos area has been recently studied in detail by Saha (1957, 1959) and Shaw (1962). The results of the present investigation are in essential agreement with their findings and therefore this subject will be only briefly discussed.

In the general context of Lumbers' (1967a) tectonic division of the Bancroft-Madoc area, the Loon Lake pluton is situated on the southeast limb of the major synclinorium between the Harvey-Cardiff arch and the Kasshabog arch (Map 3).

The regional structure of Chandos Township is outlined in Figure 4.5.1. The prominent structural features of the region are two major sets of folds. The principal fold set trends generally northeast and is vaguely parallel to the synclinorium axis. It also extends roughly in the same direction

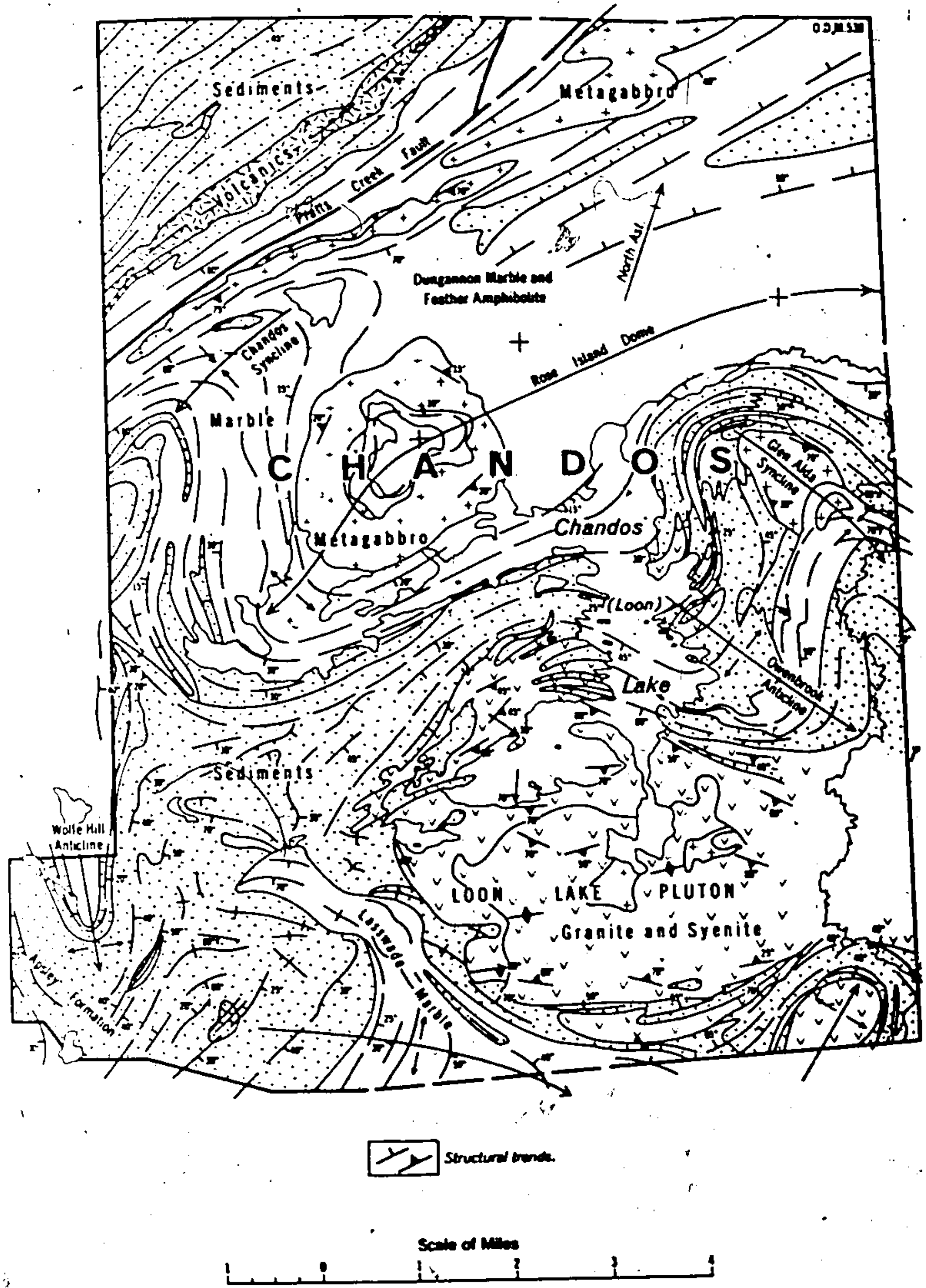
Sediments
Metagabbro
Volcanics
Prins Creek Fault
Dungannon Marble and
Feather Amphibolite
North Ax.
Chandos Syncline
Rose Island Dome
Marble
C H A N D O S
Glen Alda Syncline
Metagabbro
Chandos
(Loon)
Lake
Greenbrook Anticline
Sediments
Wolfe Hill Anticline
LOON LAKE PLUTON
Granite and Syenite
Lasswade Marble
Apsley Formation
Structural trends.
Scale of Miles
1
0
1
2
3
4

Figure 4.5.1 Structural Features of Chandos Township (after Shaw, 1962).

as the general regional trend of strikes and lithological discontinuities. The development of this fold trend is correlated with the metamorphic event dated at 1125±25 million years which also produced the regional metamorphism of amphibolite facies in this area (Shaw, 1962; Lumbers, 1967a; Jennings, 1969). These folds mostly dip southwest, but in the Apsley region some of them also dip northeast. The other set, composed of west to northwest trending cross-folds, is younger than that of the northeast trend and roughly perpendicular to it (Saha, 1957, 1959; Shaw, 1962). These successive foldings formed a number of poorly defined domes and basins in the area. This regional structural pattern has been complicated in the southern part of Chandos Township by the intrusion of the pluton, which caused complex and intense deformations of the surrounding rocks, particularly the marbles. These deformations also include cross-folding and crumpling, the intensity and frequency of which increase toward the contact.

Foliation, defined as a planar structure outlined by the parallel orientation of platy and lath-like minerals, is the prominent structural feature in most supracrustal rocks of the Apsley region. It is generally parallel with not only the compositional banding or lithological layering, but also the main lithological boundaries. Around the pluton, the foliation of the country rocks is predominantly parallel to the contact and usually dips toward the body. The amount of dip, however, increases as one approaches the pluton.

Lineation, including elongation of minerals (such as amphibole) and small crenulations in the foliation surface, is generally parallel to the axis of the fold in which it occurs.

Two major faults have been recognized in the study area (Map 1). The first one, with ENE trending (about N 60° E) is roughly parallel to the Pratts Creek fault and possibly controls the axis of South Bay of Chandos Lake. Its continuation on the east side of Chandos Lake was not detected; this may be due to very scarce outcrops in this swampy area. The second fault with NNW trending is possibly the continuation of the distinct lineament, which was detected north of Chandos Lake (e.g. Shaw, 1962; Lumbers, 1967a). The fault probably controls the major axis of Chandos Lake, trending N 30° W. This direction is also parallel to one of the main joint sets in the area.

In the southern part of the pluton was recognized a fault with NE trending, which is possibly only of local significance (Map 1). Faults cross-cut all rock types and are accompanied in places by shear zones. They appear to be roughly vertical. The nature and amount of displacement, however, is difficult to determine.

4.6 Summary

1. The vicinity of the Loon Lake pluton is composed of

three distinct lithological units of supracrustal rocks. In order of decreasing abundances, they are gneisses, marbles and amphibolites.

2. The prograde regional metamorphism in the Chandos region probably corresponds to "the low-pressure intermediate type amphibolite facies" of Miyashiro (1961) or "medium stage of metamorphism" of Winkler (1970).

3. Comparison of the natural mineral assemblages with experimentally determined mineral equilibria (assuming $P_{H_2O} = P_{total}$) suggest a temperature range of about 620-700°C and a pressure range of about 4.5-6.0 kb for this regional metamorphism.

4. The intrusion of the Loon Lake pluton superimposed contact metamorphism on these already regionally metamorphosed rocks.

5. The contact metamorphism in the aureole of the pluton probably corresponds to the K-feldspar-cordierite hornfels facies of Winkler (1967). The contact metamorphism, however, took place at a greater depth than the typical shallow-seated contact metamorphism.

6. Tentative estimation of the physical condition of contact metamorphism (assuming $P_{H_2O} = P_{total}$) indicates a maximum temperature range of about 750-820°C and a pressure range of about 2.5-4 kb. This estimated temperature is relatively close

to that derived from the coexisting calcite-dolomite pair.

7. The aluminous gneisses which are characterized by the presence of garnet and sillimanite and/or cordierite and occur in the contact aureole of the pluton, are probably a residuum after the extraction of granitic material from the Apsley biotite gneiss. Some leucogranitic rocks present in the contact aureole in association with aluminous gneisses probably represent such extracted granitic material.

8. The regional structural pattern, which is characterized by two major sets of folds, has been complicated in the southern part of Chandos Township by the intrusion of the pluton, which caused complex and intense deformations of the surrounding rocks.

CHAPTER 5

GEOLOGY AND PETROGRAPHY OF THE PLUTON

5.1 General Features of the Pluton

The Loon Lake pluton is a roughly ovoidal-shaped mass about 16 square miles in area, with an east-west diameter of about 5 miles and a north-south diameter of about 3.5 miles. About a third of this area, however, is covered by lake and swamps. All the eastern side of the pluton is covered by the Crowe River Swamp.

The pluton is a steeply dipping, zoned intrusion. The core of the pluton is formed by leucocratic monzonite, while the outer zone is composed mainly of quartz monzonite. Several elongated masses of basic rocks up to 500 m long occur as isolated bodies within the pluton, most of them in the central part. To a smaller extent, the basic bodies occur also on the periphery of the pluton (Map 1).

Apart from these three rock types, a conformable belt of granodioritic gneisses has been distinguished in the outer quartz monzonitic zone of the pluton (Map 1). This belt probably represents merely a septum or screen of partially assimilated and migmatized gneisses.

These four lithological units can usually be readily recognized in the field by their texture and mineral contents. In places, however, their distinctness is not so obvious and consequently, the borders between zones on Map 1 are locally somewhat arbitrary.

5.2 Structure

The intrusion is generally conformable with the surrounding rocks, but in places the relation is discordant, as indicated, for example, by the intersecting of the foliation of country rocks by the pluton. Cloos (1934) estimated that not more than 10-15% of the contact between the pluton and surrounding rocks would be discordant. It appears that the pluton is structurally independent of the regional pattern. The pluton has not been affected by the main events of regional deformation and metamorphism dated at 1125±25 million years (Silver and Lumbers, 1965; Lumbers, 1967a) nor is its shape related to the regional structural pattern. There is no continuation of the structures of the country rocks into the pluton. Furthermore, the regional structures are disrupted by the intrusion.

In the vicinity of the pluton, bands of marble show apparent forcing aside by the intrusion. Fold axes within these distorted metamorphic layers are approximately parallel to the contact. Also, axes of minor folds within gneisses are parallel to the contact and perpendicular to the lineation in the pluton. Somewhat more complicated is the western side of the pluton, where the structures within about 500 m from the contact become more complex toward the contact. But once again the trend parallel to contact prevails. Shaw (1962) suggested that the pluton warped the surrounding rocks into apparent conformity with its outline.

All these features together with the presence of rotated angular inclusions in the pluton and agmatitic structures suggest that the pluton is post-tectonic. It was forcefully injected, and it shouldered aside and in places refolded the walls (Shaw, 1962). But chilled zones against country rocks are absent.

Planar arrangement of hornblende and biotite, tabular crystals of feldspars and in places also the arrangement of the inclusions and schlieren in parallel planes produce foliation in the pluton. The rocks are distinctly foliated especially along the margin, but in the centre of the body, monzonite is usually massive and homogeneous with indistinct foliation. Foliation in the pluton has been interpreted by Saha (1957, 1959) and Shaw (1962) as primary flow foliation because of its concentric disposition, its sweep around inclusions, the rotation of inclusions, the post-tectonic character of the pluton, etc. Foliate structure is concentrically arranged roughly parallel with the contact. Generally, it dips steeply at angles of about

50-85° toward the centre of the body, suggesting that the pluton has the shape of an assymetric funnel with contacts and internal structures that dip inward. Lineation, including mineral aggregate streaks and elongation of minerals can be observed only rarely and mainly near the contact. In general, it is subparallel to the dips of foliation.

The rocks of the pluton are relatively well-jointed. The system of joints does not appear, however, to show clear relation to the other structures of the pluton and to the mechanics of intrusion (Cloos, 1934; Saha, 1957, 1959). The two most prominent sets of joints are roughly vertical. The first set has north-northeast trending, while the second has northwest trending. Both these joint sets are also prominent in the surrounding rocks. It appears that these joints were formed under regional stress. In places, the thin pegmatitic and leucogranitic veins conform to these directions.

5.3 Contact Relations

The pluton-country rock contact is relatively sharp in the southern and northeastern parts of the body where it touches calcareous gneiss and mafic hornfels. Although even there, the country rocks are migmatized to a varying degree in the form of veins and lenses of quartz-feldspathic material with a granitic to aplitic and pegmatitic appearance (Map 1).

The calcomagnesian gneisses and mafic hornfelses, even as inclusions, are usually only fragmented with abrupt contacts and without apparent alteration, indicating that migmatization in these rocks is possibly mainly of arteritic character. The degree of migmatization increases toward the contact.

On the western and northwestern side of the pluton, the contact is gradational with a zone of migmatites up to 500 m wide. This zone, in which the gneisses are intimately mixed with granitic rocks containing in places even ghost structures of assimilated rocks, has been described in detail by Shaw (1962). Once again, the proportion of granitic material increases toward the pluton. Some of these granitic rocks are the product of the partial melting of gneisses more or less in situ, as has been suggested earlier (c.f. section 4.3). In places, however, there is evidence that the generation of some migmatitic rocks in the contact aureole was accompanied by the injections of granitic material from the pluton. Thus it appears that both these processes - anatexis of country rocks and bodily injections of granitic rocks from the pluton - participated in the formation of this migmatite zone.

The composition and amount of melt formed by anatexis of gneisses depends not only on pressure and temperature, but also on the composition of gneisses, particularly on the component ratio Ab/An of plagioclase in the rock. The higher the An content of a plagioclase in a gneiss, the higher the temperature of the beginning of anatexis (c.f. Winkler and Von Platen, 1961; Winkler, 1967). In the surrounding rocks, the most acid plagioclase is present in the biotite gneisses, which in the contact aureole also carry the largest volume of granitic material and contain the widest zone of migmatization. Conversely, the calcomagnesian gneisses with the most basic plagioclase show the lowest degree of anatectic migmatization. It is of interest that Ermanovics has pointed out that "rocks with partial melt portions probably have large permeability with respect to invading or evading components, so that large pegmatitic concentrations may result" (1967, p.144). Perhaps this may be one of the reasons why the western and northwestern sides of the aureole composed of biotite gneisses, which produced the largest volume of granitic segregation during partial melting, have also the largest amount of pegmatitic and aplitic concentrations.

On Map 1 the different zones of migmatization have been arbitrarily drawn in the places where the proportion of granitic material makes up to 20, 40 and 66% of the volume (c.f. Legend to Map 1). At the weste[illegible]n and northwestern sides of the pluton, the boundary between the migmatite zone and the pluton proper is also rather arbitrary, marking the places at which granitic material prevails over country rocks by a ratio of 2:1.

The contact between the monzonite core and the outer zone formed by quartz monzonite appears to be relatively sharp but gradational. The sharp variation in lithology can be noticed between outcrops about 200 feet apart. Locally, a gradual transition about 150 feet wide between the outer granitic zone and the core has been observed. Granitic rocks of the outer zone, however, also cross-cut monzonite (Saha, 1957, 1959).

In the field, the contact between monzonitic rocks and basic inclusions appears to be gradational in places. This is indicated by the fact that the potash feldspar "may be locally so abundant that the diorites pass into monzonites" (Shaw, 1962, p.13). In places, however, the basic rocks are cross-cut by the leucocratic monzonite and also microscopic studies show that the composition of plagioclase and modal amounts of felsic minerals change abruptly at the contact, suggesting that the contact is not really gradational and indicating that the basic rocks are older than the main rock types of the pluton.

5.4 Age of the Pluton

The age of the Loon Lake pluton is only poorly known. In the absence of any isotope dating of the pluton, the age can only be estimated indirectly. The superimposition of the contact aureole on rocks which were already regionally metamorphosed to the amphibolite facies grade and the independence of the pluton on regional structures suggest that the pluton postdates the culmination of the metamorphic event dated at 1125±25 million years (the U/Pb dates of zircon, Silver and Lumbers, 1965; Lumbers, 1967a). The extensive mobilization of hornfelses and some other features, however, indicate that the pluton was emplaced into the already heated regionally metamorphosed rocks and diastrophism was probably still continuing when the intrusion took place. But the relatively large difference between the estimates of pressure for contact and regional metamorphism requires a time interval between these two events during which load pressures were lowered an appreciable amount. It appears that even when the pluton was emplaced well after the culmination of regional metamorphism, both these events might be part of one major cycle of orogenesis. The Loon Lake pluton, however, appears to be older than the intrusions of pegmatites and calcite-fluorite-apatite veins which were emplaced about one billion years ago (U/Pb ages of zircon, Silver and Lumbers, 1965; Rb/Sr, U/Pb, Pb/Pb, Th/Pb, K/Ar ages, Shafiqullah et al., 1973). Thus it may be suggested that the pluton was emplaced between about 1125 and 1000 million years ago.

5.5 Petrography

5.5.1 Introduction

The modal compositions of representative rocks comprising the pluton have been classified according to the modified

Johannsen's (1932) system (Figure 5.1) and are given in Appendix 1 (Table A.1.1-4). Apart from the granodiorite gneiss unit, most analyses of the core of the pluton indeed correspond to monzonite, while most of those from the outer zone of the pluton fall into the field of quartz monzonite. In a few cases, however, rocks which can be classified as monzonites also occur in the outer quartz monzonitic zone of the pluton (c.f. Appendix 1, Figure 5.1). Rocks from basic inclusions can be classified as diorite or syenodiorite. Rocks corresponding to gabbro (i.e. containing plagioclase An>50 and mafic minerals >50%) have not been found in the basic bodies. For completeness, modal analyses of Saha (1957) and D.M. Shaw (unpublished results given in Appendix 1) are also shown in Figure 5.1.

5.5.2 Quartz Monzonite

Quartz monzonite (map unit 9) forms the bulk of the outer core of the pluton. In spite of the fact that the quantitative mineral composition of this zone is variable, rocks of granitic or granodioritic composition are only sparsely present (c.f. Figure 5.1). Also many leucocratic and aplitic dikes in the vicinity of the pluton, particularly at the northeastern side of the intrusion, have a modal composition corresponding to quartz monzonite.

This rock type is medium to coarse-grained with its grain size ranging usually from about 1-5 mm. Its colour is

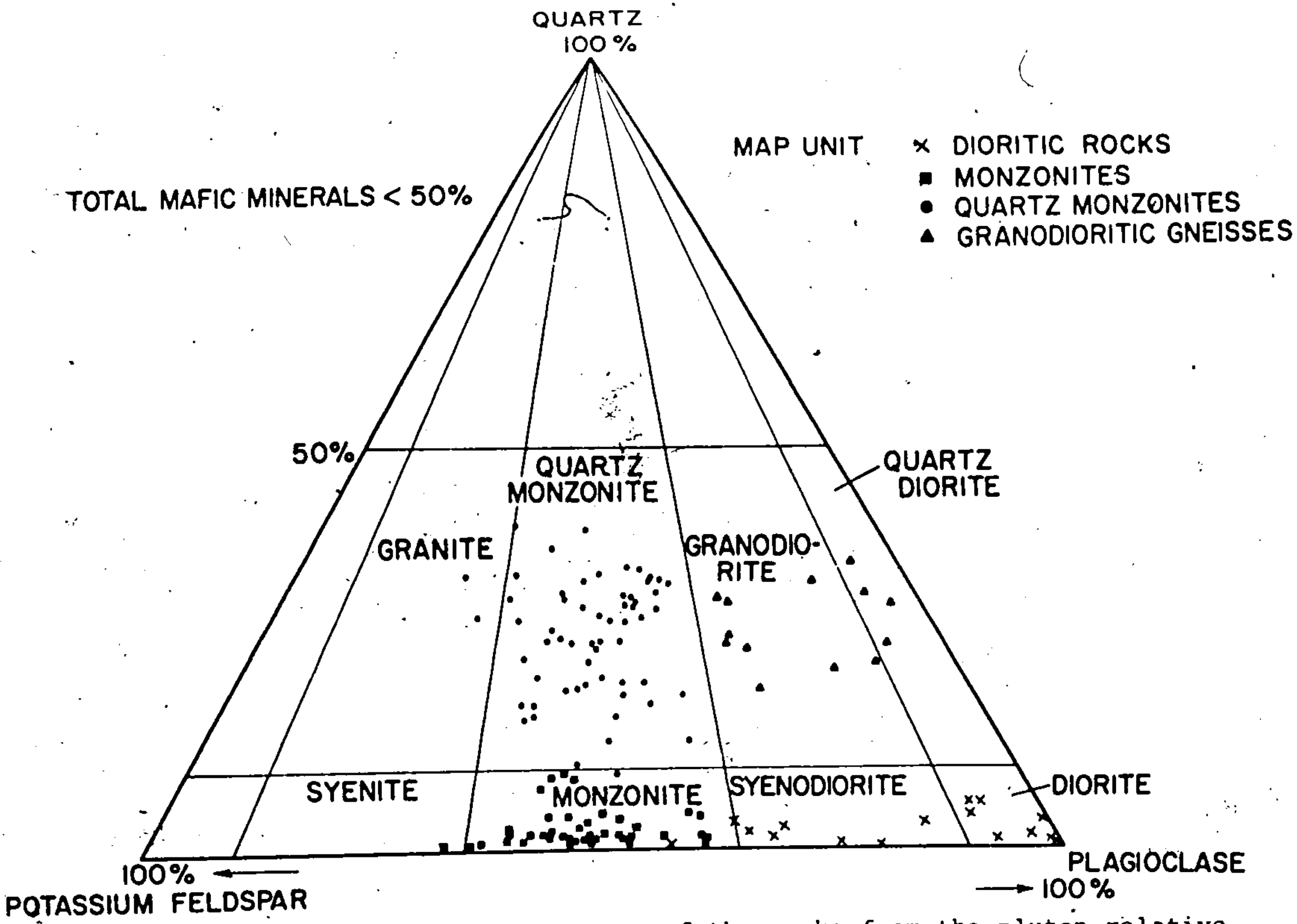

Figure 5.1 Distribution of modal analyses of the rocks from the pluton relative to the classification scheme (subdivision of the quartz-potassium feldspar-plagioclase diagram: 10-35-65-90% plagioclase; 10-50% quartz)

light gray to light pink, due largely to the white or pink feldspars and gray quartz. Quartz monzonite is composed of plagioclase, potash feldspar, quartz and biotite, which is the prevalent ferromagnesian mineral. Rarely, varieties containing subordinate amounts of hornblende in addition to biotite also occur. Subordinate and accessory amounts of magnetite, ilmenite, sphene, apatite, zircon, tourmaline, allanite and secondary muscovite, calcite, epidote and chlorite are present.

The texture of quartz monzonite is hypidiomorphic granular, with features of cataclastic and mortar texture in places. Plagioclase forms subhedral to anhedral crystals with a composition ranging from albite to oligoclase (An 8-An 20). Potassium feldspar is anhedral to subhedral, frequently microperthitic and in places shows cross-hatch twinning, although this is sometimes vaguely defined. Quartz occurs as anhedral grains usually with undulose extinction.

Biotite is subhedral and pleochroic from Y, Z - dark reddish-brown to X - light brown-yellow. Hornblende forms individual crystals up to 2 mm long with strong dark green pleochroism.

Locally, magnetite and ilmenite crystals have a corona of tiny granular sphene which probably developed during the late-stage deuteric recrystallization of these minerals with exsolution of titanium. Sphene also forms individual, usually euhedral crystals. Apatite is a common accessory mineral.

It forms colourless elongated prismatic crystals, which attain a maximum length of about 1 mm. Zircon is a rare accessory mineral in quartz monzonite. Pegmatitic and aplitic dikes are abundant throughout the outer zone of the pluton. In places they even grade into quartz monzonite.

5.5.3 Monzonite

This rock type (map unit 8) is coarse-grained, massive, usually grayish or brownish-pink in colour. It essentially consists of potash feldspar, plagioclase, subordinate amounts of quartz and about 5-10% mafic minerals. The principal mafic mineral is biotite, but in places hornblende and rarely clinopyroxene are also abundant. The accessory sphene, magnetite, ilmenite, apatite, and secondary calcite, epidote, chlorite and muscovite are frequently encountered.

The texture of these rocks is allotriomorphic to hypidiomorphic granular with locally pronounced features of mortar and cataclastic texture. In places where mortar and cataclastic textures are present, the aggregates of the large grains of feldspars with an average grain size of about 2-5 mm are separated by thin mortar laminae with a grain size of about 0.1 mm composed essentially of feldspars with minor amounts of quartz. In places, however, monzonite does not contain any evidence of shearing. Monzonitic rocks show subtle changes in mineral composition throughout this zone but rocks corresponding to syenite are only very seldom encountered (c.f. Figure 5.1 and Appendix 1).

Plagioclase forms anhedral granular crystals ranging from about 0.1-4 mm in size. Its composition varies from about An 12 to An 25. Potassium feldspar is subhedral to anhedral, ranging from 0.1-5 mm in size. Most of the larger crystals of potassium feldspars are perthitic but the texture and size of exsolved albite is quite variable. Cross-hatched twinning is occasionally present, but only poorly defined.

Quartz forms small anhedral interstitial grains ranging from about 0.1-0.8 mm with an undulose extinction. Hornblende occurs as subhedral prisms up to 2 mm long with pleochroism X - light yellow-green; Y - brown-green; Z - dark green, and an extinction angle c∧Z 17-19°. Clinopyroxene forms small, up to 0.5 mm large crystals which are colourless or very pale green with an extinction angle c∧Z 38-40°. Biotite occurs in the form of subhedral flakes up to 2 mm large. In places, two types of biotite seem to be present. "Secondary" biotite with pleochroism X - straw; Y, Z - grayish-brown, is associated with the cores of ragged hornblende, while "primary" biotite occurs as crystals with a scheme of pleochroism X - pale yellowish-brown; Y, Z - red-brown without any obvious reaction relation to hornblende.

Mutual relations of mafic minerals indicate that in order of decreasing age, the ferromagnesian minerals are clinopyroxene, hornblende and biotite.

Sphene forms euhedral to subhedral crystals or irregular aggregates usually associated with clusters of ferromagnesian minerals. It also occurs as fine-grained aggregates which rim magnetite and ilmenite.

In places, monzonitic and quartz monzonitic rocks probably underwent recrystallization as indicated by thin rims of clear untwinned albite around plagioclase (c.f. Saha, 1957, 1959).

5.5.4 Basic Rocks

Among the basic rocks (map unit 7) there is a wide variation of mineral composition which is probably caused by both original igneous variation and later alteration.

Diorite[1] and syenodiorite imperceptibly pass into each other. In general, syenodiorite occurs predominantly at the outer part of the basic bodies. Petrographically, syenodiorite differs from diorite mainly by higher content of potash feldspar and also biotite.

Syenodiorite and diorite are dark gray, medium to coarse-grained, massive but occasionally weakly foliated. They have usually a hypidiomorphic granular texture with some features of cataclastic texture and are composed chiefly of plagioclase, biotite and hornblende with varying amounts of pyroxene, quartz and potash feldspar. Calcite, ilmenite, magnetite, sphene and apatite are present in accessory amounts. Plagioclase forms subhedral to anhedral crystals up to 2.5 mm large, which frequently have normal and continuous zoning. The composition of plagioclase corresponds to andesine.

---

[1] For the sake of simplicity, the term "diorite" is used further in the text to include these two rock types

Clinopyroxene is abundant in some places, while in others it occurs only as small relics rimmed by hornblende or is missing completely. It forms subhedral pale green or colourless crystals with local exsolution of orthopyroxene. Clinopyroxene has a composition $Wo_{42}En_{44}Fs_{14}$ (sample 232) as estimated from the single crystal determination of unit-cell parameters (J. Griep, personal communication).

Elongated crystals of hornblende are up to 3 mm long with pleochroism X - brownish-yellow; Y - brownish-green; Z - green. Despite the fact that hornblende locally replaces clinopyroxene, most of the hornblende in these rocks appears to be of primary origin. Biotite forms large subhedral flakes or large scaly aggregates with pleochroism X - pale brownish-yellow; Y, Z - dark brown. Biotite is a late mineral. It not only replaces other ferromagnesian minerals, but also large flakes of biotite lie usually in the poorly defined foliation planes. The amount of potassium feldspar is highly variable. There is a tendency for an increase of its content toward the margins of of the bodies. Potash feldspar is commonly interstitial and locally shows evidence of growth at the expense of plagioclase. In general, textural relations indicate that the potash feldspar in basic rocks is late in origin. The petrography of the modification of basic rocks by felsic magma was documented and described in detail by Saha (1957).

In the central part of the pluton, the basic bodies occur in the vicinity of inclusions of mafic hornfelses from which they also differ by texture and grain size.

5.5.5 Granodioritic Gneiss

These rocks (map unit 10) form a roughly conformable belt in the quartz monzonite zone. They probably represent septa or screens of biotite and biotite-hornblende gneisses, which were partially assimilated and migmatized. Locally, the original foliation of gneisses has been destroyed and mafic minerals indicate recrystallization usually with a faint parallel orientation. In other places, gneisses retain their original banded character and mafic portions contain large porphyroblasts of feldspars.

These rocks seem to be deformed by magmatic flow. Consequently, it might suggest considerable movement during the emplacement of the pluton. Apart from the different fabric, the gneissic rocks contain higher amounts of mafic minerals and also higher contents of plagioclase (relative to potash feldspar) than the typical granitic rocks of the pluton (c.f. Figure 5.1).

Deuteric alteration in all these four rock-type units is relatively widespread throughout the pluton. Apart from effects mentioned earlier, it includes the chloritization of biotite and hornblende, development of epidote, muscovite (sericite) and carbonate mainly in plagioclase grains, etc. It is possible, however, that some muscovite is related to a late magmatic stage rather than a post-magmatic deuteric phase.

5.5.6 Inclusions

Inclusions of country rocks are frequently encountered throughout the outer zone of the pluton particularly along its periphery. They measure from several centimeters to a hundred meters in size and their volume decreases gradually toward the centre of the pluton. In the monzonite core of the pluton, they are much less abundant. The inclusions are commonly oval or discoid in shape and show different degrees of alteration. Some inclusions, especially those of biotite gneiss are partially assimilated and have given way even to nebulitic structures, while others have sharp boundaries and appear to be unaltered. Many inclusions consist of aluminous and mafic hornfelses (c.f. section 4.3). Most elongated inclusions tend to be oriented parallel to a foliation in the host plutonic rocks. Locally, however, inclusions are also rotated.

In the core of the pluton, a single inclusion about

5 m long of partially serpentinized dunite has been found. The contact relationship between dunite and monzonite is concealed and also flow-layering or related structures and textures have not been observed. Partially serpentinized olivine makes up at least 95% of the rock with only minor amounts of orthopyroxene and magnetite and traces of clinopyroxene present. Olivine has a composition of about Fo_{90}, based on refraction index measurements on one sample. Olivine is commonly strained and granulated with features of mortar texture.

5.6 Compositional Variation

In order to determine whether there is a significant regional trend in the variation of the composition of the pluton, it was intended to use trend surface analysis. Despite the fact that Saha's work suggested that the pluton was suitable for such studies, no polynomial surface of low order could give a good approximation to the composition pattern in the pluton. Although the attempt to use trend surface analyses was unsuccessful, some general systematic trends of compositional variation within each main zone of the pluton are present and have already been demonstrated by Saha (1957, 1959) and Shaw (1962).

The outer quartz monzonitic zone is relatively inhomogeneous, but no significant recorded spatial variation has been observed. Saha (1957, 1959), however, has recorded a positive correlation between the amount of mafic minerals and

An-content of plagioclase within this zone. The rocks of the monzonitic core subtly vary in a more systematic manner with respect to their locations within the pluton. Saha (1957) demonstrated that the potassium feldspar to plagioclase ratio increases toward the margin of this zone, while the basicity of plagioclase and the amount of mafics decrease in this direction; also, the ratio biotite to hornblende plus pyroxene increases outwards. Hornblende occurs chiefly in the central part of this zone; its content decreases outwards and it is nearly absent close to the contact with the outer zone of the pluton. Clinopyroxene occurs only in the central part of the monzonite zone together with hornblende and biotite.

Similar trends are present also in the basic bodies, which show a tendency to become more acidic from the centre toward the margin. These changes include an increase in potash feldspar content and the ratio biotite to hornblende plus pyroxene. As already noted above, they are not, however, due only to the original igneous variation, but some of them are probably related to interaction with felsic magma (Saha, 1957, 1959; Shaw, 1962). Potash feldspar and biotite in the basic rocks appear to be of late origin.

5.7 Potassium Feldspars

The Loon Lake pluton also displays variations of the structural state of potash feldspars. In most of the pluton, potassium feldspar is represented by cross-hatched twinned microcline, while some monzonitic rocks have untwinned orthoclase as the dominant K-feldspar. Potassium feldspars in the felsic rocks of the Loon Lake pluton are mostly microperthitic.

In order to determine the variation of the structural state and composition of potassium feldspar in relation to the lithology and spatial position in the pluton, potash feldspars from quartz monzonite and monzonite were examined by X-ray diffraction (c.f. Appendix 1) using the following data:

(1) obliquity (or triclinicity);
(2) unit-cell parameters;
(3) the three peak method of Wright (1968).

The bulk composition of perthitic potash feldspar was determined by Orville's method (1960, 1963, 1967).

5.7.1 Obliquity

The angular separation of the (131) and ($1\bar{3}1$) reflections in X-ray diffraction patterns was defined by Goldsmith and Laves (1954) as a measure of obliquity. This method, however, is applicable only to crystals with relatively high obliquity. For feldspars with low obliquity, the reflections (131) and ($1\bar{3}1$) interfere and form a single broadened reflection. The reflections were sufficiently resolved up to the angular separation corresponding to obliquity of about 0.4 for the X-ray goniometer used in the course of this work.

In some of the examined samples, orthoclase[1] coexists with microcline, and the proportions of orthoclase and microcline in such cases were roughly estimated by a comparison of the diffraction patterns with those of artificial mixtures of orthoclase and microcline prepared by Steiger and Hart (1967). As they pointed out, the detection limit for orthoclase in such a composite is usually 5% or more, whereas for microcline, it is 20% or higher, depending on the obliquity. According to the data on (131) and (1$\bar{3}$1) reflections, the structural state of the potassic phases of perthite of 28 studied samples can be divided into four types:

I - maximum or near maximum microcline (obliquity 0.8-1.00);

II - intermediate microcline (obliquity 0.5-0.70) with or without subordinate orthoclase and maximum to near maximum microcline (obliquity 0.80-1.00) with subordinate orthoclase;

III - low to intermediate microcline (having a single, but broadened 131 reflection) with or without subordinate maximum or near maximum microcline;

IV - orthoclase (having a single but sharp 131 reflection).

The results of the X-ray study are listed in Table 5.1.

---

[1] The term "orthoclase" as used here refers simply to an untwinned potassium feldspar with a single sharp 131 reflection.

Table 5.1 Obliquity and composition of potassium feldspar; composition of coexisting plagioclase

Sample No.	1	2	3	4	5	6	7
57	P				I	0.92	
58	P	83	95*		I	0.91	
59	P				I	0.93	
147	P		94		I	0.91	
26	QM	82	93	16	II	0.65	
27	QM	82	93*	13	II	0.93	~10% orthoclase
44	QM	80	93*	16	I	0.93	
45	QM				I	0.84	
53	QM	80	94	11	II	0.65	~25% orthoclase
115	QM	79	94*	9	I	0.91	
117	QM		94	11	I	0.92	
131	QM				II	0.60	
141	QM		94	9	I	0.81	
143	QM				I	0.81	
163	QM	85	94	13	I	0.89	
203	QM				II	0.58	
94	M				IV	0	
95	M				III	low	
102	M	75	94*	12	I	0.91	
198	M				IV	0	
200	M	85	93	25	IV	0	
207	M	72	93	22	IV	0	
222	M	82	92	20	IV	0	
223	M				II	0.66	
225	M				III	low	
226	M	83	93*	22	IV	0	
228	M	78	93	18	III	low	~30% max. microcline
251	M	76	94*	13	I	0.88	

1. Host rock: P=pegmatite; QM=quartz monzonite; M=monzonite
2. Bulk composition of perthitic K-feldspar (wt.% Or) determined by Orville's method
3. Composition of the potassic phase of perthite (wt.%) determined from the unit-cell data (*) or by the "three-peak method"
4. Anorthite content of coexisting plagioclase determined optically
5. Type of obliquity (c.f. section 5.7.1)
6. Obliquity = $12.5\,[d(131) - d(1\bar{3}1)]$
7. Second potassic phase

5.7.2 Unit-Cell Parameters

The computer-refined unit-cell parameters of seven potassic phases of perthites were determined from the X-ray diffraction patterns according to the method outlined by Wright and Stewart (1968). The cell dimensions are given in Appendix 1 and plotted on the graph of Wright and Stewart (1968) (Figure 5.2) which shows the variation of the "b" and "c" parameter with the structural state and the dependence of the "a" dimension on composition. This graph shows that the potassic feldspars for which the (131) and (1$\bar{3}$1) reflection can be resolved and which have the characteristic cross-hatched twinning, lie on the microcline side, whereas the one (226) with only the orthoclase (131) reflection and which simultaneously lacks the grid-twinning, lies close to the orthoclase line.

5.7.3 Three-Peak Method

The three-peak method devised recently by Wright (1968) was also used for estimation of the structural state and composition of ten potassic phases of perthitic alkali feldspars. Wright (1968) has shown that the "a", "b" and "c" cell dimensions can be linearly related to the ($\bar{2}$01), (060) and ($\bar{2}$04) reflections. The reflections (060) and ($\bar{2}$04) serve for estimation of the structural state while the ($\bar{2}$01) reflection can be used for estimation of the composition. As in the unit-cell graph, the potassic phases with separated (131) and (1$\bar{3}$1) reflections fall

Figure 5.2 Unit-cell parameters of potassic phases of perthites plotted on a b-c graph of Wright and Stewart (1968) simplified after Tilling (1968). Cross contours (dashed lines) represent the values of a. Potassic phase with a single, sharp (13$\bar{1}$) reflection was calculated as monoclinic.

Figure 5.3 Potassic phases of perthites plotted on a 060-$\bar{2}$04 graph of Wright (1968) simplified after Tilling (1968). Cross contours (dashed lines) represent 2θ values of ($\bar{2}$01) reflection.

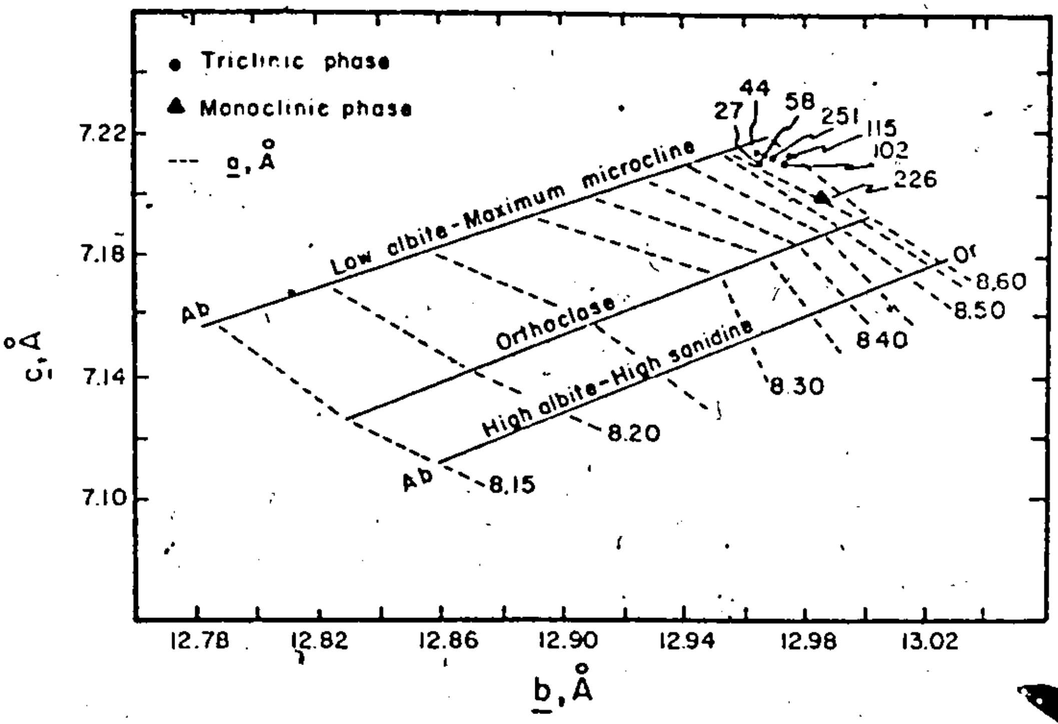

Figure 5.2

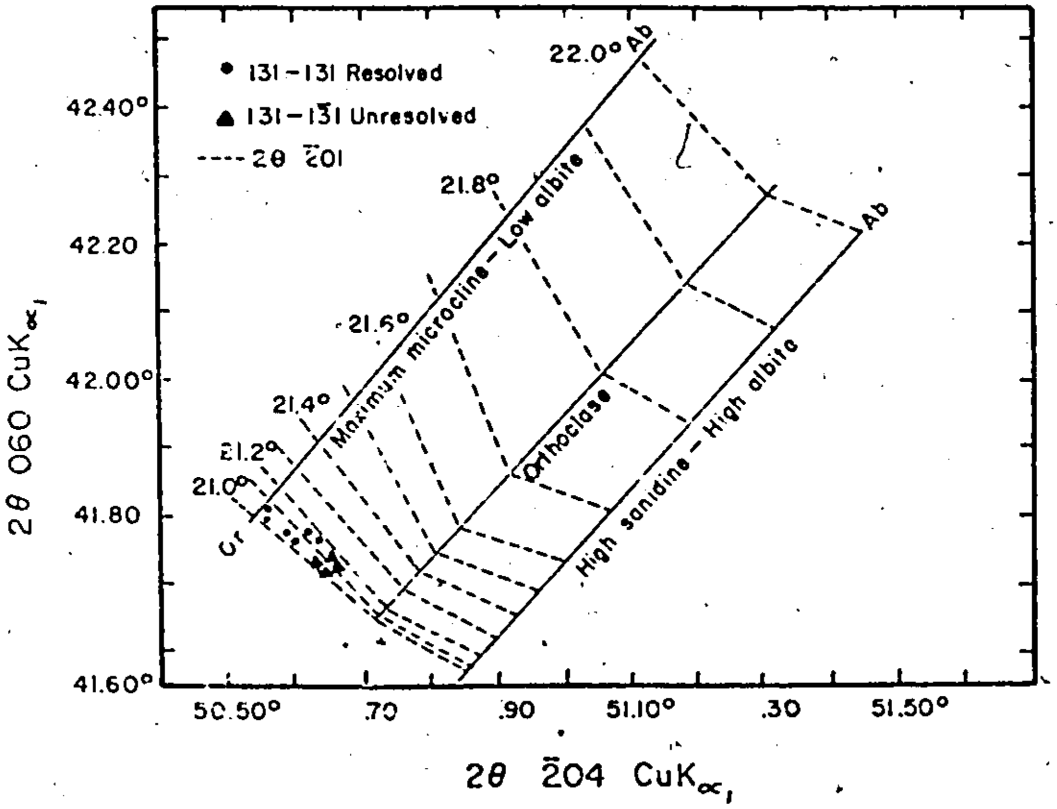

Figure 5.3

close to the maximum microcline-low albite series (117, 141), while those with the single (131) reflection (200, 207, 222) are close to the orthoclase series (Figure 5.3).

5.7.4 Composition of the Potassium Feldspars

The bulk composition of fourteen potash feldspars is given in Table 5.1 which also shows the composition of the exsolved potassic phases of these perthites determined from the unit-cell data or by the "three-peak method". As the data in Table 5.1 suggest, there is no obvious relationship between the bulk composition of perthite and the structural state or the composition of the potassic phase or the lithology of the pluton. Keeping in mind that Orville's method is relatively crude and that only a small number of samples were examined, it indicates that the bulk composition of the K-feldspars was not a deciding factor in determining the structural state of potassic phases of perthites in the pluton. The composition of exsolved potassic phases varies within rather narrow limits of about $Or_{92}Ab_{08}$ - $Or_{95}Ab_{05}$.

5.7.5 Variation in the Structural State

Despite the relatively small number of samples studied, it appears that the regional variations of the structural state within the pluton reveal a zonal pattern. In general, microcline is the principal K-feldspar in the outer zone, whereas orthoclase occurs in the centre of the pluton. The regional distribution of the four feldspar structural types based on (131) and ($1\bar{3}1$) reflections (Table 5.1) show that Type I is characteristic of most of the outer portion of the pluton. The central part of the pluton contains predominantly Type IV and in places also Type III (c.f. Map 2). It seems, however, that the structural types are not dependent on the main lithological zones of the pluton. Some monzonitic rocks (samples 102, 251) contain maximum or near maximum microcline (Type I), while intermediate microcline (Type II) is locally present in quartz monzonite.

Several hypotheses have been invoked to explain the variation in the structural state of potash feldspars such as observed in the pluton. Heier (1957) and Mackenzie and Smith (1961) have suggested that the triclinicity is a function of the temperature of formation and that the former increases as the latter decreases. Despite the fact that in the Loon Lake pluton there is a general tendency for K-feldspars from monzonite to have a lower obliquity than those from quartz monzonitic rocks, it appears that this hypothesis cannot explain the presence of maximum microcline in some monzonites.

Eskola (1951), Karamata (1961) and Smithson (1963) have pointed out that deformation facilitates the inversion from a monoclinic to a triclinic state. But in the pluton, the degree of deformation shows no obvious relation to the structural state of feldspar. Some rocks with pronounced shearing contain orthoclase, while many undeformed rocks have maximum microcline as the dominant alkali feldspar. It suggests that deformation was not a deciding factor for the structural state of K-feldspar.

Marmo et al. (1963) noted that triclinicity might be positively correlated with an abundance of myrmekite, but in the rocks studied, this has not been found. On the contrary, myrmekite is even more common in rocks with low obliquity than in those with maximum microcline. Also, reheating during the intrusion of younger plutonics (Tilling 1968) could hardly be postulated as the cause of zonation in the structural state. Even if the quartz monzonite represents a younger intrusion than the monzonite core, the presence of maximum or nearly maximum microcline in some monzonites negates such a process. No evidence has been found for any other alternative explanations, for example, that the low obliquity of K-feldspars in the interior of the pluton was produced by reheating caused by a near-surface but not exposed younger intrusive. Thus the variation seems to be of primary origin in the sense of Tilling (1968). This would suggest that potash feldspars of the outer zone inverted faster and indicate the presence of a catalyzing agent, which caused the feldspar inversion in the outer zone to be more rapid than in the core. The catalytic effect of volatiles, particularly water on this inversion, has been confirmed experimentally (e.g. Donnay et al., 1960; McConnel and McKie, 1960); the latter authors noted that the rate of transformation increases as the square-root of the total water pressure.

Kennedy (1955) has suggested that water will migrate to the cooler, outer portions of a magma and also has a higher concentration in the cooler parts. Also as a rule, pegmatites contain maximum microcline, as the only potassium feldspar. It is generally accepted that pegmatites crystallized under high f_{H_2O} conditions.

Likewise, the migration of water from the country rocks into the pluton might be significant. On the basis of oxygen isotope studies, Y.N. Shieh (personal communication) has suggested such inward migration. It might be speculated that the pluton acted as a sink and water diffused out of the wall-rocks, possibly concentrating in the periphery of the pluton.

Thus in both cases (the pluton represents either a closed system with a temperature gradient or an open system with water migrating out of the country rocks), water would probably concentrate more in the periphery of the pluton than in the centre. Such a distribution of water in the pluton is consistent with the presence of microcline in the outer zone, and orthoclase in the centre of the pluton and suggests a catalytic effect of H_2O on the orthoclase-microcline inversion in the pluton. It is not clear, however, whether the relative distribution of f_{H_2O} which could exist at solidus temperatures or at the temperature at which oxygen isotope exchange ceased, was maintained at the lower temperature of feldspar inversion.

5.8 Some Considerations on the Emplacement of the Pluton

The relation between the basic rocks and the other main lithological units of the pluton is not clear. The cross-cutting of dioritic rocks by monzonite and the small lenses of basic rocks, presumably dislocated from larger bodies, show that they are older than the pluton proper, and that they were solidified at a time when monzonite and quartz monzonite were still mobile.

Also, despite the fact that most bodies occur in the centre of the Loon Lake pluton, their presence at the south-western periphery of the pluton (c.f. Map 1) argues against the differentiation of monzonitic and dioritic rocks mainly in situ from a single magma as suggested by Ermanovics (1967). It appears that the basic rocks probably "represent inclusion or roof pendants of gabbros previously injected into the paragneisses" (Shaw, 1962, p. 13), which might or might not be genetically related to the bulk of the pluton.

In the absence of any conclusive petrographic evidence for the co-genesis of basic rocks and monzonite, the only indication for this relationship appears in comparison with similar plutons in this part of the Grenville Province. A number occur not only in the Bancroft-Madoc area (c.f. Lumbers, 1967a), but also in the Westport-Gananoque region (e.g. Westport, Perth Road, South Lake, Ganaoque plutons) and in some of these plutons, basic rocks (gabbro-diorite) are present in association with monzonitic and granitic rocks.

Regarding the monzonitic and quartz monzonitic zones of the pluton, it appears that they represent separated intrusions of magma as indicated by the cross-cutting of monzonite by quartz monzonite (c.f. Saha, 1957, 1959). Since the contact between the monzonitic core and the quartz monzonitic outer zone, however, seems in places to be relatively sharp but gradational, the older intrusion - monzonitic - was probably not completely crystallized and still behaved somewhat plastically as quartz monzonite intruded. Thus, the time interval between these two intrusions was probably short. Petrographic similarities and rapid successive intrusions of the two felsic rock types may suggest a genetic relation between them.

Although, as noted earlier, some granitic rocks were formed by partial melting of the surrounding rocks in situ or nearly so and assimilation of country rocks did occur, these mechanisms seem inadequate to generate the bulk of the quartz monzonitic zone. There are many observations indicating that the quartz monzonite intruded into its present position (as evidenced, for example by (1) the contact metamorphic aureole, (2) the frequently abrupt manner in which the pluton cross-cuts structural features of the country rocks, (3) angular inclusions of country rocks with sharp contacts and diverse orientations, frequently rebroken, dilated and veined by the quartz monzonite, etc.). Also, a general lack of correlation between the composition of the wall-rocks and adjacent rocks of the pluton negate excessive marginal assimilation of more acid country rocks in situ.

Apart from the roughly concentrical arrangement of the two main zones of the pluton, the monzonitic core also shows subtle but systematic progressive acidification toward the margin, as demonstrated by Saha (1957, 1959) and Shaw (1962). Saha (1957) concluded that neither assimilation of country rocks nor assimilation of basic rocks in the centre of the monzonitic body could produce such systematic variation.

The mineral composition of the monzonite indicates that the rocks occurring in the centre of the monzonite core started to crystallize earlier than those which are present around the margin, as suggested by the increase of the anorthite content of plagioclase from the margin toward the interior, the presence of pyroxene, the first mafic mineral to crystallize, only at the centre of the monzonite zone and the increase of the content of mafic minerals toward the centre. There is no evidence, however, that the rocks were differentiated in situ. On the contrary, as Shaw (1962) pointed out, when magma was injected "it must have already crystallized to a notable extent because the solid crystals were oriented during flow to give the foliation and lineation now visible" (p.16). This indicates that the variation of mineral composition was present in the monzonitic magma before its emplacement, suggesting that the systematic variations in the monzonitic core might have been due to the flowage differentiation. Bhattacharji and Smith (1964) and Bhattacharji (1966, 1967) have experimentally demonstrated that solid particles accumulate in a flowing liquid in the region of the maximum longitudinal velocity component away from the margins, at or near the centre. It suggests that the early precipitated crystals moved from the wall toward the centre and might have caused the concentric variation in the monzonite core.

5.9 Summary

1. The Loon Lake pluton is a post-tectonic, steeply dipping, assymetrical funnel-shaped intrusion.

2. The pluton was emplaced after the culmination of the metamorphic event dated at 1125±25 m.y., but it is older than the intrusions of pegmatites and calcite-fluorite-apatite veins which were emplaced about one billion years ago.

3. The pluton is surrounded by a migmatite zone of variable width. Both the partial melting of country rocks and bodily injections of granitic rocks from the pluton probably participated in the formation of the migmatite zone.

4. The pluton consists of two main zones, which have a roughly concentrical arrangement. The core of the pluton is formed by monzonite and the outer zone by quartz monzonite.

Several large isolated bodies of basic rocks (syenodiorite, diorite) occur within the pluton, most of them in the central part of the pluton. In order of decreasing age the rock types are: basic rocks, monzonites and quartz monzonites. Apart from these three rock types, a conformable belt of granodioritic gneisses occursin the outer quartz monzonitic zone of the pluton. This belt probably represents merely a septum or screen of partially assimilated and migmatized gneisses.

5. The Loon Lake pluton is also zoned with respect to the structural state of potassium feldspars. It is suggested that this variation was controlled by the distribution of water within the body.

6. Petrographic similarities and rapid successive intrusions of the two felsic rock types might suggest a genetic relation between them. The relation between the basic and felsic rocks of the pluton is uncertain. It appears that the basic rocks "represent inclusion or roof pendants of gabbros previously injected into paragneisses" (Shaw, 1962, p.13).

7. The process of flowage differentiation probably played a significant role during the emplacement of monzonite.

CHAPTER 6

GEOCHEMISTRY OF THE LOON LAKE PLUTON

The results of chemical analyses of the rocks and mineral separates from the Loon Lake pluton are listed in Appendix 1. The analytical methods together with their precision and accuracy are given in Appendices 1 and 2 and the sample locations are shown on Map 2.

6.1 Chemistry of the Rocks

6.1.1 Major Elements

As expected from the modal analyses, the chemical data of monzonite and quartz monzonitic rocks show a bimodal distribution for silica and alumina (Figure 6.1.1), although with a transition between the two maxima. Some rocks (e.g. 142) occurring in the outer zone of the pluton (but not geographically close to the monzonitic core) correspond chemically to monzonite.

Quartz monzonitic and monzonitic rocks have a subalkaline character as shown by the molar ratio $(Na_2O+K_2O)/Al_2O_3$, which is always less than one. In general, the quartz monzonite from the Loon Lake pluton is poorer in CaO, MgO and FeO and richer in K_2O than Nockolds' (1954) average of quartz monzonite

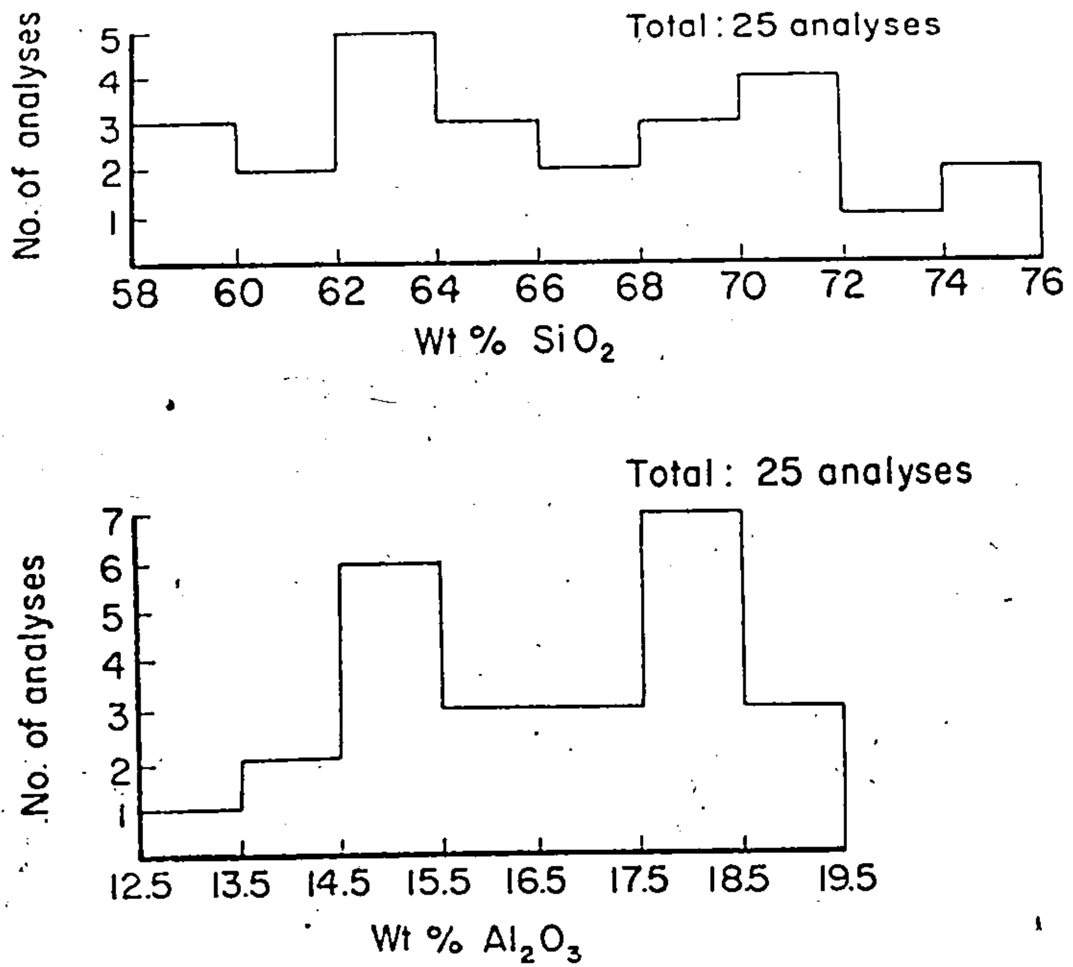

Figure 6.1.1 Histograms of SiO_2 and Al_2O_3 distributions in the felsic rocks

and richer in Al_2O_3 and Na_2O than his average of calc-alkali granites (Table 6.1.1). On the other hand, it is rather similar to the Rockport granitic rocks from this part of the Grenville Province given by Sauerbrei (1966).

The leucocratic fine-grained granitic rock, which was probably generated by the partial melting of the country rocks (sample 259, see chapter 4.3.1) is characterized by a higher content of silica and lower content of Al_2O_3, CaO, MgO and iron (c.f. Table 6.1.1) in comparison with a typical quartz monzonite from the Loon Lake pluton.

The average chemical composition of monzonite is relatively close to that of the alkali syenites of Nockolds (1954) although the CaO, Na_2O and iron contents are slightly higher and Al_2O_3 and K_2O lower in alkali syenites (Table 6.1.2). Once again, the average of the Loon Lake pluton monzonites is very similar to that of the Westport monzonites of Sauerbrei (1966), but differs from the potassic syenite from the Umfraville gabbro complex, especially in its low content of Fe (Table 6.1.2).

The dioritic rocks of the Loon Lake pluton show a distinct chemical variation particularly in CaO, MgO and K_2O (Appendix 1). The petrography of these rocks, as indicated by the presence of the late patches of potassium feldspar and large scaly aggregates of biotite, suggest, however, that some of these variations might be of a secondary origin (c.f. Saha, 1957, 1959; Shaw, 1962). Thus the evaluation of the magmatic

Table 6.1.1 Comparison of average composition of granitic rock types

	1	2	3	4	5	6	7	8
SiO_2 (wt.%)	70.98	71.92	63.53	69.15	66.88	72.08	73.86	77.79
TiO_2	0.36	0.37	0.99	0.56	0.57	0.37	0.20	0.15
Al_2O_3	14.74	14.59	15.80	14.63	15.66	13.86	13.75	11.59
Fe_2O_3	1.20	1.36	3.19	1.22	1.33	0.86	0.78	1.18
FeO	1.30	0.78	2.00	2.27	2.59	1.67	1.13	0.58
MnO	0.03	0.02	0.06	0.06	0.07	0.06	0.05	0.01
MgO	0.43	0.31	1.15	0.99	1.57	0.52	0.26	0.06
CaO	1.15	1.21	2.85	2.45	3.56	1.33	0.72	0.21
Na_2O	3.79	3.30	3.91	3.35	3.84	3.08	3.51	3.36
K_2O	5.43	5.50	5.14	4.58	3.07	5.46	5.13	5.00
P_2O_5	0.08							
H_2O	0.37							0.13
H_2O-	0.06							0.05
CO_2	0.08							0.05
Total	100.00	99.36	98.62	99.26	99.14	99.29	99.39	100.16

1. Average of quartz monzonite from the Loon Lake pluton (average of 12)
2. Average Rockport granite (average of 17), Sauerbrei (1966)
3. Average Frontenac granite (average of 29), Sauerbrei (1966)
4. Average of 121 quartz monzonites, Nockolds (1954)
5. Average of 137 granodiorites, Nockolds (1954)
6. Average of 72 calc-alkali granites, Nockolds (1954)
7. Average of 48 alkalic granites, Nockolds (1954)
8. Leucogranite - 259

Table 6.1.2 Comparison of average composition of monzonitic and syenitic rock types

	1	2	3	4	5	6
SiO_2 (wt.%)	62.55	61.98	61.86	59.41	55.36	58.72
TiO_2	0.82	0.82	0.58	0.83	1.12	1.12
Al_2O_3	18.03	17.92	16.91	17.12	16.58	18.31
Fe_2O_3	1.81	2.60	2.32	2.19	2.57	3.78
FeO	1.69	1.52	2.63	2.83	4.58	2.08
MnO	0.07	0.06	0.11	0.08	0.13	0.07
MgO	0.90	1.12	0.96	2.02	3.67	1.39
CaO	1.80	1.69	2.54	4.06	6.76	1.85
Na_2O	4.77	5.33	5.46	3.92	3.51	5.01
K_2O	6.90	5.92	5.91	6.53	4.68	6.03
P_2O_5	0.20					0.29
H_2O	0.35					0.20
H_2O-	0.08					0.13
CO_2	0.03					0.19
Total	100.00	98.96	99.28	98.99	98.96	99.17

1. Average of monzonite from the Loon Lake pluton (average of 12)
2. Average Westport monzonite (average of 6), Sauerbrei (1966)
3. Average of 25 alkali syenites, Nockolds (1954)
4. Average of 18 calc-alkali syenites (Leucocratic), Nockolds (1954)
5. Average of 46 monzonites, Nockolds (1954)
6. Potassic syenite, Umfraville complex, Lumbers (1967a)

affinities of dioritic rocks is not straightforward. Also, there is no clear geological evidence linking them with their descendants, as for example, in a layered intrusion. The presence of normative olivine in most samples, even those that are least altered, indicates the undersaturated character for the diorites, in spite of the fact that none of these rocks contains modal olivine. When the chemical compositions of dioritic rocks are compared with those of gabbroic and dioritic rocks from the surrounding area, it appears that they are somewhat similar to those of the late gabbro and diorite group of Lumbers (1967a) - for example, the Umfraville gabbro complex (except in alkalies, particularly K_2O, which is notably higher in most of the basic rocks from the pluton) - but differ from those of his earlier diorite group, represented for example by the Jocko Lake or Tudor complexes. From the latter group, they differ particularly by a higher content of Fe and Ti.

A common problem of many composite, predominantly felsic plutons containing several intrusive phases, is whether such intrusions have been formed from a single parental magma, and if so whether such magma is a product of the magmatic differentiation of a more basic one. In order to evaluate whether the behaviour of the felsic rocks of the pluton is consistent with some process of magmatic differentiation, their compositions have been plotted in synthetic systems. Since monzonitic and quartz monzonitic rocks contain more than 80% of normative feldspars and quartz, the system Or-Ab-An-Q-H_2O appears to be a good model for these rocks. Figure 6.1.2 shows the normative composition of felsic rocks from the pluton in relation to the Q-Ab-Or ternary diagram. Most of the granitic rocks fall within Winkler and Von Platen's (1961) granitic field, while the rest, except one, together with monzonites fall into the field of syenitic rocks from the Gardar province of Greenland (Watt, 1966).

Quartz monzonites loosely cluster in the low temperature region of the Ab-Or-Q projection with about 30% of normative quartz. The diagram also shows the gap between the bulk of granitic rocks of the pluton and that which is associated with aluminous hornfelses and is thought to be generated by partial melting of the country rocks in situ or nearly so.

The monzonitic rocks cluster near the feldspars' join at Or_{40} to Or_{50} extending to about 10% of quartz. A comparison with the experimentally-determined melting minima shows that monzonites fall toward the Or corner from the alkali feldspar minima as the minimum or eutectic in the pure feldspar join, as determined experimentally, varies from Or_{40} at 1 kb P_{H_2O} to Or_{29} at 10 kb P_{H_2O} (c.f. Luth et al., 1964; Kleeman, 1965). But "this shift appears to be the general case with syenitic rocks" and it "is probably generated by the confluence of the boundary surfaces of plagioclase, ferroaugite, fayalitic olivine, Fe-Ti oxide, and liquid. Although the calcic pyroxene might be expected to be dominant in this respect" (Morse, 1968, p.114).

Figure 6.1.2 Normative composition of felsic rocks from the Loon Lake pluton in relation to the quartz-albite-orthoclase ternary system. The solid line encloses analyses of 1190 granitic rocks (Winkler and Von Platen, 1961). Dashed line shows the field of syenitic rocks from the Gardar province of Greenland (Watt, 1966). Dashed-dotted and dotted lines represent field boundaries at indicated Ab/An ratios at 2 kb P_{H_2O}. Squares denote ternary minima or eutectics at various P_{H_2O} with an Ab/An ratio of 2.9(■1 = 2 kb; ■2 = 4 kb; ■3 = 7 kb; ■4 = 10 kb P_{H_2O}) (both taken from Winkler, 1967) ■5 marks the position of the temperature minimum at 2 kb and Ab/An = ∞ (Tuttle and Bowen, 1958).

○ - monzonite
● - quartz monzonite
× - leucogranite 259

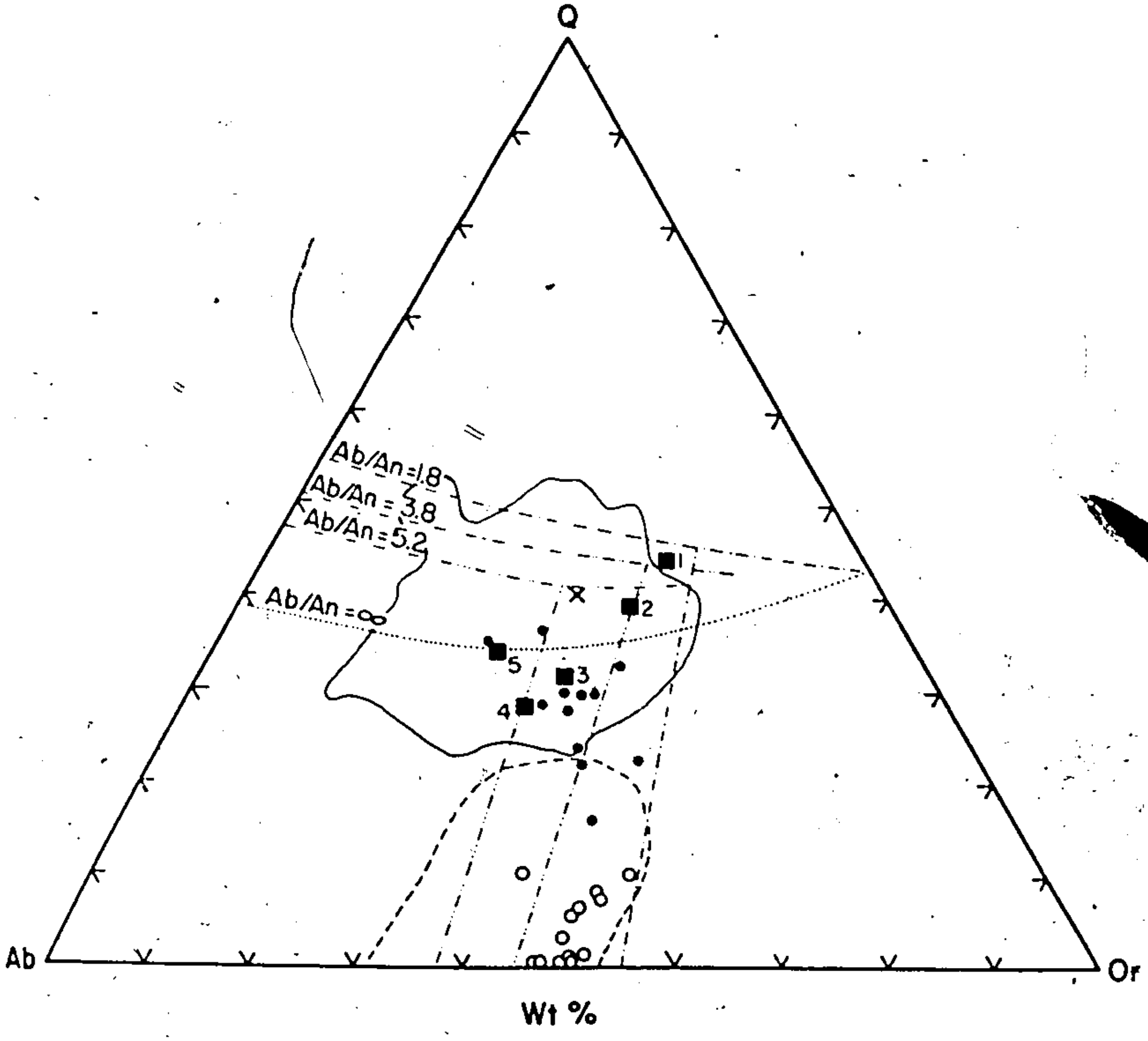
Q
Ab/An=1.8
Ab/An=3.8
Ab/An=5.2
Ab/An=∞
1
2
3
4
5
Ab
Or
Wt %

Even if monzonites and quartz monzonites form clusters, there seem to be several transitional rocks. The fact that all analyses lie on the alkali feldspar side of the ternary minima is compatible with a derivation of these rocks from a single magma. The gradual increase in normative quartz toward the silica apex might suggest that the zoning in the Loon Lake pluton is due to fractional crystallization.

Figure 6.1.3 shows the normative percentages of albite, anorthite and orthoclase in the rocks from the pluton plotted on the H_2O-saturated and silica-saturated plane of the Or-Ab-An-Q tetrahedron and their relation to the low temperature trough of Kleeman (1965). Most of the quartz monzonites and monzonites fall into the thermal trough and the rest of them lie on the plagioclase side of the low temperature region within the 2% contour of Tuttle and Bowen (1958) for "normal granites".

The position of the felsic rocks in the Or-Ab-An-Q-H_2O system indicates an igneous rather than a metasomatic origin for monzonite and quartz monzonite from the Loon Lake pluton and it suggests that these rocks probably resulted from "crystal-liquid equilibrium" (Tuttle and Bowen, 1958).

Coexisting potash feldspars and plagioclases from felsic rocks are plotted on the An-Ab-Or diagram in Figure 6.1.4. The composition of coexisting feldspars (c.f. Table 5.1) and the trend of their variation is consistent with the experiment of Yoder et al. (1957) and also with the composition of

Figure 6.1.3 Normative composition of felsic rocks in relation to the anorthite-albite-orthoclase ternary system. The boundaries of the low temperature trough are shown (solid lines) and range from $Or_{29}Ab_{71}$ at 10 kb to $Or_{45}Ab_{55}$ at 1 kb P_{H_2O}. Dashed lines show uncertainty due to the possibility of analytical error (Kleeman, 1965). The irregular boundary is the 2% contour of Tuttle and Bowen (1958, Figure 67) enclosing most granitic rocks that contain more than 80% normative Ab+Or+Q.

○ - monzonite
● - quartz monzonite
× - leucogranite 259

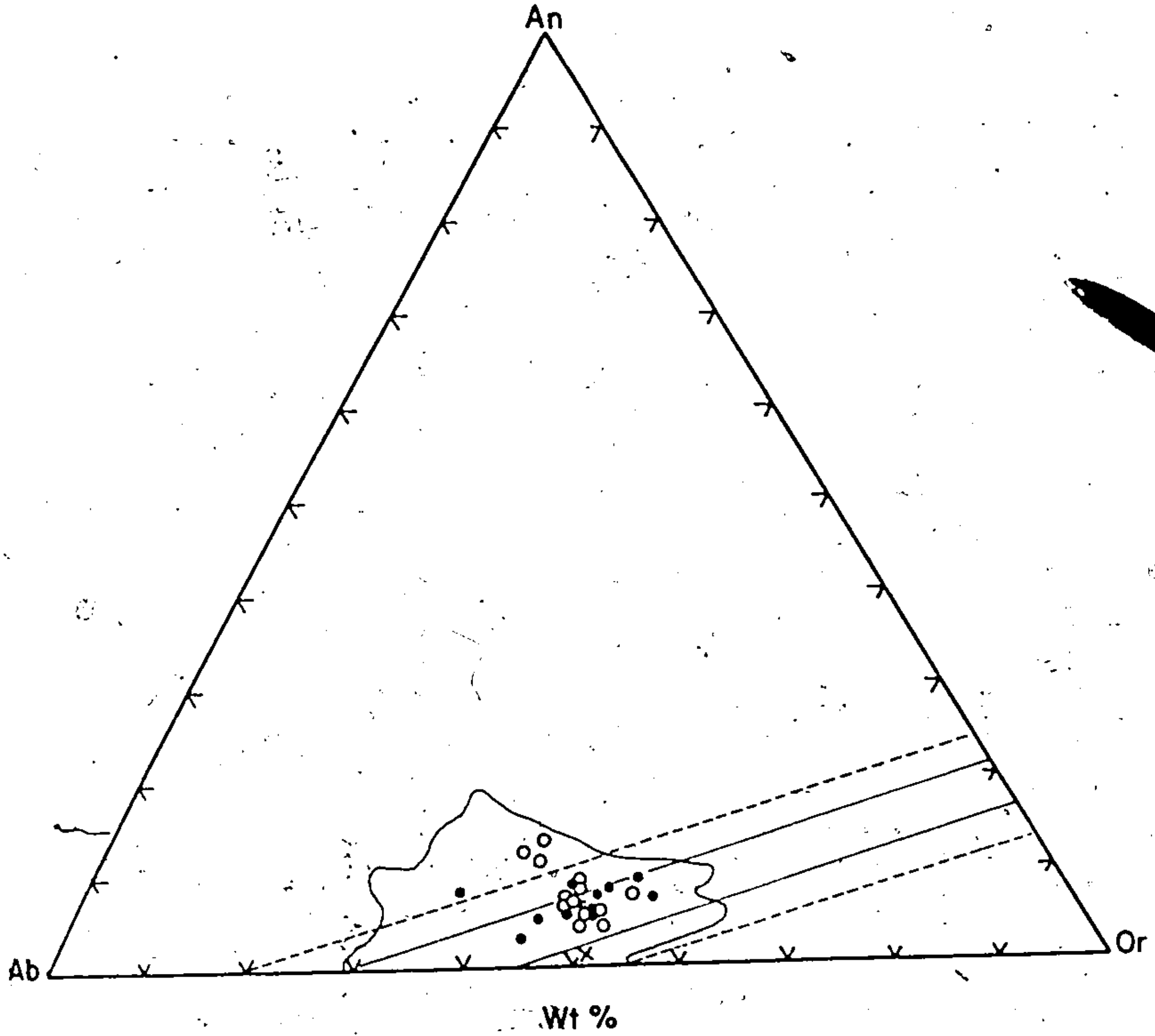
An
Ab
Or
Wt %

Figure 6.1.4 An-Ab-Or diagram showing the composition of coexisting feldspar pairs from the felsic rocks. The coexisting feldspars are connected by tie lines. Also, two pairs of synthetic feldspars of Yoder et al. (1957) with their respective temperatures are shown.

Compositions of potassium feldspar were determined by Orville's (1960, 1967) method while those of plagioclase were determined optically. Since the An contents of potash feldspar and Or contents of plagioclase were not determined, the feldspars were plotted along the joins.

● - feldspar pairs from monzonite

☐ - feldspar pairs from quartz monzonite

△ - feldspar pairs of Yoder et al. (1957)

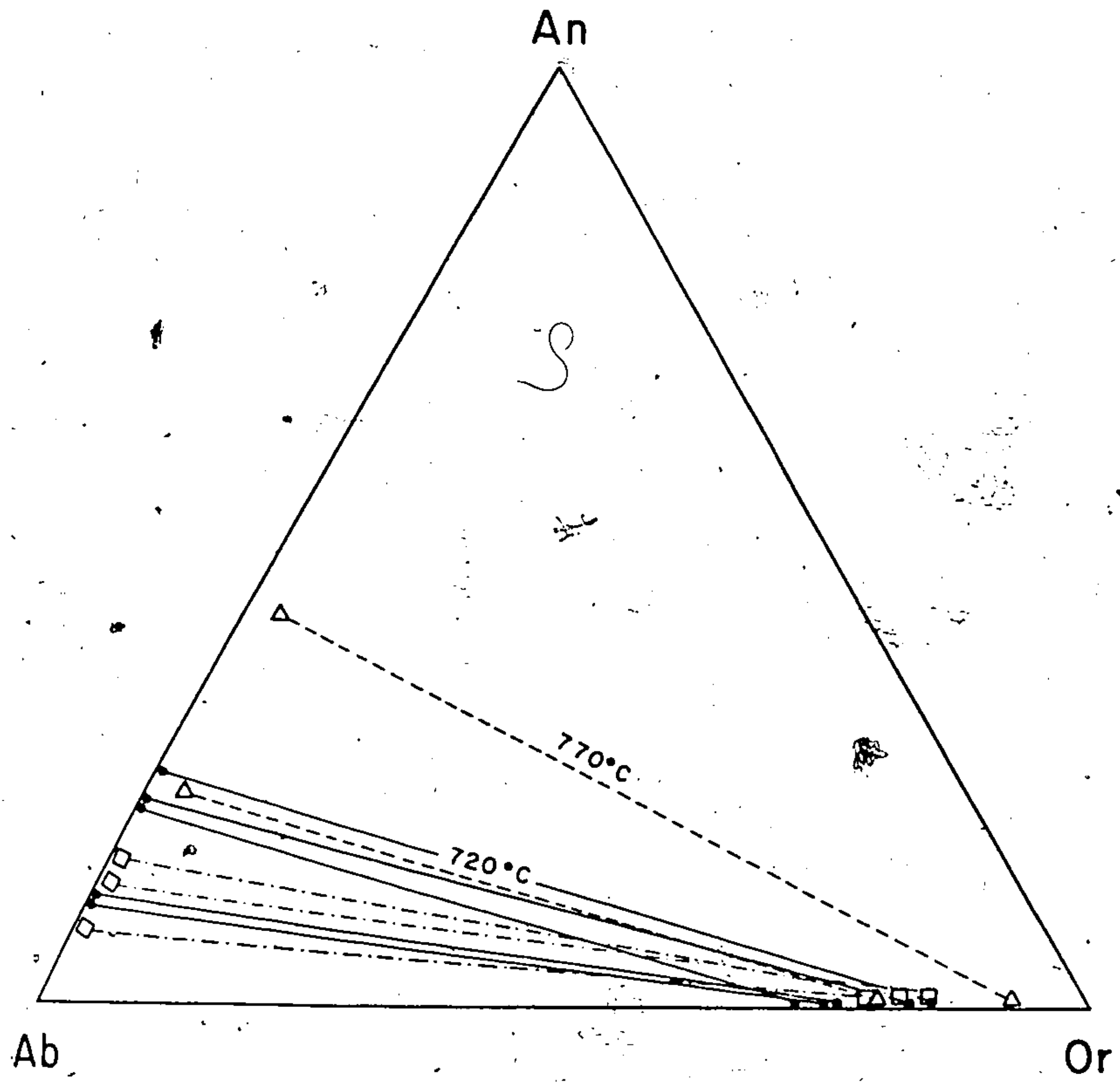
An
770 °C
720 °C
Ab
Or

coexisting feldspars from other magmatic rocks (c.f. Carmichael, 1963; Ewart, 1969; Mursky, 1972) thus indicating a magmatic origin for these rocks. The trend of variations of feldspars may once again suggest a genetic relation between these two felsic rock types.

The contents of major elements in the rocks from the pluton have been plotted on the variation diagrams against the differentiation index (D.I.) of Thornton and Tuttle (1960) in Figures 6.1.5-14. Other differentiation indexes such as Larsen's yield rather similar trends. Figure 6.1.5 shows that the monzonitic rocks are clustered on either side of the lines separating saturated from undersaturated rocks, while quartz monzonites lie within the oversaturated field of Thornton and Tuttle (1960). Dioritic rocks which lie in their undersaturated field show some scatter in the content of SiO_2 although a definite trend is observed, increasing toward the more acid types.

When the three main rock types are treated as a series, silica steadily increases from dioritic to monzonitic rocks. Even when the D.I. values for monzonites and quartz monzonites partly overlap, the latter show higher silica contents, notably changing the gentle slope of the variation trend between monzonite and diorite. Aluminum slightly increases in diorite as rocks become more felsic. The content of Al_2O_3 in quartz monzonite is lower than that from monzonite with similar D.I. values (Figure 6.1.6). The differences in silica and alumina

Figure 6.1.5 Variation of SiO_2 as a function of D.I. (= a sum of wt.% of norm. Ne+Lc+Ks+Ab+Or+Q) with fields for undersaturated, saturated and oversaturated rocks (after Thornton and Tuttle, 1960)

■ - diorites ● - quartz monzonites
○ - monzonites ✕ - leucogranite 259
(Symbols identical for Figures 6.1.6-6.1.15)

Figures 6.1.6-6.1.14

Variations of oxides of major elements as a function of D.I.

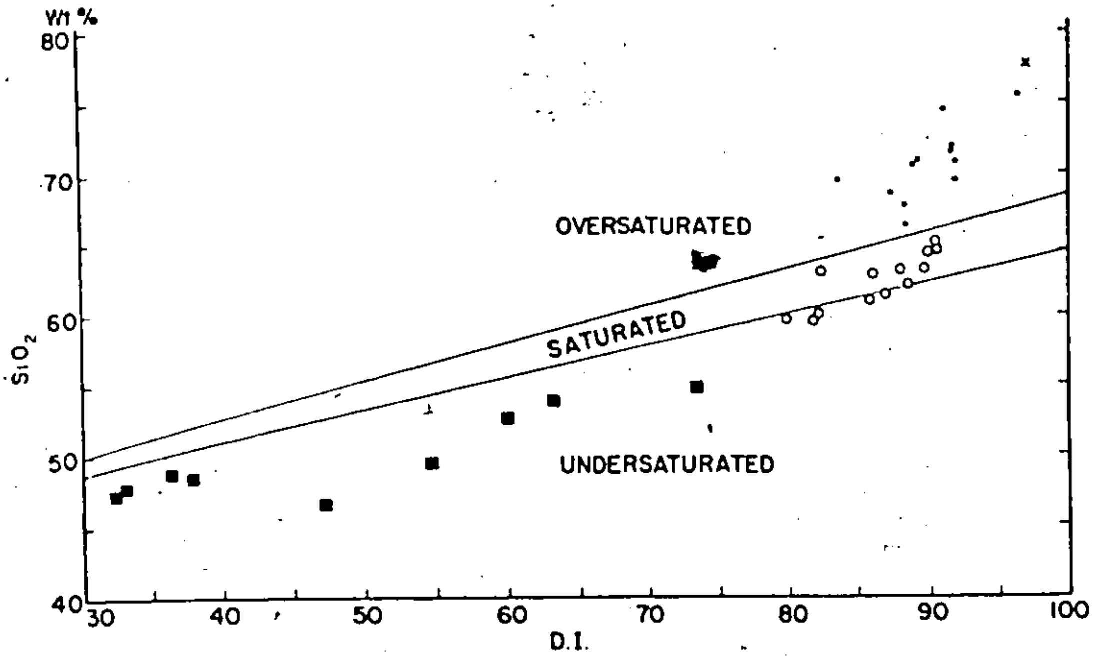

Figure 6.1.5

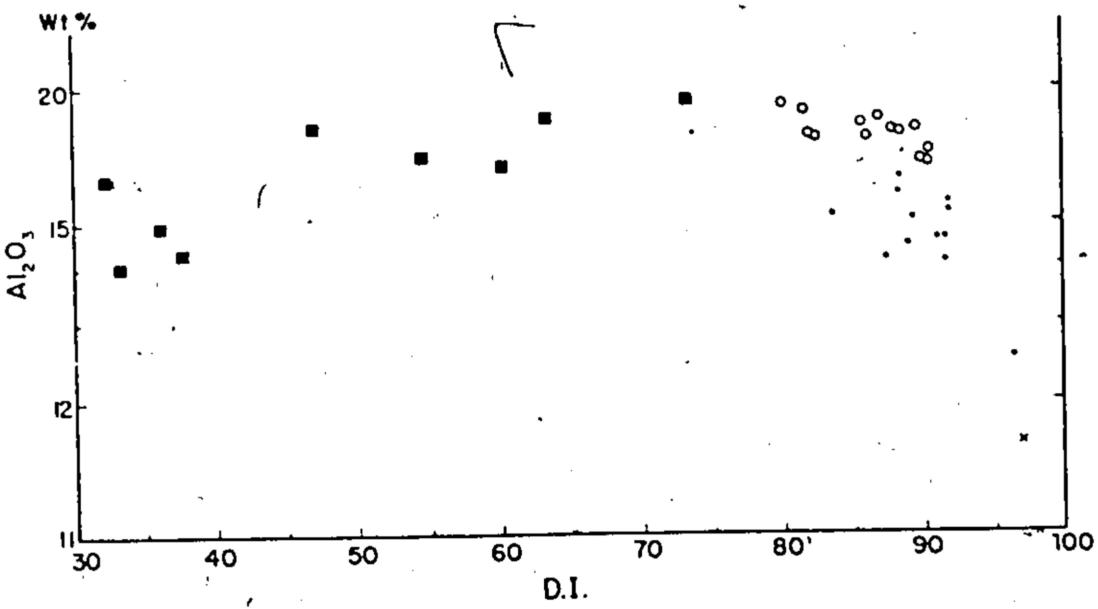

Figure 6.1.6

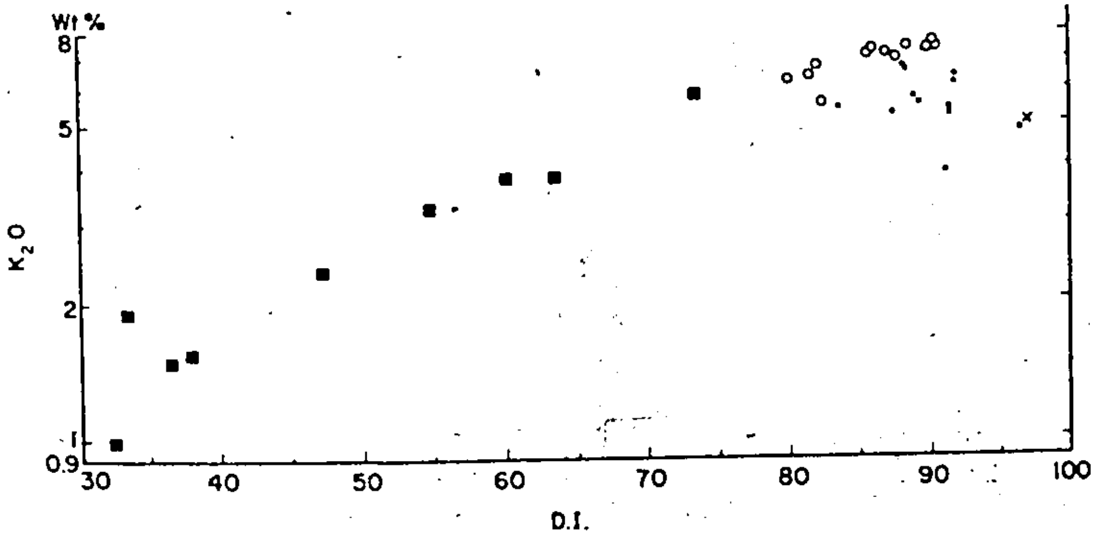

Figure 6.1.7

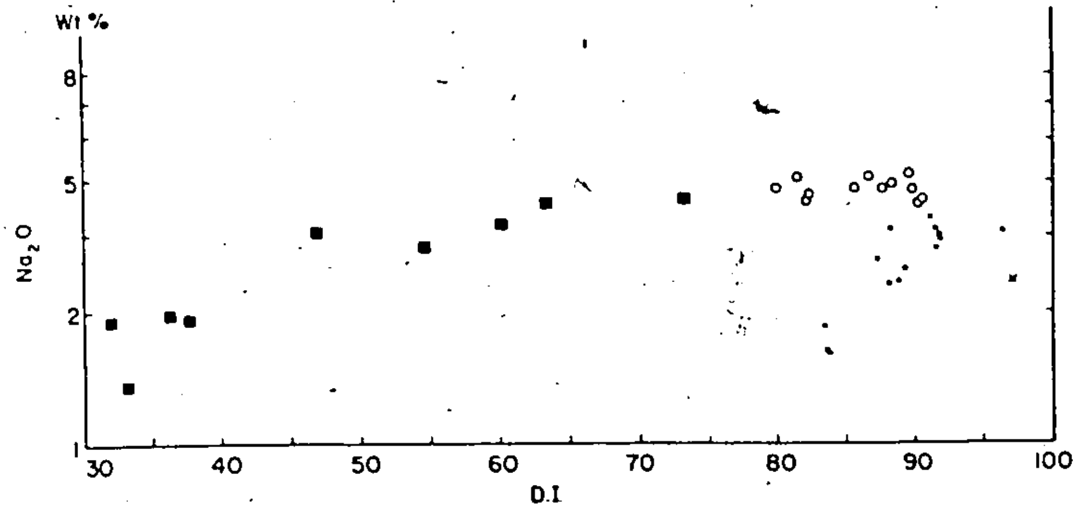

Figure 6.1.8

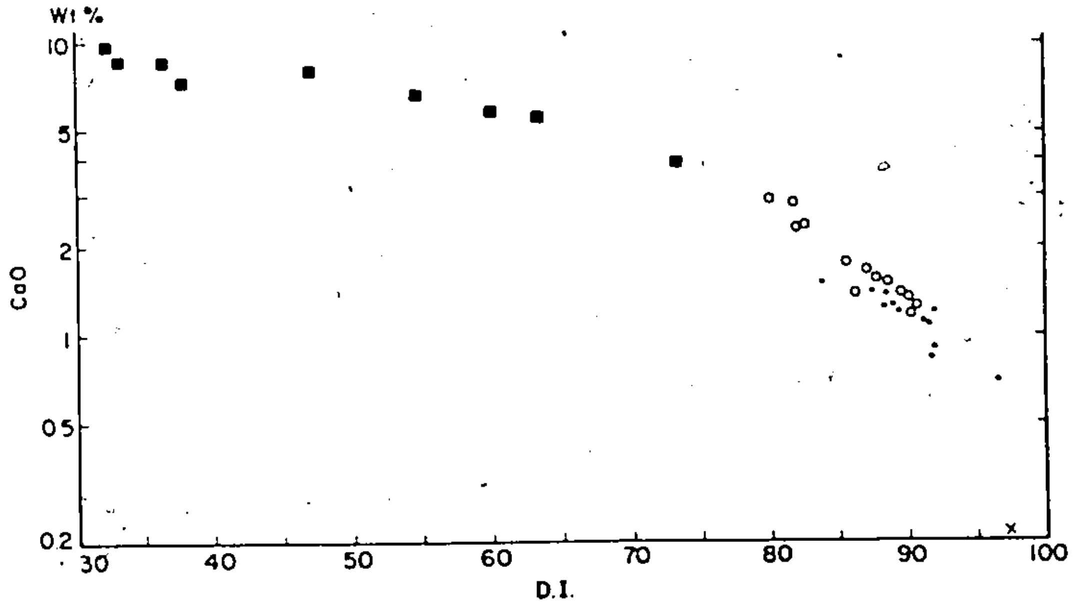

Figure 6.1.9

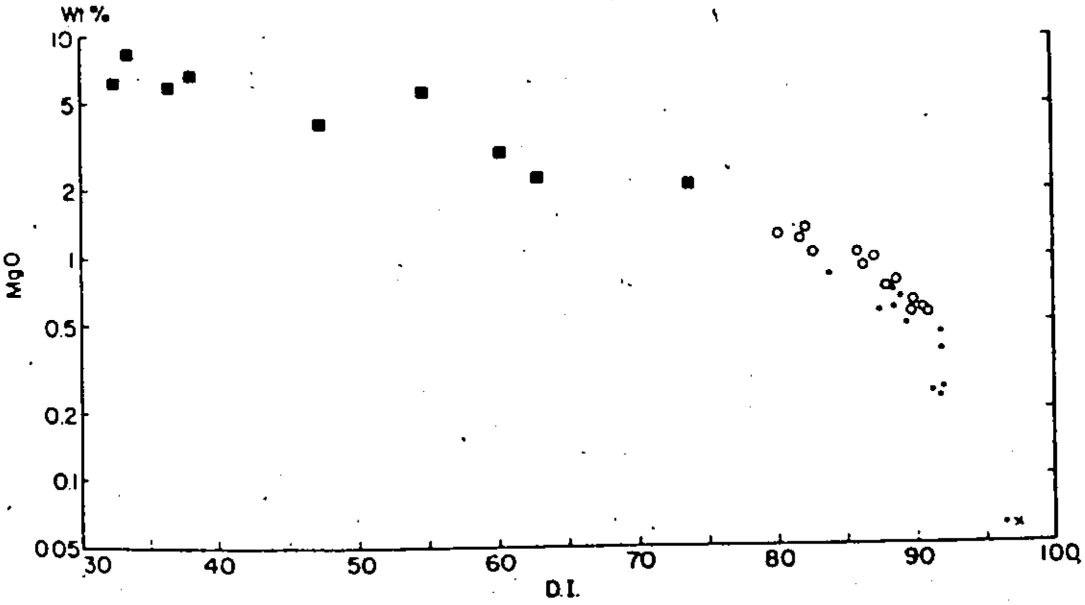

Figure 6.1.10

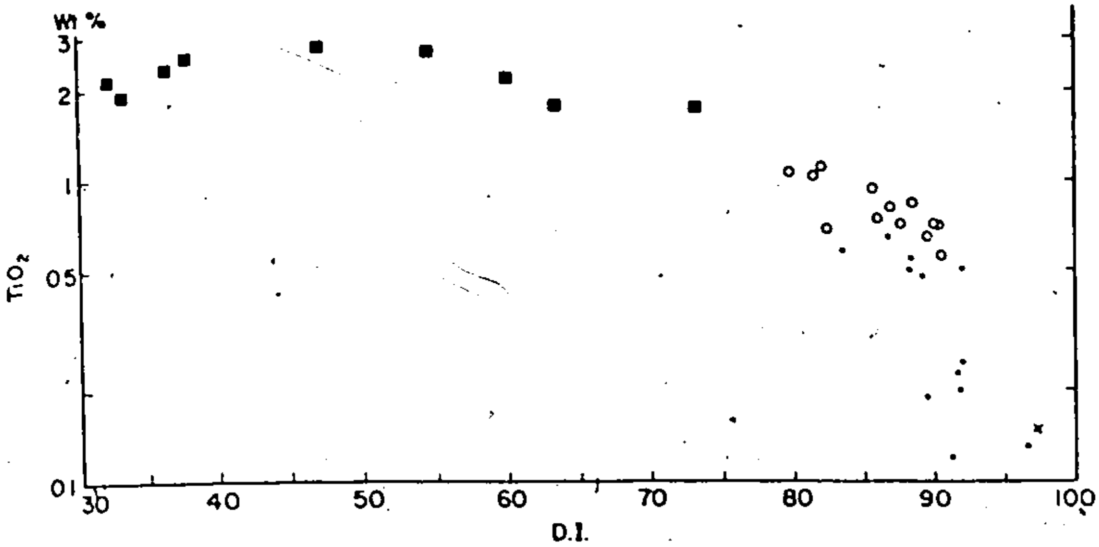

Figure 6.1.11

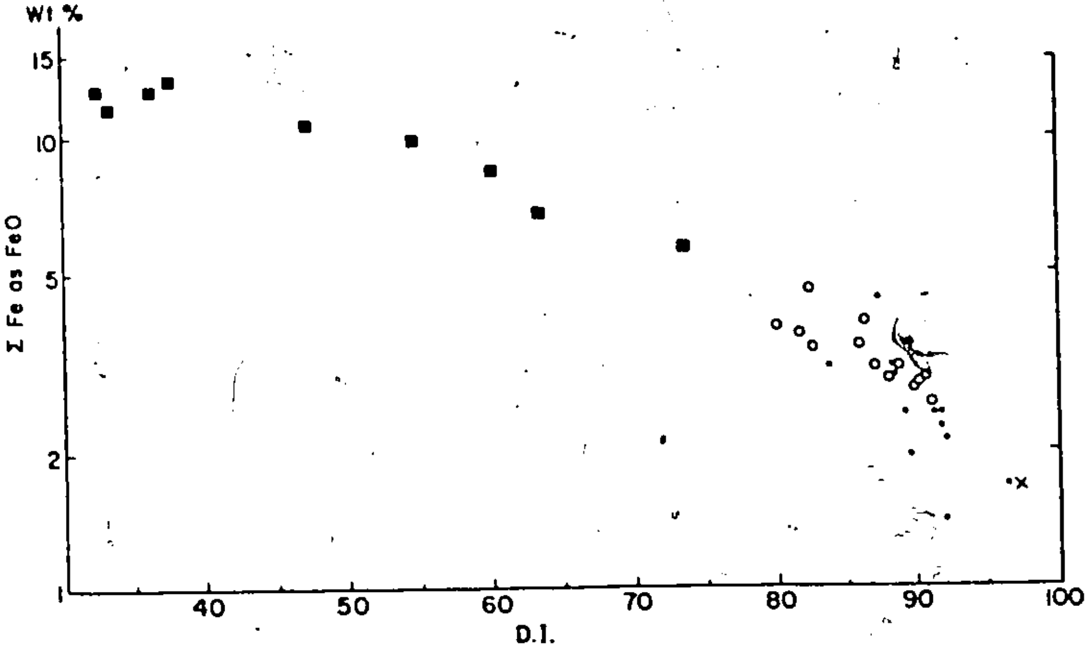

Figure 6.1.12

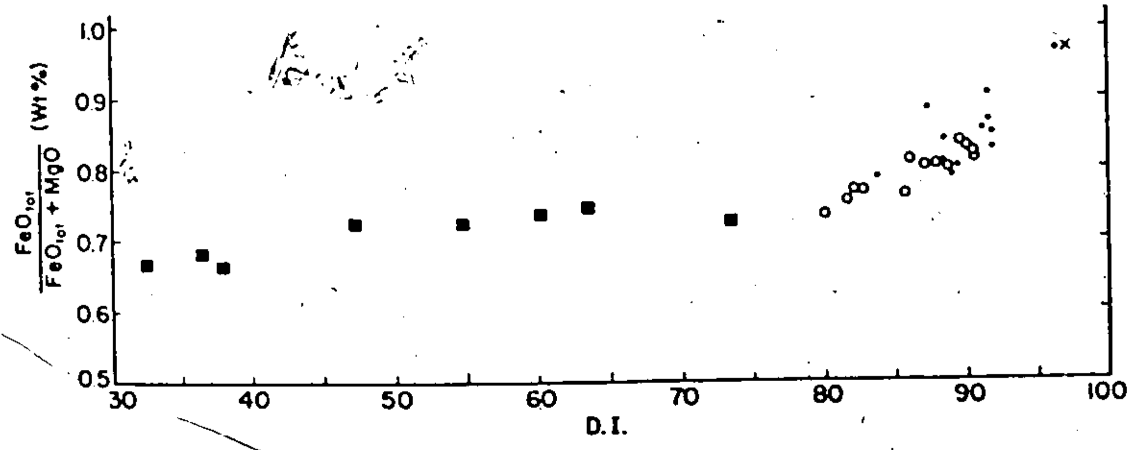

Figure 6.1.13

Figure 6.1.14

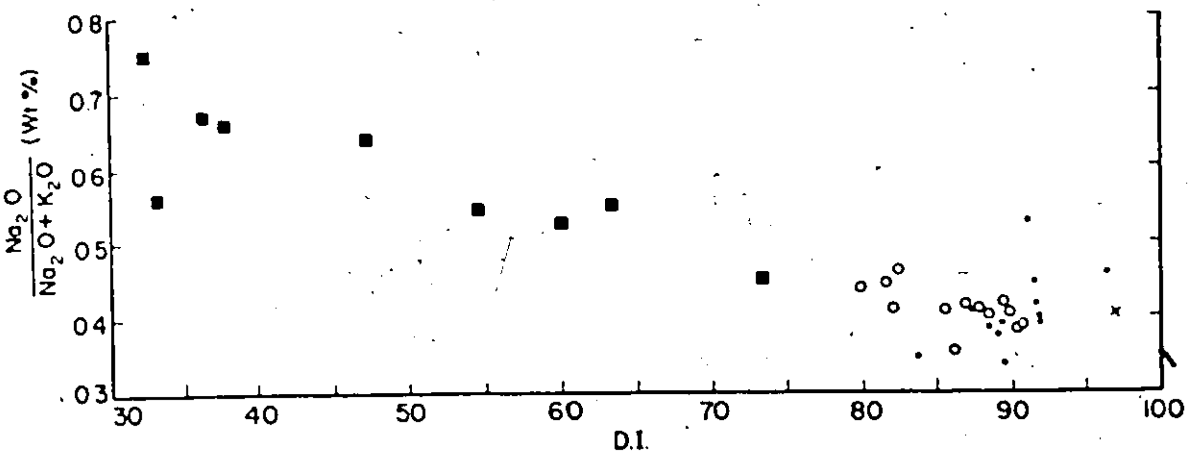

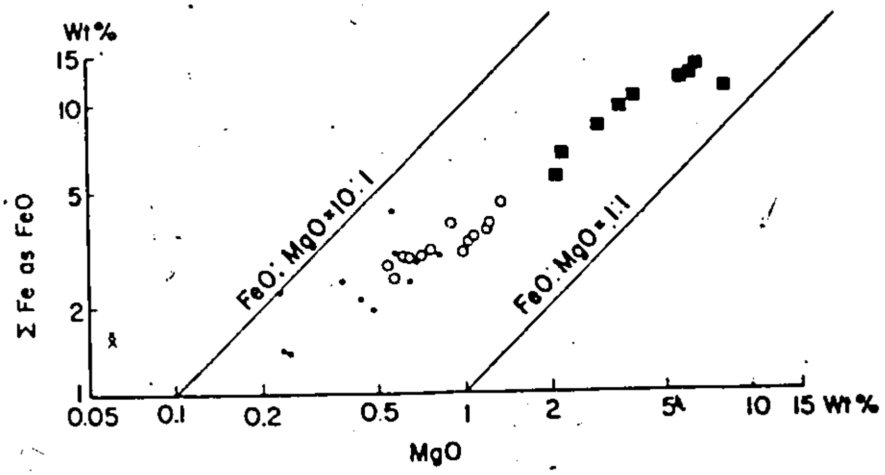

Figure 6.1.15 Relation between FeO_{total} and MgO

contents between these felsic rocks with a comparable D.I., reflect the higher content of quartz and lower amounts of feldspars in quartz monzonites in comparison with monzonites, while the contents of mafic minerals remain roughly constant.

Sodium increases slightly from dioritic to monzonitic rocks, while potassium shows a sharp rise in the same direction (Figures 6.1.7-8). Once again, quartz monzonites have lower contents of these two elements in comparison with monzonites for comparable D.I. values, expressing the smaller amounts of modal feldspars in the former rocks. The concentration of K in some dioritic rocks, however, is rather high in comparison with similar rocks (c.f. Currie and Ermanovics, 1971).

Total iron, titanium, calcium and magnesium decrease steadily toward the higher D.I. values, with Fe and Ti dropping sharply in the most acid granitic rocks (Figures 6.1.9-12). In spite of some scatter, the Na_2O/Na_2O+K_2O ratio progressively decreases from the dioritic toward the felsic rocks, while the $FeO_{total}/FeO_{total}+MgO$ ratio slightly increases in the same direction (Figures 6.1.13-14). Figure 6.1.15 shows a strong decrease in the Fe and Mg contents toward the more acid rocks of the pluton and illustrates the increasing Fe/Mg ratio in monzonite and quartz monzonite with the decrease of their concentration. Dioritic rocks, however, show only relatively small variations of the Fe/Mg ratio, in spite of the large variation of the absolute concentrations of these elements (in comparison with the felsic rocks).

In terms of $CaO-Na_2O-K_2O$, the variation in the rocks from the intrusive phases of the Loon Lake pluton are presented in Figure 6.1.16. The dioritic rocks indicate a large variation in the relative proportions of these elements with a smooth trend toward the Na-K join. Monzonite and quartz monzonite are clustered together along the Na-K join with a large overlap between them. Also on the plot of $(Na_2O-K_2O)-FeO_{total}-MgO$ (Figure 6.1.17), monzonite and quartz monzonite overlap while the variation trend of basic rocks demonstrates pronounced enrichment in alkalies.

When monzonitic and dioritic rocks are treated as a series on all these variation diagrams, they show smooth trends from the basic to the acid end with a nearly complete chemical gradation between them. These variations are consistent with, but do not prove the process of magmatic differentiation, since even if the rocks show a complete gradation, they might have been formed from two magmas with intermediate types having been developed by assimilation and hybridization (Nockolds and Allen, 1956). But the fact that at least some of the variations in the chemical composition of dioritic rocks are of primary magmatic origin is indicated by the variations of the Fe/Mg ratio, the variation of modal basicity of plagioclase, etc. On the other hand, some variations in diorites might be of secondary origin as suggested by petrographic features

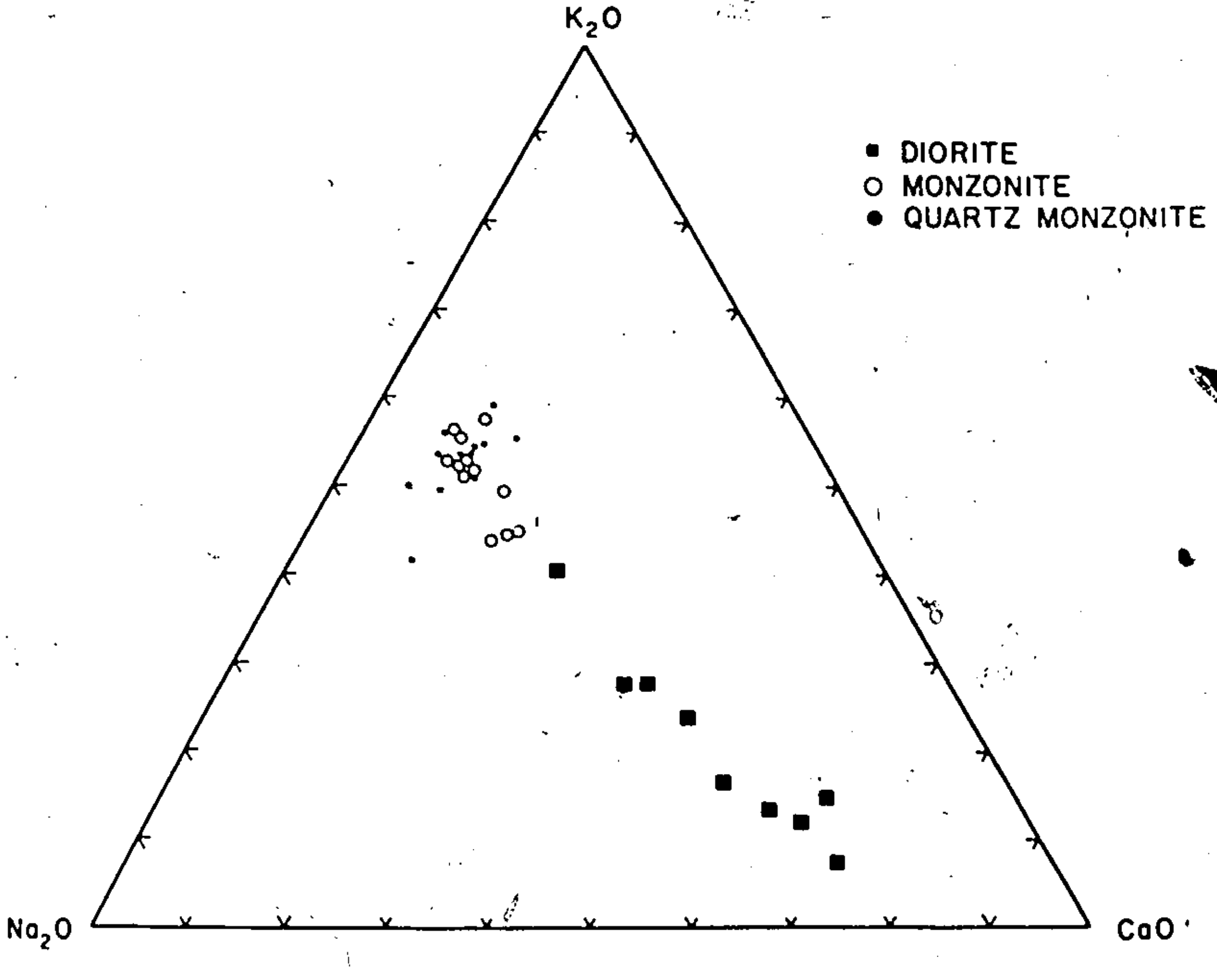

Figure 6.1.16 Na_2O-K_2O-CaO diagram

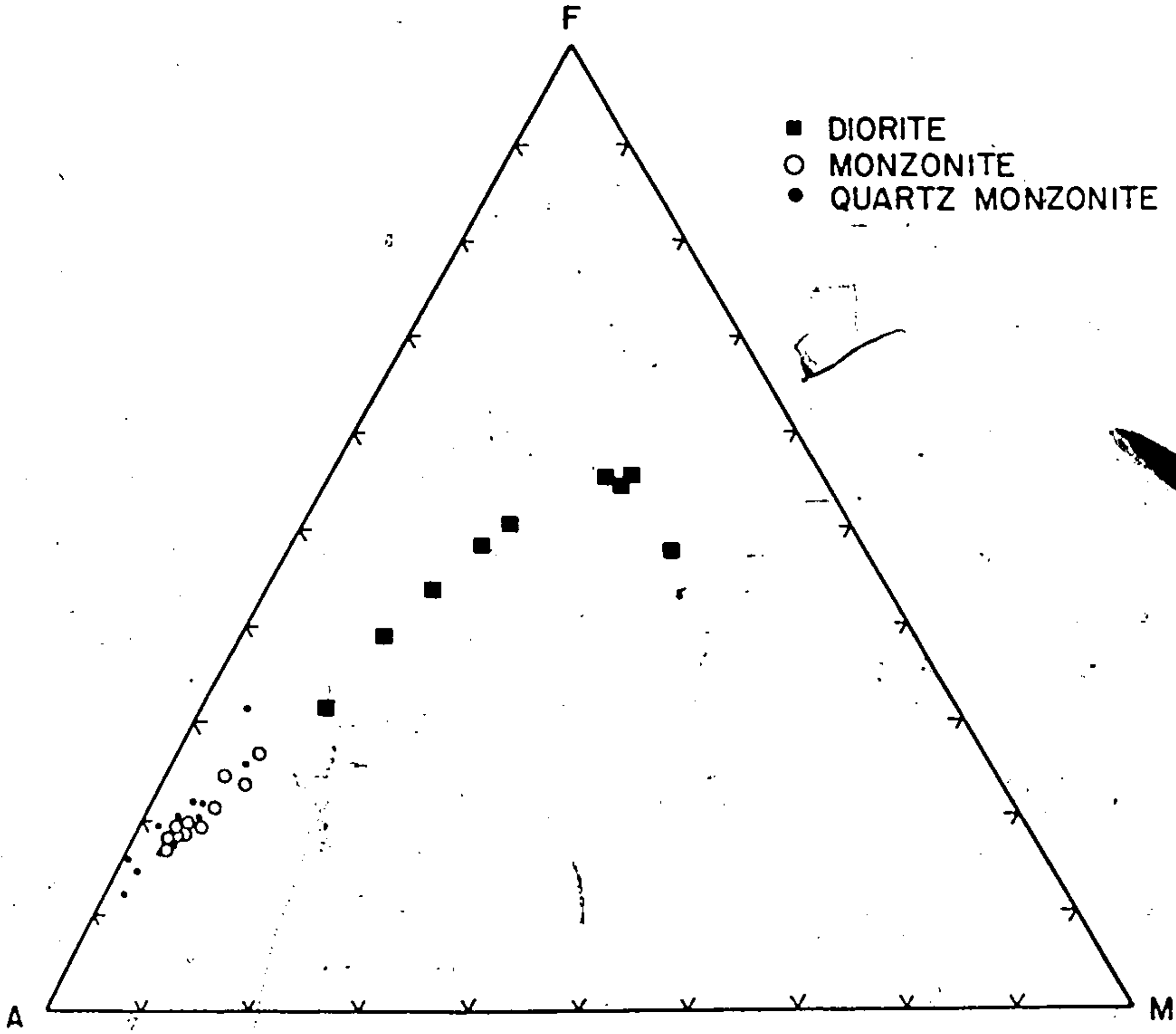

Figure 6.1.17 AFM diagram (A = Na_2O+K_2O; F = FeO_{total}; M = MgO)

(e.g. late microcline and biotite, textural evidence for replacement in diorite) which indicate an interaction between felsic rocks and diorite. Thus, it is difficult to evaluate to what degree the smooth trends in these diagrams are due to primary magmatic variation and to what degree they represent secondary alteration. Consequently, these diagrams do not appear to be conclusive as far as a possible genetic relationship between basic and felsic rocks of the pluton is concerned.

The variation trends for felsic rocks are compatible with those produced by magmatic differentiation and suggest a genetic relation between quartz monzonites and monzonites. It appears that the main difference between monzonites and quartz monzonites is quartz content. It is also of interest that one leucogranite (259), which is thought to be the product of partial melting, represents "the most differentiated" rocks on the variation diagrams.

6.1.2 Trace Elements

6.1.2.1 Rubidium

The contents of Rb in the rocks from the pluton are plotted against the differentiation index in Figure 6.1.18. The increase of Rb from dioritic toward more acid rocks is similar to trends reported from comparable suites of rocks and predicted by crystal-chemical principles. Rb concentration in monzonite

Figure 6.1.18 Variation of Rb as a function of D.I.

■ - diorite
▲ - monzonite
• - quartz monzonite
✕ - leucogranite 259

(symbols identical for Figures 6.1.19-6.1.21 and Figures 6.1.23-6.1.27 and Figures 6.1.29-6.1.37)

Figure 6.1.19 Variation of the K/Rb ratio as a function of D.I.

Figure 6.1.20 Relation between the K/Rb ratio and modal content of biotite

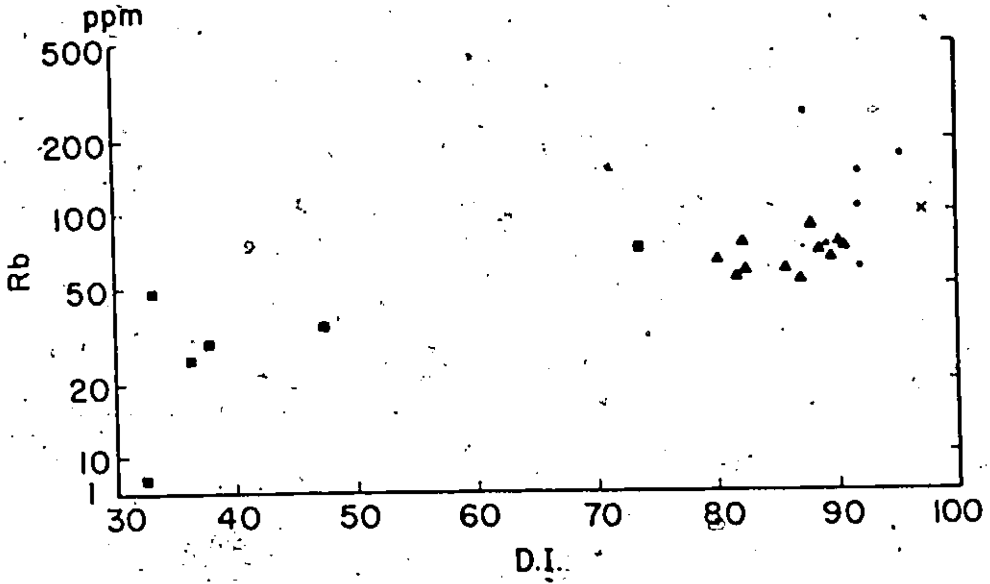
ppm
500
200
100
50
20
10
1
Rb
30
40
50
60
70
80
90
100
D.I.

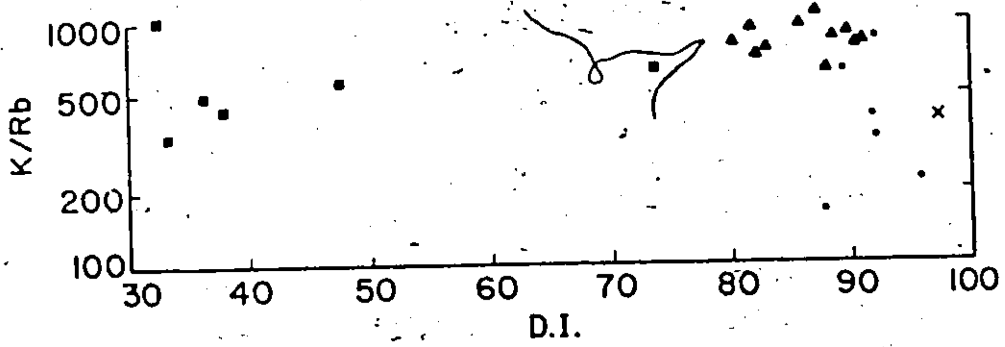
1000
500
200
100
K/Rb
30
40
50
60
70
80
90
100
D.I.

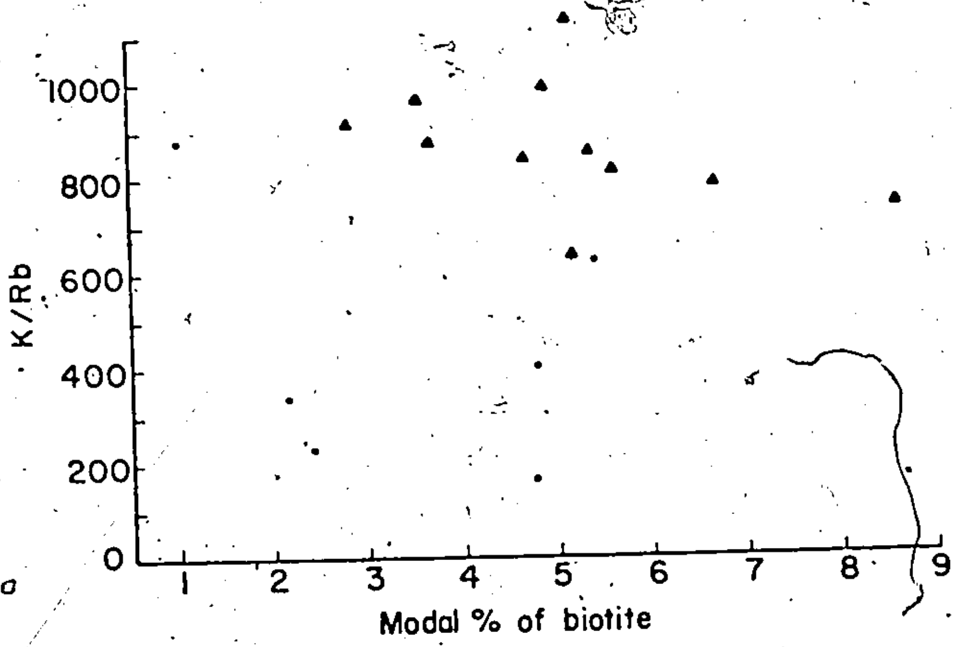
1000
800
600
400
200
0
K/Rb
1
2
3
4
5
6
7
8
9
Modal % of biotite

is relatively constant, varying between 50-100 ppm. These values are lower than world averages for syenites and monzonites, given by Heier and Adams (1964) as 124 and 136 ppm, respectively. In general, quartz monzonites have higher Rb contents than monzonites, but in many cases lower than the averages of 200, 170 and 150 ppm calculated for granitic rocks (Vinogradov, 1962; Heier and Adams, 1964; Taylor, 1965, respectively). The content of Rb in the Loon Lake pluton is comparable to the values given by Sauerbrei (1966) for rather similar plutons in the Westport area.

The close geochemical association between K and Rb, due to a very similar character, is well documented. As Goldschmidt (1954, p.164) already pointed out, the K/Rb ratio decreases toward the more acid rocks in a consanguinous igneous series. The tendency for Rb to become enriched relative to K under processes of extreme differentiation is usually ascribed to the 10% larger ionic radius (e.g. Heier and Adams, 1964; Taylor, 1965). Thus, the K/Rb ratio can be a good indication of such differentiation processes (Taylor, 1965; Shaw, 1968). The variation of the K/Rb ratio in the rocks from the pluton as a function of D.I. is illustrated in Figure 6.1.19. The relatively constant K/Rb ratios in monzonite contrast with a sharp decrease in quartz monzonite. Since Rb is mainly concentrated in biotite, the relatively constant K/Rb ratio and Rb content in monzonites might indicate that biotite fractionation was not prominent.

The tendency of the K/Rb ratio and Rb abundances in quartz monzonites to decrease toward the more acid rocks is consistent with the process of magmatic differentiation.

In most crustal rocks, the variation of the K/Rb ratio is usually limited, with an average of about 230 (Heier and Adams, 1964; Taylor, 1965; Shaw, 1968). Ahrens et al. (1952) and Heier and Taylor (1959a) concluded that the values in excess of 440 must be considered as anomalous. The high K/Rb ratios for basaltic achondrites and some oceanic tholeiites led to a suggestion that "values in excess of ~500 may represent mantle or deep crust material" (Reynolds et al., 1969, p.268). Relative to the "normal" K/Rb value of crustal rocks, the ratios in the rocks of the Loon Lake pluton are very high, particularly in monzonites and some quartz monzonites (~600-1150). Dioritic rocks have lower values on the average than monzonite although still higher than typical crustal values. The high K/Rb ratios in monzonites and some quartz monzonites are similar to the values of comparable rocks from the Westport area (Sauerbrei, 1966) and also to some mangeritic and monzonitic rocks associated with anorthosites (e.g. Reynolds et al., 1969; Green et al., 1972).

It has been suggested that the high K/Rb ratio in syenitic rocks might be due to the variable contents of biotite (c.f. Nash and Wilkinson, 1971). Therefore, in Figure 6.1.20 the K/Rb ratios of the rocks from the pluton were plotted against the biotite content of the rocks. The lack of any distinct trend in this diagram indicates that the K/Rb ratio in the felsic rocks does not depend on the amount of biotite present in a rock. (Alternative explanations for the high K/Rb ratio in monzonites and some quartz monzonites will be considered in a later section).

The data for the Loon Lake pluton are shown on a plot of Rb content against the K/Rb ratio in Figure 6.1.21. The variation trends for some well-known series, each comprising a span of rocks from basic to acid, are given for comparison in Figure 6.1.22. They include the plutonic rocks of the South California batholith, and volcanic rock suites from the Lassen Peak and Lesser Antilles (after Dupuy, 1970). For these series, magmatic differentiation is generally accepted as the main process responsible for the formation of the different rock types. Also shown are rhyolite ignimbrites from New Zealand which were probably derived from andesites by partial melting (Ewart et al., 1968; Dupuy, 1970). These diagrams are preferred to the conventional K/Rb-K plot, since K shows relatively smaller variation in comparison with Rb.

The rocks from the Loon Lake pluton are separated into two distinct trends, similar to those of other suites of rocks attributed to magmatic differentiation. The first trend, with lower Rb values includes only dioritic rocks[1], while the

---

[1] Contrary to the previous variation diagrams (section 6.1.1 and Figures 6.1.18-19), dioritic rocks in this Figure include only rocks which petrographically appear to be least altered.

Figure 6.1.21 Variation of the K/Rb ratio as a function of Rb in the rocks from the pluton

Figure 6.1.22 Variations of the K/Rb ratio as a function of Rb in some well-known rock series (after Dupuy, 1970)

curve a - South California batholith
b - Lassen Peak
c - Lesser Antilles
× - andesite, New Zealand
● - ignimbrite (rhyolite), New Zealand

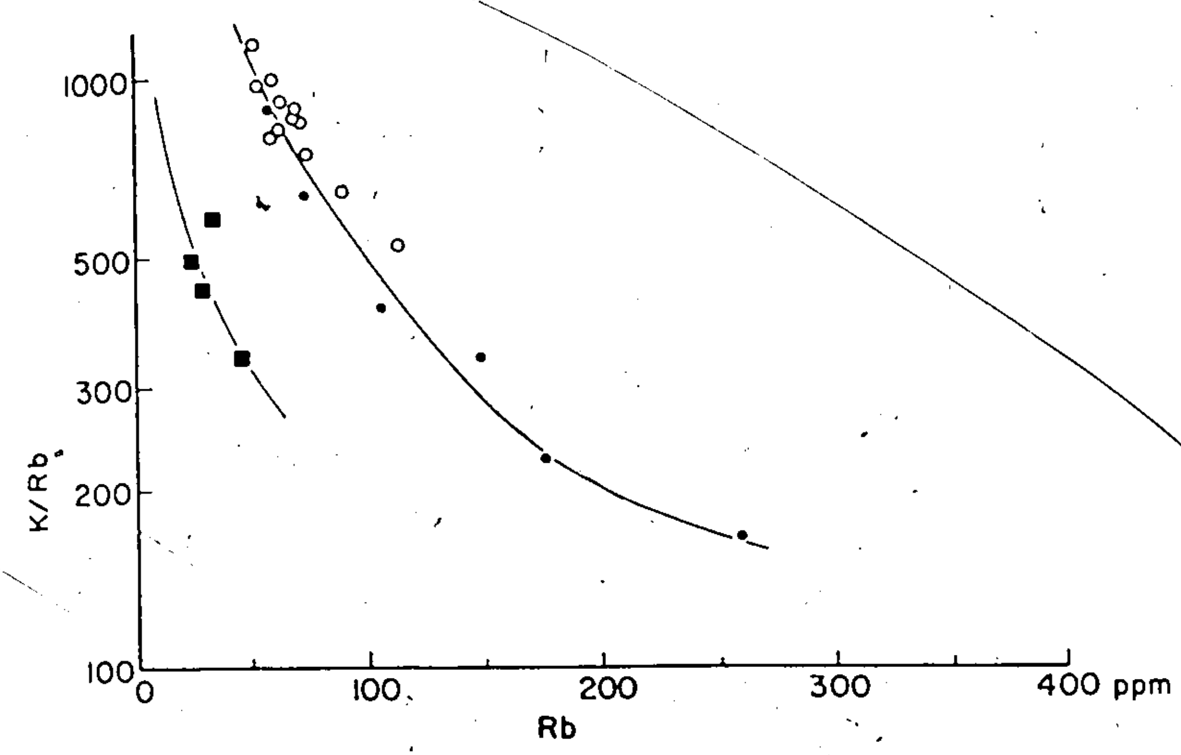
1000
500
300
200
100
K/Rb
0
100
200
300
400 ppm
Rb

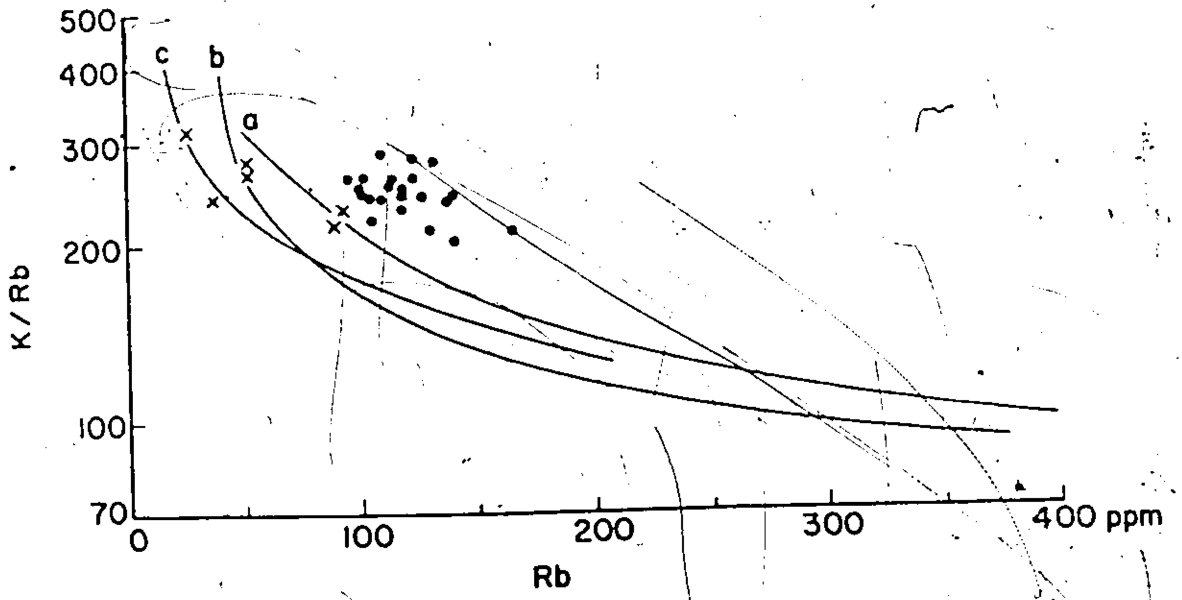
500
400
300
200
100
70
K/Rb
c
b
a
0
100
200
300
400 ppm
Rb

other represents monzonites and quartz monzonites. These separated trends suggest that basic and felsic rocks are probably not genetically related. Another possible explanation, that the separated dioritic trend reflects only the secondary changes, is difficult to evaluate. But it does not appear very probable that secondary modification would produce a trend similar to those of differentiation but separated from that of felsic rocks from the pluton. On the other hand, the well-defined trend for basic and felsic rocks might suggest that these rocks underwent relatively extensive magmatic differentiation.

6.1.2.2 Strontium

In the rocks from the Loon Lake pluton, the highest amount of Sr is present in dioritic rocks, ranging from about 850-1800 ppm. The Sr concentration in monzonite is highly variable and ranges from about 70-850 ppm. The low Sr content is generally confined to rocks from the periphery of the monzonite core of the pluton. The average Sr content of monzonitic rocks is of an order similar to Sauerbrei's (1966) average (~300 ppm) for equivalent rocks from the Westport area and also is of similar magnitude as the average estimated by Turekian and Kulp (1956) for high Ca-granitic rocks (440 ppm). Quartz monzonite has a low Sr content, varying from about 30-260 ppm.

During the process of fractionation of basic magma, Sr may behave in two different ways (Nockolds and Allen, 1953).

It may increase gradually to a maximum concentration in the intermediate rocks and then decrease in highly differentiated rocks (e.g. Noll, 1934; Wager and Mitchell, 1951; Taylor, 1965). On the other hand, Sr may only gradually decrease from basic to acid rocks (Nockolds and Allen, 1953). These features can also be deduced from Figure 6.1.23 (after Dupuy, 1970) which shows that in igneous rocks in general, the highest concentrations of Sr may be encountered in both acid and basic rocks.

A comparison of the Ca-Sr relationship in the pluton with the general variation of these elements in igneous rocks (Figure 6.1.23) shows that the monzonite and quartz monzonite are plotted in the field of "acid" igneous rocks, while dioritic rocks fall slightly outside the field for "basic" igneous rocks given by Dupuy (1970).

Figure 6.1.24 gives the variation of Sr contents in the Loon Lake pluton as a function of D.I. Sr shows some scatter when only dioritic rocks are considered, but a sharp decrease with the increase of D.I. is apparent in monzonite and quartz monzonite. This pronounced decline of Sr content toward the more acid rock types is also reflected by an increase of the Ca/Sr ratio in felsic rocks (Figure 6.1.25), which is typical for "highly differentiated granites because of the additional removal of much of Sr by capture in the earlier K-minerals" (Kolbe, 1965, p.187). The overall tendency for the decrease of the Ca/Sr ratio with the increase of Ca in the felsic rocks, despite the

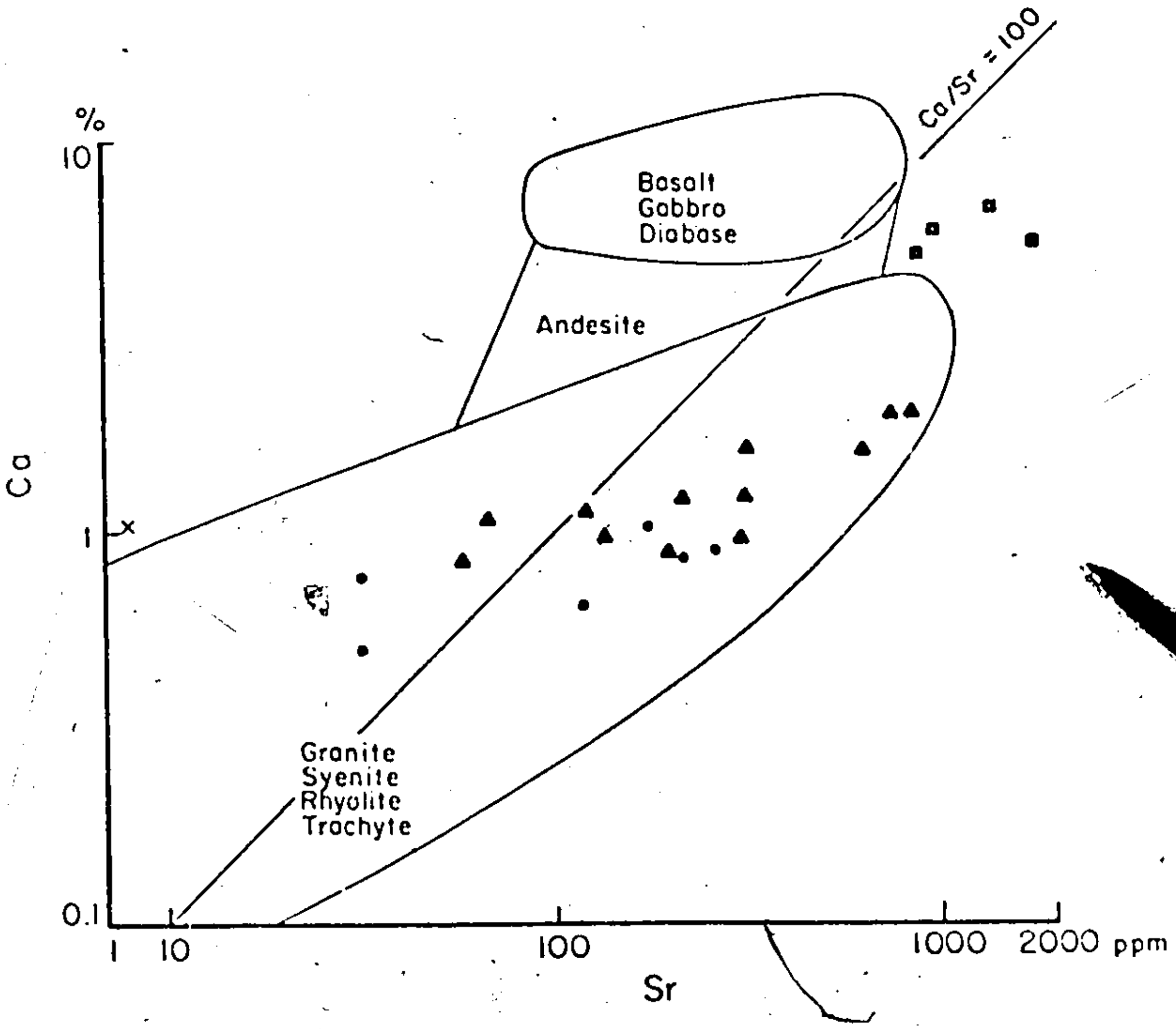

Figure 6.1.23. Relation between Ca and Sr. The outlined fields show generalized relationship in common igneous rocks (after Dupuy, 1970)

Figure 6.1.24 Variation of Sr as a function of D.I.

Figure 6.1.25 Variation of the Ca/Sr ratio as a function of D.I.

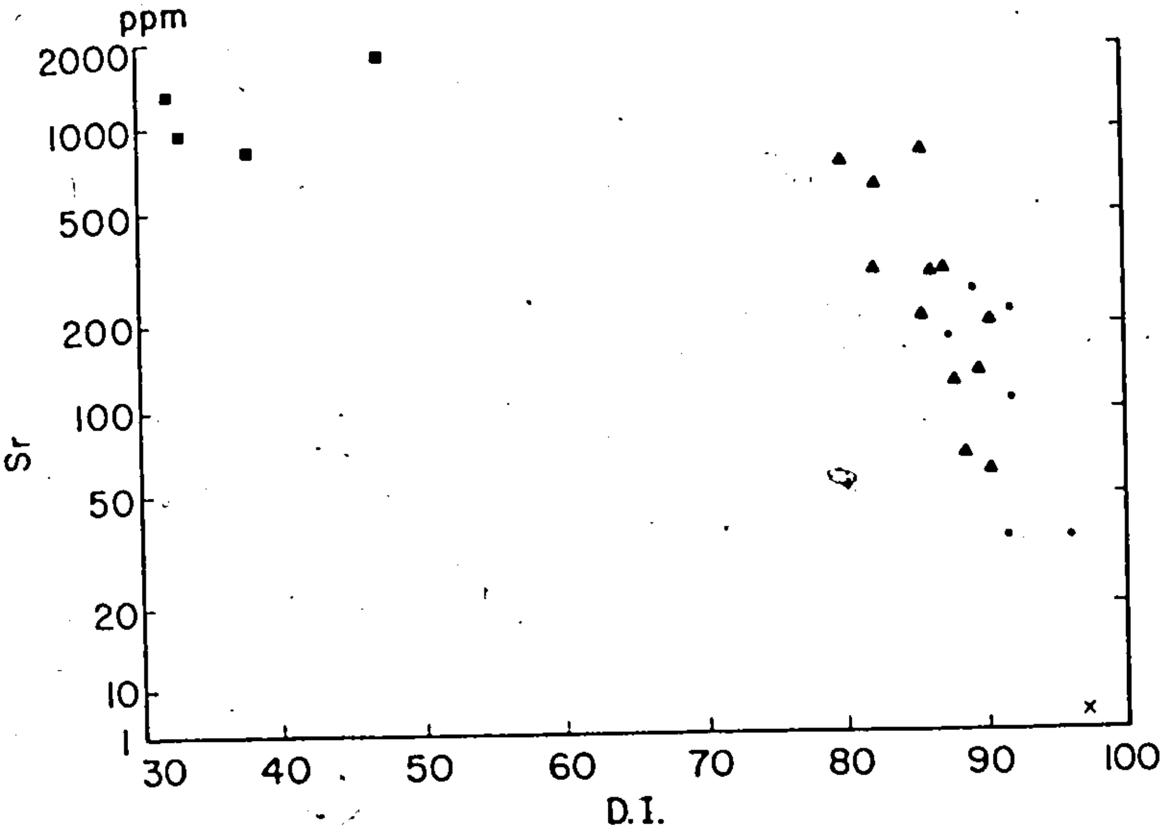
ppm
2000
1000
500
200
100
50
20
10
1
Sr
30
40
50
60
70
80
90
100
D.I.

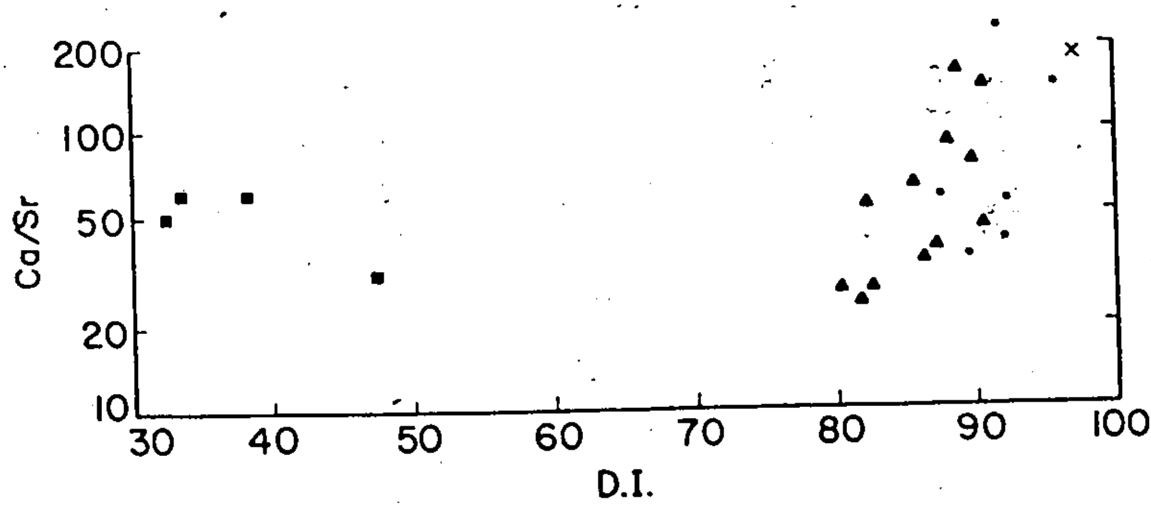
200
100
50
20
10
Ca/Sr
30
40
50
60
70
80
90
100
D.I.

slight positive correlation between Ca and Sr, can be deduced from Figure 6.1.23.

The variation of Rb as a function of Sr is shown in Figure 6.1.26, together with the generalized relationship of Rb and Sr in some igneous rocks (after Hedge, 1966). Diorite, monzonite and quartz monzonite show a negative correlation between Rb and Sr. The trend of the Rb/Sr ratio to increase toward the more acid rocks is consistent with that predicted for differentiating silicate liquids. It is of interest that the quartz monzonites fall on this diagram in the trachytic field in spite of the fact that they have enough quartz for rhyolite.

Figure 6.1.27 shows the Ca/Sr ratio of the rocks from the pluton plotted as a function of Sr concentration, while on Figure 6.1.28 are outlined for reference the trends of the well-defined magmatic sequences and also acid volcanic rocks from New Zealand, which are thought to be the result of partial melting (Ewart et al., 1968; Dupuy, 1970). The rocks of the Loon Lake pluton form two distinct trends - one for dioritic and the second for monzonitic and quartz monzonitic rocks. As in the K/Rb-Rb diagram, the separated trend for dioritic rocks may argue against the genetic link between basic and felsic rocks from the pluton (assuming that the separated trend does not reflect only a secondary alteration). On the other hand, the well-defined trend for basic rocks might suggest that diorites

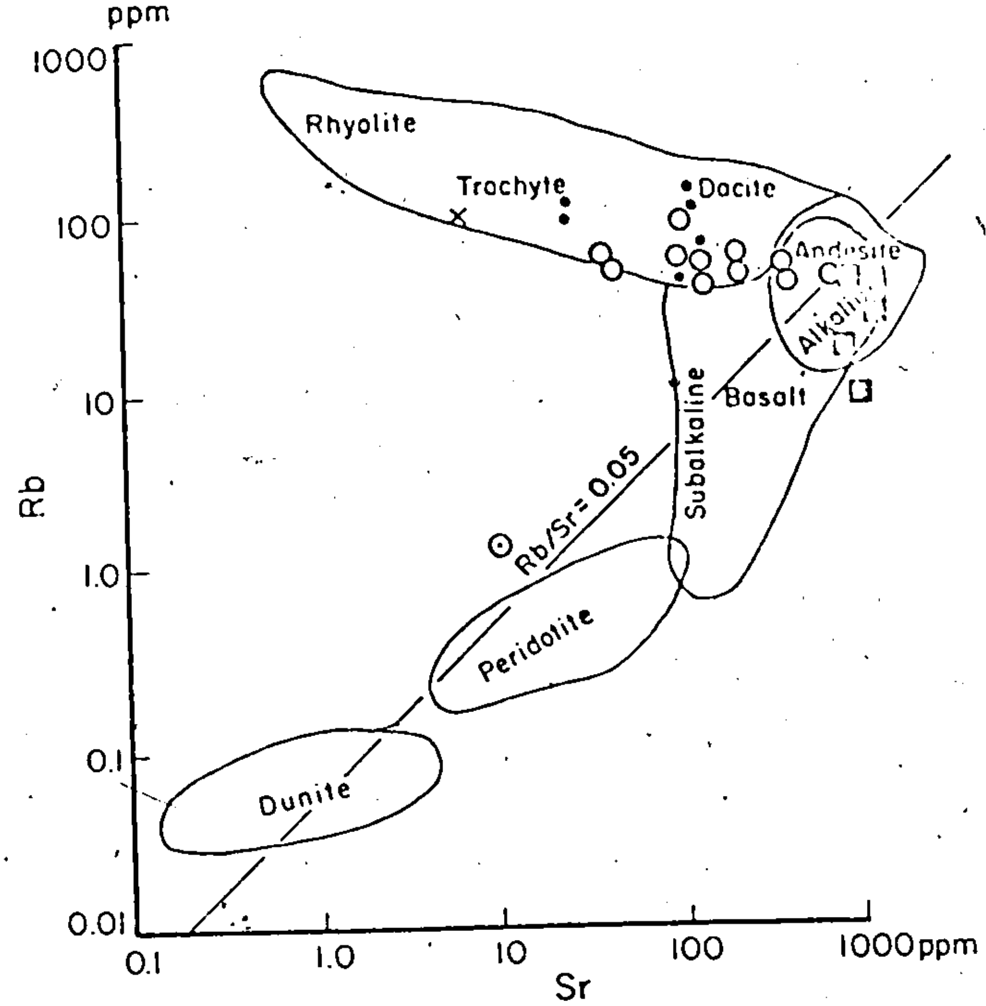

Figure 6.1.26 Relation between Rb and Sr. The outlined fields show generalized relationship in common igneous rocks (after Hedge, 1966)

⊙ - dunite 130

Figure 6.1.27 Variations of Ca/Sr ratio as a function of Sr in the rocks from the pluton

Figure 6.1.28 Variations of Ca/Sr ratio as a function of Sr in some well-known rock series (after Dupuy, 1970)

curve a - Skaergaard intrusion
b - Lassen Peak
c - Lesser Antilles
× - andesite, New Zealand
▲ - ignimbrites (rhyolite), New Zealand

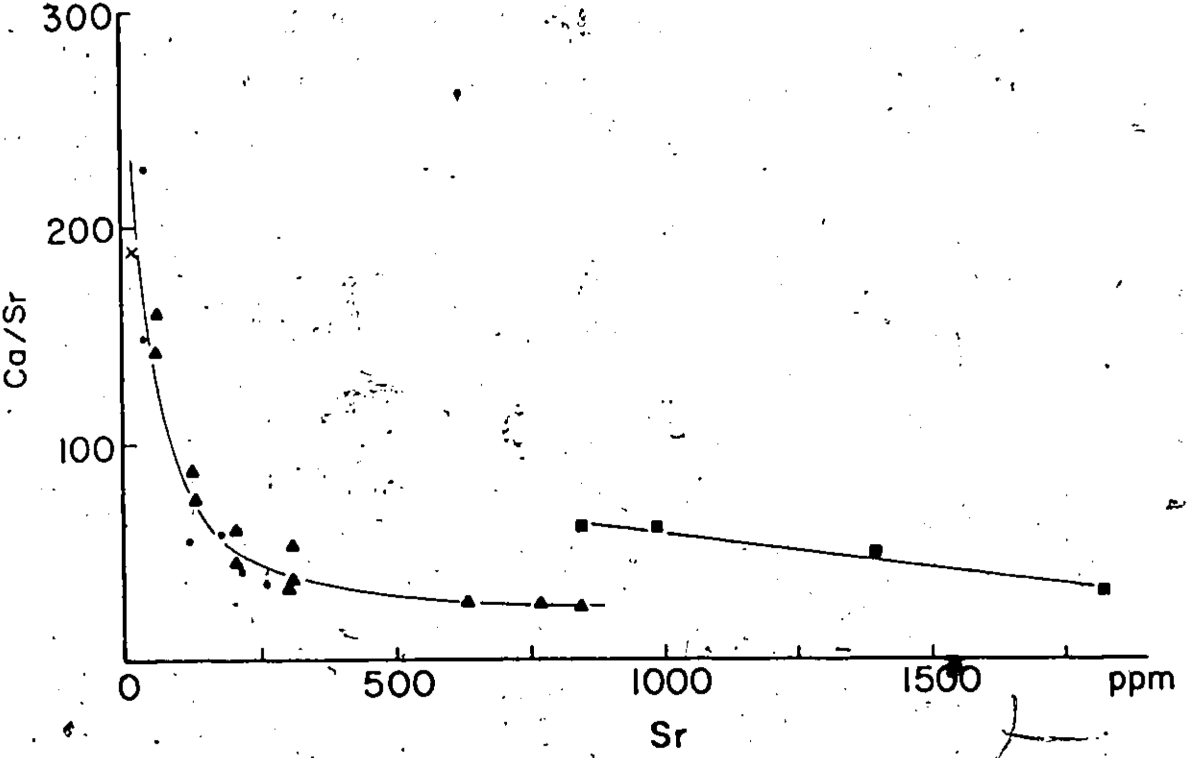
300
200
100
Ca/Sr
0
500
1000
1500
ppm
Sr

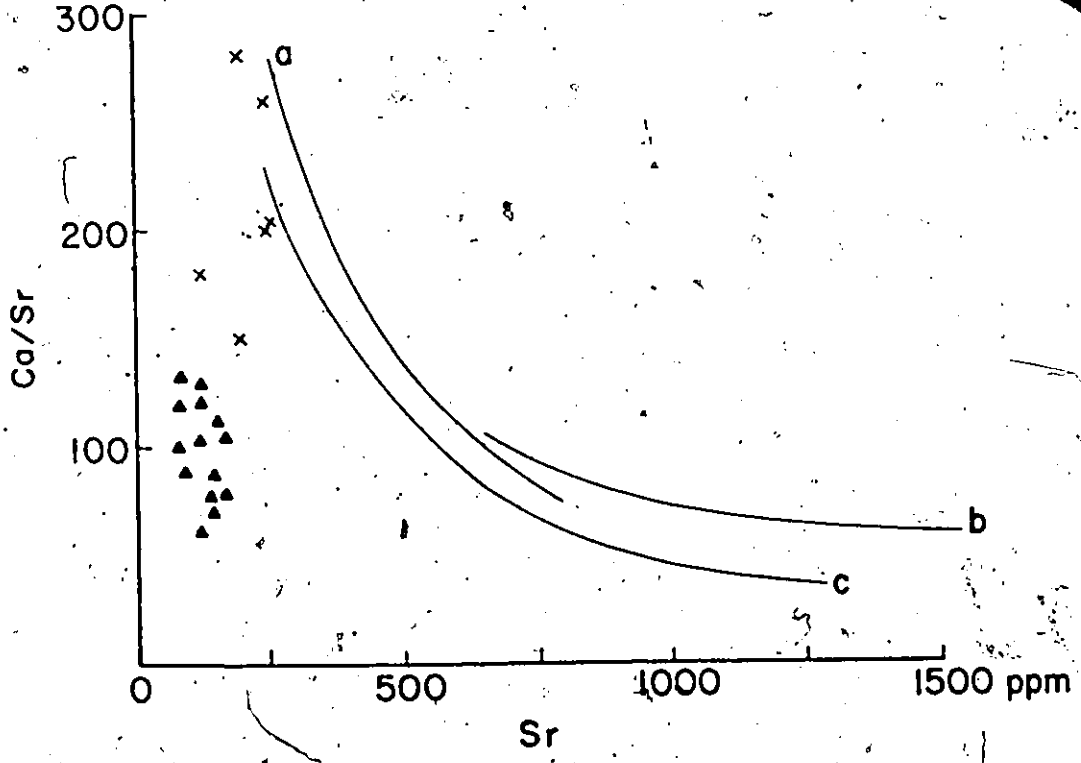
300
200
100
Ca/Sr
a
b
c
0
500
1000
1500 ppm
Sr

underwent magmatic differentiation.

The smooth trends and the wide range of variation of felsic rocks are of interest. The similarity of their trend to that of magmatic series indicates that magmatic differentiation has been the prominent process during their formation. Since the variation of Sr is mainly controlled by feldspars, it suggests that feldspar fractionation has played a significant role in the genesis of these rocks.

6.1.2.3 Barium

The content of Ba in the rocks from the pluton is very variable, but compared with other recorded values of similar rocks and rock suites, it is on the average relatively high, particularly in monzonites and some dioritic rocks (c.f. Figure 6.1.29, after Dupuy, 1970). In monzonites, it varies from about 450-5200 ppm, whereas Turekian and Wedepohl (1961) have given 1600 ppm as the average crustal values for comparable rocks.

In magmatic rocks, Ba is mostly associated with potassium, being captured in early K-minerals (e.g. Hei[illegible], 1962, 1966; Taylor, 1965). Partly due to the relatively late crystallization of the main K-minerals during the process of progressive fractionation, Ba gradually increases and then it may sharply fall in the late differentiation stages (Nockolds and Allen, 1953; Taylor, 1965).

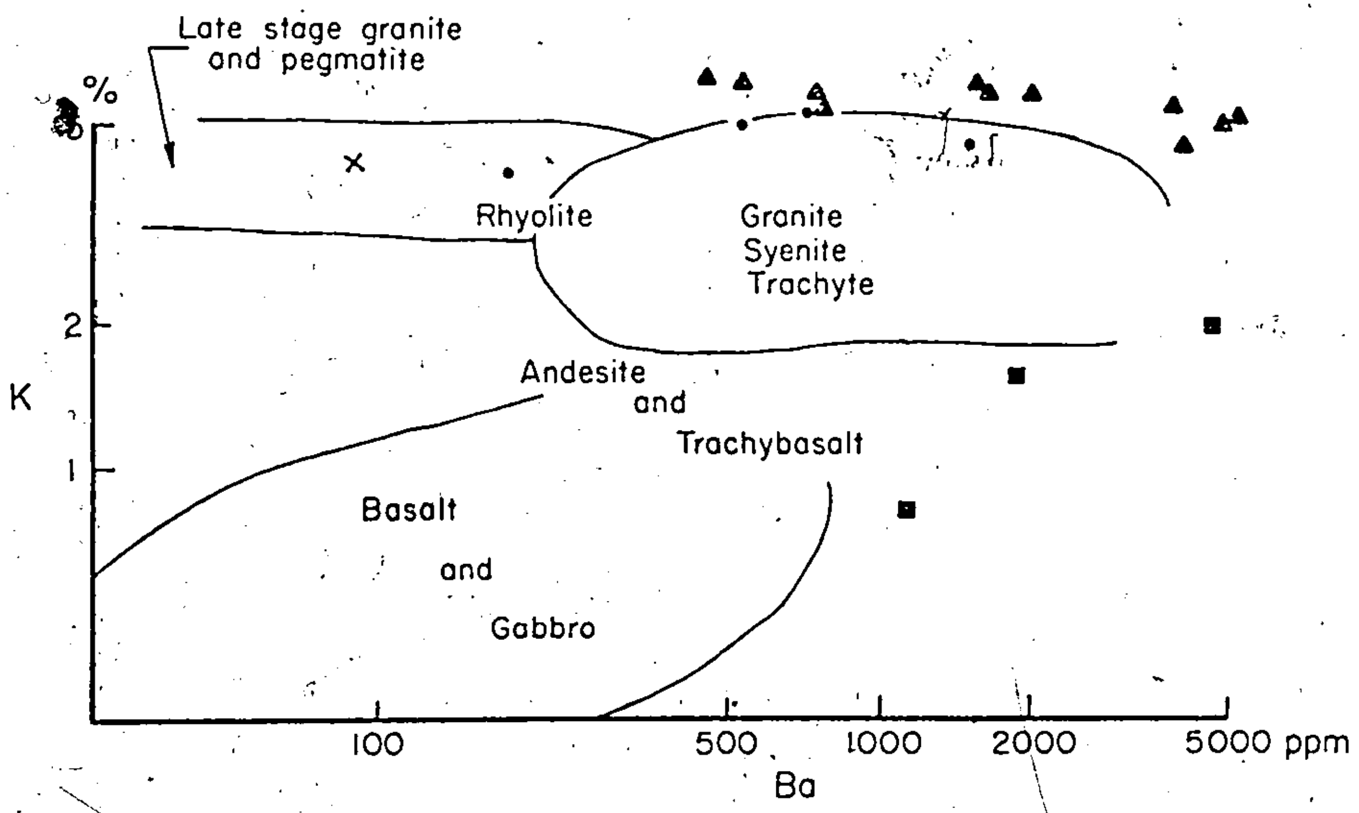

Figure 6.1.29 Relation between K and Ba. The outlined fields show generalized relationship in common igneous rocks (after Dupuy, 1970)

The variation trend of Ba for monzonite and quartz monzonite as a function of D.I. shows a sharp decline toward the more acid rocks (Figure 6.1.30). This trend of Ba is also reflected by the steep variation of the K/Ba and 100xBa/K+Ca ratios (Figure 6.1.31-32), which are characteristic for the late stages of highly differentiated magma (Nockolds and Allen, 1953, 1954; Kolbe, 1965). The variation trend of Ba is rather similar to that of Sr. The good covariance between these two elements observed in the Loon Lake pluton is a common case of a genetically related series, particularly with granitic and syenitic rocks (c.f. Siedner, 1965). Philpotts and Schnetzler (1970a) have shown that the only phenocrysts in which the concentration of Sr and Ba is greater than in the coexisting liquid are the feldspars and micas. While plagioclase and K-feldspar have a concentration of Sr larger than that in the liquid, Ba is concentrated in potassic feldspar and mica. The observed smooth variation trend for Ba and Sr in the pluton is consistent with the crystallization of feldspars as the major phases, which would preferentially take up the Sr and Ba from the liquid so that the progressively more acid residual rocks would be depleted in these two elements. The values of the Ba/Sr ratio remain relatively constant throughout the monzonite and quartz monzonite of the pluton (Figure 6.1.33), which is rather similar to the Ba/Sr trend produced during extreme differentiation of the Paresis alkali igneous suite (Siedner, 1965, Fig. 8).

Figure 6.1.30 Variation of Ba as a function of D.I.

Figure 6.1.31 Variation of the K/Ba ratio as a function of D.I.

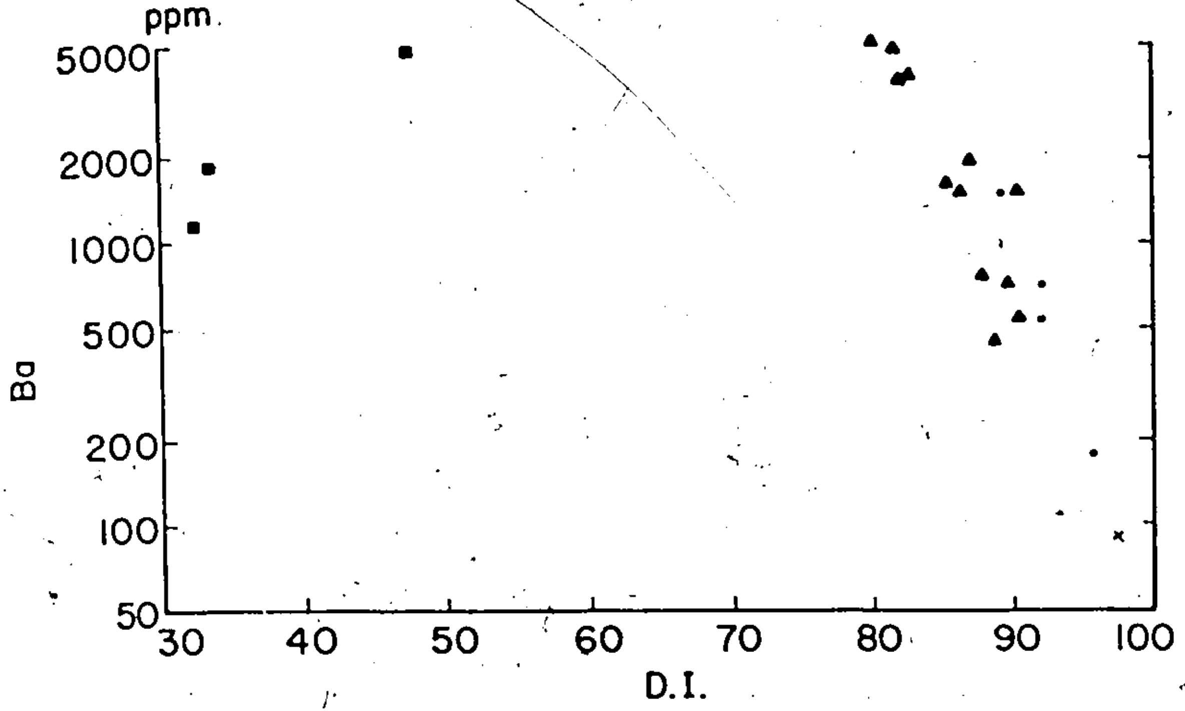
ppm.
5000
2000
1000
500
200
100
50
Ba
30
40
50
60
70
80
90
100
D.I.

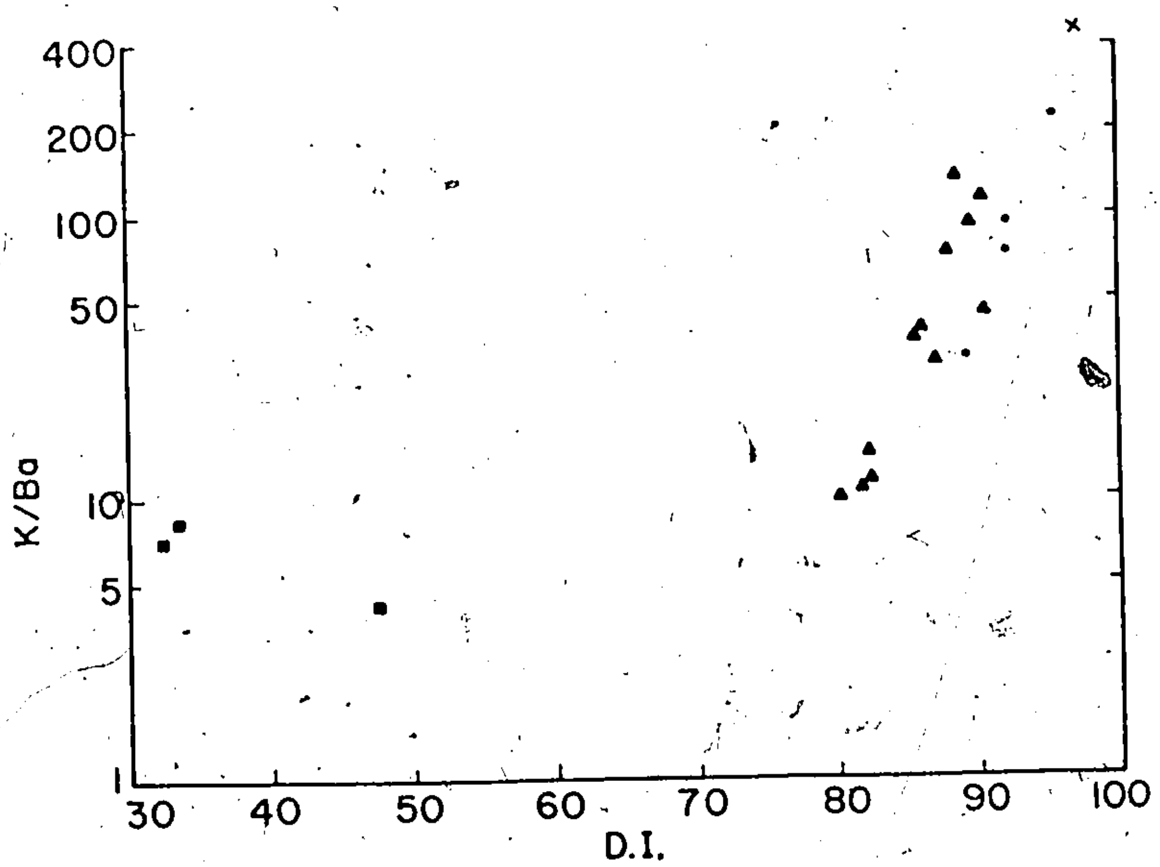
400
200
100
50
10
5
1
K/Ba
30
40
50
60
70
80
90
100
D.I.

Figure 6.1.32 Variation of the 100xBa/Ca+K ratio as a function of D.I.

Figure 6.1.33 Variation of the Ba/Sr ratio as a function of D.I.

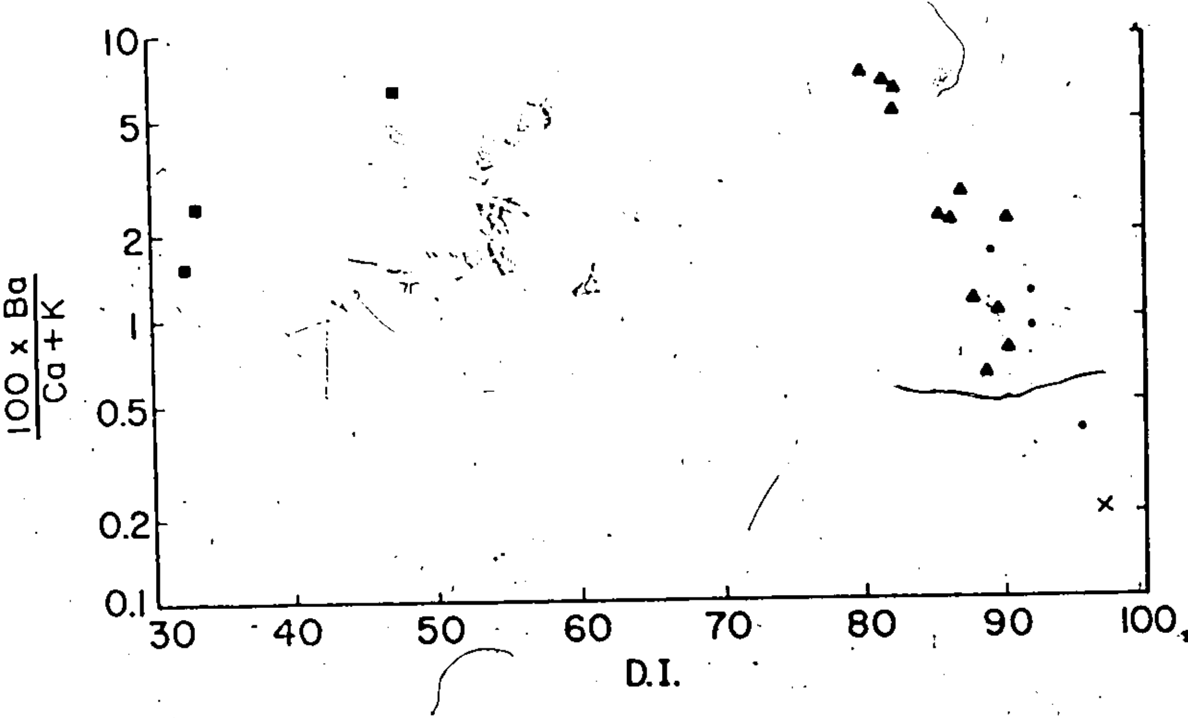
10
5
2
1
0.5
0.2
0.1
100 x Ba / Ca + K
30
40
50
60
70
80
90
100
D.I.
×

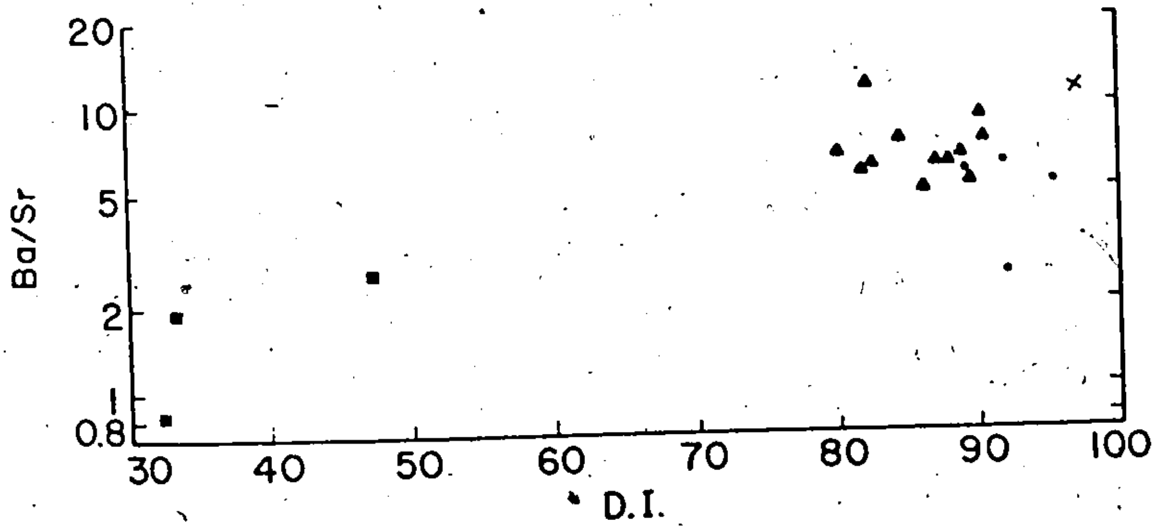
20
10
5
2
1
0.8
Ba/Sr
30
40
50
60
70
80
90
100
D.I.
×

The variation trends for monzonitic rocks indicate that these rocks are very strongly fractionated mainly by feldspars. The dominant feldspar fractionation is probably the reason why Rb is less fractionated than Ba and Sr, since Rb is mainly present in mafic minerals (biotite). The generally high content of Ba, however, suggests that the original monzonitic magma, as a whole, did not have to be the late product of highly differentiated magma (c.f. Figure 6.1.29).

With regard to the relationship between monzonites and quartz monzonites, it appears that these rock types are genetically closely related (probably comagmatic) and both underwent extensive fractional crystallization. The large overlap between monzonites and quartz monzonites on practically all these variation diagrams (in section 6.1.1-2), however, indicates that some quartz monzonites are less fractionated than acid monzonites (i.e. monzonites with high D.I. values). Consequently, it suggests that these two rock types as a series are not simply products of continuous magmatic differentiation of a single magma leading to accumulation of residual quartz and that a more complex process was probably involved.

6.1.2.4 Thallium

The content of Tl in dioritic rocks ranges from about 75-440 ppb with the average close to 210 ppb. Quartz monzonites and monzonites have higher Tl concentrations, varying from about 640-1030 ppb and from 340-700 ppb, respectively. All these values are comparable with the estimated crustal averages for similar rocks given by Albuquerque and Shaw (1972).

The close geochemical coherence between Rb and Tl, first noted by Ahrens (1948), is also apparent in the rocks from the pluton (Figure 6.1.34). The range of variation of Rb/Tl-ratios in quartz monzonite (116-145), monzonite (107-151) and diorite (101-191) are relatively close to the crustal average for this ratio (~150) given by Albuquerque and Shaw (1972). In general, the coherence of Rb/Tl is more pronounced than that for K/Rb or K/Tl. Like Rb, the concentration of Tl increases relative to K with fractionation in a series of differentiation (e.g. Siedner, 1968; Zlobin and Lebedev, 1960) and thus "the K/Tl ratio should be a sensitive index of fractionation in a differentiated sequence" (Taylor, 1965, p.151). The felsic rocks of the pluton show a distinct variation trend of the K/Tl ratio, which decreases toward the more acid members (Figure 6.1.35). A separated trend for dioritic rocks (if it does not reflect only secondary alteration) might once again suggest that these rocks are not genetically related to the felsic ones.

The K/Tl ratios particularly for monzonite are very high in comparison with the average value for crustal igneous rocks, ~30,000 (Albuquerque and Shaw, 1972), indicating strong depletion of Tl relative to K in these rocks. The impoverishment of Tl is of a magnitude similar to that of Rb, as suggested

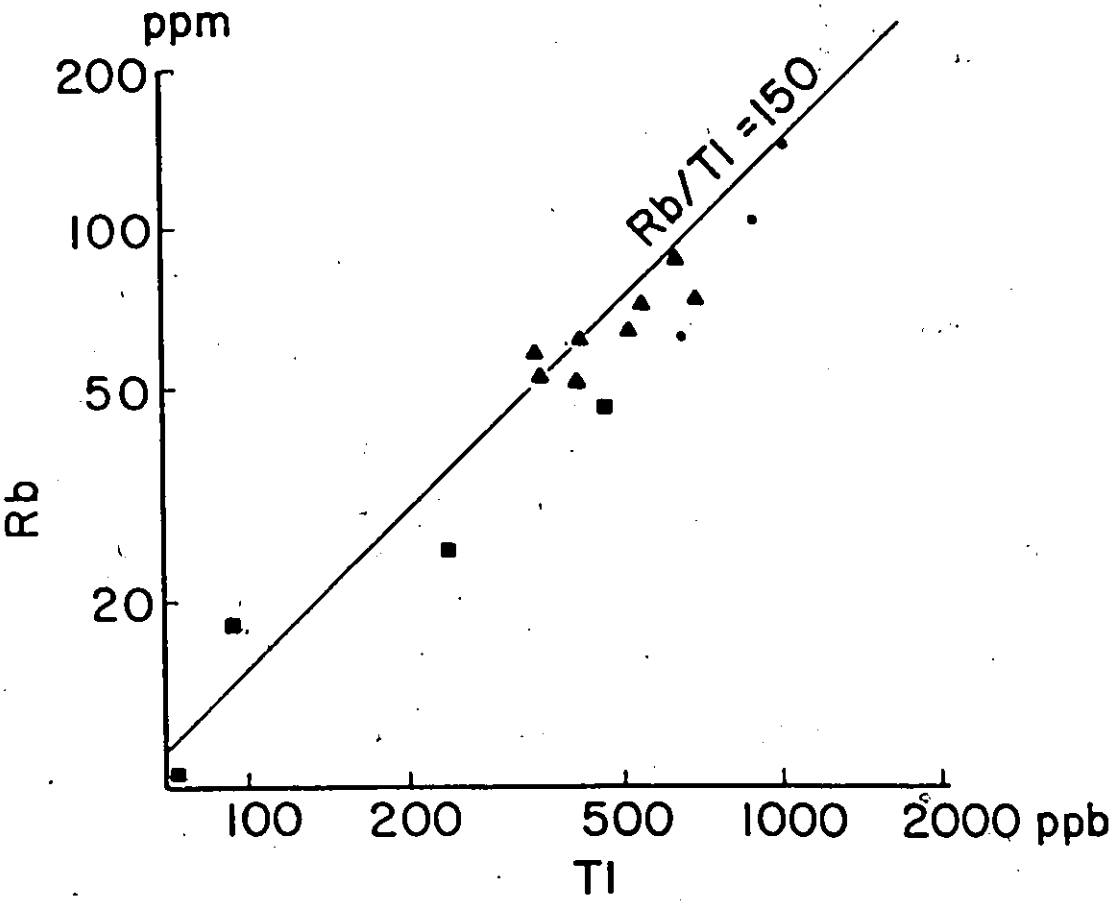

Figure 6.1.34 Relation between Rb and Tl

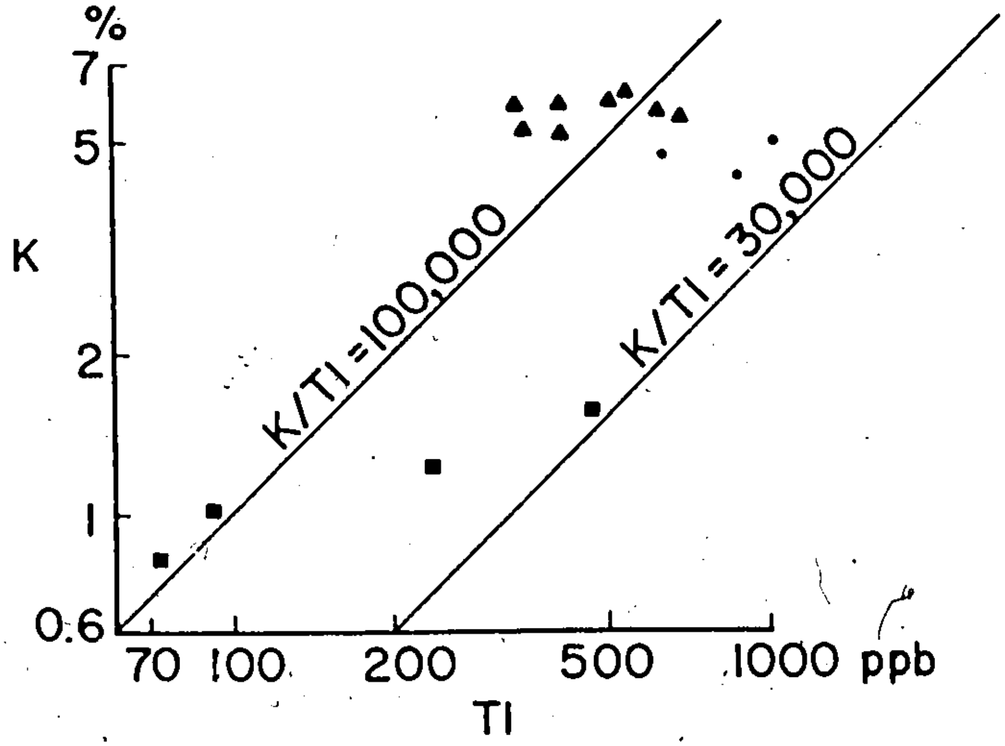

Figure 6.1.35 Relation between K and Tl

by the "normal" Rb/Tl ratio.

As noted earlier, the high K/Rb ratio and its similarity to some oceanic tholeiites led to the suggestion of a mantle or deep crust origin for these rocks. The high values for the K/Tl ratio are also comparable to Hawaiian basalts and some alkali rocks but differ from the ranges of other terrestrial rocks (Albuquerque et al., 1972). The Rb/Tl ratios, however, lie well within the ranges for continental rocks, unlike Hawaiian basalts and alkali rocks. The general impoverishment of Rb and Tl in the felsic rocks from the pluton is of interest. As will be discussed below, it is probably related to the deficiency of these elements in a parental magma.

6.1.2.5 Rare Earth Elements

In a recent summary of the geochemistry of REE, Herrmann (1970) concluded that there are three major trends of fractionation of REE during the magmatic differentiation of plutonic rocks. In the first type, exemplified by the South California batholith (Towell et al., 1965), the total REE content and their relative fractionation increases with the differentiation. The second type, described by Balashov (1963) from the Susamyr batholith (Central Tien Shan, USSR) shows the absolute concentration of REE and the degree of their fractionation passes a maximum. Finally, the Skaergaard type (Haskin and Haskin, 1968) shows an increase of total REE with differentiation, but there is little change in relative abundances.

The last two trends, however, are not well established. With regard to the Susamyr batholith, the complex might not be the result of magmatic differentiation of basic magma, but probably "was derived in large part from pre-existing continental rocks in which REE had already been somewhat enriched" (Goles, 1968, p.245). The distribution of some other trace elements in this complex was interpreted as a result of melting and assimilation of crustal rocks and not of fractional crystallization of basic magma (Tauson et al., 1956).

The recent study of the REE distribution in the Skaergaard intrusion (Haskin et al., 1971) shows that the apparent lack of relative REE fractionation in the whole-rocks is probably due to the REE-rich liquid trapped between cumulus minerals. They concluded that "the high amounts of trapped liquid present in most of the rocks explain why the relative abundances in the rocks remain close to those of the liquid" (p.213).

Thus, it appears that during magmatic differentiation, the total REE abundances in igneous rocks usually increase with fractionation (Taylor, 1965; Mason, 1966). This is also indicated by the fact that the concentration of REE in most rock-forming phenocrysts of volcanic rocks are smaller than those of coexisting "groundmass" (Onuma et al., 1968; Schnetzler and Philpotts, 1968, 1970; Higuchi and Nagasawa, 1969; Dudas et al., 1971). The increase of absolute concentrations of REE during differentiation is usually accompanied by relative enrichment of light REE over heavy ones (Schilling and Winchester, 1966, 1969). Nagasawa and Schnetzler (1971), however, suggested that crystallization of mafic minerals or larger amounts of REE-bearing accessories (e.g. zircon) could produce a decrease of total REE abundances in the residual magma.

With respect to the Eu anomaly, "basic rocks usually show normal Eu contents in chondrite-normalized REE patterns, while many differentiated rocks show negative Eu anomalies" (Nagasawa, 1973, p.301).

In order to correlate the REE abundances with the petrochemistry of the rocks from the pluton, the La concentrations have been plotted against the differentiation index in Figure 6.1.36. The La content in diorites shows a tendency to increase with the increase of the D.I. values. Some diorites, however, have a concentration of La very similar to that of basic monzonites despite the fact that their D.I. values are markedly lower.

Regarding the monzonites, the large increase of La contents toward the more acid rocks indicates that monzonites underwent extensive magmatic differentiation. Quartz monzonites, however, lie well off the variation trend of monzonite and perhaps even their La abundances show a tendency to decrease with the increase of the D.I. values. It is also of interest that leucogranite (259), which is thought to be a product of partial

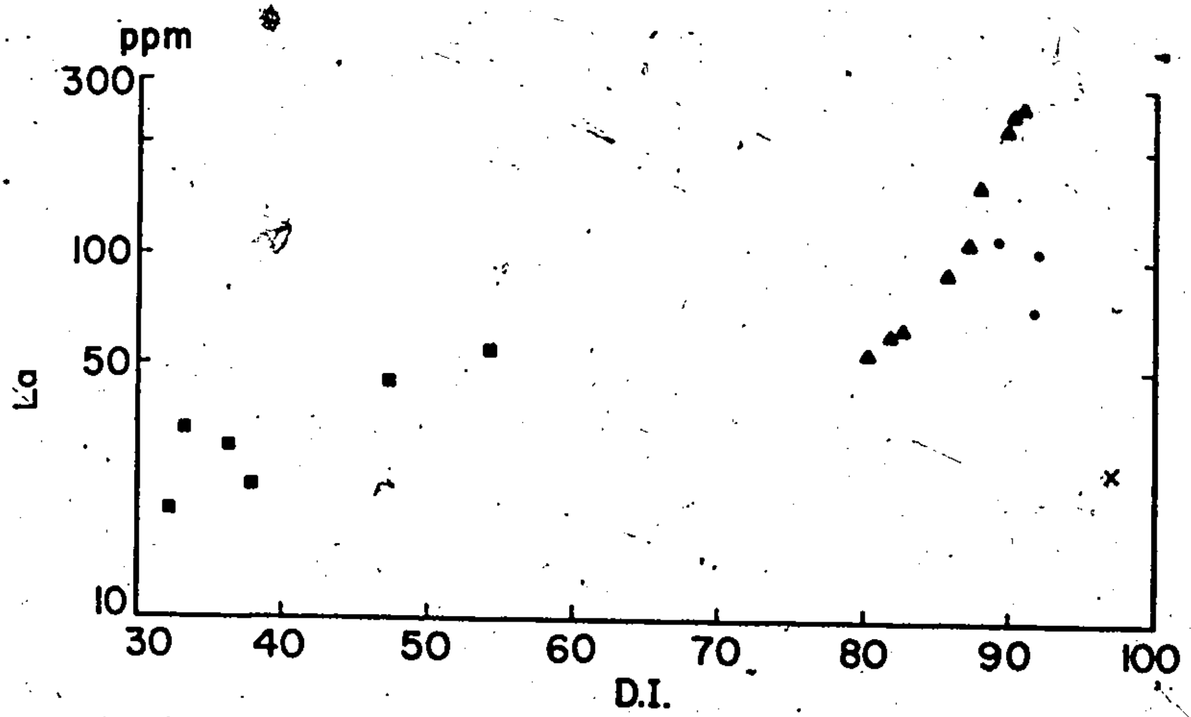

Figure 6.1.36 Variation of La as a function of D.I.

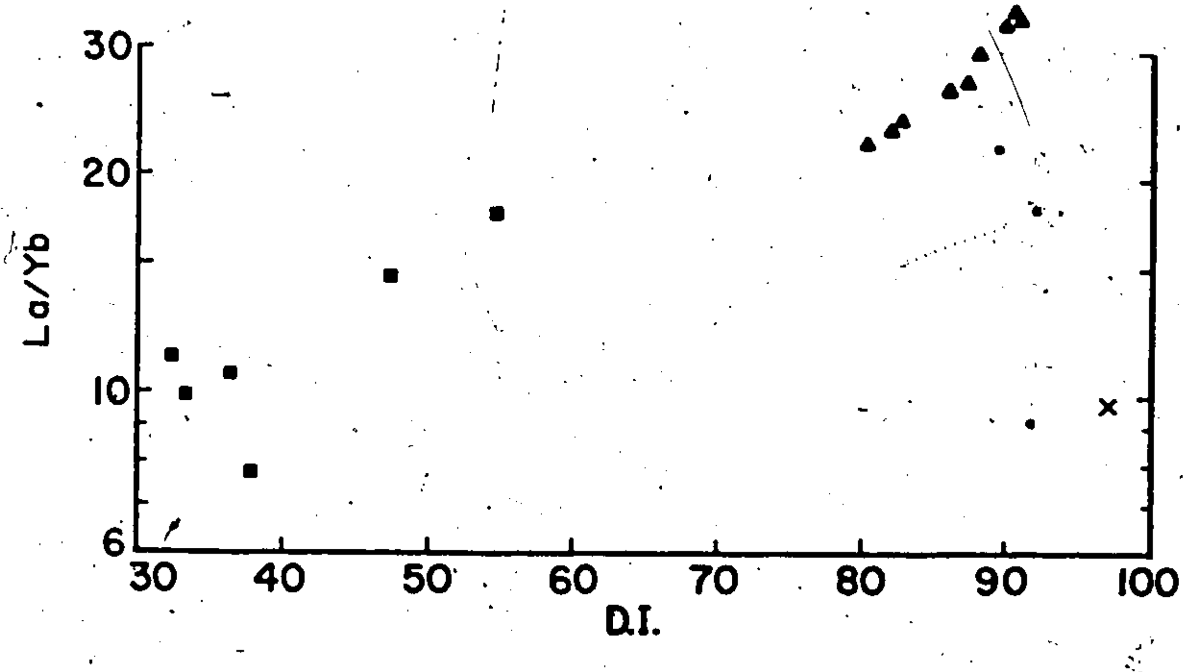

Figure 6.1.37 Variation of the La/Yb ratio as a function of D.I.

melting of the country rocks, has the lowest La content.

A trend, rather similar to that of La, is also displayed by the La/Yb ratio which is a good index of relative REE fractionation (Gast, 1968). Figure 6.1.37 shows a general tendency for the La/Yb ratio in dioritic and monzonitic rocks to increase with the increase of the D.I. values. Quartz monzonites, once again, have a lower La/Yb ratio than monzonites of comparable D.I. values. The trends for diorites and monzonites are consistent with those produced by magmatic differentiation, but they are not conclusive as far as a possible genetic relationship between these two rock types is concerned.

Figures 6.1.38-43 show the REE distributions of the whole-rocks represented by means of Coryell-Masuda plots (Coryell et al., 1963), in which whole-rock REE concentrations are divided element for element by average values for chondrites (Frey et al., 1968, c.f. Appendix 2) and plotted against REE atomic numbers. The chondrite-normalized patterns in all the rocks are enriched relative to chondritic meteorites, although each of the three main rock types of the pluton has distinct REE contents and degree of relative enrichment.

Insofar as dioritic rocks are concerned, six whole-rock samples have been analyzed for the REE (Figure 6.1.38). Regardless of the large variation of the chemical composition and absolute contents of REE of these rocks (Figure 6.1.36), the relative REE distribution patterns seem to remain substantially

Figure 6.1.38 REE distribution in dioritic rocks from the pluton

○ - sample 321
◆ - sample 199-4
□ - sample 199-5
■ - sample 70
◇ - sample 783
⧯ - sample 53-5

Figure 6.1.39 REE distribution in continental basic rocks

○ - gabbro, Skaergaard (Frey et al., 1968)
◪ - gabbro, Stillwater (Frey et al., 1968)
▲ - gabbro, Duluth (Frey et al., 1968)
□ - Deccan Plateau basalt (Frey et al., 1968)
■ - composite of dioritic rocks (< 60% SiO_2) (Haskin et.al., 1966)

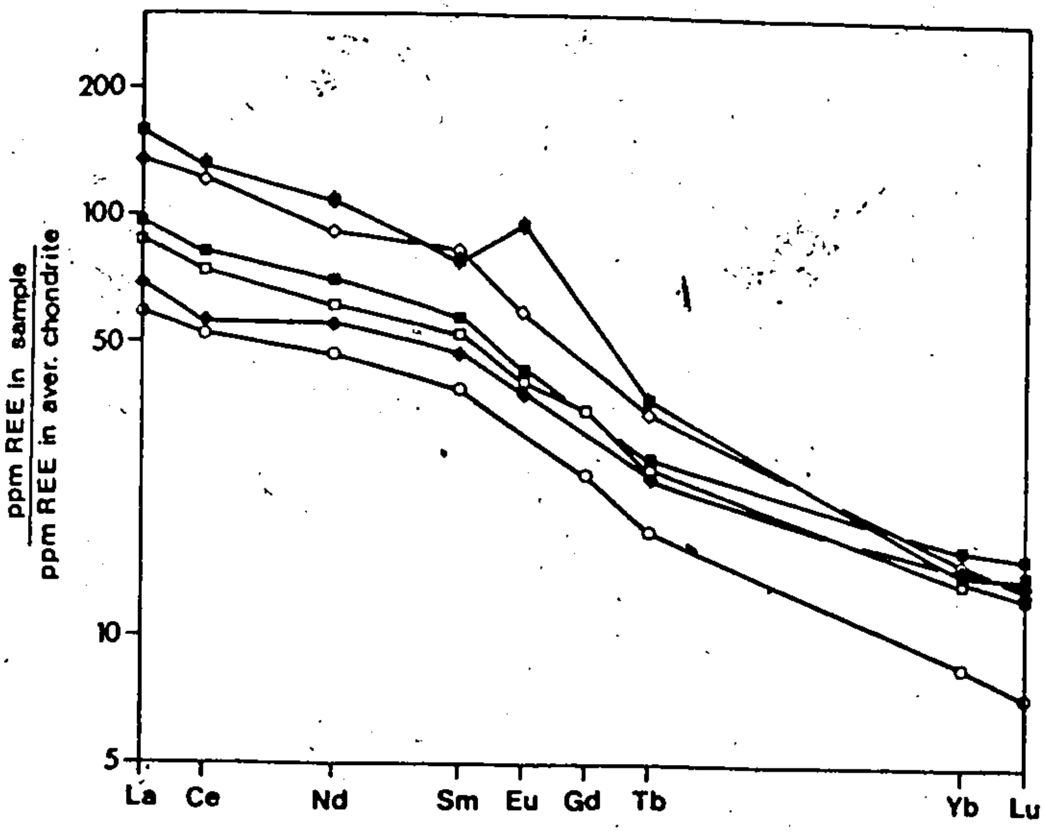
200
100
50
10
5
ppm REE in sample / ppm REE in aver. chondrite
La
Ce
Nd
Sm
Eu
Gd
Tb
Yb
Lu

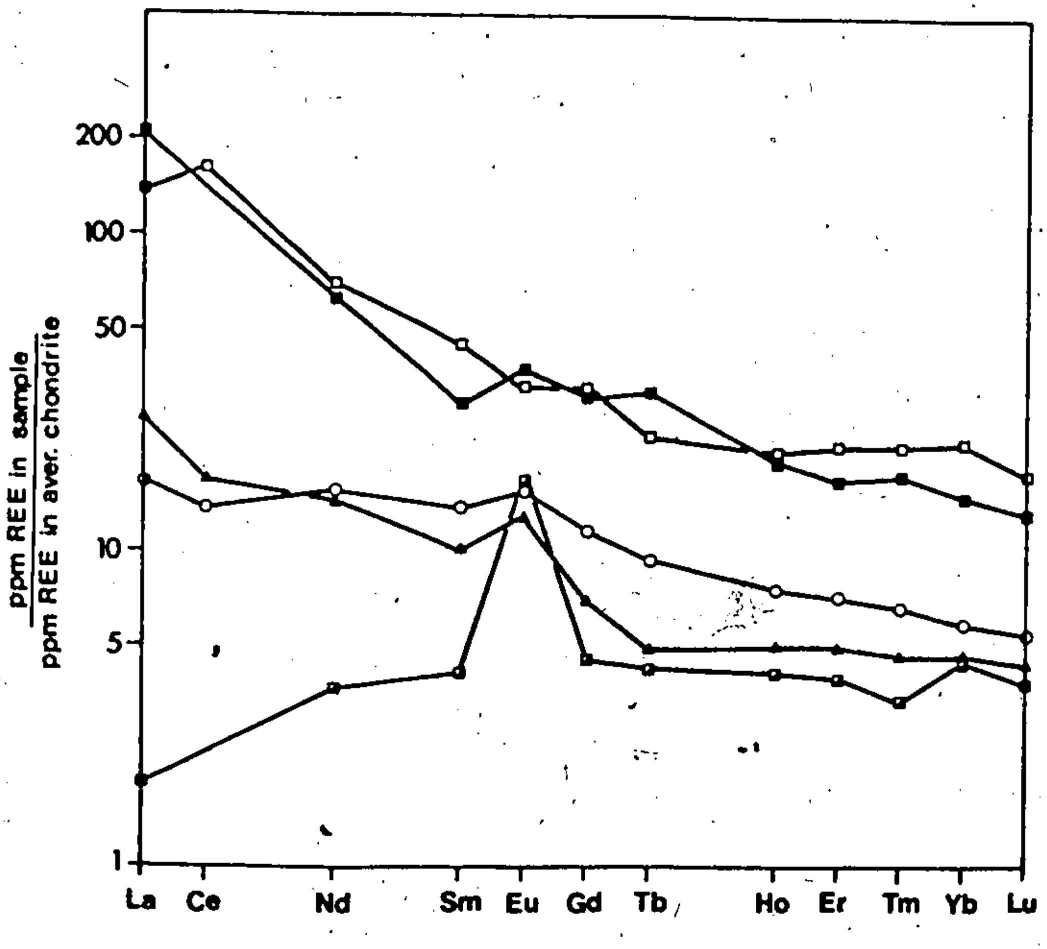
200
100
50
10
5
1
ppm REE in sample / ppm REE in aver. chondrite
La
Ce
Nd
Sm
Eu
Gd
Tb
Ho
Er
Tm
Yb
Lu

unchanged. They are characterized by well-fractionated patterns with gradual enrichment from Lu to La without distinct Eu anomalies (except sample 53-5).

The REE patterns of several continental basic rocks, mainly from layered intrusions, are plotted for comparison in Figure 6.1.39, together with the dioritic composite (<60% SiO_2) of Haskin et al. (1966). The basic rocks of the pluton differ from some of the layered intrusions (e.g. Stillwater) but are similar to the dioritic composite and Deccan basalt (Frey et al., 1968). REE distribution patterns similar to those of the Loon Lake pluton have also been recorded by Green et al. (1972) for Precambrian gabbros from Lofoten-Vesteraalen, Norway.

As noted above, the tendency for the absolute REE content and the La/Yb ratio in diorites to increase with the increasing D.I. values suggests that these rocks underwent magmatic differentiation. The positive correlation of total REE concentration with the alkalinity in basic rocks has been found by Schilling and Winchester (1966, 1969), Balashov and Nesterenko (1966) and Frey et al. (1968).

Sample 53-5 is of interest since it has a positive Eu anomaly not observed in other dioritic rocks. Feldspars are the only common rock-forming minerals which are relatively enriched in Eu (e.g. Chase et al., 1963; Haskin et al., 1966; Philpotts and Schnetzler, 1968). Thus a probable cause of the positive Eu anomaly in this sample is the incorporation of an excess of feldspars. If the Eu anomaly is a primary feature of the rock 53-5 generated during magmatic differentiation, it would suggest that this sample is at least partially of cumulative origin. The more "differentiated" character of the rock 53-5 in comparison with other analyzed diorites (as indicated by the higher value of the D.I.) combined with the positive Eu anomaly could hardly be explained by a simple magmatic differentiation without accumulation of feldspars (c.f. Philpotts and Schnetzler, 1968). The presence of a positive Eu anomaly is, however, also consistent with the process of hybridization. An adding of feldspars during hybridization could generate the observed Eu anomaly in diorite. It should be pointed out that this rock contains more than 20% of K-feldspar in mode (c.f. Appendix 1) and K-feldspar in dioritic rocks appears to be of late origin. In the absence of the REE determination of mineral phases of rock 53-5, a quantitative evaluation of the Eu anomaly, however, cannot be done.

Even if the variations of REE in diorites in general are suggestive of magmatic differentiation, these variations appear to be also compatible with hybridization or assimilation. Since monzonites (apart from basic ones) have a higher absolute content of REE than basic rocks, then partial assimilation or hybridization of diorites by monzonites might produce the observed trends.

The chondrite-normalized REE patterns of monzonite from the pluton are shown in Figure 6.1.40. The REE patterns given in Figure 6.1.40 have been separated into two sections merely to avoid complexity. The REE patterns of monzonite are well-fractionated and progressively enriched from Lu to La, relative to chondrite meteorites (except for Eu). The fractionation patterns are similar but differ slightly in absolute REE contents and in the degree of relative fractionation. More variation is seen with Eu and the Eu/Eu* values (which indicate the ratio of the observed europium abundance - Eu-to that predicted - Eu*-by graphical extrapolation between the values of Sm and Tb or Gd)[1]. Figure 6.1.40 once again shows a general tendency for the La/Yb ratio to increase with the increase of the absolute REE abundance and the decrease of the Eu/Eu* ratio. These variations are comparable with the trends attributed to fractional crystallization (Balashov, 1963; Towell et al., 1965; Haskin and Haskin, 1968; Schilling and Winchester, 1969). The increase of the La/Yb ratio from 22-34 is probably due to the removal of mafic minerals (clinopyroxene, hornblende and biotite) from the liquid.

The Eu/Eu* ratios of monzonites (Figure 6.1.40) display a tendency to decrease toward the more acid rocks. This variation trend is similar to those for Sr and Ba (Figures 6.1.24 and 6.1.30). The parallel behaviour of Eu suggests that it is probably partially present as Eu^{2+}. The relative depletion of Eu

---

[1] In the course of this work, the Eu* values were obtained by extrapolating from Sm to Tb (c.f. Buma et al., 1971), since Gd was not always determined.

Figure 6.1.40 REE distribution in monzonites from the pluton

top:

◪ - sample 251
○ - sample 96
■ - sample 102
□ - sample 125

below:

○ - sample 94
◪ - sample 207
⧯ - sample 224
□ - sample 198
■ - sample 228

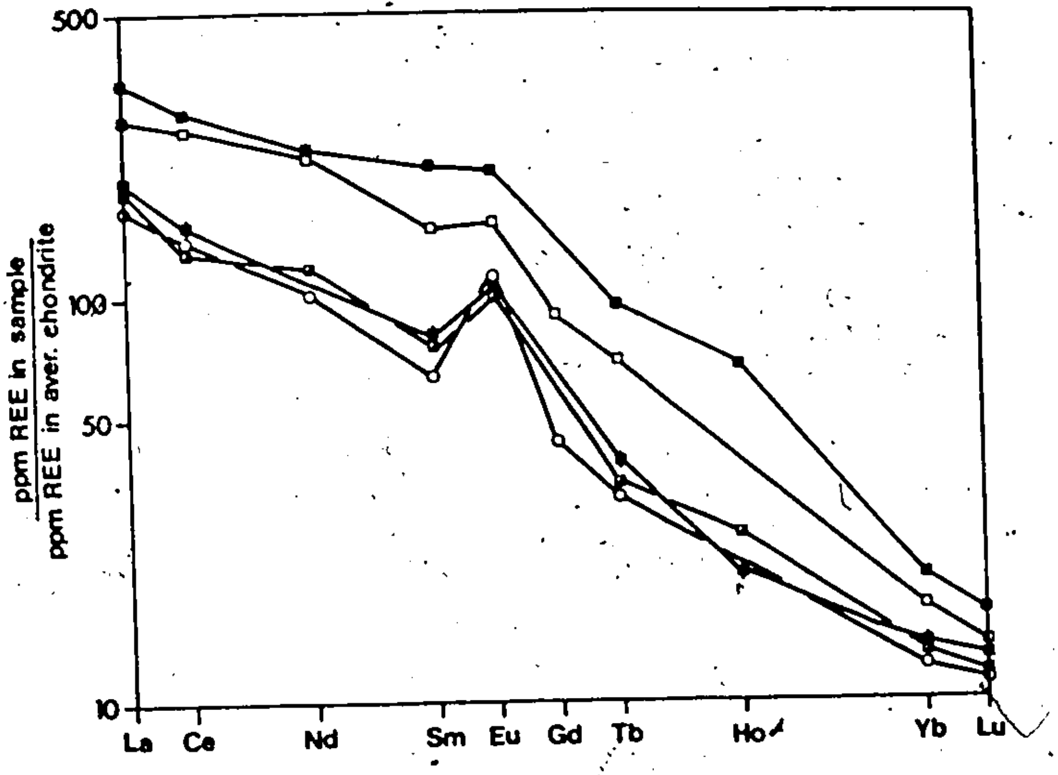
500
100
50
10
ppm REE in sample / ppm REE in aver. chondrite
La
Ce
Nd
Sm
Eu
Gd
Tb
Ho
Yb
Lu

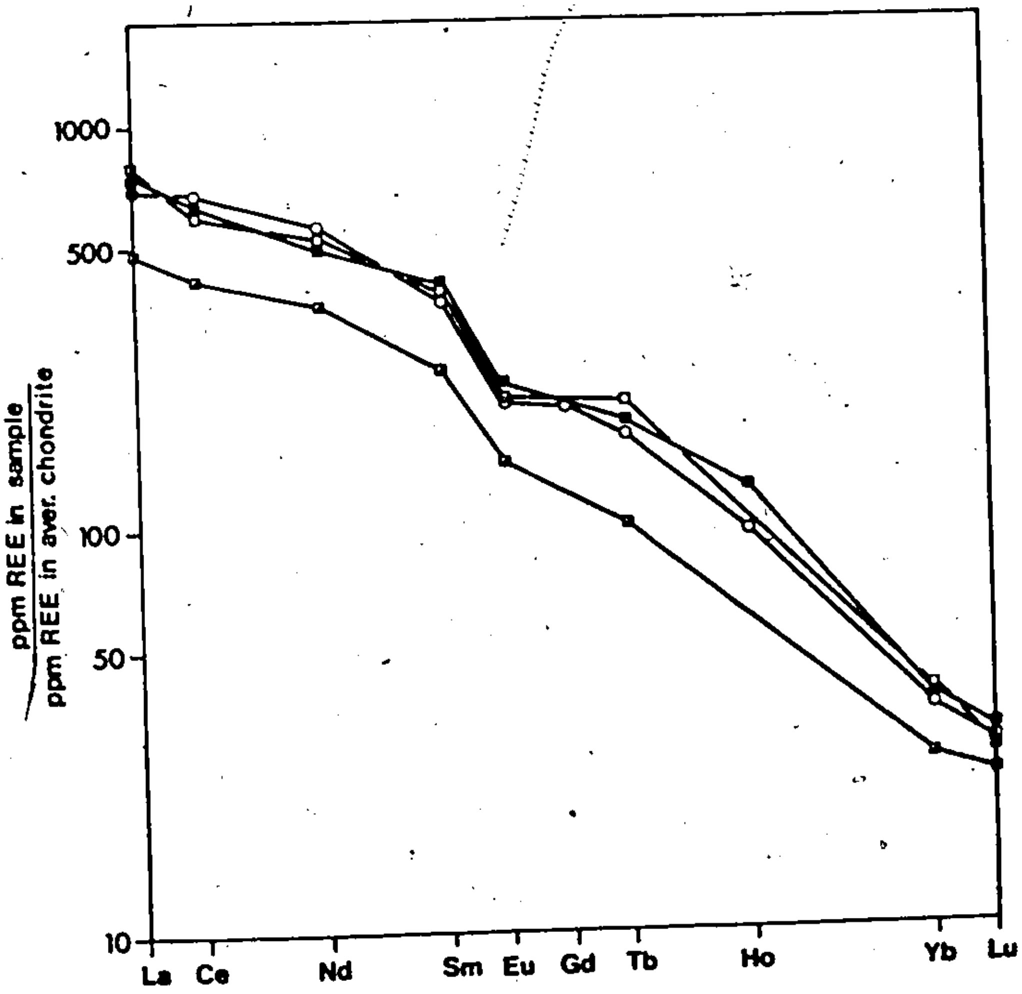
1000
500
100
50
10
ppm REE in sample / ppm REE in aver. chondrite
La
Ce
Nd
Sm
Eu
Gd
Tb
Ho
Yb
Lu

paralleled by the fall of Sr and Ba with the increase of the D.I. values is readily explained by the removal during magmatic differentiation of significant amounts of feldspars, which concentrate not only Ba and Sr but also Eu^{2+} (Taylor et al., 1968; Schnetzler and Philpotts, 1970), "whereas the remaining trivalent rare earth elements would follow their usual trend of being concentrated in the residual melts" (Towell et al., 1965, p.3493).

Arth and Hanson (1972) have suggested that the decrease of the Eu/Eu* ratio with the increasing total REE contents is characteristic for magmas, which are partly residual or cumulative (with a positive Eu anomaly) and partly differentiated (with a negative Eu anomaly) due to the addition or removal of feldspars. This appears to hold true also for monzonites from the pluton. It should be noted that the monzonites with low values of D.I. and La contents and positive Eu anomalies occur in the centre of the monzonite core of the pluton where rocks, as indicated by petrography, are more basic (e.g. containing more An-rich plagioclase, clinopyroxene, hornblende, while the outer part of the monzonite body contains biotite as the only mafic mineral and more Ab-rich plagioclase), and probably crystallized somewhat earlier than the outer zone. As will be discussed later, these observations are consistent with the process of flowage differentiation where early-formed crystals (mainly feldspars) are concentrated toward the core and thus they could be partially of a cumulative nature, while progressively

Figure 6.1.41 REE distribution in quartz monzonites from the pluton

○ - sample 115
■ - sample 27
□ - sample 26

Figure 6.1.42 REE distribution in granitic composites

■ - granitic composite (60-70% SiO_2) (Haskin et al., 1966)
□ - granitic composite (> 70% SiO_2) (Haskin et al., 1966)
○ - Finnish granitic composite (Haskin et al., 1966)
▮ - Precambrian granitic composite (Haskin et al., 1968a)

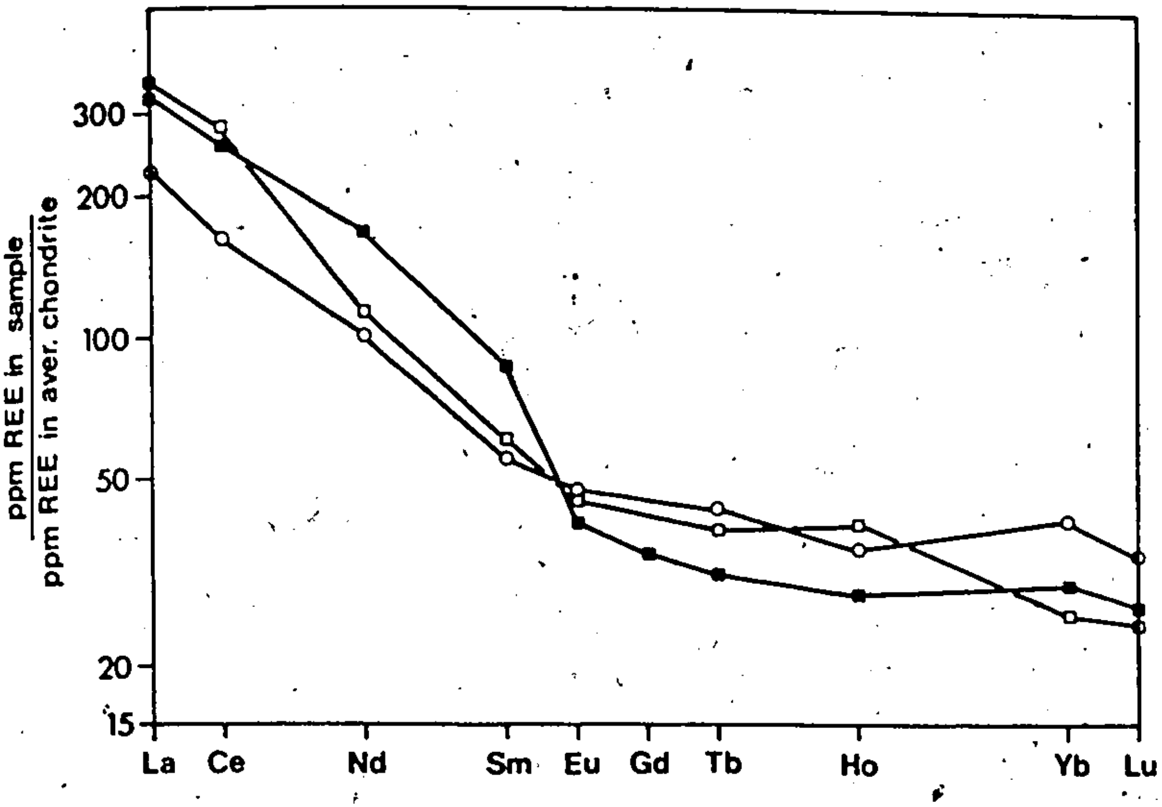
ppm REE in sample / ppm REE in aver. chondrite
300
200
100
50
20
15
La
Ce
Nd
Sm
Eu
Gd
Tb
Ho
Yb
Lu

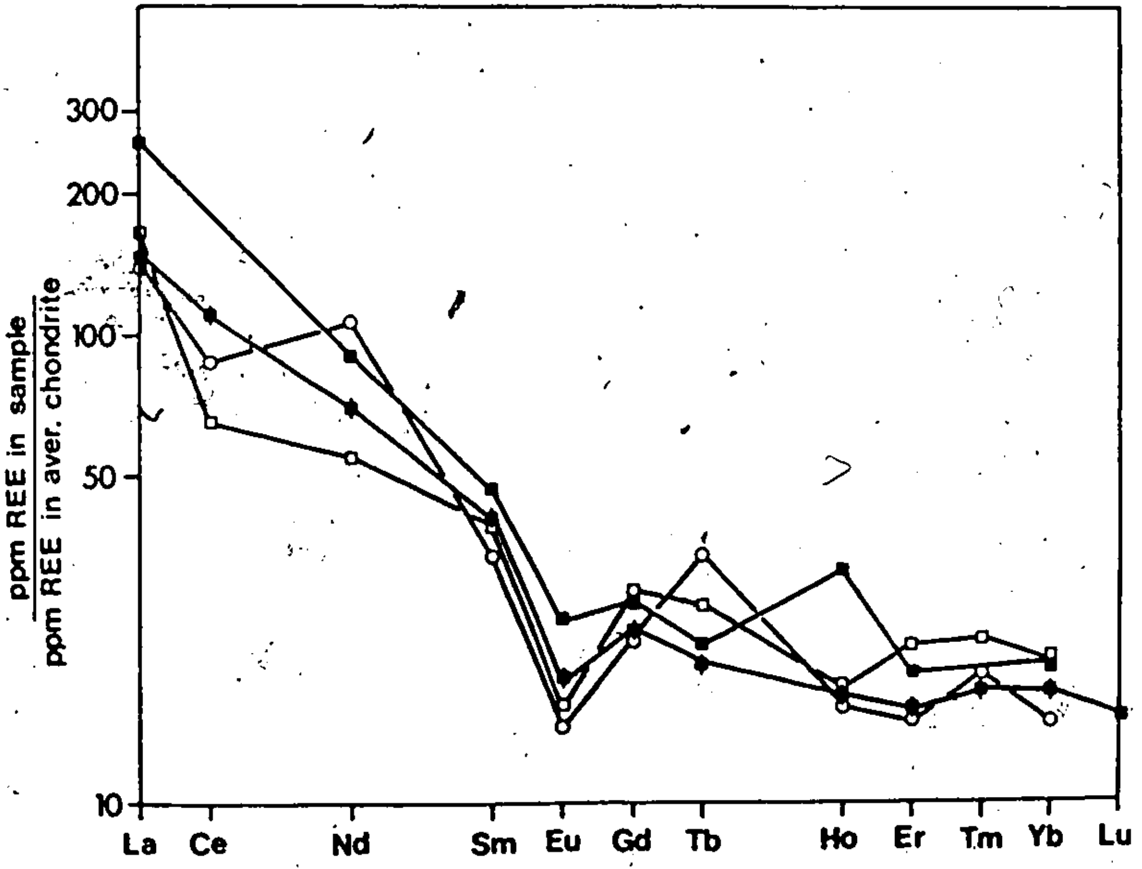
ppm REE in sample / ppm REE in aver. chondrite
300
200
100
50
10
La
Ce
Nd
Sm
Eu
Gd
Tb
Ho
Er
Tm
Yb
Lu

more differentiated liquids would be concentrated at the borders.

The REE contents of quartz monzonites normalized to chondrites are given in Figure 6.1.41. For comparison, the REE abundances in four granitic composites (Haskin et al., 1966, 1968a) are shown in Figure 6.1.42.

In general, REE distribution patterns of quartz monzonite are similar to those observed in other granitic rocks (e.g. Haskin et al., 1966; Taylor et al., 1968; Nagasawa, 1970; Buma et al., 1971; Condie and Lo, 1971). They have the typical enrichment in light REE relative to chondrites, with or without a small Eu depletion and with relatively small fractionation of heavy REE. But the REE patterns of quartz monzonites differ from those of acid monzonites. Quartz monzonites have less fractionated patterns, lower absolute contents of REE and lack significant negative Eu anomalies in comparison with acid monzonites. These differences once again indicate that some quartz monzonites are less fractionated than acid monzonite.

6.1.3 Dunite

The major chemical constituents of dunite (SiO_2, MgO, FeO, Fe_2O_3 and H_2O) essentially reflect the modal abundance of olivine and the extent of its serpentinization. A rather low content of alumina is consistent with the absence of spinel in the mode.

Unfortunately, two factors have made an evaluation of the geochemistry and petrogenesis of this rock difficult. First is the absence of definite geological or petrographic criteria for identifying the affinities and nature of this rock (c.f. Thayer, 1964, 1967; Irvine and Findlay, 1972) including also, for example, concealed contacts of the single poorly exposed small body of dunite (c.f. section 5.5.6). The second factor is the serpentinization and other possible alteration processes which further complicate the chemistry of the original rocks.

With respect to serpentinization, there is a controversy over whether this alteration was an isochemical process, except for the addition of volatiles, that caused expansion or whether serpentinization is a "constant volume" process involving major chemical changes (c.f. Hotstetler et al., 1966; Thayer, 1966). It appears, however, that some elements such as Ca, Al, Ti and K could be removed by serpentinization (Page, 1967; Miyashiro et al., 1969). These chemical changes may have also involved trace elements of alkali and alkali earth groups as shown by Shih (1972). Frey (1969) and Shih (1972) demonstrated, however, that REE (except perhaps light ones) are not removed during serpentinization or related processes and tend to preserve their original distribution.

The REE pattern of dunite from the pluton is given in Figure 6.1.43 together with those of dunites from a layered intrusion, nodules in alkali olivine basalts and alpine ultramafic bodies.

Figure 6.1.43 REE distribution in dunite 130 and some ultrabasic rocks

◩ - dunite 130

Layered intrusion:

■ - Muskox dunite (Frey et al., 1971)

□ - Matheson serpentinite (Frey et al., 1971)

Nodules in basalts:

○ - Mt. Leura dunite (Frey et al., 1971)

Alpine ultramafics:

△ - Shikoku dunite (Frey et al., 1971)

◐ - Twin Sisters dunite (Frey et al., 1971)

▮ - Cazadero peridotite (Frey et al., 1971)

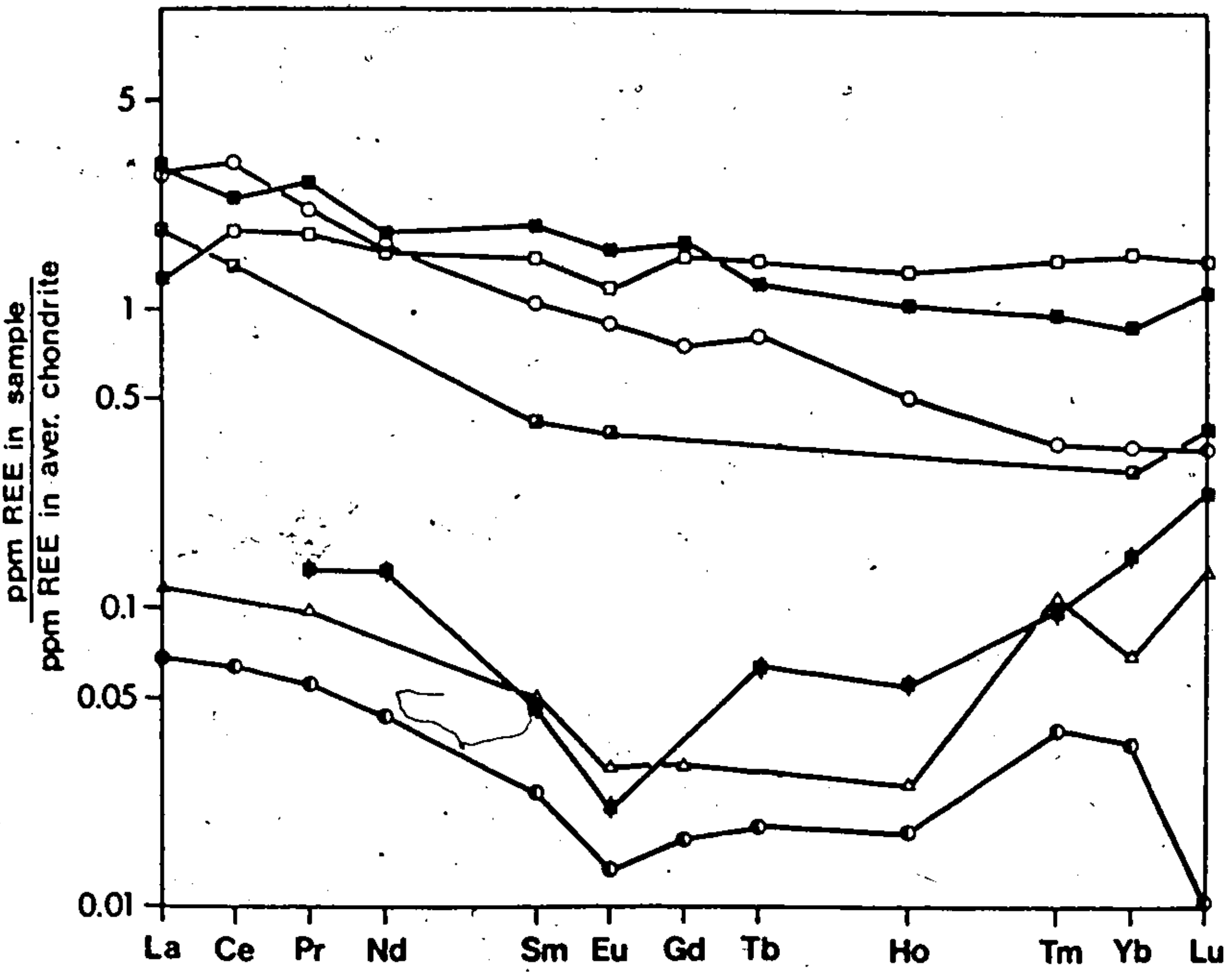
ppm REE in sample / ppm REE in aver. chondrite
5
1
0.5
0.1
0.05
0.01
La
Ce
Pr
Nd
Sm
Eu
Gd
Tb
Ho
Tm
Yb
Lu

The dunite from the pluton has absolute REE abundances similar to those of chondrites, while their distribution pattern is enriched in the light REE relative to the chondritic REE distribution. In comparison with REE distribution trends of ultramafic rocks of continental origin (Frey et al., 1971), it differs markedly from those of an alpine environment, but is similar to those of layered intrusions and nodules from alkali basalts. Even if serpentinization affected the light REE distribution, the nearly flat pattern for heavy REE differs from the distinct V-shaped patterns of the alpine-type ultramafics. The light REE enrichment observed in the analyzed dunite is also not expected either for undifferentiated mantle material or for simple residuum after basaltic liquid extraction (Frey, 1970).

It appears that the REE pattern of dunite is not dominated by olivine. This is probably a common case for "the ultramafic rocks of a layered intrusion" because "it is quite likely that trapped interstitial liquids have contributed a large fraction, perhaps nearly all, of the REE. Even small amounts of trapped liquid could drastically change the relative REE abundances" (Frey et al., 1971, p.2066).

Another possible explanation for the light REE enrichment in dunite from the pluton is contamination by crustal rocks, which are commonly enriched in the light REE and contain many times higher amounts of total REE. The similarity of relative and absolute REE abundances to those from other layered intrusions and nodules, however, might indicate a negligible contamination, if at all, by crustal rocks.

The data on hand are not sufficient to elucidate the petrogenesis of dunite and the possible relationship to the rocks of the pluton, particularly to dioritic rocks. It appears, however, that dunite from the pluton might represent a xenolith brought up during the intrusion of monzonite.

6.2 Chemistry of Minerals

In this section, a discussion of major and some trace element (Li, Ba, Sr, Rb) concentrations in minerals is grouped according to minerals; the REE abundances in minerals are treated separately for the sake of simplicity. The estimated purity of mineral fractions is given in Appendix 1.

6.2.1 Amphibole

One amphibole from diorite (sample no. 70) has been analyzed for both major and trace elements. The chemical composition and structural formula is given in Table 6.2.1.

The structural formula for amphibole was calculated on the basis of 24 (O, OH, F, Cl) using the computer program described by Jackson et al. (1967), assuming the generalized formula $X_2Y_5Z_8O_{22}$ (OH, F, Cl)$_2$. The analysis is within Leake's (1968) limits for "superior analyses" of calciferous and subcalciferous amphibole and compositionally corresponds to his

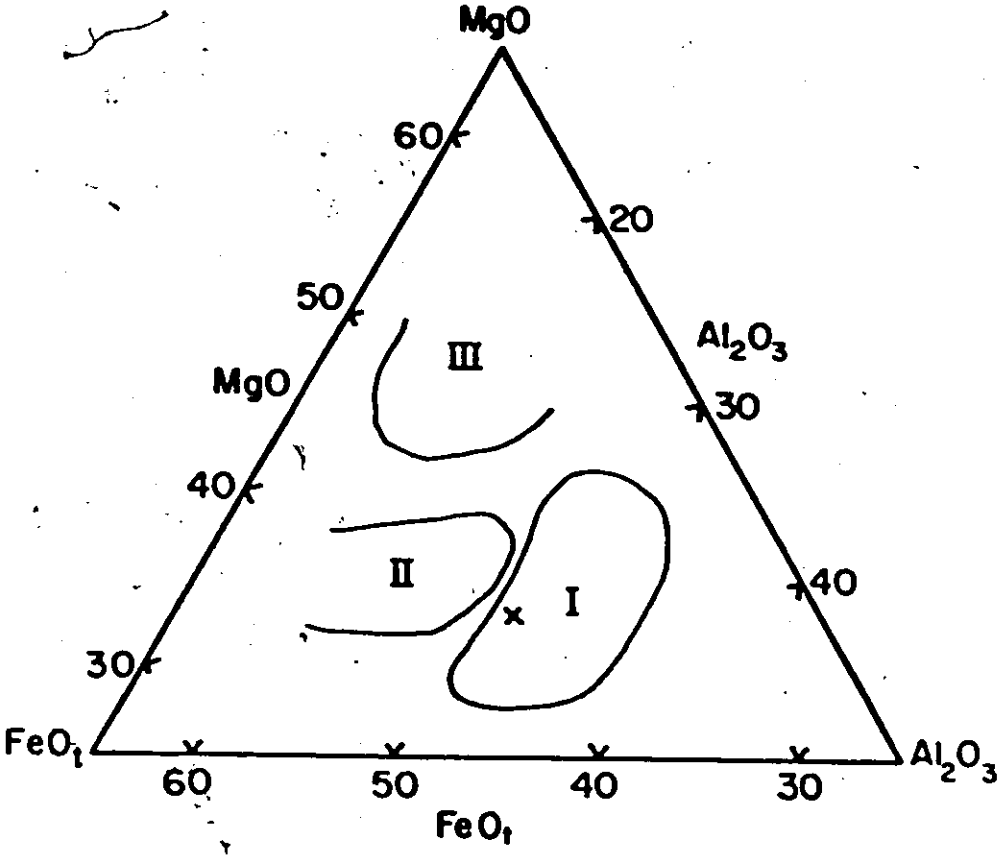

Figure 6.2.1

Portion of triangular diagram with apices MgO, total iron as FeO, and Al_2O_3, showing compositional fields of hornblendes from Caledonian plutonic rocks (Nockolds and Mitchell, 1948) and composition of hornblende from diorite of the Loon Lake pluton.

I. Field of hornblendes from hornblendites and appinitic diorites

II. Field of hornblendes from normal diorites and granodiorites

III. Field of hornblendes formed by replacement of pre-existing pyroxenes or amphiboles

x = hornblende from diorite 70 - Loon Lake pluton

Table 6.2.1 Chemical compositions and calculated formulae of amphibole and biotites from the rocks of the Loon Lake pluton

	AMPHIBOLE	BIOTITES					
Sample No.	70	94	251	102	26	115	27
Host rock	D	M	M	M	QM	QM	QM
		Chemical analyses (wt.%)					
SiO_2	44.53	38.97	37.84	37.52	36.98	33.58	37.90
TiO_2	1.17	3.08	1.32	1.60	2.67	2.64	2.33
Al_2O_3	10.08	13.25	14.35	14.40	16.09	14.94	14.70
Fe_2O_3	5.07	2.23	3.24	2.98	3.23	4.42	3.32
FeO	10.37	13.18	15.32	15.97	15.88	26.01	14.32
MnO	0.26	0.33	1.24	1.25	0.30	0.57	0.96
MgO	12.31	14.67	12.65	12.02	10.83	3.88	11.35
CaO	11.59	0.39	0.26	0.17	0.08	0.50	0.14
Na_2O	1.27	0.10	0.08	0.05	0.04	0.02	0.04
K_2O	0.95	9.31	9.25	9.05	9.71	7.64	9.41
H_2O^+	1.69	2.08	2.70	3.05	2.67	3.54	2.18
H_2O^-	0.03	0.08	0.22	0.15	0.06	0.08	0.07
F	0.17	1.74	1.81	2.05	1.00	0.79	3.17
O≡F	0.07	0.73	0.76	0.86	0.42	0.33	1.33
Total	99.42	98.68	99.52	99.40	99.12	98.28	98.56

Table 6.2.1 continued

Sample No.		70		94		251		102		26		115		27	
Host rock		D		M		M		M		QM		QM		QM	
Structural formulae number of ions based on 24 (O,OH,F,Cl) per formula unit															
Si	Z	6.61	8.00	5.92	8.00	5.76	8.00	5.69	8.00	5.66	8.00	5.40	8.00	5.77	8.00
Al^{iv}		1.39		2.08		2.24		2.31		2.34		2.60		2.23	
Al^{vi}	Y	0.37	5.12	0.29	5.92	0.33	5.83	0.27	5.70	0.57	5.79	0.23	5.59	0.41	5.58
Fe^{3+}		0.57		0.25		0.37		0.34		0.37		0.53		0.38	
Ti		0.13		0.35		0.15		0.18		0.31		0.32		0.27	
Mg		2.72		3.32		2.87		2.72		2.47		0.93		2.58	
Fe^{2+}		1.29		1.67		1.95		2.03		2.03		3.50		1.82	
Mn		0.03		0.04		0.16		0.16		0.04		0.08		0.12	
Ca	X	1.84	2.39	0.06	1.89	0.04	1.86	0.03	1.79	0.01	1.92	0.09	1.67	0.02	1.86
Na		0.37		0.03		0.02		0.01		0.01		0.01		0.01	
K		0.18		1.80		1.80		1.75		1.90		1.57		1.83	
OH		1.67	1.75	2.11	2.95	2.74	3.61	3.09	4.07	2.73	3.21	3.80	4.20	2.21	3.74
F		0.08		0.84		0.87		0.98		0.48		0.40		1.53	

Table 6.2.1 continued

Sample no.	70	94	251	102	26	115	27
Host rock	D	M	M	M	QM	QM	QM
$\frac{Fe^{3+}}{Fe^{2+} + Fe^{3+}}$		0.132	0.160	0.144	0.155	0.133	0.173
$\frac{Fe_{total}}{Fe_{total} + Mg}$		0.367	0.447	0.465	0.493	0.813	0.461
mole fraction of annite		0.279	0.325	0.338	0.339	0.583	0.304
			Trace elements				
Li (ppm)	12	116	370	239	135	375	766
Rb "	n.d.	374	417	420	498	732	991
Sr "	169	52	60	48	49	66	59
Ba "	269	3923	403	305	1084	322	699
Tl (ppb)	60	2641	2017	2553	-	4146	5765
			Element ratios				
Mg/Li	5711	763	206	303	484	62	89
K/Rb		207	184	179	162	87	79
D.I.	33.3	80.1	88.0	90.5	89.1	91.7	92.0

Host rock: D=diorite; M=monzonite; QM=quartz monzonite
D.I. = value of differentiation index for host rock
n.d. = not detected
- = not determined

magnesio-hornblende.

For the purpose of comparison, amphibole from the Loon Lake pluton has been plotted on the $MgO-FeO_{total}-Al_2O_3$ triangular diagram (Figure 6.2.1) of Nockolds and Mitchell (1948). It falls in the field defined by them for the "early" primary amphibole of hornblendites and appinitic diorites and well outside the field of amphibole formed by the replacement of former pyroxene or amphibole.

The Li content of amphibole is very low (12 ppm), but comparable with values for amphiboles from, for example, suites of calc-alkali rocks (e.g. Nockolds and Mitchell, 1948; Haslam, 1968; Leelanandam, 1970). Also the concentration of Sr and Ba (169 ppm and 269 ppm, respectively) are comparable with the contents of amphibole from calc-alkali rocks (e.g. Nockolds and Mitchell, 1948; Sen et al., 1959; Leelanandam, 1970).

6.2.2 Biotite

Six biotites from monzonite and quartz monzonite have been analyzed for major and trace elements. The chemical composition and the structural formulae of biotite are given in Table 6.2.1.

In general, biotites from the Loon Lake pluton are similar compositionally to those from other comparable plutonic rocks compiled by Rimsaite (1967) and Deer et al. (1962). (Biotite 115 appears to be partially chloritized as is also indicated by its low K contents). The structural formulae were calculated on the basis of 24 (O, OH, F, Cl) according to the method described by Jackson et al. (1967) to the general formula $X_2Y_{4-6}Z_8O_{10}(OH, F, Cl)_4$. Twelve-coordinated large cations - K, Na and Ca of X group sum from 1.67 to 1.92, somewhat less than the ideal 2.00. This group consists mainly of K, while Ca and Na occur only in very small amounts. Also, Rb, Ba and Sr are probably proxying for twelve-coordinated cations (Dodge et al., 1969). The elements of the octahedral group, totalling from 5.59-5.92 are also deficient in comparison with 6.00 in the idealized trioctahedral micas. The relation between the octahedral cations is shown graphically in Figure 6.2.2 taken from Foster (1960). All but one biotite (115) fall into the field of Mg-biotite. Figure 6.2.2 also indicates that the main variation in this cation group is a slight decrease in Mg and increase in Fe^{2+} toward the more acid host rocks. The calculated formulae show that 2.08 and 2.60 Al atoms substitute for Si in the tetrahedral layer, but only a small portion of Al (less than 0.60) is present in the octahedral layer. But "the variation of aluminum content and its distribution between four and six-coordination sites in biotites is not understood" (White, 1966, p.191). Li is also included in the Y group, since it is believed to be substituting in the octahedral site (Nockolds and Mitchell, 1948). The amount of monovalent anions OH and F is highly variable, but in most cases total less than the ideal 4.00. The relatively high average content of F in biotite from monzonite suggests that a high activity of fluorine was present during the crystallization of monzonite. If a conclusion of Putman and Alfors (1969) holds true that "for crystallization of biotite under magmatic condition, fractional crystallization would tend to yield relatively higher fluorine contents in later crystals and tend to increase the proportion of fluorine in volatile fraction remaining in the magma" (p.61), then the higher average content of F in monzonite might indicate that biotites from the monzonite underwent, on the average, a higher degree of fractionation than those from quartz monzonite.

The content of Li in biotites from quartz monzonite ranging from about 135-770 ppm increases progressively with the increase of the acidity of the host rocks; a similar trend is shown also by those from monzonite, in which the concentration of Li varies from about 115-370 ppm. This trend, however, is not apparent if both rock types are treated together as a series. The Mg/Li ratio in biotites decreases toward the more acid members if these two rock types are considered separately (c.f. Table 6.2.1).

Strontium is present in biotites in low concentration, in the range 48-66 ppm. Barium shows a general tendency to decrease in biotites from the more acid rocks of each main rock type. Rubidium increases progressively as the host rocks become more acid. While the increase of Rb in biotites from monzonite is relatively small, those from quartz monzonite show a sharp increase with the increase of acidity of the host rocks. The increase of the Rb concentration in biotites is accompanied by a simultaneous increase of Tl (c.f. Table 6.2.1).

It appears that the absolute concentration of Rb in biotite is controlled by the content of Rb in the whole-rock. Biotites from the monzonite have low Rb contents, accompanied by a relatively high K/Rb ratio (~200) similar to those of biotites from andesites and from inclusions in alkali basalts (Jakes and White, 1970), but markedly different from those of granitic or metamorphic biotites (Lange et al., 1966; White, 1966; Whitney, 1969).

The experimental works of Wones and Eugster (1965) have shown that the partitioning of magnesium, ferric and ferrous iron in biotites for the equilibrium assemblage biotite-potassium feldspar-magnetite depends mainly on temperature, water vapor pressure and oxygen fugacity. Since in both the monzonites and the quartz monzonites these minerals are present, their experimental data can be applied to an estimation of conditions during the crystallization of biotite. Relevant data for biotite from the pluton are summarized in Table 6.2.1.

Comparison of biotites from the pluton with Wones and Eugster's (1965) estimated position of "buffered" biotite solid solutions in the ternary system $K\ Fe_3^{3+}Al\ Si_3O_{12}(H_{-1})$ - $K\ Fe_3^{2+}Al\ Si_3O_{10}(OH)_2$ - $K\ Mg_3Al\ Si_3O_{10}(OH)_2$ shows that the

Figure 6.2.2 Relation between octahedral cations (atomic %) of biotites from the Loon Lake pluton. The mineral fields are taken from Forster (1960)

▲ - biotite from monzonite
● - biotite from quartz monzonite

Figure 6.2.3 Fe^{3+}-Fe^{2+}-Mg diagram (atomic %) of biotites from the Loon Lake pluton. The lines represent the composition of "buffered" biotites in the ternary system $K\ Fe^{3+}_3\ Al\ Si_3O_{12}(H_{-1})$-$K\ Fe^{2+}_3\ Al\ Si_3O_{10}(OH)_2$-$K\ Mg_3\ Al\ Si_3O_{10}(OH)_2$ (after Wones and Eugster, 1965)

× - biotite from monzonite
● - biotite from quartz monzonite

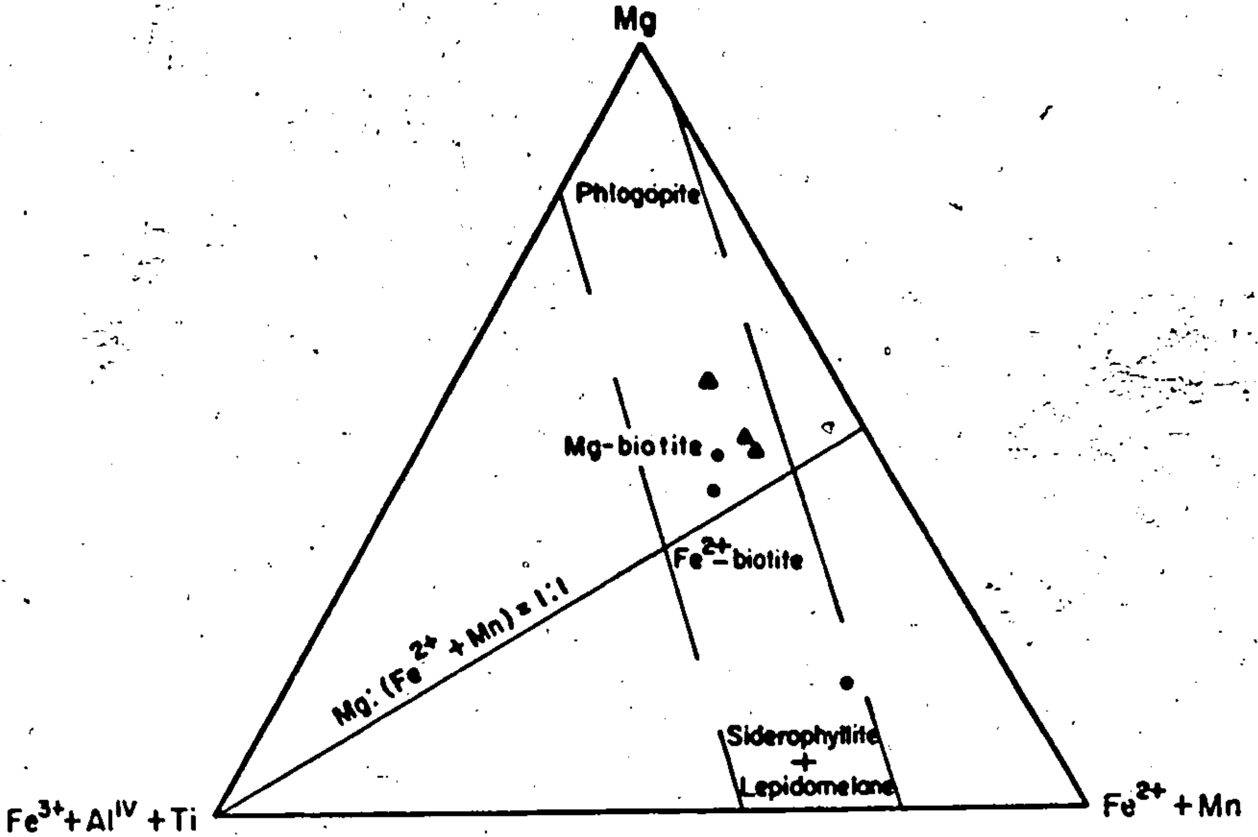
Mg
Phlogopite
Mg-biotite
Fe2+-biotite
Mg:(Fe2+ + Mn) = 1:1
Siderophyllite + Lepidomelane
Fe3+ + AlIV + Ti
Fe2+ + Mn

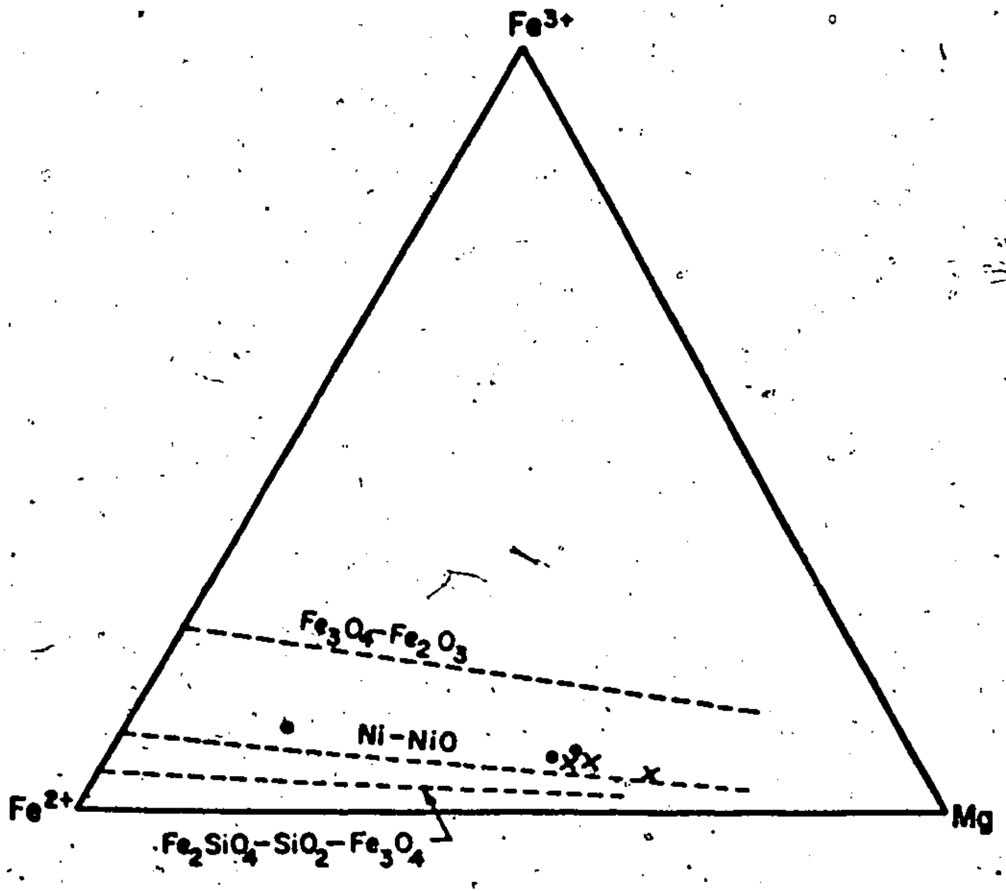
Fe3+
Fe3O4-Fe2O3
Ni-NiO
Fe2+
Mg
Fe2SiO4-SiO2-Fe3O4

Figure 6.2.4 Stability of biotite of specific Fe/(Fe+Mg) values as a function of oxygen fugacity and temperature from 2070 bars total pressure (from Wones and Eugster, 1965). The heavy curve labelled 0 represents the maximum phlogopite stability; the area bounded by the curve labelled 100 is the annite stability field. Light-weight lines and dotted lines represent "buffer" curves

X - biotite from monzonite
● - biotite from quartz monzonite

Figure 6.2.5 Calculated stability curve for biotite from monzonite 251

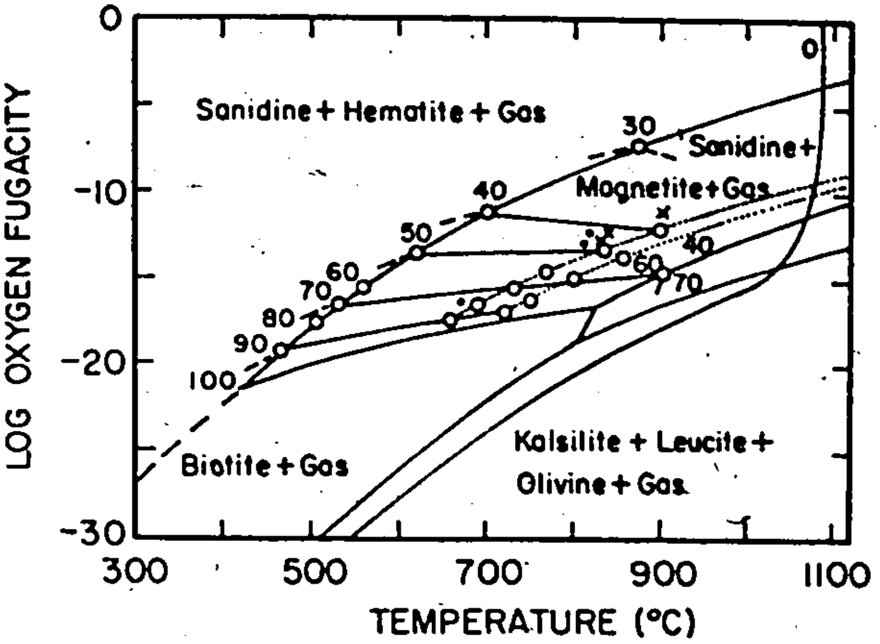

Figure 6.2.4

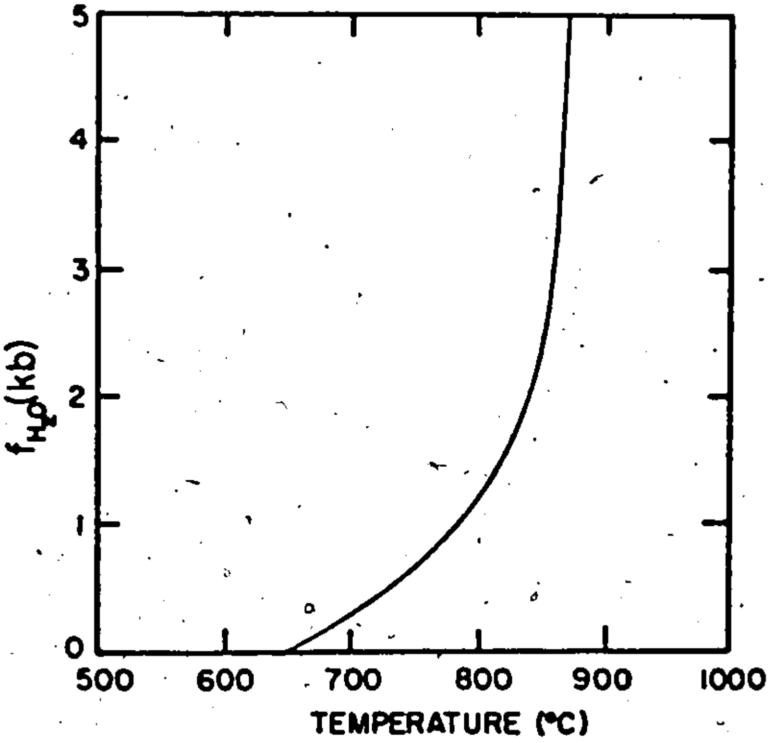

Figure 6.2.5

biotites studied follow closely the Ni-NiO buffer curve (Figure 6.2.3), although they have a composition consistent with oxygen fugacities slightly higher than those in equilibrium with the Ni-NiO buffer.

Since buffer equilibria are strongly temperature dependent, the compositions of biotite vary with the temperature. Biotites from the pluton suggest that during crystallization, the oxygen fugacity decreased with decreasing temperature (Figure 6.2.4). Thus the Fe/(Fe+Mg) ratio appears to be at least a relative measure of the temperature of biotite crystallization in the Loon Lake pluton. It is of interest that biotite from the centre of the monzonitic core (94) indicates the highest temperature while that from the margin of the quartz monzonitic zone (115) suggests the lowest temperature.

The application of the experimental data of Wones and Eugster (1965) to biotites from the pluton involves, however, several assumptions. The most important one is that substitutions other than Fe ⇌ Mg do not significantly influence the stability of biotite.

In spite of this limitation, the available data were used for the calculation of the stability curve of biotite from monzonite 251, according to the equation 6^{11} of Wones and Eugster (1965). Assuming the equilibrium coexistence of biotite with K-feldspar and magnetite, the results of this calculation are given in Figure 6.2.5. For the calculation, oxygen fugacity was considered to be slightly above the Ni-NiO buffer, ideal solution was assumed for the activity of K Al Si_3O_8 in alkali feldspar while a value of 1.00 was used for the activity of Fe_3O_4 in magnetite (c.f. Dodge et al., 1969; Ragland, 1970). The mole fraction of annite was taken as the percentage of Fe^{2+} in the octahedral group assuming an ideal octahedral occupancy of six (c.f. White et al., 1967; Dodge et al., 1969). The stability curve of biotite may be shifted to a somewhat lower temperature region according to the experimental data of Rutherford (1969). For the pressure of 2.5-4 kb suggested in section 4.3, the resulting temperature does not differ significantly from the estimates suggested in section 4.3, considering that the stability curve for biotite in Figure 6.2.5 probably represents an upper limit.

6.2.3 Feldspars

Feldspars are the most abundant minerals in the rocks of the Loon Lake pluton. Plagioclase occurs in all three main rock types in major amounts, whereas potash feldspar is the major constituent in monzonite and quartz monzonite. In dioritic rocks, potash feldspar is present in highly variable amounts (c.f. Appendix 1).

6.2.3.1 Plagioclase

Two plagioclases from diorites (321 and 70) have been analyzed for major and trace elements. The chemical composition and structural formulae of plagioclases are given in Table 6.2.2. There is a good agreement between the optical values and the chemical analyses of these two plagioclases (c.f. Table 6.2.2).

The dioritic rocks are characterized by a plagioclase of andesine composition (Table 6.2.2). The Or contents of plagioclase is of interest since Sen (1959) suggested that the content of potassium in solid solutions of plagioclase increases with the increasing temperature of crystallization. The two analyzed plagioclases, however, show a tendency for an increase of potassium concentration with increasing Ab content, similar to those found by Ribbe and Smith (1966) and Ewart and Taylor (1969). This suggests that the increase of K is associated with decreasing crystallization temperatures.

The K content of plagioclase from diorite is within the range of the concentration in andesine compiled by Heier (1962) and Anderson (1966). Ba concentrations of plagioclase are relatively high in comparison with the average given by Heier (1962) for andesine (383 ppm), but analogous to values for plagioclase from comparable rocks, compiled by Anderson (1966). The higher content of Ba in plagioclase probably explains the relatively high concentrations of Ba in diorite compared to "typical" diorite or gabbro. A comparison of the Ba concentration in plagioclase from the pluton confirms Ewart and Taylor's (1969) observation that Ba exhibits a positive correlation with

Table 6.2.2 Chemical compositions and structural formulas of feldspars from the rocks of the Loon Lake Pluton

	PLAGIOCLASE		POTASSIUM FELDSPAR		
Sample	321	70	94	251	27
Host rock	D	D	M	M	QM
			Chemical analyses (wt.%)		
SiO_2	56.59	57.70	63.84	64.74	64.83
Al_2O_3	26.94	26.37	19.12	18.48	18.54
CaO	8.90	7.02	0.29	0.03	0.02
Na_2O	5.96	6.32	1.72	0.72	0.75
K_2O	0.52	1.22	13.15	15.43	15.58
SrO	0.34	0.43	0.10	0.02	0.04
BaO	0.10	0.12	1.48	0.22	0.20
Rb_2O			0.02	0.02	0.05
Total	99.35	99.18	99.72	99.66	100.01

Structural formulas

number of ions based on 32 oxygens per formula unit

		321		70		94		251		27	
Si	Z	10.23	15.97	10.43	16.05	11.83	16.01	11.98	16.01	11.97	16.00
Al		5.74		5.62		4.18		4.03		4.03	
Ca	X	1.72	3.98	1.36	3.91	0.06	3.91	0.01	3.93		
Na		2.09		2.21		0.62		0.26		0.27	3.96
K		0.12		0.28		3.11		3.64		3.67	
Sr		0.04		0.05		0.01					
Ba		0.01		0.01		0.11		0.02		0.01	
Rb										0.01	

Table 6.2.2. continued

			Mol. %		
An	43.83	35.26	1.52	0.15	0.10
Ab	53.12	57.44	16.33	6.61	6.81
Or	3.05	7.30	82.15	93.24	93.09
$\frac{Ab}{Ab+An}$	0.55	0.62			
$\frac{Ab}{Ab+An}$ (opt.)	0.57	0.60			
			Trace elements		
Li (ppm)	5	9	n.d.	n.d.	n.d.
Rb (ppm)	n.d.	18	141	158	482
Tl (ppb)	62	128	472	1044	1943
			Element ratios		
K/Rb		563	774	810	268
K/Ba	4.9	9.3	8.2	65	74
Ba/Rb		61	94	12	3.6
Ba/Sr	0.3	0.3	16	11	5.2
Rb/Tl		141	299	151	248
Ca/Sr	22	14	2.5	1.2	0.4
D.I.	32.4	33.3	80.1	88.0	92.0

Host rock: D=diorite; M=monzonite; QM=quartz monzonite

opt. = composition of plagioclase determined optically

D.I. = value of differentiation index for host rock

n.d. = not detected

Ab content. Ribbe and Smith (1966) concluded that Ba may occur at the 0.0X% level in plagioclase crystallized at a high temperature.

Both plagioclases contain substantial amounts of strontium (Table 6.2.2), well above the average given by Heier (1962) for andesines (898 ppm). With regard to the distribution of strontium in the plagioclase of basic rocks, it has been found that Sr increases as the An content decreases (Wager and Mitchell, 1951; Iida, 1961; Butler and Skiba, 1962; Hall, 1967), while in acid rocks the concentrations of Sr decrease as the An content decreases (Sen et al., 1959; Hall, 1967; Ewart and Taylor, 1969). The variation of Sr in investigated plagioclases is consistent with that observed in basic rocks - Sr decreases with the increase of An content. The significance of the Ca/Sr variation in plagioclase, however, is uncertain. It was thought that the "Sr/Ca ratio is a sensitive guide to fractionation in plagioclase" (Taylor, 1965, p.155). But recently Berlin and Henderson (1968, 1969a,b) have demonstrated that "the increasing Sr/Ca ratio in plagioclase is dominated by the amount of augite (and/or hornblende) to crystallize and usually does not give any indication of Sr-Ca fractionation in the plagioclase" (Berlin and Henderson, 1969b, p.423).

Rubidium, which was detectable in only one plagioclase by the method used for analysis (c.f. Appendix 1), is rather low, resulting in a high K/Rb ratio (563) for this plagioclase.

Also, the concentration of Li in both plagioclases is very low - 5 and 9 ppm, respectively. Lithium is probably related to the impurities of micaceous material in plagioclase. An alternative explanation has been invoked by Ewart and Taylor (1969). They have suggested the presence of Li in solid solution in the feldspar lattice. Heier (1960) has also suggested that Li^{1+} substitutes for Na^{1+} in feldspars.

6.2.3.2 Potassium Feldspar

The major and trace elements have been determined in three potassium feldspars. The chemical composition and structural formulae of K-feldspars are given in Table 6.2.2. The structural formulae of K-feldspars, like those of plagioclase, were calculated on the basis of 32 oxygens by the method described by Jackson et al. (1967). Two samples show a certain degree of discrepancy between the composition determined by the Orville method (c.f. Table 5.1) and by wet chemical analysis, probably because "the heavy liquid separates are apparently unsuitable for an estimate of bulk compositions of the perthites" (Ragland, 1970, p.181).

Ba decreases sharply in potassium feldspars as the host rocks become more acid. Feldspar from the central part of the monzonite core of the pluton (94) has the highest Ba content. The lower concentrations are found in the potassium feldspars from the outer part of the monzonite body and from quartz monzonite.

Since Ba is strongly concentrated in the earliest-formed K-feldspars (Heier, 1962), it would indicate that the inner part of the monzonite core crystallized earlier than the outer part of the monzonite.

Table 6.2.2 shows that the potassium feldspar from more basic monzonites (94) also has the highest content of Sr, followed by that from quartz monzonite (27). Feldspar from acid monzonite (251) has the lowest concentration. Since "the strontium contents of alkali feldspars are unlikely to have been affected by unmixing and recrystallization" (Hall, 1967, p.846), such a sequence of Sr concentration in feldspars could hardly be explained by continuous magmatic differentiation of a single magma.

Rubidium increases in the potassium feldspars from the progressively more acid rocks. Those from monzonite have very low contents of Rb (~150 ppm), while the potassium feldspar from quartz monzonite shows a value of 482 ppm. These low concentrations of Rb in potassium feldspars, resulting in an abnormally high K/Rb ratio, appear to be characteristic for feldspars from syenites and granulites (Taylor and Heier, 1958; Heier and Taylor, 1959a; Upton, 1960). Also, the Tl content in potash feldspars increases as the host rocks become more acid. The concentrations of Tl in K-feldspars from the Loon Lake pluton are comparable with values compiled by Albuquerque and Shaw (1972).

Taylor and Heier (1960) have pointed out that "Ba and Rb are considered the best elements to use to elucidate the fractionation processes in K-feldspars" and "the Ba/Rb ratio should be a critical guide to any fractionation process" (p.57) since Ba is concentrated in early formed phases and Rb is concentrated in late phases.

The sharp decrease of the Ba/Rb ratio in the feldspars studied is consistent with such a process. Similarly, the variation of some other element ratios (e.g. K/Ba, K/Rb) in feldspars from the Loon Lake pluton is compatible with the process of magmatic differentiation (contrary to the variation of Sr contents in K-feldspars, which is probably not readily consistent with a process of continuous magmatic differentiation - see above). The decrease of Ba in the potassium feldspars accompanied by a simultaneous decrease in the Ba/Sr ratio from about 15 to 5 is comparable to the range found by Heier and Taylor (1959b) in alkali feldspars from highly differentiated pegmatites. The small number of samples studied, however, is not sufficient to elucidate the fractionation process in detail. Also, the explanation of the distribution trends of trace elements in minerals of plutonic igneous rocks is not straightforward, as demonstrated by Berlin and Henderson (1968, 1969a,b).

6.2.4 Coexisting Biotites and Potassium Feldspars

With regard to the distribution of trace elements between coexisting biotite and K-feldspar, the divalent cations

Sr and Ba are substantially concentrated in K-feldspar. This general tendency for the relative enrichment of Sr and Ba in K-feldspars in comparison with biotite is usually attributed to a coupled substitution, enabling these elements to substitute for potassium. Apart from the valence difficulty, Taylor (1965) ascribed the very low level of Sr in micas to the difficulties for the usually 8 or 10-coordinated Sr to occupy the larger 12-coordinated K-positions of micas.

The evaluation of the mineralogical control of Ba distribution shows that more than 90% of the total Ba content of monzonite and quartz monzonite is present in K-feldspars. On the other hand, rubidium is considerably concentrated in biotite in comparison with K-feldspar. Also, the K/Rb ratio increases on passing from biotite to potash feldspar. Rb obviously enters the large 12-coordinated K-site of biotite structure in preference to the 8 to 10-coordinated K-site of feldspars.

The "fractionation coefficient" -

$$F/B = \frac{(K/Rb)\ \text{K-feldspar}}{(K/Rb)\ \text{biotite}}$$

(Lange et al., 1966) ranges from 3.4-4.4 and has a mean value of 3.8. Comparable values for these mineral pairs have been reported from granitic rocks (Lange et al., 1966; Dupuy, 1967, 1968; Barbieri et al., 1968; Whitney, 1969; Dodge et al., 1970). The mean value of 3.8 would fall between the experimentally-determined values for the distribution coefficient ratio of synthetic sanidine-phlogopite pairs at temperatures of 500° and 700°C (values 4.5 and 3.2, respectively, Beswick and Eugster, 1968). The similarity of the fractionation coefficient from the Loon Lake pluton to those from other granitic rocks suggest that the very high K/Rb ratios in feldspars and in rocks do not result from the generation of localized crystal chemical factors, as suggested by Taylor and Heier (1958), Heier (1962), Taylor (1965), Ewart and Taylor (1969), etc., but that they probably depend mainly on the composition of an original liquid.

The partitioning of the elements between coexisting minerals could also be used to evaluate the hypothesis of Currie and Ermanovics (1971) for the generation of zoned - monzonitic and granitic - plutons in the neighbouring Westport area and suggested also for the Loon Lake pluton (Ermanovics, 1967, 1970). Their diffusional process of migration of silica and alkalies as a cause for the generation of the monzonitic core and granitic rim of a pluton is not compatible with equilibrium conditions. The equilibrium conditions have been evaluated by the distribution of K and Rb among coexisting biotite and K-feldspar. The partitioning of K and Rb between two phases can be theoretically expressed as log a K/Rb biotite = log a K/Rb potassium feldspar+log K, where a = the activity; K = distribution coefficient - constant for given P-T conditions (c.f. Banno and Matsui, 1965; White, 1966). If an ideal solution is assumed, the activity will be approximately equal to the concentration.

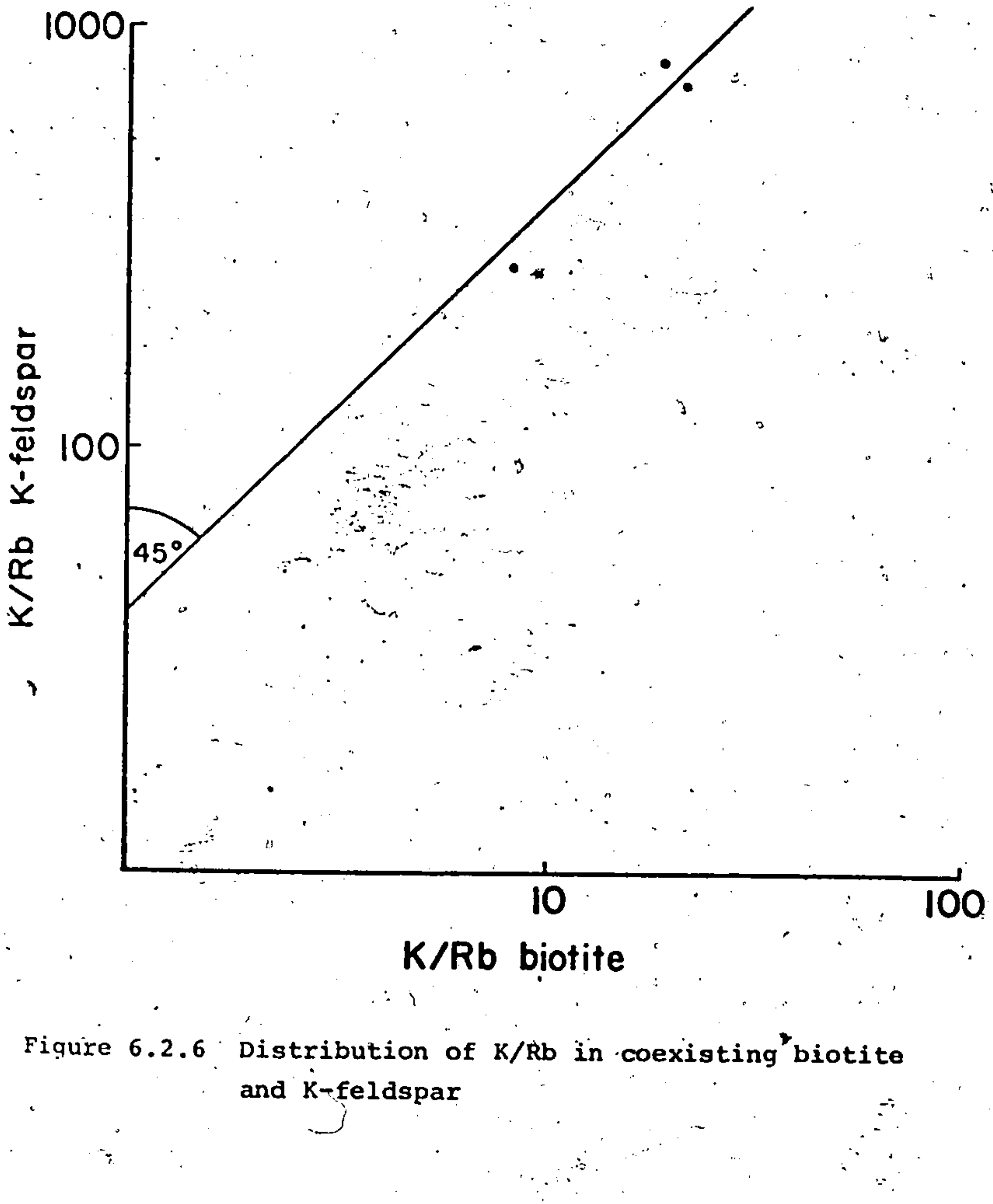

Figure 6.2.6 Distribution of K/Rb in coexisting biotite and K-feldspar

The ratio K/Rb in biotites is plotted logarithmically against the ratio K/Rb in K-feldspars in Figure 6.2.6. The coexisting mineral pairs from the felsic rocks of the Loon Lake pluton fall close to a line with a theoretical slope of 45°, thus indicating that biotite and K-feldspar attained at least approximate equilibrium.

6.2.5 Rare Earth Elements in Minerals

In order to readily compare the mineral and whole-rock REE fractionation trends and also to compare them with REE patterns for these minerals reported previously by other authors, the REE abundances in mineral phases from the rocks of the pluton have been normalized to chondrites.

6.2.5.1 Dioritic Rocks

Major mineral constituents of two dioritic rocks have been analyzed for the rare earths. Analyzed minerals include hornblende, biotite and plagioclase from diorite 70 and clinopyroxene and plagioclase from diorite 321.

Figures 6.2.7-8 show the REE fractionation trends for both minerals and whole-rock analyses of these two diorites. REE patterns for both feldspars are typical for plagioclase (Towell et al., 1965; Schnetzler and Philpotts, 1970; Nagasawa and Schnetzler, 1971). They are gradually depleted from La to Lu with strong positive Eu anomalies. The steady depletion of REE toward Lu is "either due to crystallochemical control or due to

Figure 6.2.7 REE distribution in biotite, hornblende, plagioclase and their host diorite 70

× - biotite

○ - hornblende

● - plagioclase

□ - whole-rock

Figure 6.2.8 REE distribution in clinopyroxene, plagioclase and their host diorite 321

○ - clinopyroxene

● - plagioclase

□ - whole-rock

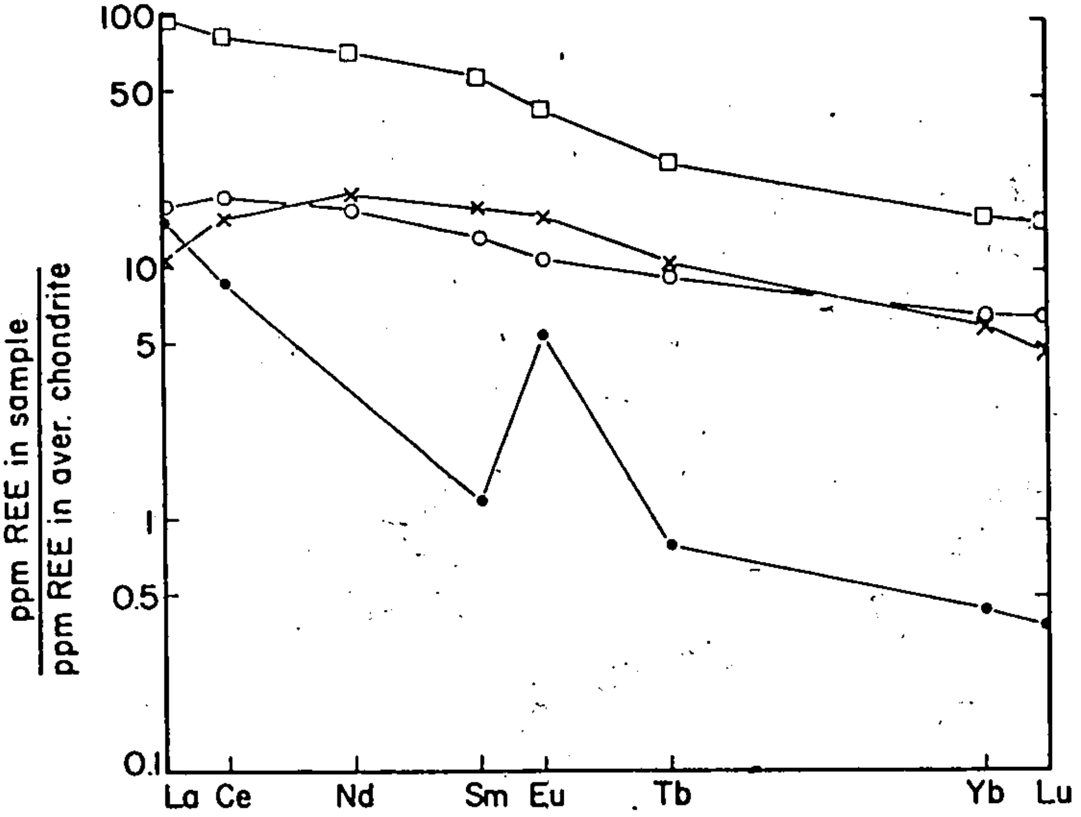
100
50
10
5
1
0.5
0.1
ppm REE in sample / ppm REE in aver. chondrite
La
Ce
Nd
Sm
Eu
Tb
Yb
Lu

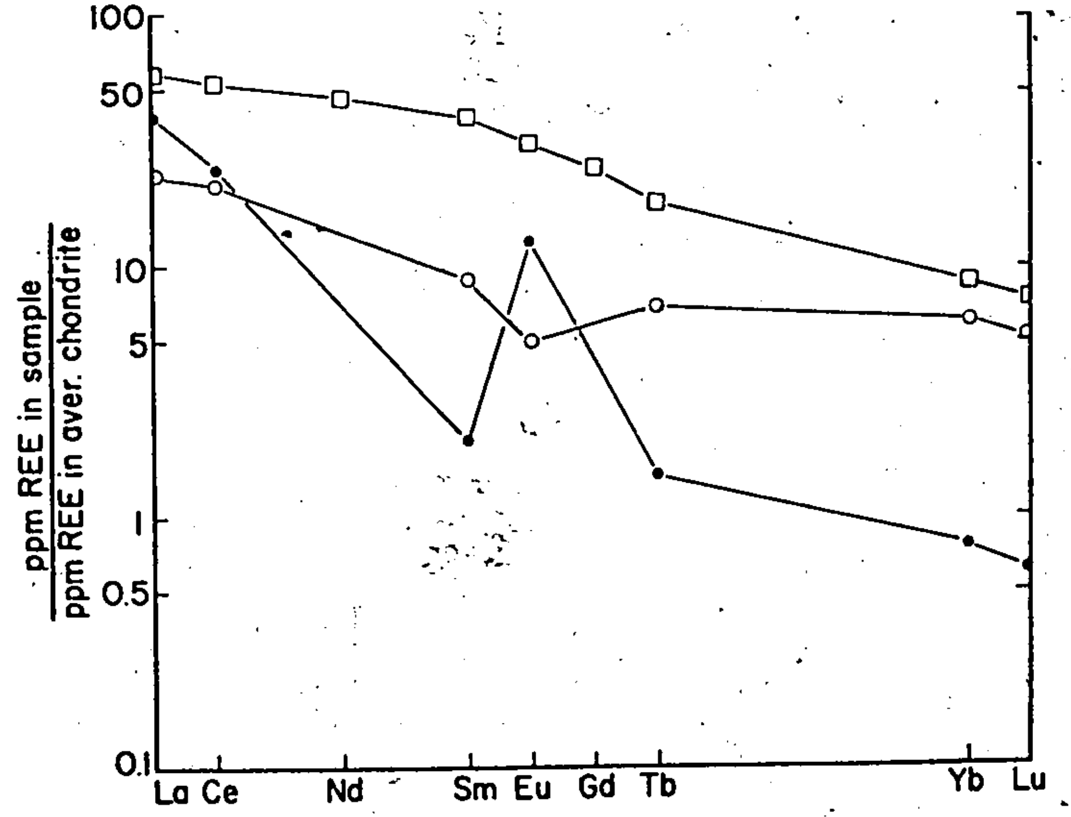
100
50
10
5
1
0.5
0.1
ppm REE in sample / ppm REE in aver. chondrite
La
Ce
Nd
Sm
Eu
Gd
Tb
Yb
Lu

close-system competition with other mafic phases like pyroxene or amphiboles" (Shih, 1972, p.59). The distinct positive Eu anomalies are characteristic for feldspars. The significant enrichment of Eu in feldspars is attributed to its partial existence as Eu^{2+} contrary to the other typically trivalent REE with the possible occasional exception of Ce. According to Philpotts (1970) and Nagasawa (1971), Eu is present in feldspars mainly in a divalent state.

The fractionation trend of clinopyroxene is similar to those given by, for example, Schnetzler and Philpotts (1970). A negative Eu anomaly in clinopyroxene might indicate that the plagioclase and clinopyroxene have crystallized at the same time and competed for REE in a closed system, although, due to the partial alteration of clinopyroxene, its fractionation trend should be treated cautiously. The REE pattern for hornblende differs slightly from that of clinopyroxene, thus supporting a suggestion that hornblende is of primary origin. The absence of Eu depletion in hornblende might indicate that plagioclase and hornblende did not crystallize at the same time and that the crystallochemical effect was a prominent factor (however, since the absolute REE abundances in hornblende are substantially higher than those in plagioclase, this argument is weakened).

The chondrite-normalized REE trend for biotite is somewhat striking. It differs from biotites of felsic rocks in the depletion at the La end of the pattern. It is also less fractionated and lacks significant Eu depletion. The similarity to the hornblende REE pattern tempts the suggestion that biotite is secondary after hornblende and is formed mainly from it. The replacement of hornblende is also indicated by petrography (c.f. section 5.5.4).

It appears, however, that most of the REE in dioritic rocks are present in accessory minerals, probably apatite and sphene (the latter, however, appears to be partially of secondary origin - c.f. Saha, 1957). The enrichment of the light REE in sphene and apatite (Fleischer and Altschuler, 1969; Nagasawa, 1970) is consistent with the observed REE patterns of dioritic rocks displaying gradual enrichment toward La. (In this connection, Figures 6.2.7-8 show that the REE patterns of these diorites cannot be explained only by the silicates analyzed).

6.2.5.2 Monzonite

REE have been determined in major mineral phases of three different monzonites, spanning the observed variation range for monzonitic rocks. Mineral phases include hornblende, biotite, K-feldspar and plagioclase from monzonite 94, biotite, K-feldspar and plagioclase from monzonite 207 and biotite, sphene, plagioclase and K-feldspar from monzonite 251.

Sample 94 represents a "basic" clinopyroxene-hornblende bearing monzonite with a low D.I. value (=80.1). Sample 251 is "acid" biotite monzonite from the outer part of the monzonite body with a high D.I. (=88.0). The composition of monzonite 207 is intermediate between them (D.I. = 81.8). Figures 6.2.9-11 show chondrite-normalized REE patterns for these rocks and their mineral constituents. REE patterns for all feldspars are comparable with published feldspar values (Towell et al., 1965; Schnetzler and Philpotts, 1968; 1970; Buma et al., 1971; Dudas et al., 1971; Nagasawa, 1971, 1973). They display gradual depletion in heavy REE with strong positive Eu anomalies. In accordance with the data of Schnetzler and Philpotts (1970), K-feldspars have lower total contents of REE than the coexisting plagioclases, but are relatively more enriched in Eu.

As noted earlier, the anomalous distribution of Eu relative to other REE is attributed to its partial presence as Eu^{2+}. Philpotts (1970) has pointed out that the Eu^{2+}/Eu^{3+} ratio can be calculated in any two equilibrated phases of a known Sr and REE concentration, assuming equal partition coefficients for Eu^{2+} and Sr between these coexisting phases. The assumption of such equivalence appears to be reasonable, not only because of the same charge, but also the difference in ionic radii falls well within Goldschmidt's 15% "substitutional limit" (Philpotts, 1970, p.259). Shanon and Prewitt (1969) give ionic radii for both Eu^{2+} and Sr^{2+} in eight-fold coordination of 1.25 Å. The Eu^{2+}/Eu^{3+} ratio calculated by Philpotts' (1970) method from K-feldspar-biotite pairs is 23 for K-feldspar from sample 94. It indicates that Eu in K-feldspars is present

Figure 6.2.9 REE distribution in hornblende, biotite, K-feldspar, plagioclase and their host monzonite 94

○ - hornblende
× - biotite
☼ - K-feldspar
● - plagioclase
□ - whole-rock

Figure 6.2.10 REE distribution in biotite, K-feldspar, plagioclase and their host monzonite 207

× - biotite
○ - K-feldspar
● - plagioclase
□ - whole-rock

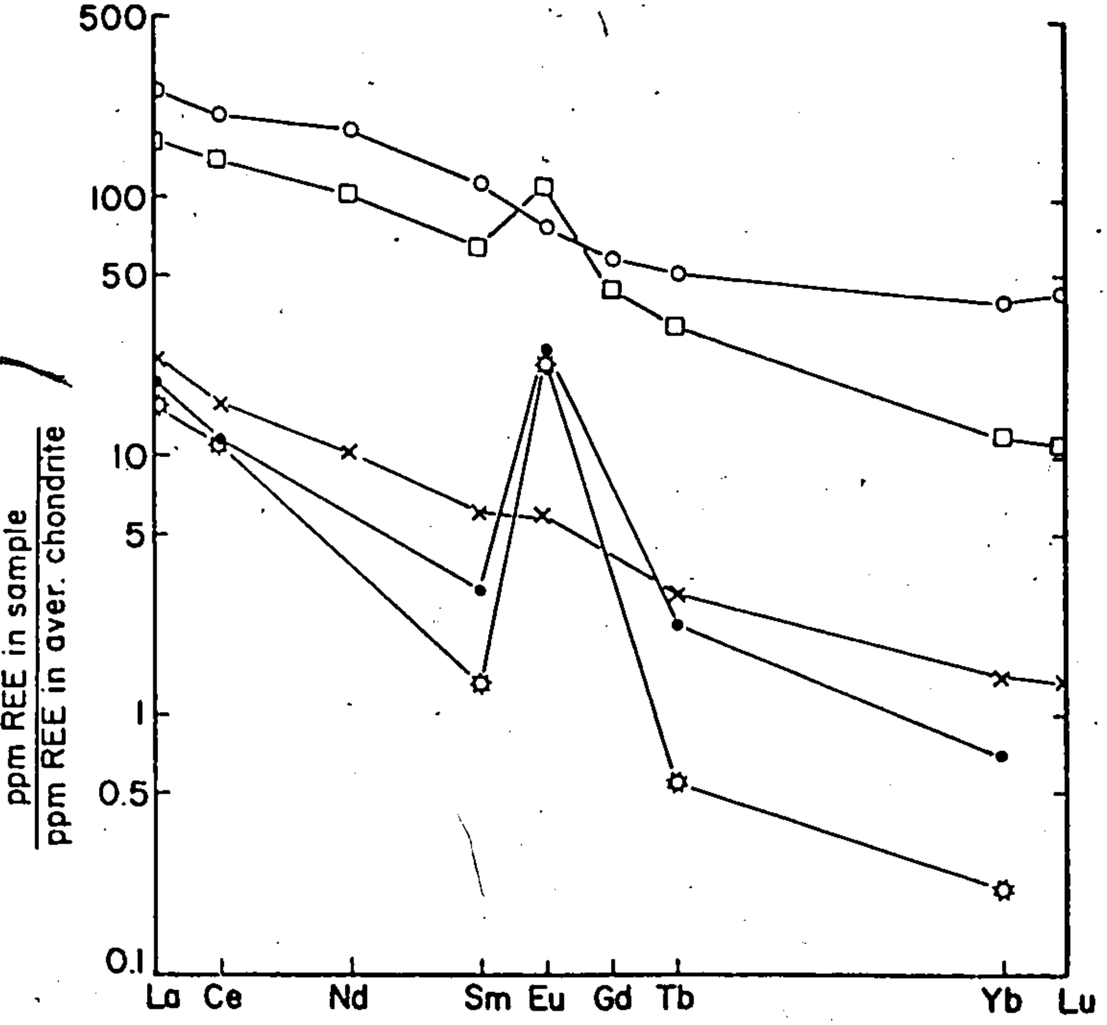
500
100
50
10
5
1
0.5
0.1
ppm REE in sample / ppm REE in aver. chondrite
La
Ce
Nd
Sm
Eu
Gd
Tb
Yb
Lu

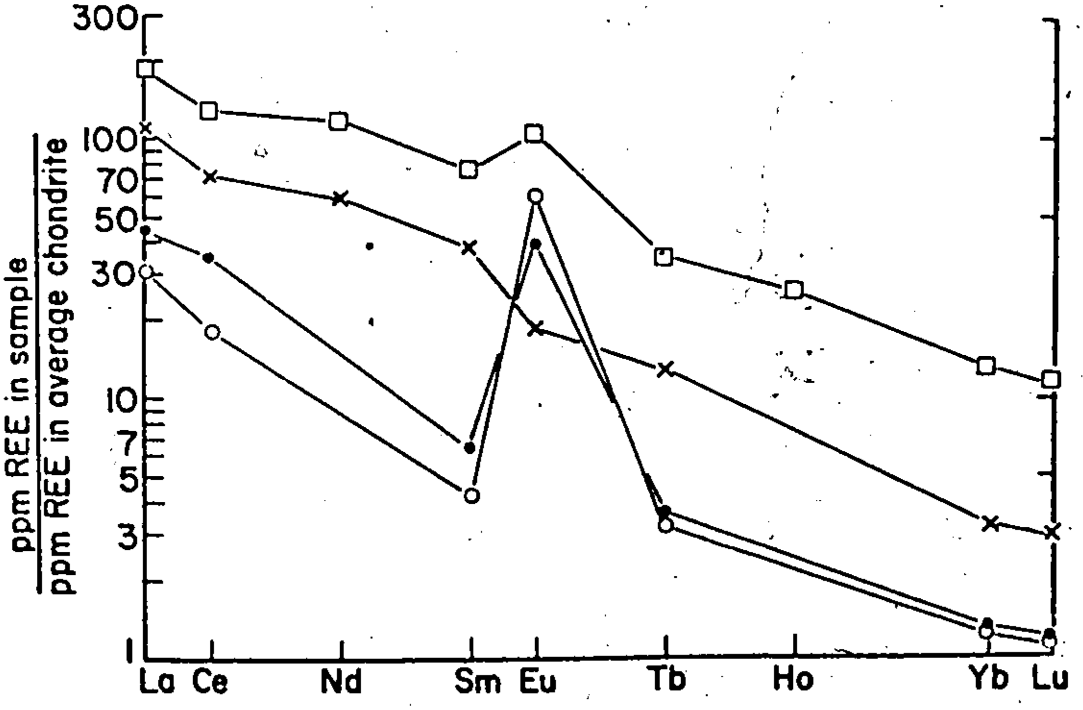
300
100
70
50
30
10
7
5
3
1
ppm REE in sample / ppm REE in average chondrite
La
Ce
Nd
Sm
Eu
Tb
Ho
Yb
Lu

Figure 6.2.11 REE distribution in sphene, biotite, K-feldspar, plagioclase and their host monzonite 251

☼ - sphene
× - biotite
○ - K-feldspar
● - plagioclase
□ - whole-rock

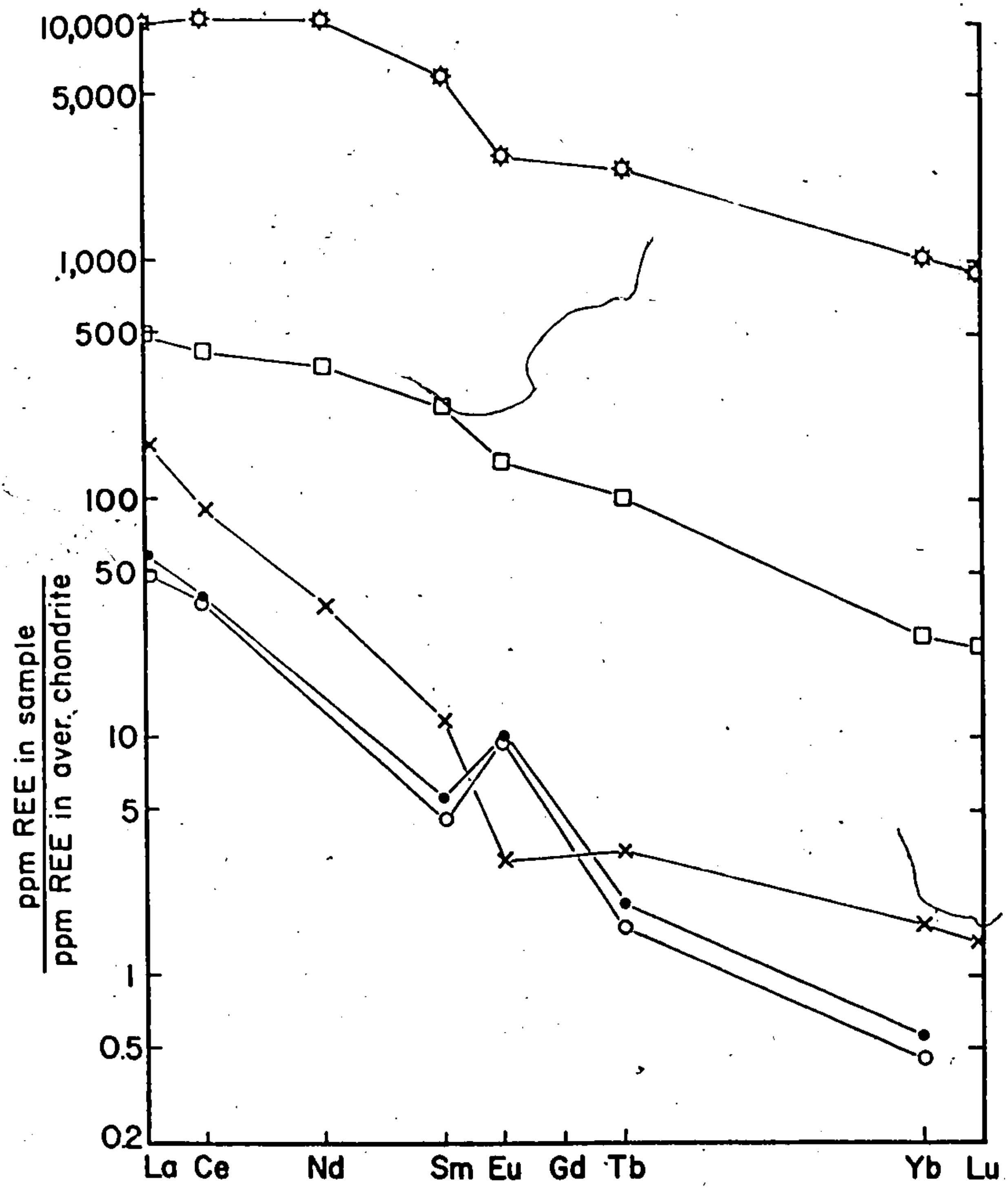
10,000
5,000
1,000
500
100
50
10
5
1
0.5
0.2
ppm REE in sample / ppm REE in aver. chondrite
La
Ce
Nd
Sm
Eu
Gd
Tb
Yb
Lu

mainly in a divalent state. Another characteristic feature is the increase of total REE in feldspars with the increase of the degree of differentiation and REE contents of their host rocks.

The REE pattern of hornblende is considerably enriched in light REE relative to chondrite, but compared to the whole-rock trend it is less fractionated favouring the heavy rare-earths. The absence of significant Eu depletion may indicate that the crystallochemical factor was predominant for the REE distribution and that hornblende could have crystallized in an open system or at a different time than feldspars.

REE patterns for biotite are similar to those recorded by Buma et al. (1971). Their degree of fractionation appears to positively correlate with the La/Yb ratio of whole-rocks. The abundances of Eu relative to other REE in biotite, similar to those of whole-rocks and feldspars, decrease with the increase of the D.I. values of the rock. On the other hand, the total REE contents of biotite increase as the D.I. values of the host rocks increase.

Sphene has by far the highest total REE concentration from analyzed minerals. Rare-earth distribution in sphene exhibits a light REE enrichment relative to chondrites with a slight maximum at Ce and Nd. In general, the observed trend is similar to that of whole-rock.

Figures 6.2.9-10 (samples 94 and 207) also show that the REE patterns of these rocks cannot be explained by the analyzed major rock-forming minerals alone. Unlike many granitic rocks (Haskin et al., 1966), the REE distribution in monzonite from the Loon Lake pluton is strongly influenced by accessory minerals, notably sphene and possibly apatite, which probably contain most of the REE of these rocks. But perhaps the most striking feature of the REE distribution in mineral separates is the variation of Eu abundance relative to other rare-earths, particularly in feldspars. The decrease of Eu anomalies paralleled by the increase of total REE abundance in feldspars and by the decrease of relative Eu abundance in the whole-rocks with the increase of the D.I. values (Table 6.2.3), suggests that the size

Table 6.2.3 Some trace element abundances in feldspars and their host monzonites

Sample No.	1	2	3	4	5	6	7	8	9
94	23.0	9.7	2.2	5.21	6.43	54.1	13300	837	80.1
207	16.0	7.8	1.8	10.20	14.70	61.2			81.8
251	3.1	2.5	0.8	16.40	19.1	158.0	1970	178	88.0

1 Eu/Eu* in K-feldspar
2 Eu/Eu* in plagioclase
3 Eu/Eu* in whole-rock
4 La (ppm) in K-feldspar
5 La (ppm) in plagioclase
6 La (ppm) in whole-rock
7 Ba (ppm) in K-feldspar
8 Sr (ppm) in K-feldspar
9 D.I. of whole-rock

of the Eu anomalies are largely controlled by the composition of the original liquid. The decrease of Eu anomalies in feldspars accompanied by the decrease of Ba and Sr and the increase of Rb (Table 6.2.3) strongly suggest that this variation in the chemical composition of monzonite is mainly due to the crystallization of feldspars with higher contents of Sr, Ba and Eu than the melt. Thus the residual liquid from which progressively more fractionated monzonites (with progressively higher D.I. values) crystallized were accordingly enriched in Rb and depleted in Sr, Ba and Eu. The gradually increased La/Yb ratio of whole-rocks, however, indicates that the fractionation of other REE was dominated by mafic and accessory minerals.

6.2.5.3 Quartz Monzonite

Major mineral constituents from three different quartz monzonites have been analyzed for REE. Analyzed mineral phases are plagioclase, K-feldspar and biotite from samples 26 (value of D.I. = 89.1), 27 (D.I. = 92.0) and 115 (D.I. = 91.7). The results for these minerals normalized to chondritic values are given in Figures 6.2.12-14, together with the REE patterns of their host rocks.

In general, the REE patterns for feldspars are similar to those from monzonite, once again with a higher total REE abundance and a smaller Eu/Eu* ratio in plagioclase than in K-feldspar. The Eu/Eu* ratios in both feldspars are comparable

Figure 6.2.12 REE distribution in biotite, K-feldspar, plagioclase and their host quartz monzonite 26

× - biotite

○ - K-feldspar

● - plagioclase

□ - whole-rock

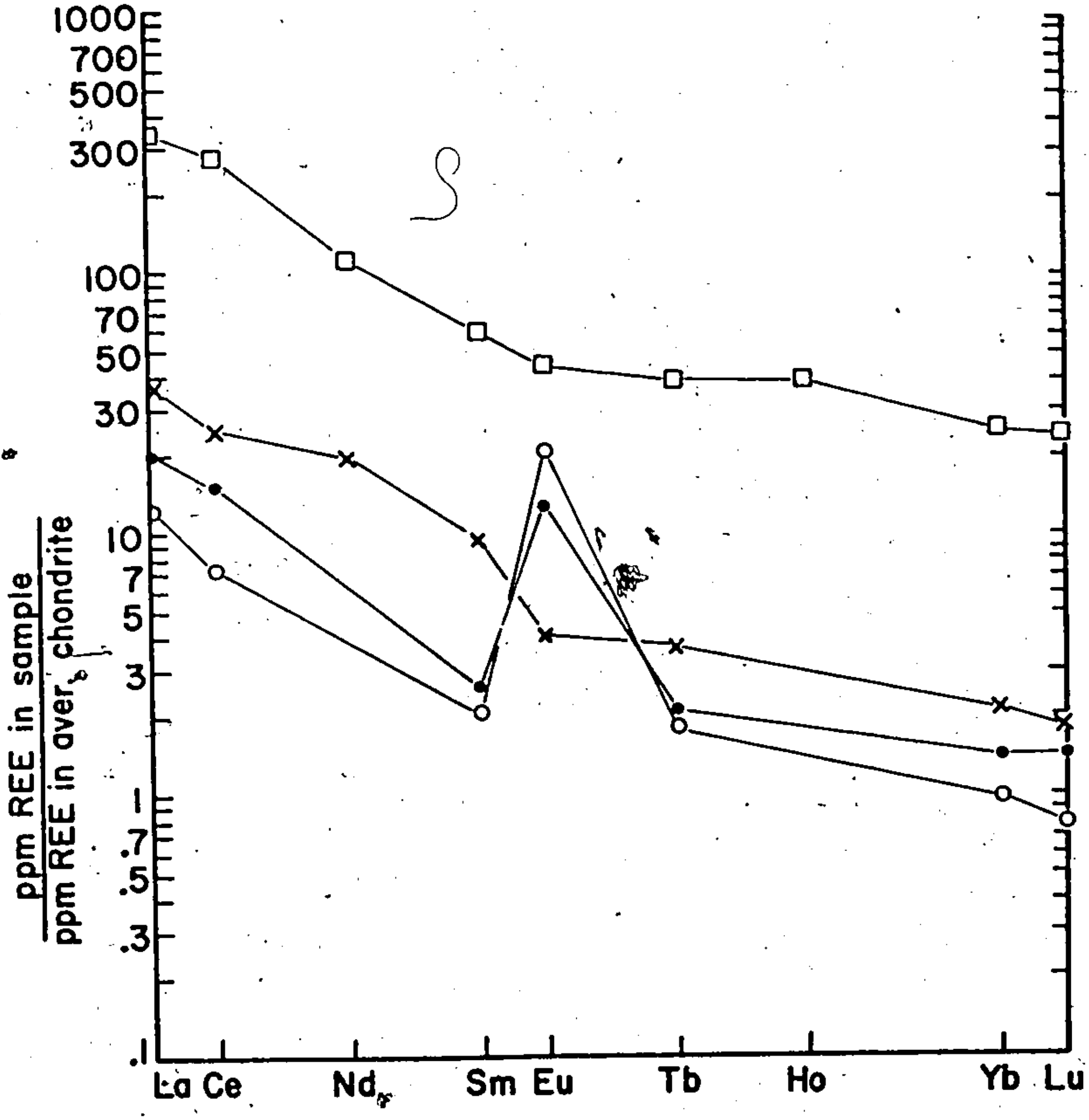
1000
700
500
300
100
70
50
30
10
7
5
3
1
.7
.5
.3
.1
ppm REE in sample / ppm REE in aver. chondrite
La
Ce
Nd
Sm
Eu
Tb
Ho
Yb
Lu

Figure 6.2.13 REE distribution in biotite, K-feldspar, plagioclase and their host quartz monzonite 115

✕ - biotite
○ - K-feldspar
● - plagioclase
□ - whole-rock

Figure 6.2.14 REE distribution in biotite, K-feldspar, plagioclase and their host quartz monzonite 27

✕ - biotite
○ - K-feldspar
● - plagioclase
□ - whole-rock

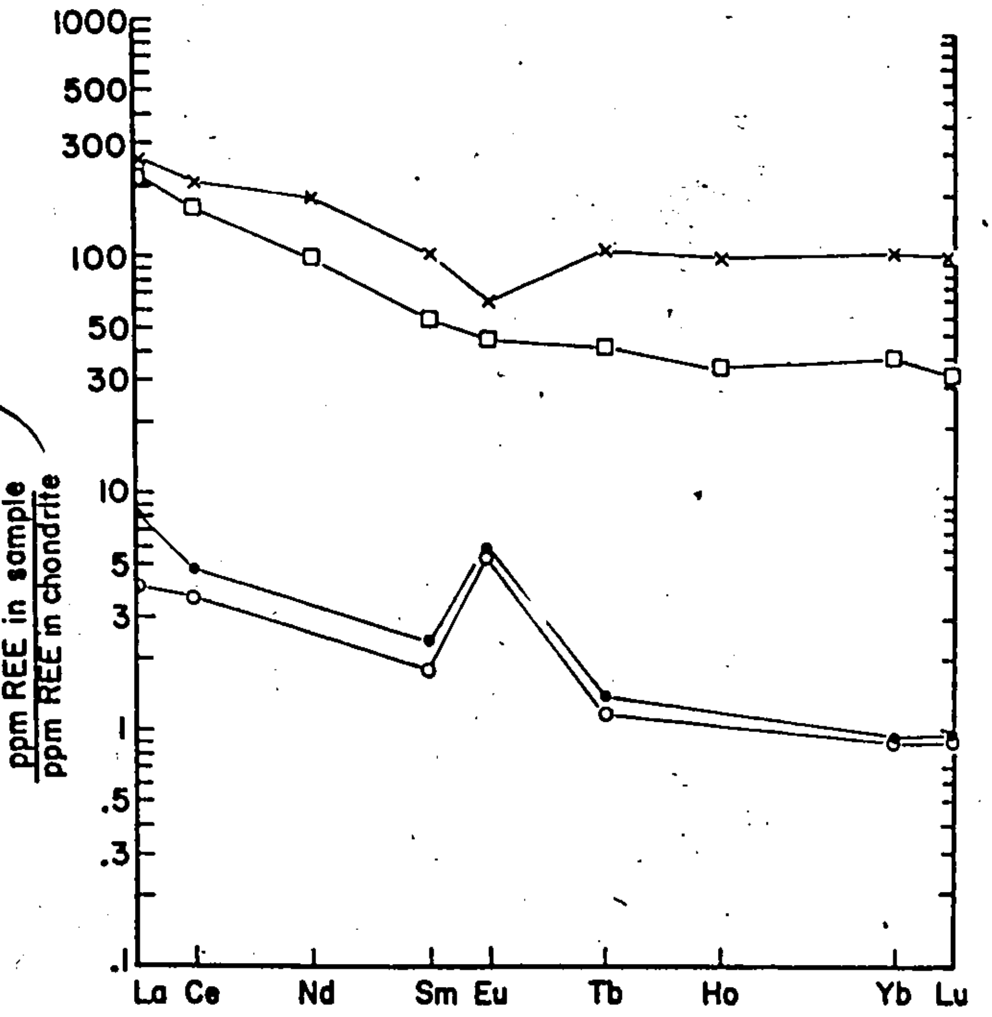
1000
500
300
100
50
30
10
5
3
1
.5
.3
.1
ppm REE in sample / ppm REE in chondrite
La
Ce
Nd
Sm
Eu
Tb
Ho
Yb
Lu

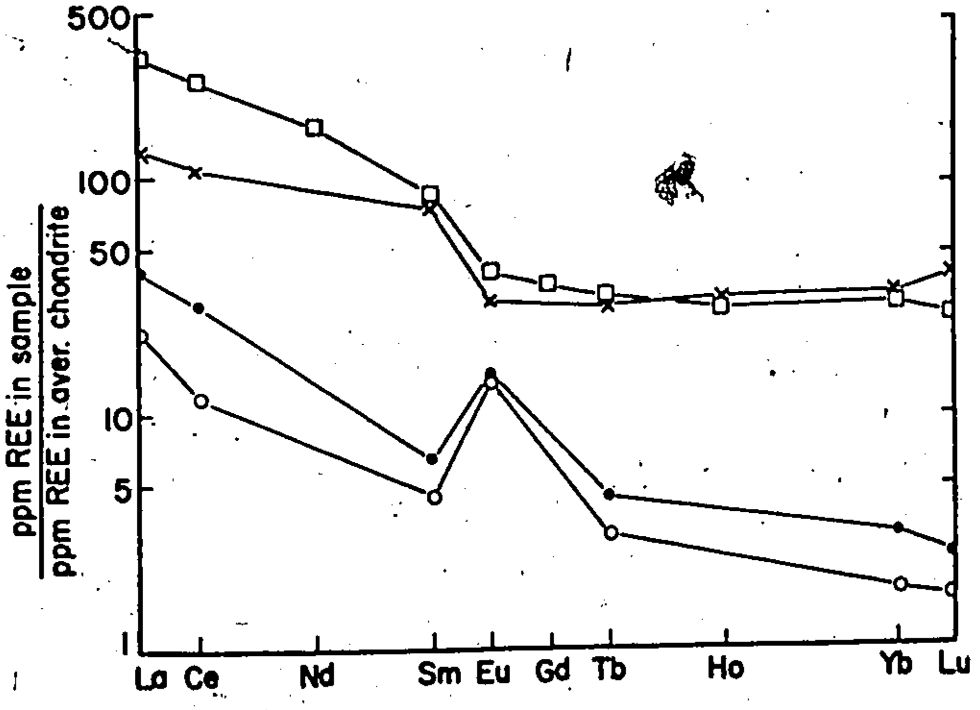
500
100
50
10
5
1
ppm REE in sample / ppm REE in aver. chondrite
La
Ce
Nd
Sm
Eu
Gd
Tb
Ho
Yb
Lu

to the Eu enrichment observed in feldspars from other granitic rocks (4-13, Towell et al., 1965; Buma et al., 1971). The Eu^{2+}/Eu^{3+} ratio calculated by Philpotts' (1970) method from K-feldspar-biotite pairs of sample 27 indicates that Eu in K-feldspars of these rocks is also mainly in a divalent state (Eu^{2+}/Eu^{3+} = 5.5 for K-feldspar 27).

Relative to the chondrite REE distribution, biotite from quartz monzonite is progressively enriched in light REE, with slight negative Eu anomalies. The absolute content of rare-earths and their relative fractionation in biotite are variable.

Among the major mineral constituents, biotite has the highest concentration of REE. A mass balance, however, shows that REE are not chiefly contained in major mineral phases (biotite and feldspars) but in accessory minerals, probably apatite and sphene. A similar distribution, where REE are predominantly present in accessory minerals, has been found in some other granitic rocks (e.g. Gavrilova and Turanskaya, 1958; Buma et al., 1971; Condie and Lo, 1971).

6.3 Summary

1. Monzonitic and quartz monzonitic rocks from the pluton have a subalkaline character.

2. Comparison with the Or-Ab-An-Q-H_2O systen suggests

that felsic rocks from the pluton resulted from "crystal-liquid equilibria" (Tuttle and Bowen, 1958).

3. The variations of major and some trace elements (Rb, Sr, Ba and Tl) in quartz monzonite are consistent with the trends produced by fractional crystallization. The variations of Ca, K, Ba and Sr in these rocks suggest a significant role for feldspars during such a process. The variations of REE, however, are not readily compatible with this mechanism. But the evaluation of REE variations is complicated by the fact that the bulk of the REE in quartz monzonites is present in accessory minerals.

4. Monzonites, as a series, show systematic chemical variations which are consistent with the trends produced by extensive fractional crystallization dominated by feldspars. The dominant feldspar fractionation is probably the reason why Rb and Tl are significantly less fractionated than Ba and Sr. Also, the variations of the Eu anomaly suggest that monzonites are partially cumulative (basic monzonites with positive Eu anomalies) and partially differentiated (acid monzonites with negative Eu anomalies), due to the accumulation or removal of feldspars.

5. The variations of the chemical composition of monzonites and quartz monzonites suggest a comagmatic origin for these two rock types. Some quartz monzonites, however, appear to be less fractionated than acid monzonites, indicating that the felsic rocks of the pluton, as a series, are not simply products

of continuous magmatic differentiation of a single magma leading to accumulation of residual quartz, and that a more complex process was involved.

6. The characteristic feature of monzonites and some quartz monzonites is very high K/Rb and K/Tl ratios relative to "normal" crustal values. These high ratios are also accompanied by relative impoverishment of Rb and Tl in both biotites and K-feldspar in comparison with those from typical granitic rocks.

7. The partitioning of K and Rb between coexisting K-feldspar and biotite from felsic rocks indicates that these two phases attained at least approximate equilibrium.

8. The composition of biotites from the felsic rocks of the pluton is consistent with oxygen fugacities slightly higher than those in equilibrium with a Ni-NiO buffer.

9. Dioritic rocks show distinct chemical variations. At least some of these variations appear to be of primary magmatic variation, suggesting that these rocks underwent magmatic differentiation. But some variations are also compatible with the process of hybridization or assimilation by felsic magma, hindering reliable evaluation of a possible genetic relation

between basic and felsic rocks of the pluton. There are, however, indications that these rocks might not be genetically related.

CHAPTER 7

PETROGENESIS

7.1 Introduction

A number of theories have been invoked to explain the origin of felsic plutons such as the Loon Lake pluton, which are zonally and concentrically arranged relative to the contacts, with progressive acidification toward the wall-rocks.

Wynne-Edwards (1957) and Saha (1957, 1959) attribute such zoning to the marginal assimilation of the more acid country rocks, while Shaw (1962) has proposed, specifically for the Loon Lake pluton, only the selective transfer of some elements, mainly silica, from the wall-rocks. Alternatively, Wright (1966) and Saha (1957, 1959) have invoked multiple intrusions of magma.

Ermanovics (1967, 1970) has suggested that the zonation in the Perth Road pluton in the Westport area may be attributed to the intrusion of a single magma with subsequent magmatic differentiation in situ or nearly so. Also, Chapman (1968) has advocated for zoned plutons in the Appalachians, the intrusion of a single but inhomogeneous magma. Acidification of the periphery of the pluton due to metamorphism (Fox, 1969) or the escape of volatiles (Emmons, 1953; Ermanovics, 1970) have also been invoked. Likewise, a process of "granitization", a large scale migration of silica and alkalies (Currie and Ermanovics, 1971) and some other mechanisms have been suggested to explain the zonation of such plutons.

Considerable field evidence can be offered to suggest that a magmatic phase existed during the formative stages of the pluton and that the pluton was forcefully injected into already metamorphosed country rocks (e.g. contact metamorphosed aureole, rotation of inclusions, dips of the wall-rocks toward the contacts, etc.).

The observational data and inferences pertinent to the Loon Lake pluton (c.f. chapter 5 and Saha, 1957, 1959) suggest that the pluton represents multiple intrusions of progressively more siliceous magma. The relative ages of the three distinct intrusive units of the pluton, as inferred in the field on the basis of cross-cutting relations, are (in order of decreasing age): diorite, monzonite, quartz monzonite (c.f. Saha, 1957, 1959; Shaw, 1962).

Other problems common to many zoned plutons representing multiple intrusions are whether the individual intrusive phases are genetically related, whether they have been formed from a single parental magma and what is the nature of the original magma.

7.2 Dioritic Rocks

The presence of basic (gabbro-diorite) bodies in several monzonitic plutons in this part of the Grenville Province might suggest a co-genetic relation between these two rock types. But in most of these plutons, basic and monzonitic rocks are considered to be genetically unrelated (Saha, 1957, 1959; Wynne-Edwards, 1967; Currie and Ermanovics, 1971, etc.). The same conclusion - unrelated origin - was suggested by Saha (1957, 1959) and Shaw (1962) specifically for the Loon Lake pluton.

The relation of dioritic rocks toward the bulk of the pluton formed by monzonitic and quartz monzonitic rocks is uncertain. Diorite is, in many places, cut by monzonite and therefore older than felsic rocks. As noted earlier, when dioritic and monzonitic rocks are treated as a series on the variation diagrams, they show smooth trends for major elements from the basic to the more acid ones. These trends for major elements are consistent with those produced by magmatic differentiation. But some of these trends are also compatible with the process of hybridization or assimilation (Nockolds and Allen, 1956). Transition rocks have compositions that could have been formed by the mixture of "basic" diorites and monzonites. But there is evidence that at least some variations are of primary magmatic origin (variation of the Fe/Mg ratio, variation of the basicity of plagioclase, etc.) thus indicating that diorites underwent magmatic differentiation. On the other hand, the petrography of these rocks suggests that a certain degree of alteration of diorites by felsic magma took place. The large flakes of biotite and patches of K-feldspar replacing other minerals appear to be related to this alteration (c.f. Saha, 1957, 1959; Shaw, 1962). The contents of these "later" minerals decrease inward from the edges of basic inclusions. The process of hybridization is also consistent with the remarkably high content of potassium in some of the basic rocks. It is also of interest that some transitional rocks have a chemical composition similar to "pyroxene syenite" of Buddington (1939) from the Adirondacks, and to shoshonites from Wyoming (Prostka, 1973), both of which are considered to be the result of hybridization and assimilation of gabbro and amphibolite by syenitic magma (c.f. Buddington, 1939; Prostka, 1973). Thus it is difficult to evaluate to what degree a smooth variation trend for major elements between monzonites and diorites resulted from magmatic differentiation or to what degree they represent the alteration of diorites by monzonitic magma.

Despite the fact that the variation trends between basic and monzonitic rocks may have been affected by hybridization, it might be suggested, however, that dioritic rocks could originally be genetically related to the bulk of the pluton. But the clarification of this possibility is complicated by uncertainties with respect to the original chemistry of diorites.

Assuming that the chemistry of diorites, which petrographically appear to be least altered, represents the original unmodified composition of basic rocks, then the variations of some elements and element ratios may argue against a genetic relation between diorites and monzonites. The Ca/Sr vs Sr (Figure 6.1.27), K/Rb vs Rb (Figure 6.1.21) and K/Tl (Figure 6.1.35) diagrams show two distinct trends - one for felsic and the second for basic rocks. Such variations suggest that these two rock types do not belong to a comagmatic series and they were not produced by magmatic differentiation of a single magma (assuming, of course, that these trends do not reflect only secondary changes in the diorites). Thus the available data are consistent with the conclusion of Saha (1957, 1959) and Shaw (1962) that the basic rocks from the Loon Lake pluton "are not early differentiates of the monzonite, but represent inclusions or roof pendants of gabbros previously injected into the paragneisses" (Shaw, 1962, p.13). But due to the uncertainty of the original composition of dioritic rocks, these conclusions about their eventual relation to the bulk of the pluton, should be treated cautiously.

The presence of the dunite inclusion in the pluton might invoke the suggestion that the sequence ultrabasic rocks (dunite) and diorite could be part of a layered intrusion. The data on hand, however, cannot unequivocally evaluate this suggestion. There is no obvious evidence that these rocks are genetically related.

7.3 Monzonite

There appear to be two aspects to the problem of the petrogenesis of the monzonite from the Loon Lake pluton. These are:

(a) the fractionation processes operating within the monzonitic magma;

(b) the origin of the monzonitic magma.

7.3.1 Fractionation within the Monzonite

Monzonitic rocks as a series show large and systematic variation, not only in the chemical composition of major and trace elements, but also in element ratios as a function of the D.I. values. These variations are consistent with extensive fractional crystallization. Such a process probably involved the crystallization of large amounts of feldspars with K/Rb, K/Tl, Ba/Rb, Eu/Eu* ratios and concentrations of Ba, Sr, etc., higher than the melt and with Ca/Sr, Rb/Sr, K/Ba ratios and contents of Rb, Tl, etc., lower than the melt. The crystallization of feldspars was also likely accompanied by smaller amounts of mafic and possibly accessory minerals (sphene and probably also apatite) with La/Yb and Fe/(Fe+Mg) ratios lower than in the melt. Thus the residual liquid from which progressively more acid monzonite crystallized was accordingly depleted in Ba, Sr, a relative concentration of Eu, heavy rare-earths, etc., and enriched in Rb, Tl, total rare-earths, a relative concentration of light REE, etc. The positive Eu anomaly, high concentration of Ba, Sr, unusually high K/Rb ratio, etc. in the basic, least fractionated monzonite (with the lowest D.I. values) emphasize the important role of feldspar fractionation and these features may be attributed largely to feldspar accumulation.

As already noted earlier, however, the monzonites as a whole are not the product of feldspar accumulation, but probably crystallized from monzonitic magma. The negative Eu anomalies in acid monzonites, the petrography, the position in the Q-Ab-Or system, the chemical variation trends, etc., indicate that feldspars are not in excess. The rather high K/Rb ratio even in rocks with a negative Eu anomaly and also in minerals, suggest that the original K/Rb ratio of magma was very high.

With regard to the actual mechanism, it seems significant that the least fractionated and most basic monzonitic rocks occur in the centre of the monzonitic body. Such a distribution is in accordance with the earlier suggestion (section 5.8) of a process of flow differentiation, which is based on the principle that the suspended particles in a flowing liquid tend to move from the walls and border zones toward the central portion. This is also consistent with the suggestion that monzonite was emplaced partly as a crystal mush (Shaw, 1962) probably containing feldspars and clinopyroxene as the main components. Shaw pointed out that during the emplacement, monzonitic magma "must have already crystallized to a notable extent because the solid crystals were oriented during flow to give the foliation and lineation now visible" (1962, p.16). It is also difficult to visualize extensive fractionation in situ which would be required to generate large variations in the chemistry of monzonitic rocks if they were emplaced as crystal mush.

7.3.2 The Origin of the Monzonitic Melt

Numerous hypotheses for the origin of syenitic and monzonitic rocks have been invoked, but none has been widely accepted. Only a few pertinent hypotheses of the origin of monzonitic magma will be discussed below.

7.3.2.1 Partial Melting of Crustal Rocks

Several hypotheses of partial melting of quartz-poor feldspathic rocks have been proposed for the origin of monzonite. Currie and Ermanovics (1971) have suggested that the monzonitic plutons in the neighbouring Westport area, which compositionally are rather similar to the Loon Lake pluton, were generated by partial melting of country rocks accompanied by diffusion which "caused silica and alkalies to migrate away from the sites of anatexis, leaving a relatively calcium-rich syenitic melt (monzonite). The mobile material collected on the margin of the anatectic masses, producing rocks of granitoid composition" and they "draw the general conclusion that monzonitic to syenitic melts can develop by anatexis followed by desilication by transport in the vapour phase" (Currie and Ermanovics, 1971, p.68). In general, this process does not appear to be readily applicable to the Loon Lake pluton. With respect to field and petrographic observations, the pluton is clearly intrusive and imposed distinct contact metamorphism on the surrounding rocks and thus could hardly be generated in situ or nearly so.

Consideration of the normative compositions of monzonitic rocks from the pluton in the system An-Ab-Or-Q, partitioning of trace elements between coexisting phases, smooth variation trends etc., indicate that an origin involving any metasomatic or diffusion processes is unlikely. This also applies to the suggestion for the introduction of late K-feldspar as a process for the generation of monzonites. As Tuttle and Bowen (1958), however, pointed out, the position of rocks in the thermal troughs of the An-Ab-Or-Q system most probably resulted from "crystal-liquid equilibrium". Thus a model of partial melting of quartz-poor feldspathic rocks without any additional diffusion or metasomatism can be considered.

The hypothesis of partial melting in the deeper crust appears to be consistent with the REE data. Figure 7.1 shows chondrite-normalized REE patterns of garnet-sillimanite-cordierite hornfelses, monzonite and the averages of the North American shale and metamorphosed North American shale (Haskin et al., 1968a), which are generally considered a good approximation

Figure 7.1 REE distribution in monzonites, aluminous hornfelses and the averages of North American shales

○ - monzonite 94

◇ - monzonite 198

▮ - monzonite 251

◐ - aluminous hornfels 67

◩ - aluminous hornfels 712-4

■ - composite of North American shales (Haskin et al., 1968a)

□ - composite of metamorphosed North American shales (Haskin et al., 1968a)

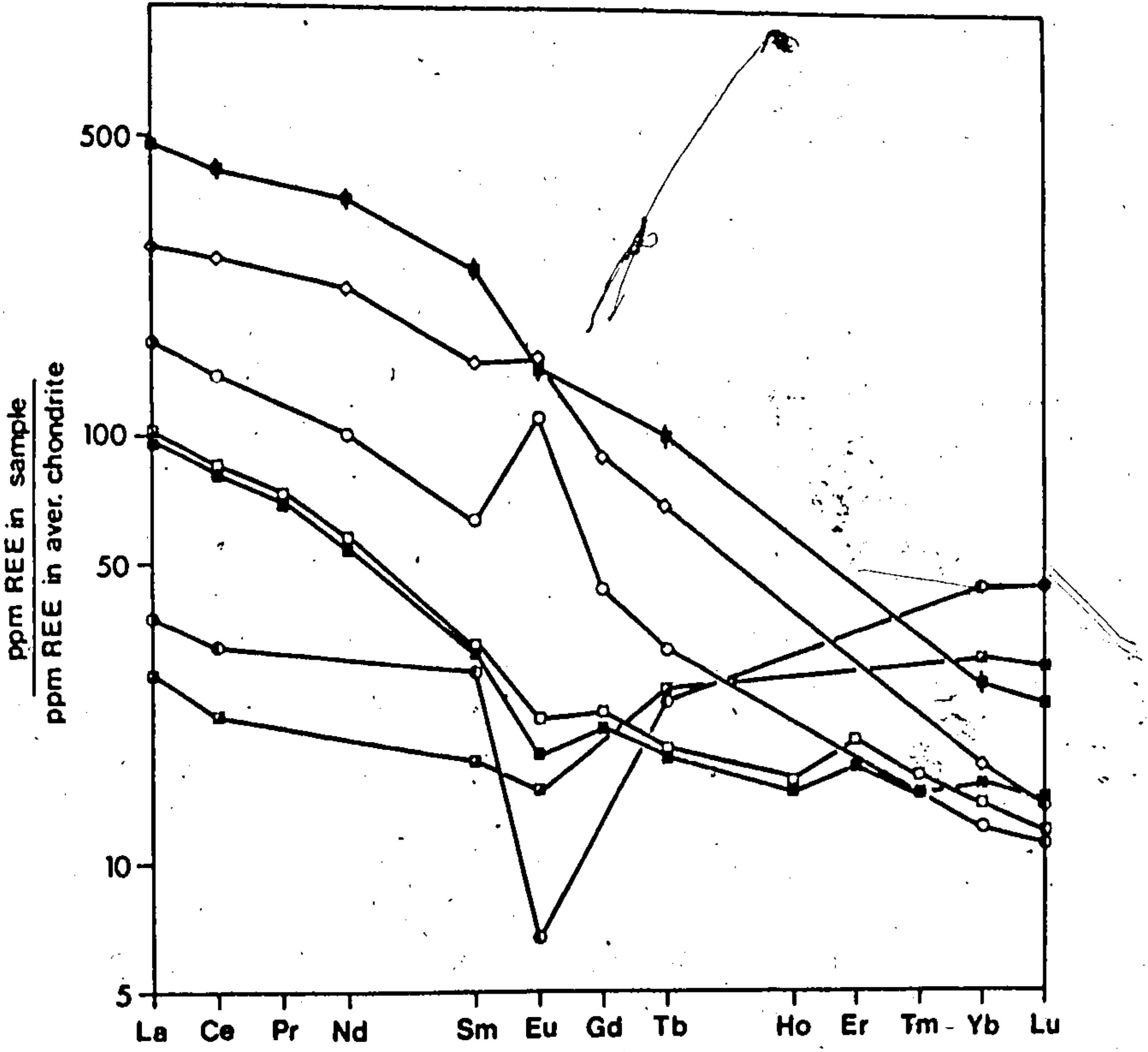
ppm REE in sample / ppm REE in aver. chondrite
500
100
50
10
5
La
Ce
Pr
Nd
Sm
Eu
Gd
Tb
Ho
Er
Tm
Yb
Lu

of the REE patterns of crustal rocks. The hornfelses are progressively enriched in heavy REE with or without a pronounced Eu anomaly. Even if the REE distributions of monzonites and hornfelses relative to the shale averages are not strictly complementary, it suggests, at least quantitatively, that the partial melting of such crustal rocks could produce monzonite, from a REE point of view. The REE patterns of these hornfelses are dominated by garnet which preferentially incorporates heavy REE (Haskin et al., 1966; Schnetzler and Philpotts, 1970), and thus the partial melting with garnet present as a residual phase (Gast, 1968) might generate the heavy REE depletion observed in monzonites. But the explanation of the K/Rb ratio in monzonite by a simple anatectic process is not so straightforward. As will be discussed below, monzonite would require derivation from a parent which also has a high K/Rb ratio.

Heier and Adams (1964), Taylor (1965), White (1966), Condie (1969), etc., have pointed out that Rb is expected to be enriched in the initial melt extracted from crustal rocks thus producing a low K/Rb ratio. On the other hand, Gast (1968) and Jakes and White (1970) have suggested that the behaviour of Rb relative to K in the initial melt is controlled largely by refractory minerals, possibly without the substantial enrichment of Rb in the melt.

Shaw (1968), Philpotts and Schnetzler (1970a) have concluded that the only common silicate minerals which generate the larger increase of the K/Rb ratio in coexisting melts are micas. Since the restite inclusions from the pluton and aluminous hornfelses from the contact aureole contain biotite as virtually the only K and Rb-bearing phase, their comparison with monzonite can be instructive. The average K/Rb ratio for six analyzed aluminous hornfelses (c.f. Appendix 1) is relatively high (=287). The restite inclusion (67) from monzonite which almost completely lacks feldspars, has a K/Rb ratio of about 170, somewhat lower than the "normal" crustal value of 230 (Shaw, 1968). This difference, however, is too small to be complementary to the high values for monzonites, which range from about 600-1100. Another problem of the depletion of Rb relative to K is the uncertainty with respect to the existence of biotite in a residue after the extraction of a partial melt of monzonitic composition, since the presence of clinopyroxene in monzonite indicates a rather anhydrous condition during the generation of monzonite (c.f. Fyfe, 1970; Brown and Fyfe, 1970). Thus in both cases (i.e. either Rb is enriched in the initial melts or the K/Rb ratio is controlled by refractory minerals), the origin of monzonite by partial melting of common crustal rocks is not compelling. The relatively high K/Rb ratio for the aluminous rocks also indicates that the garnet-sillimanite-cordierite hornfelses are not the residue after the extraction of monzonite, but it is consistent with the earlier suggestion that these rocks represent restite after partial melting of crustal rocks with the extraction of a melt, probably of granitic composition.

The difficulties of generating the high K/Rb ratio apply also to the partial melting of dioritic rock or amphibolite (Green et al., 1972), assuming that their K/Rb ratio does not differ very significantly from the crustal value. Anatexis of these rocks would not yield a melt with an appropriate trace element concentration, with the presence of either amphibole or perhaps large amounts of clinopyroxene in the residue with garnet, since the presence of amphibole (Hart and Aldrich, 1966) and probably also occasionally clinopyroxene in the residue (c.f. Philpotts and Schnetzler, 1970a; and see below), lower the K/Rb ratio in the melt. On the other hand, the high degree of partial melting would probably not generate a magma with such large absolute contents of alkalies and low concentrations of Ca, Mg and Fe. The difficulties with high absolute contents of alkalies and low concentrations of Ca, Mg and Fe also apply to another alternative explanation - the selective melting of hornblende, which has a high K/Rb ratio.

More plausible seems to be a two-stage melting process in the lower crust, perhaps similar to that proposed by Reynolds et al. (1969) and Green et al. (1972). A first partial melting stage would produce a residuum with a high K/Rb ratio followed by a second stage with a higher degree of melting where feldspars contribute significantly to the melt formed. These melts from the second stage might correspond to the monzonite. In order to put the hypotheses into a geological context, Reynolds et al. (1969) have suggested the stratification of the continental crust with respect to the K/Rb ratio and a large depletion of Rb relative to K in the lower crustal region, mainly due to enrichment of Rb in "anatectic melts generated at the depth and subsequent migration of the liquids to higher levels" (Reynolds et al., 1969, p.276). Then subsequent melting in the lower crust would generate magma with a high K/Rb ratio. In order to give rise to the high contents of alkalies and the high K/Rb ratio, such a process would require the melting of mainly feldspars, thus producing distinct positive Eu anomalies in the derivative melts (assuming that during the partial melting of granulites, for example, the REE were not strongly affected by RE-bearing accessory minerals of the "source material", then perhaps the positive Eu anomalies might be cancelled out or become unnoticable).

Apart from basic monzonite, however, pronounced positive Eu anomalies were not observed. Also it is not apparent if this process could generate a magma with such high absolute contents of potassium and rare-earths as are present in monzonite. It is also of interest that the chemical sequence of intrusions in the Loon Lake pluton is the reverse of that expected from the partial melting of crustal rocks, unless the intrusions would represent magmas produced during a waning cycle of anatexis (Hall, 1966; Erikson, 1969).

7.3.2.2 Contamination of Basic Magma

This theory attributes the origin of syenitic and monzonitic rocks to an assimilation of crustal rocks by basic magma (e.g. Chapman, 1968). Although the hypothesis cannot be completely eliminated by the available data, it is not very compelling for the genesis of monzonite from the Loon Lake pluton.

The assimilated material would have to be enriched in alkalies, particularly in potassium, far above the abundances in common rocks. For example, if the least altered and differentiated diorite from the pluton (321) assimilated country rocks in a 1:1 ratio to form monzonite, the country rock would have to contain about 12% K_2O and 7% Na_2O. If the ratio of magma to assimilated material is greater than 1:1 as is more probable, the concentration of alkalies in the assimilated material would have to be even higher. Also, if gabbroic rocks which are associated with or assumed to be parental magma of syenitic rocks (e.g. gabbro from the neighbouring Umfraville complex - Lumbers, 1967a - or "parental magma" of gabbro-syenite series from the Appalachians - Butler and Ragland, 1969), were used in similar calculations, the content of alkalies in the assimilated rocks would have to be even higher. Another problem involving this hypothesis is the relative lack of intermediate rocks. Also, as Condie and Lo have pointed out "alkali igneous rocks are rare in early Precambrian terrains" (1971, p.1116). Thus it appears that assimilation was not a dominant process for deriving monzonite from a basic magma.

7.3.2.3 Contamination of Acid Magma

The alternative hypothesis of assimilation is that of Fenton and Faure, who suggested that syenites are "the results of assimilation of metasedimentary gneisses, schists and marbles by a normal granitic magma" (1969, p.16). Granite, however, would have to assimilate large amounts of hornblende gneiss and marble (Shand, 1930, 1943) in order to decrease the content of silica in granitic magma. But low concentrations of Ca, Mg and Fe in monzonite negate such large-scale assimilation. Such assimilation would also probably not explain the high content of alkalies and mafic-poor character of monzonite. This mechanism is further complicated by a large amount of superheat in granitic magma required for the assimilation of vast amounts of crustal rocks. Also, experimental studies (c.f. Wyllie and Watkinson, 1970) argue against such a process. Wyllie and Watkinson concluded that "if we consider the effects of limestone assimilation in a granite magma, the available experimental data suggest strongly that the dominant effect is to cause it to crystallize with little change in composition of the liquid portion of the magma" (1970, p.371). Thus this process is a rather unlikely explanation for the origin of the monzonite from the Loon Lake pluton.

7.3.2.4 Derivation from More Basic Magma

Morse has pointed out that syenitic and monzonitic rocks and "their extrusive equivalent trachytes" because of " their small volume in the crust and frequent well-defined association with logically parental magma series, render their derivation from basalt quite credible and in some cases the parent-daughter relationship is clearly demonstrable" (1968, p.112). This conclusion is supported by the experimental studies of Green and Ringwood (1968), which indicate that syenitic and monzonitic magma indeed can be produced from basalt. The chemical composition of monzonitic rocks is consistent with this hypothesis even if the available data cannot prove it conclusively. The normative composition of these rocks (Figures 6.1.2-3) suggests that monzonite is formed in response to crystal-liquid equilibria. Elements such as K, Ba, REE, which are strongly concentrated by a process of fractionation, are enriched in monzonites, while ferromagnesian elements (Ni, Co, V, Cr - McCammon, 1968) are depleted. Also, well-fractionated REE patterns are comparable with such a process. The similarity of the chemical composition of monzonite to well-defined comparable plutonic rock series, and even to some trachytic rocks (Philpotts et al., 1971; Nagasawa, 1973) suggests that monzonite from the pluton has been derived from more basic magma.

7.3.2.5 Other Considerations

The high K/Rb and K/Tl ratios in monzonites and some quartz monzonites are of considerable petrogenetic interest. There is a number of possible explanations for the impoverishment of Rb and Tl relative to K in these rocks, but only the most appropriate hypotheses are considered here.

The ratio K/Rb for feldspars (Philpotts and Schnetzler, 1970a) shows that they discriminate against Rb. Since feldspars usually form more than 90% of these rocks, it might be suggested that feldspar accumulation may have played a significant role in the genesis of these rocks, and that they might be of cumulative origin. Apart from the basic monzonites, however, these rocks do not appear to be of such an origin, as already discussed in section 7.3.1.

Beswick (1973) has suggested that early separation and removal of biotite would leave the residual liquid impoverished in Rb relative to K. Biotite in monzonitic rocks, however, appears to be the last mafic mineral to crystallize. Likewise, the relatively high K/Rb ratio in biotite could hardly be explained by this process.

Heier (1966) has suggested that the enrichment of K relative to Rb, reported in some nepheline syenites, may either reflect the original chemistry of the primary magma or the removal, at some stage during crystallization, of Rb in an escaping gas phase. The possibility of gas escape is difficult to assess.

The partitioning of trace elements between coexisting phases indicating at least an approach to the approximate equilibrium, the systematic variation of major and trace elements with differentiation, relatively constant "crustal" values of Rb/Tl ratios in the rocks from the pluton and similarly high K/Rb in other monzonitic and nepheline syenitic bodies in this region (Payne, 1966; Sauerbrei, 1966), indicates that the Rb depletion is not due to the losses of late stage magmatic fluids or to "the migration of alkalies in either gaseous or fluid phase" (Bell et al., 1973, p.1026).

The similarity of the "fractionation coefficient" F/B from the Loon Lake pluton to those from other granitic rocks, which, however, have "normal" crustal values of the K/Rb ratio, the lack of any apparent relationship between modal biotite and the K/Rb ratio of host rocks and also high K/Rb not only of feldspars but also of biotite, suggest that the high K/Rb ratio in monzonite is probably inherited from the original liquid from which they crystallized. The Rb depletion appears to be a characteristic feature of many nepheline syenites, syenites and monzonites (Heier and Taylor, 1964; Heier, 1964, 1966; Payne, 1966; Sauerbrei, 1966; Reynolds et al., 1969; Green et al., 1972). Thus the Rb and Tl depletion, if it is an original feature of magma, as suggested, lead to some speculations with respect to the nature of the "source material".

Payne (1966) has suggested that the high K/Rb ratios of nepheline syenite from the Blue Mountains body (south of the Loon Lake pluton), which are more similar to those of mantle-derived rocks (c.f. Lessing et al., 1963) than to crustal rocks, indicate a mantle origin for the nepheline syenite magma. Such an origin of nepheline syenite is also corroborated by Sr isotope data (Krogh, 1964; Krogh and Hurley, 1968).

As discussed previously, the mineralogical and chemical similarities of the Loon Lake pluton to zoned plutons in the Westport area (e.g. Westport and Gananoque plutons) which have been dated at between 1100-1000 million years (Krogh and Hurley, 1968) - about the same age as that estimated for the Loon Lake pluton - is remarkable and has already been noted by Ermanovics (1967, 1970). The data of Sauerbrei (1966) show that these plutons in the Westport area also have a high K/Rb ratio (~550). In this respect it is of interest that Krogh and Hurley (1968), on the basis of a low initial ratio Sr^{87}/Sr^{86}, have concluded that these plutons "do not represent the Archean basement and were not derived by weathering or melting of such a basement" (p.7120), and inferred their mantle origin.

The similarity between these bodies and the Loon Lake pluton, even in their high K/Rb ratios, which are also comparable with those from the apparently mantle-derived Blue Mountains nepheline syenite, might indicate that the magma from which the monzonitic rocks of the Loon Lake pluton were derived is of upper mantle or lower crust origin. The high K/Rb ratio might also suggest that monzonitic magma was not contaminated to a large degree by crustal rocks with a "normal" K/Rb ratio, since significant contamination would probably cause a sizeable decrease in this ratio.

The trace element abundances can provide some limitations on the character of the "source material", but "because of the large fluctuations and essentially unknown values of distribution coefficients" (Jakes and White, 1972, p.26), the constraints are treated only qualitatively. The high contents of K, Ba, Sr, REE and strongly fractionated REE patterns and low concentrations of ferromagnesian elements in monzonitic rocks indicate that they may be derived from a very small degree of partial melting and/or extensive fractional crystallization of more primitive material. (Of course, these two processes are not mutually exclusive. If melting took place, then it was followed by solidification, which might have allowed extensive fractionation).

The distribution coefficients suggest that the residuum or cumulate of the monzonitic rocks contained minerals, probably garnet, which discriminate against light REE. The high K/Rb ratio negates the presence of amphibole in equilibrium with monzonitic liquid, while a high concentration of Sr and the absence of negative Eu anomalies exclude large amounts of plagioclase, although both these minerals might partially determine the geochemical characteristic of monzonite. The high contents of K and high K/Rb ratio also, of course, exclude K-feldspar as a possible phase in a residuum. Despite the fact that the presence of larger amounts of biotite in equilibrium with the monzonitic liquid is a tempting explanation for the high K/Rb ratio, the high concentrations of Ba and K and possibly also water undersaturated conditions during the generation of monzonitic magma, are not readily consistent with biotite coexisting with a monzonitic melt. The "inert" phases (with respect to K, Ba, Rb, Sr and REE) such as olivine or orthopyroxene, could have coexisted with the monzonitic liquid even in large amounts, as could likewise probably clinopyroxene (assuming that clinopyroxene had lower K/Rb ratios than the coexisting melt). There is an uncertainty with respect to the presence of clinopyroxene in equilibrium with monzonitic liquid. Clinopyroxene usually has a lower K/Rb ratio than the coexisting melt (c.f. Shaw, 1968; Gast, 1968); however, Philpotts and Schnetzler (1970a) have reported that occasionally clinopyroxene has this ratio higher than that of the melt, thus leading to the decrease of the ratio in the coexisting melt.

In conclusion, it appears that monzonites, as a whole, are not the product of the accumulation of feldspars, but they probably crystallized from monzonitic magma. Such a magma was probably formed by fractional crystallization of basic deep-seated magma, or partial melting of lower crust/upper mantle rocks. Garnet, orthopyroxene, olivine and possibly clinopyroxene might have been residual or cumulative minerals during the generation of monzonitic magma.

7.4 Quartz Monzonite

With respect to the petrogenesis of quartz monzonitic rocks, the important problem appears to be the relation between them and monzonites. The gradual increase of normative quartz toward the granite minimum in the Q-Ab-Or projection (Figure 6.1.2) and smooth trends between monzonitic and quartz monzonitic rocks in many variation diagrams could suggest a continuous fractional crystallization of a single magma. This interpretation, however, is not supported by a close inspection of the data. Apart from the contents of silica and alumina, the chemical composition of some quartz monzonite is rather similar to monzonite, as is also shown by the large overlap between these two rock types on the variation diagrams for both major and trace elements and for element ratios. It is difficult to envisage any sort of continuous process of fractional crystallization of a single parental magma leading to accumulation of residual quartz producing monzonites and subsequently quartz monzonites, some of which are less fractionated than the acid (most fractionated) monzonites. The more fractionated REE patterns of monzonite, the presence of a negative Eu anomaly in acid monzonite and its absence or near absence in the granitic rocks also argues against such a process. Likewise, the acid monzonites have a less basic plagioclase than those of some quartz monzonites, while during the process of continuous magmatic differentiation, progressive enrichment of the Ab component in feldspars would be expected (Bowen, 1928; Yoder et al., 1957 - assuming that P_{H_2O} varied systematically during the period of crystallization). This indicates that monzonite and quartz monzonite may not be related directly to each other through liquid-crustal reactions. The similarity and continuity of the chemical properties of the rocks, however, strongly suggest a close genetic relationship, since the idea of a second unrelated intrusion of chemically rather similar magma would involve too much coincidence. Also, the systematic variations of chemical composition between these two rock-types indicate that quartz monzonite is not a product of partial melting of wall-rocks, enhanced by monzonitic magma, but genetically unrelated to it.

Accepting a genetic relationship between monzonite and quartz monzonite, several hypotheses can be invoked in order to explain the observed variations. From a purely chemical point of view, Shaw's (1962) suggestion of the migration of silica out of the surrounding rocks is quite compelling. The geological data, however, are not readily compatible with such a mechanism. This process could hardly explain a general lack of correlation between the composition of wall-rocks and adjacent rocks of the pluton, relatively sharp borders between monzonite and quartz monzonite, etc. Likewise, the partitioning of trace elements between coexisting phases, indicating the attainment of at least approximate equilibrium, the normative compositions of these rocks, which fall into the low temperature troughs of An-Ab-Or-Q systems, smooth trends on variation diagrams, etc., negate extensive metasomatic effects. These arguments also contradict the hypothesis of Currie and Ermanovics (1971) based upon the large scale migration of elements by diffusion.

Toulmin (1964) has suggested for associated syenitic and granitic rocks from New England that syenite represented an accumulation product of the granitic magma. This hypothesis is also not applicable for the Loon Lake pluton. Monzonite, as a whole, does not have any characteristics of an accumulative residuum with respect to the granitic rocks (e.g. chemistry, overlap of basicity of plagioclase); cumulative rocks do not form smooth chemical trends with the residual liquids on the variation diagrams (Nockolds and Allen, 1956; Philpotts, 1966). Furthermore, "it is difficult to imagine how accumulative residues could be emplaced prior to the residual liquids" (Erikson, 1969, p.2232). Some other processes might be suggested and discussed but it appears that the models consistent with the greatest proportion of the observational data and the inferences that can most reasonably be derived from them would incorporate basically two processes:

(a) from a single magma, two portions were tapped and each of these subsequently underwent further differentiation along independent but similar paths;

(b) monzonitic magma was in part intruded into the present position and in part it reacted with and fractionally melted crustal rocks (perhaps the granitic or gneisses layer of Jacoby, 1971) and then subsequently intruded.

The first model is comparable with that proposed by Upton (1960) for the Kungnat syenite complex in southwestern Greenland and later corroborated by McDowell and Wyllie (1971). Upton (1960) has suggested the mechanical separation of already differentiated and stratified magma into parts and then "superimposed on the primary differentiation of the ... magma are the secondary effects of differentiation proceeding independently and simultaneously in each of the two isolated magma portions" (Upton, 1960, p.121). Such a mechanism may probably explain most features of chemical variations in quartz monzonites. Some variations of REE in quartz monzonites, however, do not appear to be readily compatible with this process. But the little data at hand cannot reliably evaluate these variations. The evaluation is further complicated by the fact that the bulk of REE in quartz monzonites is present in accessory minerals, which might mask and hinder those trends. Assuming, however that the variations of REE observed in three analyzed quartz monzonites represent significant and meaningful trends, then the general tendency of the La/Yb ratio and total REE contents of quartz monzonite to decrease with the increase of the D.I. values contrasts with the predicted trends, which suggest the increase of this ratio and total REE with fractionation (Taylor, 1965; Haskin et al., 1966). Also, the lack of variation of the Eu/Eu* ratio in quartz monzonites (contrary to the distinct variation in monzonites) might indicate that these rocks did not undergo extensive fractional crystallization (assuming that a possible variation of the Eu/Eu* ratio would not be masked by other REE-rich phases, particularly accessories).

The alternative explanation for the absence of Eu anomalies, that is, the variation of redox conditions (Philpotts, 1970; Philpotts and Schnetzler, 1970b) during fractionation, is probably contradicted by the composition of biotite, which suggests that the felsic rocks of the pluton crystallized under about the same redox conditions.

As noted above, these considerations regarding REE, however, are only speculative and must be treated cautiously. On the other hand, there are many indications that quartz monzonites indeed underwent magmatic differentiation (c.f. section 6.1.1-2 and below).

The second model envisages the existence of monzonitic magma, which in part intruded and in part partially melted and reacted with crustal rocks, producing the quartz monzonite. A similar process has been suggested by Chapman (1968) for the syenite-granite complexes of the White Mountains magma series and by Barker et al. (1972) for the Pikes Peak batholith, Colorado.

As earlier discussed (section 4.3) the temperature imposed on the wall-rocks by the pluton was well above the temperature of the beginning of their partial melting. Thus it is probable that magma which ascended through crustal rocks could hardly avoid a partial melting of gneissic or granitic rocks where it came into contact with them. Partial melting of the latter might produce ~~a~~ granitic anatectic melt, which by mixing with monzonite could form quartz monzonite. In this respect, it is of interest that quartz monzonite (259) probably generated by the partial melting of country rocks and the normative composition of which falls close to the ternary minimum on the Q-Ab-Or projection, lies at the most differentiated end of the smooth chemical trends on the variation diagrams. It shows that mixing of monzonitic magma with anatectic melt might have produced the many observed variations of the quartz monzonitic rocks.

There is geological evidence (see above) that the bulk of the quartz monzonitic zone of the pluton could not be generated in situ or nearly so. Also, the emplacement of monzonite partially as crystal mush (Shaw, 1962) required monzonitic magma to react with an anatectic melt deeper in the crust. Thus it appears that the Apsley gneiss was not, at least in the dominant part, the parental material for an anatectic melt. A question arises whether somewhat deeper under the present surface, there were quartz-feldspathic rocks, which could generate the granitic anatectic melt, and if so, whether such a partial melt could also resemble leucogranite (259).

On the basis of gravity data, Jacoby (1971) has concluded that the Bancroft area, including the Hastings basin with the Loon Lake pluton, is underlain at depths of not more than 3 km by a thick, more or less uniform, granitic or gneissic layer, probably corresponding to the basement complex of the Grenville supergroup (Wynne-Edwards, 1972). Jacoby (1971) has indicated that the rocks of this layer are not very different in composition from the leucocratic biotite gneiss (the Apsley gneiss). Also, Wynne-Edwards (1972) pointed out that the basement rocks correspond to quartz-feldspathic gneisses, probably not very different from those of the Apsley gneiss group. The overall chemical and petrographical similarities of assumed rocks of the basement complex (Wynne-Edwards, 1972) to the Apsley gneiss suggest that the products of the partial melting of both these rocks would be rather similar, particularly since the composition of partial melts corresponds to the low-melting fractions of these rocks. It indicates that even if the anatectic melt might have varied from place to place, these variations were probably not large. This might suggest that leucogranite (259) resulting from partial melting of the Apsley gneiss, could also resemble a partial melt of the basement rocks, which might have mixed with monzonite.

The thickness of the basement complex of the Grenville Supergroup is unknown, but Jacoby (1971) indicated its presence at the depth of 6 km from the present surface. Considering that the pluton was emplaced at the pressure of 2.5-4 kb, the depth at which monzonitic magma reacted with anatectic melt was probably adequate for their "mixing".

The "mixing" process can readily explain a variation of REE, i.e. the tendency for the decrease of the La/Yb ratio and total REE contents in quartz monzonitic rocks with the increase of D.I. values, and the absence of Eu anomalies (assuming that these REE variations are petrogenetically significant). It may also explain why some rocks (e.g. sample 142) with chemical and modal compositions clearly corresponding to monzonite, occur in the outer quartz monzonitic zone of the pluton.

But it does not seem very likely that this process alone could produce variation trends for quartz monzonites such as observed, for example, on the Ca/Sr vs Sr or K/Rb vs Rb diagrams (Figures 6.1.21, 6.1.27). The trends observed in quartz monzonites are similar to those produced by fractional crystallization and strongly suggest such a process. The two models proposed (a "mixing" process and that involving partially independent differentiation) are not mutually exclusive. Each only stresses the relative significance of a particular mechanism, even if both processes were probably operative. When monzonitic magma moved upward through a deep zone of crust, where the rocks were already undergoing high-grade metamorphism and possibly partial melting, it is likely that the magma became contaminated with anatectic granitic melt. On the other hand, if quartz monzonitic magma was already emplaced as a crystal mush as suggested earlier, it is probable that magma underwent a certain degree of fractional crystallization, at least during its emplacement (e.g. by flowage, differentiation, crystal settling, etc.).

7.5 Summary

1. The relation of diorite to the felsic rocks is not clear, but there are some indications that the basic and felsic rocks might not be genetically related.

2. The variation trends of monzonites are consistent with extensive fractional crystallization and indicate the important role of feldspars during such a process. The actual mechanism of this fractionation probably involved flowage differentiation.

3. Monzonitic magma was probably formed by partial melting of lower crustal/upper mantle rocks, or by fractional

crystallization of basic deep-seated magma.

4. Quartz monzonite was probably generated by both assimilation and fractional crystallization of monzonitic magma, even if the latter was most likely the dominant process. The process of assimilation is envisaged as a "mixing" of monzonitic magma with granitic melt produced by partial melting of crustal rocks, perhaps those of the basement complex of the Grenville Supergroup.

CHAPTER 8

EVOLUTION OF THE PLUTON

In order to present a coherent but tentative interpretation of the observed data, several aspects of the pluton, some of them already mentioned, will be discussed below.

Buddington (1959) defined three depth zones of granite emplacement. The Loon Lake pluton is similar in many aspects to his mesozonal plutons, which he defined as those emplaced at a depth of between 4 and 10 miles and a temperature range of country rocks, before intrusion, of 250° to 500°C. This is consistent with the earlier suggestion that the pluton is post-tectonic, but that it was emplaced into a region where diastrophism was still continuing. Also, the petrography shows that despite the primary igneous characteristics of the pluton there is some textural evidence that post-emplacement deformation locally occurred. The felsic magma was probably at a maximum temperature of about 750° to 820°C and pressures between 2.5 to 4 kb at the time of intrusion. This estimate probably represents the upper limits (assuming $P_{H_2O} = P_{total}$) since $P_{H_2O} < P_{total}$ may be expected to lower the estimated temperature. Bateman and Wahrhaftig (1966, p.125) have cast doubts on the validity of the assumption that $P_{H_2O} = P_{total}$ and "certainly this is not a valid general assumption during plutonic crystallization" (Putman and Alfors, 1969, p.74). The estimated temperatures, however, agree well with the experimental data of McDowell and Wyllie (1971) for similar syenitic and granitic rocks from the Kungnat syenite complex, Greenland.

In agreement with their data, which shows that the above-estimated conditions are below the liquidus, it appears that the intrusion was emplaced partially as crystal mush (c.f. Shaw, 1962). Equilibrium oxygen fugacities during crystallization of felsic rocks were probably slightly above the Ni-NiO buffer.

The pluton was probably emplaced between 1125 and 1000 million years ago. This age is comparable with those of monzonitic plutons in the Westport area, which might be of the same or similar origin. In this respect, it is of interest that mangeritic, monzonitic, syenitic and quartz monzonitic rocks, which are associated with anorthosites in the Adirondack complex, have a Rb/Sr age of about 1055 m.y. (Heath and Fairbairn, 1968) and an age of 1130 m.y. was given by Silver (1968) from cogenetic U/Pb isotope systems in zircons.

The Loon Lake pluton is a composite body consisting of three distinct rock types. In order of decreasing age, these rock types are diorite, monzonite and quartz monzonite. Dioritic rocks form the larger bodies chiefly in the inner part of the monzonitic core and might "represent inclusions or roof pendants of gabbros previously injected into paragneisses" (Shaw, 1962, p.13). The petrographic features indicate that diorites underwent extensive hybridization by felsic magma, particularly around the margin of these basic bodies, thus obscuring their original chemical composition. But it appears that dioritic rocks also underwent a certain degree of magmatic differentiation. The relation of diorite to the two main intrusive phases (monzonite and quartz monzonite) is not clear. There are some indications that the basic and felsic rocks might not be genetically related.

With regard to monzonite and quartz monzonite, there is numerous evidence for their igneous emplacement. This includes the contact metamorphic aureole, the locally discordant relation against the country rocks, disoriented inclusions of frequently refractory wall-rocks, the igneous differentiation trends, the position of the normative composition of these rocks in the low temperature troughs of the An-Ab-Or-Q systems, etc.

Tectonic data indicate that the pluton has the shape of an assymetrical funnel and appears to be most consistent with a roughly vertical emplacement of magma by forceful intrusion (forceful in the sense that the wall-rocks were pushed outward and upward with no implication as to unusual magmatic or tectonic forces). The pluton is probably narrowing with depth (Cloos, 1934; Saha, 1957; Jacoby, 1971) and like many syenitic and basic bodies in this region, it "intruded through narrow feeder zones from great depth" (Jacoby, 1971, p.72).

The body represents multiple intrusions with the monzonitic core being older than the quartz monzonitic outer zone. The period of time which separated the emplacement of these intrusions, however, was relatively short. It appears that quartz monzonite intruded when the monzonite core was probably not yet completely consolidated. The chemistry and the close spatial association of monzonite with quartz monzonite suggest that these intrusive phases are genetically related, but not through crystal-liquid reactions. It has been suggested that both these intrusive units are related to a single monzonitic magma, which in part intruded (monzonite) and in part evolved further (quartz monzonite) and subsequently intruded, following the previous intrusion of monzonite into its present position. The chemical and mineralogical variations and differences between these two series are consistent with a short period of time between the emplacement of these intrusions, during which either differentiation proceeded in the subjacent chamber, or magma mixed with and assimilated an anatectic granitic melt from quartz feldspathic country rocks. But it is probable that both these processes were operative in generating quartz monzonite.

There is no evidence that the monzonitic rocks represent cumulus. The available data suggest the former existence of monzonitic melt, which was not a product of the remobilization of the granitic basement, but which may be of an upper mantle or lower crust origin. A melt was probably derived from more basic material by either fractional crystallization or partial melting. Even if no attempt has been made to quantitatively evaluate the nature of this "source rock" (Gast, 1968; Shaw, 1970), the trace elements provide a number of constraints on the character of the source material. It appears that monzonite could have been in equilibrium with garnet, clino- and orthopyroxene, and olivine, but equilibrium with amphibole, plagioclase and K-feldspar is not likely.

Systematic mineralogical variations in the monzonitic core of the pluton cannot readily be explained by differentiation *in situ*, but are suggestive of the flowage differentiation. It appears that flowage differentiation probably occurred during the upward rise of magma yielding a centre of crystal cumulate and a border liquid of more acid and fractionated monzonite. Such a process could also explain the large but spatially systematic chemical variation within the monzonitic core of the pluton.

CHAPTER 9

CONCLUSION

1. The Chandos area underwent, at about 1125±25 m.y. ago, the prograde regional metamorphism corresponding to the "low-pressure intermediate type of amphibolite facies" of Miyashiro (1961) or "medium stage of metamorphism" of Winkler (1970). Estimated metamorphic conditions suggest a temperature range of about 620-700°C and a range for total pressure of about 4.5-6.0 kb.

2. On these regionally metamorphosed rocks, the pluton superimposed the contact metamorphism of the K-feldspar-cordierite hornfels facies of Winkler (1967). An estimation of the metamorphic conditions indicates a maximum temperature range of about 750-820°C and a range of about 2.5-4 kb for total pressure.

3. Under these conditions, an anatexis of country rocks in the contact aureole took place. The aluminous gneisses probably represent a residuum after partial melting of the Apsley gneiss.

4. The pluton is a post-tectonic funnel-shaped

intrusion emplaced at about 1075±75 m.y. ago. The pluton represents multiple intrusions of magma. In order of decreasing age, the intrusive units are diorite, monzonite and quartz monzonite.

5. The relation of diorite to the felsic rocks is not clear, but there are some indications that the basic and felsic rocks might not be genetically related.

6. Monzonites and quartz monzonites are probably related to a single magma but, as a series, these rocks are not simply a product of continuous magmatic differentiation leading to accumulation of residual quartz.

7. The distinct chemical variations within monzonites are consistent with extensive fractional crystallization and indicate the important role of feldspars during this process. The actual mechanism of this fractionation probably involved the flowage differentiation.

8. Monzonitic magma was formed by partial melting of lower crustal/upper mantle rocks, or by fractional crystallization of basic deep-seated magma.

9. Quartz monzonite was probably generated by both fractional crystallization of monzonitic magma and "mixing" of this magma with granitic melt produced by partial melting of

crustal rocks. The former process; however, probably prevailed.

REFERENCES

ABRAHAM, E.M. (1951) The geology in the vicinity of aeromagnetic anomalies on the Bancroft and Coe Hill sheets (preliminary report). Ont. Dept. Mines, Prelim. Rept., 1951-52.

ADAMS, F.D. and BARLOW, A.E. (1910) Geology of the Haliburton and Bancroft areas, Province of Ontario. Geol. Surv. Can. Mem. 6, 419p.

AHRENS, L.H. (1948) The unique association of Tl and Rb in minerals. Jour. Geol., 56, 578-90.

______, PINSON, W.H. and KEARNS, M.M. (1952) Association of rubidium and potassium and their abundance in common igneous rocks and meteorites. Geochim. Cosmochim. Acta, 2, 229-42.

AKELLA, J. and WINKLER, H.G.F. (1966) Orthorhombic amphibole in some metamorphic reactions. Contr. Mineral. Petrol., 12, 1-12.

ALBUQUERQUE, C.A.R. de, MUYSSON, J.R. and SHAW, D.M. (1972) Thallium in basalts and related rocks. Chem. Geol., 10, 41-8.

______ and SHAW, D.M. (1972) Thallium. In Handbook of Geochemistry (ed. K.H. Wedepohl), Ch. 81, Vol. II-I. Springer-Verlag.

ALTHAUS, E. (1967) The triple point andalusite-sillimanite-kyanite. Contr. Mineral. Petrol., 16, 29-44.

______ (1969) Das System Al_2O_3-SiO_2-H_2O. Experimentelle untersuchungen und folgerungen für die petrogenese der metamorphen Giesteine. Neues Jahrb. Mineral., Abh. 111, 74-161.

______, KAROTKE, E., NITSCH, K.H. and WINKLER, H.G.F. (1970) An experimental re-examination of the upper stability limit of muscovite plus quartz. Neues Jahrb Miner. Monats., 6, 325-36.

ANDERSON, A.T. (1966) Mineralogy of the Labrieville anorthosite, Quebec. Amer. Mineral., 51, 1671-711.

ARTH, J.G. and HANSON, G.N. (1972) Quartz diorites derived by partial melting of eclogite or amphibolite at mantle depths. Contr. Mineral. Petrol., 37, 161-74.

BALASHOV, Y.A. (1963) Regularities in the distribution of the rare-earths in the earth's crust. Geochem., USSR (English trans.), 2, 107-24.

BALASHOV, Y.A. and NESTERENKO, G.V. (1966) Distribution of the rare-earths in the traps of the Siberian platform. Geochem. Intern., 3, 672-79.

BANNO, S. and MATSUI, Y (1965) Eclogite types and partitioning of Mg, Fe and Mn between clinopyroxene and garnet. Proc. Japan Acad., 41, 716-21.

BARBIERI, M., FORNASERI, M. and PENTA, A. (1968) Rubidio e potassio nelle nuclanti dei Colli Albani, Di Vico del Cimino. Period. Mineralogia, 37, 243-98.

BARKER, J.F. (1972) Rare-earth elements in the Whitestone anorthosite. Unpub. M.Sc. thesis, McMaster University, Hamilton.

BARKER, F., WONES, D.R. and SHARP, W.N. (1972) Some aspects of the chemistry, mineralogy, petrology and genesis of the Pikes Peak batholith, Colorado. Geol. Soc. Amer., Ann. Mtgs., Program with abstracts, p.444.

BARTH, T.F.W. (1933) The large pre-Cambrian intrusive bodies in the southern part of Norway. 16th Intern. Geol. Congress, Washington, 297-309.

______ (1956) Studies in gneiss and granite. Skr. Norske Vidensk.-Akad. I. Mat-Naturv. Klasse, 35p.

______ (1962) The feldspar geological thermometers. Norsk Geol. Tidssk., 42 (Feldspar Vol.), 330-9.

______ (1968) Additional data for the two feldspar geothermometer. Lithos, 1, 305-6.

BATEMAN, P.C. and WAHRHAFTIG, C. (1966) Geology of the Sierra Nevada. In Geology of Northern California (ed. E.H. Bailey.), Calif. Div. Mines and Geol. Bull., 190, 107-72.

BELL, K., DAWSON, J.B. and FARQUHAR, R.M. (1973) Strontium isotope studies of alkalic rocks: the active carbonatite volcano Oldoinyo Lengai, Tanzania. Geol. Soc. Amer. Bull., 84, 1019-30.

BERLIN, R. and HENDERSON, C.M.B. (1968) A re-interpretation of Sr and Ca fractionation trends in plagioclases from basic rocks. Earth and Plan. Sci. Lett., 4, 79-83.

______ and ______ (1969a) The distribution of Sr and Ba between the alkali feldspar, plagioclase and ground mass phases of porphyritic trachytes, and phonolites. Geochim. Cosmochim. Acta, 33, 247-55.

BERLIN, R. and HENDERSON, C.M.B. (1969b) Trace element fractionation trend in minerals. Earth and Plan. Sci. Lett., 5, 423-24.

BEST, M.G. (1966) Structural geology of Precambrian rocks south of Bancroft, Ontario. Can. Jour. Earth Sci., 3, 441-55.

BESWICK, A.E. (1973) An experimental study of alkali metal distributions in feldspars and micas. Geochim. Cosmochim. Acta, 37, 183-208.

______ and EUGSTER, H.P. (1968) The distribution of potassium and rubidium between sanidine and phlogopite. Geol. Soc. Amer. Ann. Mtgs., Program with abstracts, 25-26.

BHATTACHARJI, S. (1966) Experimental scale model studies on flowage differentiation in sills. Geol. Soc. Amer. Spec. Paper 87, p.11 (Abs.).

______ (1967) Scale model experiments on flowage differentiation in sills. In Ultramafic and Related Rocks (ed. P.J. Wyllie). J. Wiley and Sons Inc., N.Y., 69-70.

______ and SMITH, C.H. (1964) Flowage differentiation. Science, 145, 150-53.

BOETTCHER, A.L. (1970) The system $CaO-Al_2O_3-SiO_2-H_2O$ at high pressures and temperatures. Jour. Petrol., 11, 337-79.

BOONE, G.M. and WHEELER, E.P. (1968) Staining for cordierite and feldspars in thin section. Amer. Mineral., 53, 327-31.

BOWEN, N.L. (1928) The evolution of the igneous rocks. Princeton Univ. Press, 334p.

BROWN, G.C. and FYFE, W.S. (1970) The production of granitic melts during ultrametamorphism. Contr. Mineral. Petrol., 28, 310-8.

BRYAN, W.B., FINGER, L.W. and CHAYES, F. (1969) Estimating proportions in petrographic mixing equations by least squares approximation. Science, 163, 926-7.

BUDDINGTON, A.F. (1939) Adirondack igneous rocks and their metamorphism. Geol. Soc. Amer. Mem. 7, 354p.

______ (1959) Granite emplacement with special reference to North America. Geol. Soc. Amer. Bull., 70, 671-747.

BUMA, G., FREY, F.A. and WONES, D.R. (1971) New England granites: trace element evidence regarding their origin and differentiation. Contr. Mineral. Petrol., 31, 300-20.

BUTLER, J.R. and RAGLAND, P.C. (1969) A petrochemical survey of plutonic intrusions in the Piedmont, Southeastern Appalachians, U.S.A. Contr. Mineral. Petrol., 24, 164-90.

______ and SKIBA, W. (1962) Strontium in plagioclase feldspars from four layered basic masses in Somalia. Min. Mag., 33, 213-25.

CARMICHAEL, D.M. (1968) Structure and progressive metamorphism in the Whetstone Lake area, Ontario, with emphasis on the mechanism of prograde metamorphic reactions. Unpub. Ph.D. thesis, Univ. Calif., Berkeley.

______ (1969) On the mechanism of prograde metamorphic reactions in quartz-bearing pelitic rocks. Contr. Mineral. Petrol., 20, 244-47.

______ (1970) Intersecting isograds in the Whetstone Lake area, Ontario. Jour. Petrol., 11, 147-81.

CARMICHAEL, I.S.E. (1963) The crystallization of feldspar in volcanic acid liquids. Quart. Jour. Geol. Soc. Lond., 119, 95-113.

CHAKRAVORTHY, P.S. and GHOSH, K.P. (1972) The coexisting kyanite, sillimanite and andalusite in regionally metamorphosed Precambrian rocks near Bansinala, Bankura District, West Bengal, India. 24th Intern. Geol. Congress, Montreal, Petrology, 88-89.

CHAPMAN, C.A. (1968) A comparison of the Maine coastal plutons and the magmatic central complexes of New Hampshire. In Studies of Appalachian Geology, Northern and Maritime. (ed. E-an Zen), 385-96.

CHASE, J.W., WINCHESTER, J.W. and CORYELL, C.D. (1963) Lanthanum, europium and dysprosium distributions in igneous rocks and minerals. Jour. Geophys. Res., 68, 567-75.

CHAYES, F. (1960) Correlation in closed tables. Carnegie Inst. Washington, Yearbook 59, 165-8.

CHESWORTH, W. (1967) The origin of certain granitic rocks occurring in Glamorgan Township, southeastern Ontario. Unpub. Ph.D. thesis, McMaster Univ., Hamilton.

CHESWORTH, W. (1971) Metamorphic conditions in a part of the Haliburton Highlands of Ontario. Lithos, 4, 219-29.

CHIANG, M.C. (1965) Element partition between hornblende and biotite in the rocks from the Loon Lake aureole, Chandos Township, Ontario. Unpub. M.Sc. thesis, McMaster Univ., Hamilton.

CHOUDHURI, A. and WINKLER, H.G.F. (1967) Anthophyllit und Hornblende in einigen metamorphen Reaktionen. Contr. Mineral. Petrol., 14, 293-315.

CHYI, L.L. (1972) Distribution of some noble metals in sulfide and oxide minerals in Strathcona Mine, Sudbury. Unpub. Ph.D. thesis, McMaster Univ., Hamilton.

CLOOS, E. (1934) The Loon Lake pluton, Bancroft area, Ontario, Canada. Jour. Geol., 42, 393-99.

CONDIE, K.C. (1969) Petrology and geochemistry of the Laramie batholith and related metamorphic rocks of Precambrian age, eastern Wyoming. Geol. Soc. Amer. Bull., 80, 57-82.

______ and LO, H.H. (1971) Trace element geochemistry of the Louis Lake batholith of early Precambrian age, Wyoming. Geochim. Cosmochim. Acta, 35, 1099-119.

CORYELL, C.D., CHASE, J.W. and WINCHESTER, J.W. (1963) A procedure for geochemical interpretation of terrestrial rare-earth abundance patterns. Jour. Geophys. Res., 68, 559-66.

CURRIE, K.L. (1971) The reaction 3 cordierite = 2 garnet + 4 sillimanite + 5 quartz as a geological thermometer in the Opinicon Lake region, Ontario. Contr. Mineral. Petrol., 33, 215-26.

______ and ERMANOVICS, I.F. (1971) Geology of the Loughborough Lake region, Ontario, with special emphasis on the origin of the granitoid rocks. A contribution to the syenite Problem. Geol. Surv. Can. Bull. 199, 85p.

DAY, H.W. (1970) Redetermination of the stability of muscovite and quartz. Geol. Soc. Amer., Ann. Mtgs., Program with abstracts, p.535.

DEER, W.A., HOWIE, R.A. and ZUSSMAN, J. (1962) Rock-forming minerals. Vol. 3 - Sheet silicates. Longmans, London, 270p.

DENECHAUD, E.B. (1969) Rare-earth activation analyses: improvement and application to Stretishorn dike and Duluth complex. Unpub. Ph.D. thesis, Univ. Wisconsin, 138p.

______, HELMKE, P.A. and HASKIN, L.A. (1970) Analysis for the rare-earth elements by neutron activation and Ge(Li) spectrometry. Jour. Radioanal. Chem., 6, 97-113.

DODGE, F.C.W., FABBI, B.P. and ROSS, D.C. (1970) Potassium and rubidium in granitic rocks of Central California. U.S. Geol. Surv., Prof. Paper 700-D, D108-15.

______, SMITH, U.C. and MAYS, R.E. (1969) Biotites from granitic rocks of the Central Sierra Nevada batholith, California. Jour. Petrol., 10, 250-71.

DONNAY, G., WYART, J. and SABATIER, G. (1960) The catalytic nature of high-low feldspar transformations. Carnegie Inst. Washington, Yearbook 59, 173-4.

DUDAS, M.J., SCHMITT, R.A. and HARWOOD, M.E. (1971) Trace element partitioning between volcanic plagioclase and dacitic pyroclastic matrix. Earth and Plan. Sci. Lett., 11, 440-6.

DUPUY, C. (1967) Coefficient de partage du rubidium entre biotite et sanidine dans les ignimbrites de Toscane, Italie. Compt. Rend., 264, 2613-5.

______ (1968) Rubidium et caesium dans biotite, sanidine et verre des ignimbrites de Toscane (Italie). Chem. Geol., 3, 81-91.

______ (1970) Contribution a l'etude des fractionnements geochimiques des alcalins, des alcalino-terreux et du gallium au cours des processus magmatiques. Unpub. D.S.N. thesis, Univ. Montpellier, France.

______, FRATTA, M. and SHAW, D.M. (1973) Partition coefficient of thallium compared with rubidium. Earth and Plan. Sci. Lett., 19, 208-212.

EMMONS, R.C. (1953) Petrogeny of the syenites and nepheline syenites of central Wisconsin. Geol. Soc. Amer. Mem. 52, 71-87.

ERIKSON, E.H. Jr. (1969) Petrology of the composite Snoqualmie batholith, Central Cascade Mountains, Washington. Geol. Amer. Bull., 80, 2213-6.

ERMANOVICS, I.F. (1967) Evidence bearing on the origin of the Perth Road pluton, southern Ontario. Unpub. Ph.D. thesis, Queen's Univ., Kingston.

______ (1970) Zonal structure of the Perth Road monzonite, Grenville Province, Ontario. Can. Jour. Earth Sci., 7. 414-34.

ESKOLA, P. (1914) On the petrology of Orijarvi region, southwest Finland. Bull. Comm. Geol. Finlande, 40, 1-272.

______ (1915) On the relation between chemical and mineralogical composition in the metamorphic rocks of the Orijarvi region. Bull. Comm. Geol. Finlande, 44, 109-43.

______ (1933) On the differential anatexis of rocks. Bull. Comm. Geol. Finlande, 103, 12-25.

______ (1951) Around Pitkäranta. Ann. Acad. Sci., Fennicae Ser. A 27, 1-90.

EVANS, B.W. (1964) Fractionation of elements in the pelitic hornfelses of the Cashel-Lough Wheelaun intrusion, Connemara, Eire. Geochim. Cosmochim. Acta, 28, 127-56.

______ (1965) Application of a reaction-rate method to the breakdown equilibria of muscovite and muscrite plus quartz. Amer. Jour. Sci., 263, 647-67.

EWART, A. (1969) Petrochemistry and feldspar crystallization in the silicic volcanic rocks, Central North Island, New Zealand. Lithos, 2, 371-88.

______ and TAYLOR, S.R. (1969) Trace element geochemistry of the rhyolitic volcanic rocks, Central North Island, New Zealand. Phenocryst data. Contr. Mineral. Petrol., 22 127-46.

______, ______ and CAPP, A.C. (1968) Trace and minor element geochemistry of the rhyolitic volcanic rocks, Central North Island, New Zealand. Total rocks and residual liquid data. Contr. Mineral. Petrol., 18, 76-104.

FENTON, M.D. and FAURE, G. (1969) The strontium isotopic composition of the Laramie Range syenite, Wyoming, and its bearing on petrogenesis. Geol. Soc. Amer., Ann. Mtgs., Program with abstracts, 15-16.

FISCHER, W. and BOCK, R. (1942) The production of pure scandium compounds. Z. anorg. u. allgem. Chem., 249, 146-97.

FLEISCHER, M. and ALTSCHULER, Z.S. (1969) The relationship of the rare earth composition of minerals to geological environment. Geochim. Cosmochim. Acta, 33, 725-32.

FOSTER, M.D. (1960) Interpretation of the composition of trioctahedral micas. U.S. Geol. Surv., Prof. Paper 354-B, 11-49.

FOX, P.E. (1969) Petrology of Adamant Pluton, British Columbia. Geol. Surv. Can., Paper 67-61, 101p.

______ and MOORE, J.M. Jr. (1969) Feldspars from Adamant pluton, British Columbia. Can. Jour. Earth Sci., 6, 1199-209.

FREY, F.A. (1969) Rare earth abundances in a high-temperature peridotite intrusion. Geochim. Cosmochim. Acta, 33, 1429-47.

______ (1970) Rare earth and potassium abundances in St. Paul's rocks. Earth and Plan. Sci. Lett., 7, 351-60.

______, HASKIN, L.A. and HASKIN, M.A. (1971) Rare-earth abundance in some ultrabasic rocks. Jour. Geophys. Res., 76, 2057-70.

______, HASKIN, M.A., POETZ, J.A. and HASKIN, L.A. (1968) Rare-earth abundances in some basic rocks. Jour. Geophys. Res., 73, 6085-98.

FRIEDMAN, G.M. (1959) Identification of carbonate minerals by staining methods. Jour. Sed. Petrol., 29, 87-97.

FYFE, W.S. (1970) Some thoughts on granitic magmas. In Mechanism of Igneous Intrusion (eds. G. Newall and N. Rast). Geol. Jour. Spec. Issue 2, 201-16.

GANGULY, J. (1972) Staurolite stability and related paragenesis: Theory, experiments and applications. Jour. Petrol., 13, 335-65.

GAST, P.W. (1968) Trace element fractionation and origin of tholeiitic and alkaline magma types. Geochim. Cosmochim. Acta, 32, 1057-86.

______, HUBBARD, N.J. and WEISMANN, H. (1970) Chemical composition and petrogenesis of basalts from Tranquility Base. Proc. Apollo 11 Lunar Sci. Conf., Vol. 2, 1143-63. Pergamon Press, N.Y.

GAVRILOVA, L.K. and TURANSKAYA, N.Y. (1958) Distribution of rare-earth in rock-forming and accessory minerals of certain granites. Geochem., USSR (English Trans.), 2, 163-70.

GEIJER, S. (1917) Faluntraktens berggrund och malmfyndigheter. Sveriges Geol. Undersokn. Ser. C, no. 275.

______ (1963) On the association of magnesia and sulphide ores in metasomatic mineralization. Arkiv. Mineral. geol., Bd. 3, 153-64.

GEOLOGICAL SURVEY OF CANADA (1950) Map 16G - Coe Hill aeromagnetic sheet. Geol. Surv. Can. Geophysics Paper no. 16 (revised 1957).

GOLDSCHMIDT, V.M. (1954) Geochemistry. Clarendon Press, Oxford. 730p.

GOLDSMITH, J.R. and LAVES, F. (1954) The microcline-sanidine stability relations. Geochim. Cosmochim. Acta, 5, 1-19.

______ and NEWTON, R.C. (1969) P-T-X relations in the system $CaCO_3$-$MgCO_3$ at high temperatures and pressures. Amer. Jour. Sci., 267, 160-90.

GOLES, G.G. (1968) Rare-earth geochemistry of Precambrian plutonic rocks. 23rd Intern. Geol. Congress, Prague, Vol. 6, 237-49.

GORDON, G.E., RANDLE, K., GOLES, G.G., CORLISS, J.B., BEESON, M.H. and OXLEY, S.S. (1968) Instrumental activation analysis of standard rocks with high-resolution γ-ray detectors. Geochim. Cosmochim. Acta, 32, 369-96.

GRABER, F.M., LUKENS, H.R. and MacKENZIE, J.K. (1970) Neutron activation analysis determination of all 14 stable rare-earth elements with group separation and Ge(Li) spectrometry. Jour. Radioanal. Chem., 4, 229-39.

GRAF, D.L. and GOLDSMITH, J.R. (1955) Dolomite-magnesian calcite relations at elevated temperatures and CO_2 pressures. Geochim. Cosmochim. Acta, 7, 109-28.

______ and ______ (1958) The solid solubility of $MgCO_3$ in $CaCO_3$. A revision. Geochim. Cosmochim. Acta, 13, 218-9

GRANT, J.A. (1959) The granite rocks of the Grenville Province in southeastern Ontario. Unpub. M.Sc. thesis, Queen's Univ., Kingston.

GREEN, T.H., BRUNFELT, A.O. and HEIER, K.S. (1972) Rare-earth element distribution and K/Rb ratios in granulites, mangerites and anorthosites, Lofoten-Vesteraalen, Norway. Geochim. Cosmochim. Acta, 36, 241-57.

_____ and RINGWOOD, A.E. (1968) Genesis of the calc-alkaline igneous rock suite. Contr. Mineral. Petrol., 18, 105-62.

GREENWOOD, H.J. (1963) The synthesis and stability of anthophyllite. Jour. Petrol., 4, 317-41.

HALL, A. (1966) A petrogenetic study of the Rosses granitic complex, Donegal. Jour. Petrol., 7, 202-20.

_____ (1967) The distribution of some major and trace elements in feldspars from the Rosses and Ardara granite complex, Donegal, Ireland. Geochim. Cosmochim. Acta, 31, 835-47.

HARKER, R.I. and TUTTLE, O.F. (1955) Studies in the system $CaO-MgO-CO_2$. Part 2. Limits of solid solution along the binary join $CaCO_3-MgCO_3$. Amer. Jour. Sci., 253, 274-82.

HARPER, C.T. (1967) On the interpretation of potassium-argon ages from Precambrian shields and Phanerozoic orogens. Earth Plan. Sci. Lett., 3, 128-32.

HART, S.R. and ALDRICH, L.T. (1966) Fractionation of K/Rb by amphiboles - implications regarding mantle composition. Science, 155, 325-7.

HASKIN, L.A., ALLEN, R.O., HELMKE, P.A., PASTER, T.P., ANDERSON, M.R., KOROTEV, R.L. and ZWEIFEL, K.A. (1970) Rare-earths and other trace elements in Apollo 11 lunar samples. Proc. Apollo 11 Lunar Sci. Conf., Vol. 2, 1213-31. Pergamon Press, N.Y.

_____, FREY, F.A., SCHMITT, R.A. and SCHMITT, R.M. (1966) Meteoritic, solar and terrestrial rare-earth distributions. Phys. Chem. of the Earth, 7, 167-322.

_____ and GEHL, M.A. (1963) The rare-earth contents of standard rocks G-1 and W-1 and their comparison with other rare-earth distribution patterns. Jour. Geophys. Res., 68, 2037-43.

_____ and HASKIN, M.A. (1968) Rare-earth elements in the Skaergaard intrusion. Geochim. Cosmochim. Acta, 32, 433-47.

HASKIN, L.A., HASKIN, M.A., FREY, F.A. and WILDEMAN, T.R. (1968a) Relative and absolute terrestrial abundances of the rare-earths. In Origin and Distribution of the Elements (ed. L.H. Ahrens), 889-912. Pergamon Press, N.Y.

______, HELMKE, P.A., PASTER, T.P. and ALLEN, R.O. (1971) Rare-earths in meteoritic, terrestrial and lunar matter. In Activation Analysis in Geochemistry and Cosmochemistry (ed. A.O. Brunfelt and E. Steinnes). Proc. NATO Advanced Study Inst., Kjeller, Sept. 1970, 227-36. Universitets-forlaget.

______, WILDEMAN, T.R. and HASKIN, M.A. (1968b) An accurate procedure for determination of the rare-earth elements by neutron activation. Jour. Radioanal. Chem., 1, 337-48.

HASLAM, H.W. (1968) The crystallization of intermediate and acid magmas at Ben Nevis, Scotland. Jour. Petrol., 9, 84-104.

HEATH, S.A. and FAIRBAIRN, H.W. (1968) Sr^{87}/Sr^{86} ratios in anorthosites and some associated rocks. In Origin of Anorthosite and Related Rocks (ed. Y.W. Isachsen), 99-110, N.Y. State Mus. Sci. Serv. Mem. 18.

HEDGE, C.E. (1966) Variations in radiogenic strontium found in volcanic rocks. Jour. Geophys. Res., 71, 6119-26.

HEIER, K.S. (1957) Phase relations of potash feldspars in metamorphism. Jour. Geol., 65, 468-79.

______ (1960) Petrology and geochemistry of high grade metamorphic and iengous rocks on Langøy, Northern Norway. Norges Geol. Unders., 207, 264p.

______ (1962) Trace elements in feldspars - a review. Norsk Geol. Tidsskr., 42, 415-54.

______ (1964) Geochemistry of the nepheline syenite on Stjernøy, North Norway. Norsk Geol. Tidsskr., 44, 205-15.

______ (1966) Some crystallo-chemical relations of nephelines and feldspars on Stjernøy, North Norway. Jour. Petrol., 7, 95-113.

______ and ADAMS, J.A.S. (1964) The geochemistry of the alkali metals. Phys. Chem. of the Earth, 5, 253-381.

______ and TAYLOR, S.R. (1959a) Distribution of Li, Na, K, Rb, Cs, Pb and Tl in southern Norwegian Precambrian alkali feldspars. Geochim. Cosmochim. Acta, 15, 284-302.

HEIER, K.S. and TAYLOR, S.R. (1959b) Distribution of Ca, Sr and Ba in southern Norwegian Precambrian alkali feldspars. Geochim. Cosmochim. Acta, 17, 286-304.

______ and ______ (1964) A note on the geochemistry of alkaline rocks. Norsk Geol. Tidsskr., 44, 197-203.

HENSEN, B.J. and GREEN, D.H. (1971) Experimental study of the stability of cordierite and garnet in pelitic compositions at high pressures and temperatures. 1. Compositions with excess alumino-silicate. Contr. Mineral. Petrol., 33, 309-30.

HERRMANN, A.G. (1970) Yttrium and lanthanides. In Handbook of Geochemistry (ed. K.H. Wedepohl), Vol. II-2, 57-71. Springer-Verlag.

HESS, P.C. (1969) The metamorphic paragenesis of cordierite in pelitic rocks. Contr. Mineral. Petrol., 24, 191-207.

HEWITT, D.F. (1956) The Grenville region of Ontario. In The Grenville Problem, Royal Soc. Can., Spec. Pub. No. 1, 22-41.

______ (1957) The Grenville Province. In The Proterozoic in Canada, Royal Soc. Can., Spec. Pub. No. 2, 132-40.

______ (1961) Nepheline syenite deposits of southern Ontario. Ont. Dept. Mines, 69, pt. 8, 1960, 194p.

______ (1962a) Some tectonic features of the Grenville Province of Ontario. In The Tectonics of the Canadian Shield, Royal Soc. Can., Spec. Pub. No. 4, 102-117.

______ (1962b) Geology of Wollaston Township, Hastings County. Ont. Dept. Mines, Geol. Rep. 11, 29-55.

______ and JAMES, W. (1956) Geology of Dungannon and Mayo Townships. Ont. Dept. Mines, 64, 1955, 65p.

______ and SATTERLY, J. (1957) Haliburton-Bancroft area. Ont. Dept. Mines, Map No. 1957b.

HIETANEN, A. (1967) On the facies series in various types of metamorphism. Jour. Geol., 75, 187-214.

HIGUCHI, H. and NAGASAWA, H. (1969) Partition of trace elements between rock-forming minerals and the host volcanic rocks. Earth and Plan. Sci. Lett., 7, 281-7.

HIGUCHI, H., TOMURA, K., ONUMA, N. and HAMAGUCHI, H. (1969) Rare-earth abundances in several geochemical standard rocks. Geochem. Jour., 3, 171-80.

______, ______, ______ and ______ (1970) Determination of rare-earth elements in rock samples by neutron activation and cation exchange. Jour. Radioanal. Chem., 5, 207-22.

HINTON, M.A. (1972) Thallium and related elements in a metamorphic rocks. Unpub. B.Sc. thesis, McMaster Univ., Hamilton.

HIRSCHBERG, A. and WINKLER, H.G.F. (1968) Stabilitätsbeziehungen zwischen Chlorit, Cordierit, und Almandin bei der Metamorphose. Contr. Mineral. Petrol., 18, 17-42.

HOLDAWAY, M.J. (1966) Hydrothermal stability of clinozoisite plus quartz. Amer. Jour. Sci., 264, 643-67.

HOLMES, A. and REYNOLDS, D.L. (1947) A front of metasomatic metamorphism in the Dalradian of Co. Donegal. Compt. Rend. Soc. Geol. Finlande, 20, 25-65.

HOTSTETLER, P.B., COLEMAN, R.G., MUMPTON, F.A. and EVANS, B.W. (1966) Brucite in alpine serpentinites. Amer. Mineral., 51, 75-98.

IIDA, C. (1961) Trace elements in minerals and rocks of the Tzu-Hakone region, Japan. Part II. Plagioclase. Jour. Earth Sci., Nagoya Univ., 9, 14-28.

IRVINE, T.N. and FINDLAY, T.C. (1972) Alpine-type peridotite with particular reference to the Bay of Islands igneous complex. In The Ancient Oceanic Lithosphere (ed. E. Irving). Publ. Earth Physics Branch, Dept. Energy, Mines, Resources, Ottawa, 97-128.

JACKSON, E.D., STEVENS, R.E. and BOWEN, R.W. (1967) A computer-based procedure for deriving mineral formulas from mineral analyses. In Geological Survey Research, 1967, U.S. Geol. Surv., Prof. Paper 575-C, 23-31.

JACOBY, W.R. (1971) A detailed gravity study of granites in the Bancroft area, Ontario. Unpub. manuscript, Gravity Div., Earth Physics Branch, Dept. Energy, Mines, Resources, Ottawa, 80p.

JAKES, P. and WHITE, A.J.R. (1970) K/Rb ratios of rocks from island arcs. Geochim. Cosmochim. Acta, 34, 849-56.

JAKES, P. and WHITE, A.J.R. (1972) Major and trace element abundances in volcanic rocks of orogenic areas. Geol. Soc. Amer. Bull., 83, 29-40.

JENNINGS, D.S. (1969) Origin and metamorphism of part of the Hermon Group near Bancroft, Ontario. Unpub. Ph.D. thesis, McMaster Univ., Hamilton.

______ and MITCHELL, R. (1969) An estimation of the temperature of an intrusion of carbonatite at the Fen complex, South Norway. Lithos, 2, 167-9.

JOHANNES, W. and WINKLER, H.G.F. (1965) Transport von Feldspäten und Quartz in Temperaturegefälle. Beitr. Miner. Petrol., 11, 250-71.

JOHANNSEN, A. (1932) A descriptive petrography of igneous rocks. Vols. 1-4, Univ. Chicago Press.

KARAMATA, S. (1961) Einfluss der geologischen Alters und des tektonischen Drucks auf die Art der Alkalifeldspate. Inst. Lucas Mallada, Cursillos y Conf., 8, 127-30.

KAY, G.M. (1942a) Development of the northern Allegheny synclinorium and adjoining regions. Geol. Soc. Amer. Bull., 53, 1601-57.

______ (1942b) Ottawa-Bonnechere graben and Lake Ontario homocline. Geol. Soc. Amer. Bull., 53, 585-646.

KENNEDY, G.C. (1955) Some aspects of the role of water in rock melts. In Crust of the Earth (ed. A. Poldervaart), Geol. Soc. Amer., Spec. Paper 62, 489-504.

KLEEMAN, A.W. (1965) The origin of granitic magmas. Jour. Geol. Soc. Austr., 12, 35-52.

KOLBE, P. (1965) Geochemical investigation of the Cape Granite, Southwestern Cape Province, South Africa. Jour. Geol. Soc. South Africa, 69, 160-99.

KROGH, T.E. (1964) Strontium isotope variations and whole-rock isochron studies in the Grenville Province of Ontario. Dept. Geol. Geophys., Mass. Inst. Tech., 12th Ann. Rep. for 1964, U.S. Atomic Energy Comm., 73-124.

______ and HURLEY, P.M. (1968) Strontium isotope variation and whole-rock isochron studies, Grenville Province of Ontario. Jour. Geophys. Res., 73, 7107-25.

KUDO, A.M. (1962) The discriminant function used in classifying some amphibolites. Unpub. M.Sc. thesis, McMaster Univ., Hamilton.

LAL, R.K. and MOORHOUSE, W.W. (1969) Cordierite-gedrite rocks and associated gneisses of Fishtail Lake, Harcourt Township, Ontario. Can. Jour. Sci., 6, 145-65.

LANGE, I.M., REYNOLDS, R.G. Jr. and LYONS, J.B. (1966) K/Rb ratios in coexisting K-feldspars and biotites from some New England granite and metasediments. Chem. Geol., 1, 317-22.

LEAKE, B.E. (1968) A catalog of analysed calciferous and subcalciferous amphiboles together with their nomenclature and associated minerals. Geol. Soc. Amer., Spec. Paper 98, 210p.

LEELANADAM, C. (1970) Chemical mineralogy of hornblendes and biotites from the charnockitic rocks of Kondapalli, India. Jour. Petrol., 11, 475-505.

LESSING, P., DECKER, R.W. and REYNOLDS, R.C. (1963) Potassium and rubidium distribution in Hawaiian lavas. Jour. Geophys. Res., 68, 5851-55.

LUMBERS, S.B. (1967a) Stratigraphy, plutonism and metamorphism in the Ottawa River Remnant in the Bancroft-Madoc area of the Grenville Province of southeastern Ontario, Canada. Unpub. Ph.D. thesis, Princeton Univ., Princeton.

______ (1967b) Geology and mineral deposits of the Bancroft-Madoc area. In Geology of Parts of Eastern Ontario and Western Quebec. GAC-MAC Guidebook, Kingston, 13-29.

LUTH, W.C. (1967) Studies in the system $KAlSiO_4$-Mg_2SiO_4-H_2O. 1. Inferred phase relations and petrologic applications. Jour. Petrol., 8, 372-416.

______, JAHNS, R.H. and TUTTLE, O.F. (1964) The granite system at pressures of 4 to 10 kilobars. Jour. Geophys. Res., 69, 759-73.

McCAMMON, B.W. (1968) A geochemical study of some igneous rocks from the Loon Lake complex using spectrographic methods. Unpub. B.Sc. thesis, McMaster Univ., Hamilton.

McCONNELL, J.D.C. and McKIE, D. (1960) The kinetics of the ordering process in triclinic $NaAlSi_3O_8$. Min. Mag., 32, 436-54.

McDOWELL, S.D. and WYLLIE, P.J. (1971) Experimental studies of igneous rock series: the Kungnat syenite complex of southwest Greenland. Jour. Geol., 79, 173-94.

MacINTYRE, R.M., YORK, D. and MOORHOUSE, W.W. (1967) Potassium-argon age determinations in the Madoc-Bancroft area in the Grenville Province of the Canadian Shield. Can. Jour. Earth Sci., 4, 815-28.

MacKENZIE, W.S. and SMITH, J.V. (1961) Experimental and geological evidence for the stability of alkali feldspars. Inst. Lucas Mallada, Cursillos y Conf., 8, 53-64.

MARMO, V., HYTONEN, K. and VORMA, A. (1963) On the occurrence of potash feldspar of inferior triclinicity within the Precambrian rocks in Finland. Bull. Comm. geol. Finlande, 212, 51-78.

MASON, B. (1966) Principles of Geochemistry. J. Wiley and Sons, N.Y., 3rd Edition, 329p.

MASUDA, A. (1967) Lanthanide concentration ratios between pyroxene and garnet. Earth and Plan. Sci. Lett., 3, 25-28.

MEHNERT, K.R. (1963) Petrographic und Abfolge der Granitisation im Schwarzwald. IV. Neues Jahrb. Mineral., Abh. 99, 161-99.

______ (1968) Migmatites and the origin of granitic rocks. Elsevior, Amsterdam. 303p.

MERRIN, S. (1962) Experimental investigations of epidote paragenesis. Unpub. Ph.D. thesis, Penn. State Univ., University Park.

______ (1963) Experimental investigations of epidote paragenesis. Geol. Soc. Amer., Spec. Paper 73, 203 (Abstr.).

MIYASHIRO, A. (1961) Evolution of metamorphic belts. Jour. Petrol., 2, 277-311.

______, SHIDO, F. and EWING, M. (1969) Composition and origin of serpentinites from the Mid-Atlantic Ridge near 24° and 30° North Latitude. Contr. Mineral. Petrol., 23, 117-27.

MORRISON, G.H. and FREISER, M. (1957) Solvent extraction in analytical chemistry. John Wiley and Sons, N.Y., 231p.

______, GERARD, J.T., TRAVESI, A., CURRIE, R.L., PETERSON, S.F. and POTTER, N.M. (1969) Multi-element neutron activation analysis of rock using chemical group separations and high resolution gamma spectrometry. Anal. Chem., 41, 1633-7.

MORSE, S.A. (1968) Syenites. Carnegie Inst. Washington Yearbook for 1967, 112-20.

MUELLER, R.F. (1966) Stability relations of the pyroxenes and olivine in certain high-grade metamorphic rocks. Jour. Petrol., 7, 363-74.

MURSKY, G. (1972) Origin and significance of zonation in a granitic intrusion. 24th Intern. Geol. Congress, Montreal, Petrology, 181-90.

NAGASAWA, H. (1970) Rare-earth concentrations in zircons and apatites and their host dacites and granites. Earth and Plan. Sci. Lett., 9, 345-64.

______ (1971) Partitioning of Eu and Sr between coexisting plagioclase and K-feldspar. Earth and Plan. Sci. Lett., 13, 139-44.

______ (1973) Rare-earth distribution in alkali rocks from Oki-Dogo Island, Japan. Contr. Mineral. Petrol., 39, 301-8.

______ and SCHNETZLER, C.C. (1971) Partitioning of rare-earth, alkali and alkaline earth elements between phenocrysts and acid igneous magma. Geochim. Cosmochim. Acta, 35, 953-68.

NASH, W.P. and WILKINSON, J.F.G. (1971) Shonkin Sag Laccolith, Montana. II. Bulk rock geochemistry. Contr. Mineral. Petrol., 33, 162-70.

NEWTON, R.C. (1966) Some calc-silicate equilibrium relations. Amer. Jour. Sci., 264, 204-22.

NOCKOLDS, S.R. (1954) Average chemical compositions of some igneous rocks. Geol. Soc. Amer. Bull., 65, 1007-32.

______ and ALLEN, R. (1953) The geochemistry of some igneous rock series. Geochim. Cosmochim. Acta, 4, 105-42.

______ and ______ (1954) The geochemistry of some igneous rock series, part II. Geochim. Cosmochim. Acta, 5, 245-85.

______ and ______ (1956) The geochemistry of some igneous rock series, part III. Geochim. Cosmochim. Acta, 9, 34-77.

______ and MITCHELL, R.L. (1948) The geochemistry of some Caledonian plutonic rocks: a study in the relationship between the major and trace elements of igneous rocks and their minerals. Trans. Royal Soc. Edin., 61, 533-75.

NOLL, W. (1934) Geochemie des Strontiums. Chem. der Erde, 8, 507.

OKRUSCH, M. (1971) Garnet-cordierite-biotite equilibria in the Steinach aureole, Bavaria. Contr. Mineral. Petrol., 32, 1-23.

ONUMA, N., HIGUCHI, H., WAKITA, H. and NAGASAWA, H. (1968) Trace element partition between two pyroxenes and the host lava. Earth and Plan. Sci. Lett., 5, 47-51.

ORVILLE, P.M. (1960) Powder X-ray method for determination of (Ab+An) content of microcline. Geol. Soc. Amer. Bull., 71, 1939-40.

______ (1962) Comments on the two-feldspar geothermometer. Norsk Geol. Tidssk., 42 (Feldspar Vol.), 340-6.

______ (1963) Alkali ion exchange between vapor and feldspar phases. Amer. Jour. Sci., 261, 201-37.

______ (1967) Unit-cell parameters of the microcline-low albite and the sanidine-high albite solid solution. Amer. Mineral., 52, 55-86.

PAGE, N.J. (1967) Serpentinization considered as a constant volume metasomatic process: A discussion. Amer. Mineral., 52, 545-9.

PAYNE, J.G. (1966) Geology and geochemistry of the Blue Mountain nepheline syenite body. Unpub. Ph.D. thesis, McMaster Univ., Hamilton.

PERCHUK, L.L. and RYABCHIKOV, I.D. (1968) Mineral equilibria in the system nepheline-alkali feldspar-plagioclase and their petrological significance. Jour. Petrol., 9, 123-67.

PHILPOTTS, A.R. (1966) Origin of the anorthosite-mangerite rocks in southern Quebec. Jour. Petrol., 7, 1-64.

______ (1970) Redox estimation from a calculation of Eu^{2+} and Eu^{3+} concentrations in natural phases. Earth and Plan. Sci. Lett., 9, 257-68.

______, MARTIN, W. and SCHNETZLER, C.C. (1971) Geochemical aspects of some Japanese lavas. Earth and Plan. Sci. Lett., 12, 89-96.

______ and SCHNETZLER, C.C. (1968) Europium anomalies and the genesis of basalt. Chem. Geol., 3, 5-13.

PHILPOTTS, J.A. and SCHNETZLER, (1970a) Phenocryst-matrix partition coefficients for K, Rb, Sr and Ba, with applications to anorthosite and basalt genesis. Geochim. Cosmochim. Acta, 34, 307-22.

______ and ______ (1970b) Apollo 11 lunar samples: K, Rb, Sr, Ba and rare-earth concentrations in some rocks and separated phases. Proc. Apollo 11 Lunar Sci. Conf., Vol. 2, 1471-86. Pergamon Press, N.Y.

PROSTKA, H.J. (1973) Hybrid origin of the absarokite-shoshonite-banakite series, Absaroka volcanic field, Wyoming. Geol. Soc. Amer. Bull., 84, 697-702.

PUTMAN, G.W. and ALFORS, J.T. (1969) Geochemistry and petrology of the Rocky Hill Stock, Tulare County, California. Geol. Soc. Amer., Spec. Paper 120, 109p.

RAGLAND, P.C. (1970) Composition and structural state of the potassic phase in perthites as related to petrogenesis of a granitic pluton. Lithos, 3, 167-89.

______, BRUNFELT, A.O. and WEIGAND, P.W. (1971) Rare-earth abundances in Mesozoic dolerite dikes from Eastern United States. In Activation Analysis in Geochemistry and Cosmochemistry (ed. A.O. Brunfelt and E. Steinnes). Proc. NATO Advanced Study Inst., Kjeller, Sept. 1970, 227-36, Universitetsforlaget.

RAMBALDI, E.R. (1973) Variation in the composition of plagioclase and epidote in some metamorphic rocks near Bancroft, Ontario. Can. Jour. Earth Sci., 10, 852-68.

RAMBERG, H. (1952) The origin of metamorphic and metasomatic rocks. Univ. Chicago Press, 317p.

READ, H.H. (1957) The granite controversy. Murby Pub. Co., London, 430p.

REID, W.P. (1969) Mineral staining tests. Mineral Industries Bull., Colorado School of Mines, 12, 20p.

REY, P., WAKITA, H. and SCHMITT, R.A. (1970) Radiochemical neutron activation analysis of indium, cadmium, yttrium and the 14 rare-earth elements in rocks. Anal. Chim. Acta, 51, 163-78.

REYNOLDS, D.H. (1947) Hercynian Fe-Mg metasomation in Cornwall. Geol. Mag., 84, 33-50.

REYNOLDS, R.C. Jr., WHITNEY, P.R. and ISACHSEN, Y.W. (1969) K/Rb ratios in anorthositic and associated charnockitic rocks of the Adirondacks and their petrogenetic implication. In Origin of Anorthosite and Related Rocks (ed. Y.W. Isachsen), N.Y. State Mus. Sci. Serv. Mem. 18, 267-80.

RIBBE, P.M. and SMITH, J.V. (1966) X-ray emission microanalysis of rock-forming minerals. IV. Plagioclase feldspars. Jour. Geol., 74, 217-33.

RICHARDSON, S.W. (1968) Staurolite stability in a part of the system Fe-Al-Si-O-H. Jour. Petrol., 9, 467-88.

______, BELL, P.M. and GILBERT, M.C. (1968) Kyanite-sillimanite equilibrium between 700° and 1500°C. Amer. Jour. Sci., 266, 513-41.

______, GILBERT, M.C. and BELL, P.M. (1969) Experimental determination of kyanite-andalusite and andalusite-sillimanite equilibria; the aluminium silicate triple point. Amer. Jour. Sci., 227, 259-72.

RIMSAITE, J.H.Y. (1967) Studies of rock-forming micas. Geol. Surv. Can. Bull. 149, 82p.

RUTHERFORD, M.J. (1969) An experimental determination of iron biotite-alkali feldspar equilibria. Jour. Petrol., 10, 381-408.

SAHA, A.K. (1957) Mode of emplacement of some granitic plutons in south-east Ontario. Unpub. Ph.D. thesis, Univ. of Toronto, Toronto.

______ (1959) Emplacement of three granitic plutons in south-eastern Ontario, Canada. Geol. Soc. Amer. Bull., 70, 1293-326.

SATTERLY, J. (1943) Mineral occurrences in the Haliburton area. Ont. Dept. Mines, 52, pt. 2.

SAUERBREI, A. (1966) The granitic rocks of the Frontenac axis. Unpub. M.Sc. thesis, Queen's Univ., Kingston.

SCHILLING, J.G. and WINCHESTER, J.W. (1966) Rare-earths in Hawaiian basalts. Science, 153, 867-9.

______ and ______ (1969) Rare-earth contribution to the origin of Hawaiian lavas. Contr. Mineral. Petrol., 23, 27-37.

SCHMITT, R.A., SMITH, R.H., LASCH, J.E., MOSEN, A.W., OLEHY, D.A. and VASILEVSKIS, J. (1963) Abundances of the fourteen rare-earth elements, scandium and yttrium in meteoritic and terrestrial matter. Geochim. Cosmochim. Acta, 27, 577-622.

SCHNETZLER, C.C. and PHILPOTTS, J.A. (1968) Partition coefficients of rare-earth elements and barium between igneous matrix material and rock-forming mineral phenocrysts - I. In Origin and Distribution of the Elements (ed. L.H. Ahrens), 929-38. Pergamon Press, Oxford.

______ and ______ (1970) Partition coefficients of rare-earth elements between igneous matrix material and rock-forming mineral phenocrysts - II. Geochim. Cosmochim. Acta, 34, 331-40.

SEN, S.K. (1959) Potassium content of natural plagioclases and the origin of antiperthites. Jour. Geol., 67, 479-95.

______, NOCKOLDS, S.R. and ALLEN, R. (1959) Trace elements in minerals from rocks of the S. Californian batholith. Geochim. Cosmochim. Acta, 16, 58-78.

SHAFIQULLAH, M., TUPPER, W.M. and COLE, T.J.S. (1973) Radiometric ages on pegmatites from the Bancroft area, Ontario, Canada. Symposium on the Geology of the Canadian Arctic Program with abstracts, Saskatoon, p.75 (Abs.).

SHAND, S.J. (1930) Limestone and the origin of feldspatoidal rocks: an aftermath of the Geological Congress. Geol. Mag., 67, 415-27.

______ (1943) Eruptive rocks. John Wiley and Sons, N.Y., 2nd Edition, 444p.

SHANON, R.D. and PREWITT, C.T. (1969) Effective ionic radii in oxides and fluorides. Acta Cryst., B25, 925-46.

SHAW, D.M. (1962) Geology of Chandos Township. Ont. Dept. Mines, Geol. Rep. No. 11, 28p.

______ (1968) A review of K-Rb fractionation trends by covariance analysis. Geochim. Cosmochim. Acta, 32, 573-601.

______ (1970) Trace element fractionation during anatexis. Geochim. Cosmochim. Acta, 34, 237-42.

______ (1972) Origin of the Apsley gneiss. Can. Jour. Earth Sci., 9, 18-35.

SHAW, D.M. and KUDO, A.M. (1965) A test of discriminant function in the amphibolite problem. Min. Mag., 34, 423-35.

SHAW, H.R. (1963) The four-phase curve sanidine-quartz-liquid-gas between 500 and 4000 bars. Amer. Mineral., 48, 883-96.

SHIEH, Y.N., SCHWARCZ, H.P. and SHAW, D.M. (1972) Correlation between O-18/O-16 ratios and chemical compositions of the Apsley gneiss from the Grenville Province of Ontario. Trans. Amer. Geophys. Union, 53, 556 (Abs.).

______, ______ and ______ (1973) An oxygen isotope study of the Loon Lake pluton and the Apsley gneiss, Grenville Province of Ontario (in preparation).

SHIH, C.-Y. (1972) The rare-earth geochemistry of oceanic igneous rocks. Unpub. Ph.D. thesis, Columbia Univ., N.Y.

SIEDNER, G. (1965) Geochemical features of a strongly fractionated alkali igneous suite. Geochim. Cosmochim. Acta, 29, 113-37.

______ (1968) The distribution of alkali metals and thallium in some South-West African granites. Geochim. Cosmochim. Acta, 32, 1303-15.

SILVER, L.T. (1968) A geochronological investigation of the Adirondack complex, Adirondack Mountains, New York. In Origin of Anorthosite and Related Rocks (ed. Y.W. Isachsen). N.Y. State Mus. Sci. Serv. Mem. 18, 233-52.

______ and LUMBERS, S.B. (1965) Geochronologic studies in the Bancroft-Madoc area of the Grenville Province, Ontario, Canada. Geol. Soc. Amer., Ann. Mtg., Program with Abstracts, p.156.

SIMONY, P.S. (1960) Origin of the Apsley paragneiss. Unpub. M.Sc. thesis, McMaster Univ., Hamilton.

SMITH, M.E. (1966) Element distribution between coexisting feldspars in high-grade metamorphic rocks from the Frontenac axis, Ontario. Unpub. Ph.D. thesis, Queen's Univ., Kingston.

SMITHSON, S.B. (1963) Granite studies: II. The Precambrian Flö granite, a geological and geophysical investigation. Norges Geol. Undersök, 219, 212p.

STEIGER, R.H. and HART, S.R. (1967) The microcline-orthoclase transition within a contact aureole. Amer. Mineral., 52, 87-116.

STEVENSON, P.C. and NERVIK, W.E. (1961) The radiochemistry of the rare earths, scandium, yttrium and actinium. National Academy of Sciences - Nuclear Science Series, NAS-NS 3020, Oak Ridge, Tennessee, 282p.

STOCKWELL, C.H. (1964) Fourth report on structural provinces, orogenies, and time-classification of rocks of the Canadian Precambrian Shield. Geol. Surv. Can., Paper 64-17, pt. 2.

STRENS, R.G.J. (1965) Stability and relations of the Al-Fe epidotes. Min. Mag., 35, 464-75.

______ (1968) Reconnaissance of the prehnite stability field. Min. Mag., 36, 864-7.

TAUSON, L.V., ZLOBIN, B.I. and LEONOVA, L.L. (1956) Raspredelenie urana v granitoidnom komplekse Susamyrskogo batolita (tsentralnyi Tyan-Shan). Geokhim., 7, 11-19.

TAYLOR, S.R. (1965) The application of trace element data to problems in petrology. Phys. Chem. of the Earth, 6, 133-214.

______, EWART, A. and CAPP, A.C. (1968) Leucogranites and rhyolites: Trace element evidence for fractional crystallization and partial melting. Lithos, 1, 179-86.

______ and HEIER, K.S. (1958) Rubidium depletion in feldspars. Nature, 182, 202-3.

______ and ______ (1960) The petrological significance of trace element variations in alkali feldspars. 21st Intern. Geol. Congress, Copenhagen, Rept. Session 14, 47-61.

THAYER, T.P. (1964) Principal features and origin of podiform chromite deposits, and some observations on the Guleman-Soridag District, Turkey. Econ. Geol., 59, 1497-1524.

______ (1966) Serpentinization considered as a constant-volume metasomatic process. Amer. Mineral., 51, 685-710.

______ (1967) Chemical and structural relations of ultramafic and feldspathic rocks in alpine intrusive complexes. In Ultramafic and Related Rocks (ed. P.J. Wyllie), J. Wiley and Sons, N.Y., 222-39.

THORNTON, C.P. and TUTTLE, O.F. (1960) Chemistry of igneous rocks. I. Differentiation index. Amer. Jour. Sci., 258, 664-84.

TILLING, R.I. (1968) Zonal distribution of variations in structural state of alkali feldspar within the Rader Creek pluton, Boulder batholith, Montana. Jour. Petrol., 9, 331-57.

TOMURA, K., HIGUCHI, H., MIYAJI, N., ONUMA, N. and HAMAGUCHI, H. (1968) Determination of rare-earth elements in rock samples by neutron activation analysis with a lithium-drifted germanium detector after chemical group-separation. Anal. Chim. Acta, 41, 217-28.

TOULMIN, P. (1964) Bedrock geology of the Salem quadrangle and vicinity. U.S. Geol. Surv. Bull. 1163-A.

TOWELL, D.G., WINCHESTER, J.W. and SPIRN, R.V. (1965) Rare-earth distributions in some rocks and associated minerals of the batholith of Southern California. Jour. Geophys. Res., 70, 3485-96.

TUREKIAN, K.K. and KULP, J.L. (1956) The geochemistry of strontium. Geochim. Cosmochim. Acta, 10, 245-96.

______ and WEDEPOHL, K.H. (1961) Distribution of the elements in some major units of the earth's crust. Geol. Soc. Amer. Bull., 72, 175-92.

TURNER, F.J. (1968) Metamorphic petrology: Mineralogical and field aspects. McGraw-Hill, N.Y., 403p.

TUTTLE, O.F. and BOWEN, N.L. (1958) Origin of granite in light of experimental studies. Geol. Soc. Amer. Mem. 74, 153p.

UPTON. B.G.J. (1960) The alkaline igneous complex of Kungnat field, south Greenland. Medd. Grønland, 123, 5-145.

VINOGRADOV, A.P. (1962) Average contents of chemical elements in the principal types of igneous rocks of the earth's crust. Geochem., USSR (English Trans.), 641-64.

WAGER, L.R. and MITCHELL, R.L. (1951) The distribution of trace elements during strong fractionation of basic magma - a further study of the Skaergaard intrusion, East Greenland. Geochim. Cosmochim. Acta, 1, 129-208.

WANLESS, R.K., STEVENS, R.D., LACHANCE, G.R. and EDMONDS, C.M. (1967) Age determinations and geological studies K-Ar isotopic ages, report 7. Geol. Surv. Can., Paper 66-17, 120p.

WATT, W.S. (1966) Chemical analyses from the Gardar igneous province, South Greenland. Grønlands Geol. Unders., Rapp. Nr. 6, 92p.

WEBER, J.N. and SMITH, F.G. (1961) Rapid determination of calcite-dolomite ratios in sedimentary rocks. Jour. Sed. Petrol., 31, 130-1.

WHITE, A.J.R. (1966) Genesis of migmatites from the Palmer region of South Australia. Chem. Geol., 1, 165-200.

______, COMPSTON, W. and KLEEMAN, A.W. (1967) A Palmer granite - a study of a granite within a regional metamorphic environment. Jour. Petrol., 8, 29-50.

WHITNEY, P.R. (1969) Variations of the K/Rb ratio in migmatitic paragneisses of the Northwest Adirondacks. Geochim. Cosmochim. Acta, 33, 1203-11.

WINKLER, H.G.F. (1967) Petrogenesis of metamorphic rocks. Springer-Verlag, 2nd Edition, 237p.

______ (1970) Abolition of metamorphic facies, introduction of the four divisions of metamorphic stage and of a classification based on isograds in common rocks. Neues Jahrb. Miner. Monats., 1970, 5, 189-248.

______ and NITSCH, K.H. (1962) Zoisitbildung beider experimentellen metamorphose. Naturwiess., 49, 605.

______ and VON PLATEN, H. (1960) Experimentelle Gesteinsmetamorphose, III. Anatektische Ultrametamorphose kalkhaltiger tone. Geochim. Cosmochim. Acta, 18, 294-316.

______ and ______ (1961) Experimentelle Gesteinsmetamorphose, V. Experimentelle anatektischer Schmelzen und ihre petrogenetische Bedeutung. Geochim. Cosmochim. Acta, 24, 250-9.

WONES, D.R. (1963) Physical properties of synthetic biotites on the join phlogopite-annite. Amer. Mineral., 48, 1300-21.

______ and EUGSTER, H.P. (1965) Stability of biotite - experiment, theory and application. Amer. Mineral., 50, 1228-72.

WRIGHT, N.P. (1966) Mineralogic variation in the Stone Mountain granite, Georgia. Geol. Soc. Amer. Bull., 77, 207-10.

WRIGHT, T.L. (1968) X-ray and optical study of alkali feldspar: II. An X-ray method for determining the composition and structural state from measurement of 2θ values for three reflections. Amer. Mineral., 53, 88-104.

______ and STEWART, D.B. (1968) X-ray and optical study of alkali feldspar. I. Determination of composition and structural state from refined unit-cell parameters. Amer. Mineral., 53, 38-87.

WYLLIE, P.J. and WATKINSON, D.H. (1970) Phase equilibrium studies bearing on genetic links between alkaline and subalkaline magmas, with special reference to the limestone assimilation hypothesis. Can. Mineral., 10, 362-74.

WYNNE-EDWARDS, H.R. (1957) The structure of the Westport concordant pluton in Grenville, Ontario. Jour. Geol., 65, 639-49.

______ (1967) Westport map-area, Ontario, with special emphasis on the Precambrian rocks. Geol. Surv. Can., Mem. 346, 142p.

______ (1972) The Grenville Province. In Variations in tectonic styles in Canada. Geol. Assoc. Can., Spec. Paper 11 (eds. R.A. Price and R.J.W. Douglas), 264-334.

YODER, H.G., STEWART, D.B. and SMITH, J.R. (1957) Ternary Feldspars. Carnegie Inst. Washington Yearbook for 1956, 206-14.

ZLOBIN, B.I. and LEBEDEV, V.I. (1960) Geochemical relationships of Li, Na, K, Rb and Tl in alkali magma and its petrogenetic significance. Geochem., USSR, (English Trans.), 101-24.

APPENDIX 1

A.1.1 Modal Analyses

Modal analyses were made on 63 samples of rocks from the pluton and 20 samples of country rocks and inclusions from the pluton. The sample locations are shown on Map 2 and the modes are given in Tables A.1.1-5 (except for those already given in the text -c.f. Tables 4.2.1, 4.2.2, 4.3.2). In Tables A.1.1-5, several modal analyses carried out by D.M. Shaw are also included. For each modal analysis, 1500 to 2000 point-counts were recorded covering an area of about 700 square millimeters.

In order to rapidly distinguish among feldspars, quartz and cordierite, the thin sections were stained with sodium cobaltinitrite for potassium feldspars, amaranth for plagioclase, and those of aluminous hornfelses also with trypan blue stain for cordierite according to the method of Boone and Wheeler (1968). The trypan blue stain was also used to distinguish between calcite and dolomite (c.f. Friedman, 1959; Reid, 1969).

Abbreviations for Tables A.1.1-5

Principal minerals in Tables A.1.1-4:

Q	Quartz	Hb	Hornblende
Kf	Potassium feldspar	Cpx	Clinopyroxene
Pl	Plagioclase	Opq	Opaque
Bi	Biotite		

Principal minerals in Table A.1.5:

Q	Quartz	Sill	Sillimanite
Pl	Plagioclase	Cd	Cordierite
Bi	Biotite	Opq	Opaque
G	Garnet		

Others:

Al	Allanite	M	Muscovite, sericite
A	Apatite	R	Rutile
Ch	Chlorite	S	Sphene
C	Carbonate	T	Tourmaline
E	Epidote	Z	Zircon
F	Fluorite		

For the other minerals, the combined modal values are given in front of the minerals in brackets.

† - indicates that the mode was visually estimated

* - indicates only a few grains

tr trace amounts

+ from Shaw (1972) or his unpublished data

Table A.1.1 Modal analyses of rocks from the quartz monzonitic zone of the pluton

Sample No.	Q	Kf	Pl	Bi	Hb	Cpx	Opq	Others
5	38.8	36.2	19.9	2.9	-	-	0.8	1.4 (M,E,Al,A*,Z*)
26	27.2	32.4	33.1	5.4	-	-	1.3	0.6 (C,S,A)
27	22.7	37.8	35.8	2.2	-	-	1.2	0.3 (A,M*,S*,Z*)
31	24.5	35.2	34.8	2.3	-	-	2.4	0.8 (M,C)
42	16.6	44.5	31.2	4.9	-	-	1.6	1.2 (M,S,A *, Z*)
44	22.3	43.2	27.9	4.2	-	-	1.7	0.7 (M,A*)
45	27.4	33.2	35.5	3.0	-	-	0.7	0.2 (M)
48	9.3	43.3	38.7	6.8	-	-	0.7	1.2 (S,M*,E*,F*,Al*)
50	17.6	35.0	39.4	5.3	-	-	0.9	1.8 (S,M,A*,Z*)
52	19.4	35.7	36.4	4.4	-	-	2.4	1.7 (M,S,A)
53	15.8	31.4	41.1	8.0	-	-	1.6	2.1 (C,M,S,E*,A*)
55	33.3	31.2	31.3	1.8	-	-	0.8	1.5 (M,S,T*)
60	25.2	29.0	34.5	7.4	-	-	1.7	2.2 (S,E,A*,Z*)
68	20.9	44.6	31.7	1.0	-	-	1.7	0.1 (S*,A*)
79	24.6	36.0	34.6	2.6	-	-	1.7	0.5 (S,M,E,A*)
81	19.1	32.8	42.0	3.2	-	-	2.3	0.6 (M,S,C,A*)
86	21.6	32.4	32.3	12.4	-	-	0.3	1.0 (S,C,A,Z*,C*,T)
88	31.4	24.7	38.0	3.1	-	-	1.8	1.0 (M,A,Z*)
98	33.4	28.0	34.3	1.0	-	-	1.6	1.7 (M,F,C,S*)
100	35.8	34.1	25.4	2.6	-	-	1.5	0.6 (S,M*,E*,Z*)
115	19.3	34.9	40.0	4.8	-	-	0.4	0.6 (C,M,S,A*)
117	26.9	25.7	37.7	6.0	-	-	0.9	3.0 (M,S,C,T*,A*,Z*)

Table A.1.1 continued

Sample No.	Q	Kf	Pl	Bi	Hb	Cpx	Opq	Others
131	30.0	29.6	38.0	2.1	-	-	0.3	
142	8.8	42.5	45.7	2.0	-	-	0.5	0.5 (A,M)
161	11.7	36.6	38.4	7.7	-	-	1.8	3.8 (M,S,C,A*,Z*)
169	13.9	33.6	36.8	12.0	-	-	1.5	2.0 (S,A,E)
174	17.7	37.5	33.9	5.8	-	-	2.0	3.1 (M,E,A,Z*)
191	26.1	25.6	31.9	13.4	-	-	1.5	1.5 (C,A,S,M*,Z*)
218	29.7	35.9	29.5	3.7	-	-	0.7	0.5 (M,A)
236	27.8	29.0	34.6	7.5	-	-	0.7	0.4 (S,A*,Z*,E*)
238	32.9	39.1	22.8	4.2	-	-	0.9	tr (A,S)
253	32.5	33.1	30.6	2.4	-	-	1.3	tr (Z*,A*)
259	39.2	30.8	28.6	0.3	-	-	1.0	
262	27.9	28.3	35.7	5.2	-	-	1.0	1.9 (S,M,Z*,A*)
264	24.1	37.7	30.7	3.5	1.6	-	1.3	1.1 (S,C,E,A*,Z*)
+710-2	32.5	26.3	37.4	1.8	-	-	0.3	2.4 (M,A,E)
+711-6	15.1	46.6	31.8	3.6	-	-	1.3	1.6 (S,M*)
+712-7	24.5	32.6	37.1	2.7	-	-	0.4	2.7 (M,A,E,S)
+712-8	27.3	28.7	38.3	4.9	-	-	0.1	0.7 (M,A,E)
+52-1	27.5	29.0	35.7	4.7	-	-	1.8	0.9 (S,A)
+182-1	19.3	38.2	35.6	3.9	-	-	1.3	1.3 (S,M,A)
+181-1	28.4	27.4	33.0	8.0	-	-	0.9	2.3 (T,S,M)

Table A.1.2 Modal analyses of rocks from the monzonitic core of the pluton

Sample No.	Q	Kf	Pl	Bi	Hb	Cpx	Opq	Others
66	1.7	52.7	38.6	5.5	-	-	1.0	0.5 (E,S,A)
67	3.4	45.8	36.1	14.2	-	-	0.3	tr (S,A)
71	0.9	45.1	39.5	6.2	4.9	-	2.1	1.3 (S,A,E)
75	1.3	40.6	45.7	9.1	0.9	-	1.2	1.2 (C,E,S,A)
94	1.1	40.9	44.9	5.6	4.4	0.4	2.2	0.5 (S,A)
95	0.8	48.4	43.3	2.6	2.6	-	1.6	0.7 (S,C,A)
96	1.4	46.8	44.6	2.8	2.0	-	1.0	1.4 (S,C,A)
102	8.0	44.9	39.4	4.7	-	-	1.1	1.9 (S,C,A)
125	8.3	47.2	37.5	5.4	-	-	0.8	0.8 (S)
197	1.4	37.3	49.7	9.3	-	-	0.7	1.6 (E,S,A)
198	0.5	45.3	43.6	4.9	1.8	0.4	2.6	0.9 (S,E,A)
200	1.9	38.8	44.9	0.4	3.8	9.0	0.7	0.6 (S,C,A)
207	1.1	45.2	41.8	3.6	5.2	-	2.2	0.9 (S,E,A)
222	1.4	32.1	50.2	9.8	3.2	-	0.7	2.6 (C,S,E,A)
223	1.4	48.0	40.8	4.2	3.1	-	1.8	0.7 (S,A,E)
224	4.1	35.1	52.5	6.7	0.5	-	0.8	0.3 (S,A,E)
225	3.3	40.1	43.7	8.6	0.7	-	1.1	2.5 (E,S,C,A)
226	1.2	46.2	43.0	5.3	2.5	-	1.3	0.5 (S,A)
228	1.0	53.1	35.4	5.1	2.2	-	2.0	1.2 (S,E,C,A)
250	1.9	45.4	46.0	2.7	0.9	-	1.1	2.0 (S,E,A)
251	3.9	43.3	43.6	5.2	tr	-	1.8	2.2 (S,E,C,A)
255	0.8	52.5	37.5	4.1	2.9	-	1.4	0.8 (S,A)
257	1.6	53.1	35.5	4.3	2.6	-	2.2	0.7 (S,A,E)
265	1.9	50.7	40.6	3.7	0.5	-	1.1	1.6 (S,C,A)
200-3	5.6	47.7	42.2	3.2	-	-	0.6	1.0 (S,A*,M*)

Table A.1.3 Modal analyses of basic rocks

Sample No.	Q	Kf	Pl	Bi	Hb	Cpx	Opq	Others
70	1.5	-	39.5	9.4	45.8	-	2.4	1.4 (A,S,Ch)
321	tr	-	55.7	9.8	4.0	24.2	6.0	tr (A)
783	tr	0.4	77.9	11.2	3.3	3.9	2.5	0.7 (C,S,A)
+199-4	2.4	3.0	36.6	11.0	38.8	-	7.0	1.2 (S,A,C)
+199-5	3.1	3.2	51.3	14.8	-	20.1	6.7	0.8 (S,A,C)
+53-2	tr	33.6	45.8	15.8	-	-	2.3	2.5 (A,S,C,M)
+53-5	-	22.2	40.0	8.9	20.7	-	5.6	2.6 (A,S,C,M)
+53-6	1.0	21.2	42.8	18.3	6.1	2.1	4.9	3.6 (A,S,C.M)
+184-4	2.2	23.7	56.0	6.9	6.4	0.7	3.3	0.8 (S,M,A)

Table A.1.4 Modal analyses of granodioritic gneisses

Sample No.	Q	Kf	Pl	Bi	Hb	Cpx	Opq	Others
61	23.2	20.3	44.8	7.1	3.5	-	0.3	0.8 (S,A*,E*)
62	27.0	5.7	52.3	10.4	2.3	-	0.3	1.9 (E,S,A*)
122	27.6	4.6	54.4	10.5	1.0	-	tr	1.8 (E,C,S*,A*)
213	20.8	18.3	44.8	9.4	4.3	-	1.7	0.7 (S,A*,Z*)
+711-7	28.5	2.9	62.7	4.4	-	-	tr	1.4 (M,S*)

Table A.1.5 Modal analyses of aluminous gneisses

Sample No.	Q	Pl	Bi	G	Sill	Cd	Opq	Others
67	9.3	0.6	9.0	40.2	15.8	20.6	4.5	tr (A)
172	22.3	30.8	22.4	11.4	7.6	3.2	2.3	tr (A)
209	21.5	44.7	26.9	5.8	0.3	-	0.6	tr (A)
+710-1	39.2	17.5	25.9	15.1	0.5	0.5	0.9	
+710-4	$40^{\dagger}$	$30^{\dagger}$	$15^{\dagger}$	$5^{\dagger}$	$3^{\dagger}$	$5^{\dagger}$	$2^{\dagger}$	
+711-1	$40^{\dagger}$	$30^{\dagger}$	$20^{\dagger}$	$9^{\dagger}$	$0.5^{\dagger}$	-	tr	tr (Z)
+711-3	$15^{\dagger}$	$40^{\dagger}$	$20^{\dagger}$	$20^{\dagger}$	$2^{\dagger}$	tr	$3^{\dagger}$	
+711-4	$40^{\dagger}$	$30^{\dagger}$	$20^{\dagger}$	-	$5^{\dagger}$	-	$4^{\dagger}$	tr (Z)
+711-15	$45^{\dagger}$	$5^{\dagger}$	$20^{\dagger}$	$20^{\dagger}$	$5^{\dagger}$	-	tr	tr (A,T)
+711-16	$35^{\dagger}$	$30^{\dagger}$	$15^{\dagger}$	$10^{\dagger}$	$5^{\dagger}$	-	$5^{\dagger}$	tr (R,T)
+711-18	$25^{\dagger}$	$30^{\dagger}$	$15^{\dagger}$	$10^{\dagger}$	$5^{\dagger}$	$10^{\dagger}$	$4^{\dagger}$	tr (A,T)
+711-19	$30^{\dagger}$	$35^{\dagger}$	$20^{\dagger}$	$10^{\dagger}$	-	-	$4^{\dagger}$	tr (A,T)
+712-4	$20^{\dagger}$	$30^{\dagger}$	$10^{\dagger}$	$20^{\dagger}$	$5^{\dagger}$	$15^{\dagger}$	tr	tr (O)

A.1.2 Sampling and Chemical Analyses

Each of the rock samples (>5 kg) was crushed and ground to <150 mesh powder. During the grinding, samples were reduced after homogenization so that the final weight of the samples was about 50 g. Some of the analyzed samples, however, are from the collection of D.M. Shaw (c.f. Shaw, 1962, 1972).

Chemical analyses for major elements, Li, Rb, Sr and Ba were performed by J.R. Muysson, McMaster University. The precision and accuracy of these analyses for major elements are given in Shaw (1972). This also applied to the chemical analyses of country rocks which were taken from Shaw (1972) and his unpublished data (all given in Tables A.1.6-9).

Li, Rb, Sr and Ba were determined by atomic absorption spectroscopy (AAS). The precision and accuracy for these elements is about 5%. Detection limits for Li and Rb are about 1 ppm, while for Ba and Sr about 5 ppm (J.R. Muysson, personal communication).

The Tl analyses were done by P. Fung, McMaster University. Thallium was determined by AAS, after extraction by an organic solvent (c.f. Dupuy et al., 1973). The precision and accuracy for these data are better than 10% of the value determined.

Table A.1.6 Chemical analyses of quartz monzonites

	26	27	68	115	253	181-1	182-1	52-1	710-2	711-6
SIO2	70.650	70.770	69.590	72.030	75.530	69.470	66.310	68.650	74.400	67.800
TIO2	.490	.220	.510	.200	.130	.590	.560	.660	.120	.500
AL2O3	14.500	15.550	15.280	14.100	12.500	15.700	16.310	14.130	14.600	15.800
FE2O3	1.410	.860	1.260	.680	.920	.330	1.580	2.590	1.010	1.900
FEO	1.160	.600	1.000	1.630	.830	2.790	1.650	2.010	.500	1.240
MNO	.020	.030	.030	.040	.020	.020	.050	.080	.010	.030
MGO	.650	.250	.450	.230	.060	.830	.580	.570	.240	.700
CAO	1.280	1.220	.900	1.090	.700	1.510	1.380	1.420	1.110	1.750
NA2O	3.380	4.000	4.010	4.100	4.040	3.840	4.080	3.530	4.300	3.730
K2O	5.640	6.040	6.240	5.130	4.750	5.370	6.520	5.720	3.840	6.470
P2O5	.150	.050	.070	.050	.010	.180	.120	.160	0.000	.120
H2O +	.300	.250	.280	.390	.730	.700	.400	.300	.140	.750
H2O -	.070	.060	.070	.040	.070	.060	.050	.080	.040	.050
CO2	.010	.120	.010	.240	.040	.100	.010	.020	.030	.030
SUM	99.710	100.070	99.690	99.950	99.430	100.870	99.600	99.580	100.340	99.480
RB	74.000	149.000	59.000	106.000	175.000	-0.000	-0.000	240.000	-0.000	-0.000
SR	262.000	220.600	118.000	34.000	34.000	-0.000	-0.000	170.000	-0.000	-0.000
BA	1528.000	537.000	716.000	0.000	179.000	-0.000	-0.000	-0.000	-0.000	-0.000
TL	637.000	1030.000	-0.000	880.000	-0.000	-0.000	-0.000	-0.000	-0.000	-0.000
LA	114.000	105.000	-0.000	74.000	-0.000	-0.000	-0.000	-0.000	-0.000	-0.000
CE	244.000	220.000	-0.000	143.000	-0.000	-0.000	-0.000	-0.000	-0.000	-0.000
ND	60.000	101.000	-0.000	61.000	-0.000	-0.000	-0.000	-0.000	-0.000	-0.000
SM	10.900	15.000	-0.000	10.100	-0.000	-0.000	-0.000	-0.000	-0.000	-0.000
EU	3.100	2.760	-0.000	3.100	-0.000	-0.000	-0.000	-0.000	-0.000	-0.000
GD	-0.000	8.700	-0.000	-0.000	-0.000	-0.000	-0.000	-0.000	-0.000	-0.000
TB	1.000	1.490	-0.000	2.050	-0.000	-0.000	-0.000	-0.000	-0.000	-0.000
HO	2.000	2.000	-0.000	7.500	-0.000	-0.000	-0.000	-0.000	-0.000	-0.000
YB	5.160	5.990	-0.000	8.100	-0.000	-0.000	-0.000	-0.000	-0.000	-0.000
LU	.840	.910	-0.000	1.160	-0.000	-0.000	-0.000	-0.000	-0.000	-0.000

	712-7	712-8	250
SIO2	71.600	70.800	72.790
TIO2	.230	.190	.150
AL2O3	14.600	15.100	16.590
FE2O3	1.720	.820	1.180
FEO	.800	1.210	.580
MNO	.010	.030	.010
MGO	.380	.490	.050
CAO	.840	1.210	.210
NA2O	3.810	3.520	3.360
K2O	5.350	5.500	5.000
P2O5	.040	.030	0.000
H2O +	.470	.460	.130
H2O -	.070	.100	.050
CO2	.060	.290	.050
SUM	100.060	99.750	100.160
RB	-0.000	-0.000	100.000
SR	-0.000	-0.000	8.000
BA	-0.000	-0.000	90.000
TL	-0.000	-0.000	-0.000
LA	-0.000	-0.000	25.700
CE	-0.000	-0.000	59.300
ND	-0.000	-0.000	36.000
SM	-0.000	-0.000	7.580
EU	-0.000	-0.000	2.420
GD	-0.000	-0.000	-0.000
TB	-0.000	-0.000	.850
HO	-0.000	-0.000	-0.000
YB	-0.000	-0.000	2.630
LU	-0.000	-0.000	.430

major elements in wt.%

trace elements, except Tl, in ppm

Tl in ppb

-0.00 - not determined

Table A.1.7 Chemical analyses of monzonites

	94	96	102	125	142	198	207	224	225	228
SIO2	59.500	63.280	64.690	65.120	62.830	61.040	59.410	62.880	59.830	61.590
TIO2	1.040	.650	.710	.570	.740	.968	1.030	.690	1.110	.830
AL2O3	19.140	18.180	16.850	17.250	17.720	18.320	18.870	17.770	17.750	18.530
FE2O3	2.060	1.720	1.300	1.490	2.420	1.850	2.070	1.530	2.390	1.930
FEO	1.930	1.220	1.740	1.180	1.690	1.740	1.820	1.990	2.470	1.360
MNO	.070	.080	.070	.040	.060	.070	.090	.070	.100	.080
MGO	1.250	.550	.640	.590	.910	1.060	1.210	1.030	1.340	.990
CAO	2.830	1.390	1.170	1.260	1.370	1.780	2.810	2.330	2.310	1.450
NA2O	4.820	5.100	4.550	4.570	3.910	4.850	5.010	4.680	4.600	5.070
K2O	6.200	7.150	7.400	7.310	7.200	7.040	6.200	5.480	6.680	7.100
P2O5	.350	.100	.160	.100	.150	.230	.340	.270	.440	.200
H2O +	.350	.200	.390	.260	.560	.300	.380	.410	.510	.440
H2O -	.050	.080	.020	.060	.070	.140	.080	.080	.090	.150
CO2	0.000	0.000	.050	.040	0.000	0.100	.020	.135	0.000	.020
SUM	99.590	99.700	99.700	99.830	99.630	99.380	99.450	99.340	99.550	99.880
RB	83.000	65.000	73.000	71.000	115.000	59.000	54.000	58.000	75.000	52.000
SR	769.000	135.000	59.000	203.000	304.000	211.000	846.000	634.000	313.000	313.000
BA	5200.000	716.000	537.000	1520.000	1570.000	1610.000	4930.000	3940.000	3850.000	1970.000
TL	417.000	515.000	550.000	-0.000	-0.000	363.000	358.000	-0.000	700.000	413.000
LA	54.100	229.000	251.000	239.000	-0.000	90.800	61.200	63.800	-0.000	111.000
CE	121.000	585.000	558.000	524.000	-0.000	230.000	113.000	131.000	-0.000	249.000
ND	61.000	337.000	296.000	313.000	-0.000	134.000	72.000	-0.000	-0.000	137.000
SM	11.500	67.000	72.600	69.100	-0.000	26.800	13.600	14.500	-0.000	37.800
EU	7.570	14.100	15.700	14.100	-0.000	10.600	7.240	7.380	-0.000	14.700
GD	11.000	51.000	-0.000	-0.000	-0.000	22.500	-0.000	-0.000	-0.000	-0.000
TB	1.510	7.940	8.540	6.540	-0.000	3.280	1.640	1.860	-0.000	4.410
HO	-0.000	6.800	8.800	-0.000	-0.000	-0.000	1.800	1.590	-0.000	4.800
YB	2.430	7.850	7.430	7.690	-0.000	3.440	2.640	2.670	-0.000	4.120
LU	.380	.970	1.630	.950	-0.000	.478	.390	.438	-0.000	.460

	251	265	200-3
SIO2	63.300	62.130	64.380
TIO2	.720	.850	.720
AL2O3	18.100	18.010	16.940
FE2O3	1.950	1.690	1.070
FEO	1.200	1.550	1.930
MNO	.070	.090	.060
MGO	.720	.770	.610
CAO	1.530	1.520	1.340
NA2O	4.810	4.930	4.790
K2O	6.910	7.390	7.130
P2O5	.100	.140	.070
H2O +	.150	.230	.430
H2O -	.070	.060	.120
CO2	.050	.050	.070
SUM	99.680	99.410	99.660
RB	90.000	70.000	-0.000
SR	123.000	68.000	-0.000
BA	779.000	448.000	-0.000
TL	663.000	-0.000	-0.000
LA	158.000	-0.000	-0.000
CE	365.000	-0.000	-0.000
ND	214.000	-0.000	-0.000
SM	44.300	-0.000	-0.000
EU	10.100	-0.000	-0.000
GD	-0.000	-0.000	-0.000
TB	4.790	-0.000	-0.000
HO	-0.000	-0.000	-0.000
YB	5.300	-0.000	-0.000
LU	.820	-0.000	-0.000

major elements in Wt. %

trace elements, except Tl, in ppm

Tl in ppb

-0.00 - not determined

Table A.1.8 Chemical analyses of basic rocks and dunite

STATEMENT OF DATA

	70	321	783	53-2	53-5	53-6	184-4	199-4	199-5	130*
SIO2	47.790	47.290	46.520	54.770	49.620	52.650	53.740	48.360	48.770	39.400
TIO2	1.880	2.120	2.710	1.710	2.610	2.130	1.710	2.520	2.310	.020
AL2O3	14.010	16.260	18.160	19.240	16.950	16.650	18.560	14.270	14.900	.320
FE2O3	4.330	5.000	.420	2.290	2.210	.900	1.870	5.860	4.730	4.110
FEO	7.560	8.140	10.130	3.570	7.720	7.480	5.020	8.050	8.430	2.800
MNO	.170	.150	.110	.070	.150	.150	.090	.160	.140	.170
MGO	8.400	6.260	4.000	2.140	3.560	2.980	2.280	6.600	5.860	41.060
CAO	8.450	9.710	7.820	3.830	6.550	5.760	5.520	7.140	8.550	.370
NA2O	2.350	2.890	4.010	4.610	3.780	4.110	4.500	2.910	2.960	0.000
K2O	1.890	.980	2.350	5.750	3.240	3.760	3.780	1.530	1.480	0.000
P2O5	.460	.330	1.390	.710	1.250	.990	.790	.460	.510	0.000
H2O+	1.770	.620	.760	.450	.830	.740	.540	1.230	.720	10.860
H2O-	.200	.120	.150	.110	.230	.170	.130	.230	.370	.730
CO2	.110	.170	.060	.130	.190	.570	.340	.120	.010	-0.000
SUM	99.370	100.040	98.590	99.380	98.690	99.040	98.870	99.440	99.690	99.840
LI	-0.000	-0.000	-0.000	-0.000	-0.000	-0.000	-0.000	-0.000	-0.000	3.700
RB	47.000	8.000	34.000	73.000	-0.000	-0.000	-0.000	29.000	25.000	1.800
SR	981.000	1400.000	1830.000	-0.000	-0.000	-0.000	-0.000	845.000	-0.000	13.500
BA	1880.000	1160.000	4690.000	-0.000	-0.000	-0.000	-0.000	-0.000	-0.000	20.900
TL	466.000	74.000	-0.000	-0.000	-0.000	-0.000	-0.000	-0.000	240.000	0.000
LA	32.300	19.400	44.300	-0.000	57.400	-0.000	-0.000	22.700	29.400	.603
CE	71.700	45.900	109.000	-0.000	114.000	-0.000	-0.000	48.100	65.300	1.720
ND	42.000	28.000	55.000	-0.000	65.000	-0.000	-0.000	33.000	37.000	0.000
SM	10.500	7.050	14.700	-0.000	14.500	-0.000	-0.000	8.610	9.570	.077
EU	2.940	2.110	4.050	-0.000	6.610	-0.000	-0.000	2.640	2.860	.027
GD	-0.000	6.100	-0.000	-0.000	-0.000	-0.000	-0.000	-0.000	8.500	0.000
TB	1.240	.840	1.610	-0.000	1.750	-0.000	-0.000	1.180	1.190	0.000
HO	-0.000	-0.000	-0.000	-0.000	-0.000	-0.000	-0.000	-0.000	-0.000	0.000
YB	3.290	1.740	3.100	-0.000	2.940	-0.000	-0.000	2.970	2.830	.059
LU	.540	.250	.460	-0.000	.480	-0.000	-0.000	.470	.440	.014

* dunite

-0.000 - not determined

0.000 - not detected

major elements in wt.%

trace elements, except Tl, in ppm

Tl in ppb

Table A.1.9 Chemical analyses of aluminous hornfelses and Apsley biotite gneisses

	67	172	710-1	710-4	711-1	711-3	711-4	711-15	711-16	711-18
SIO2	45.850	58.020	59.100	55.200	53.600	54.740	60.000	58.000	57.300	57.900
TIO2	2.170	1.130	1.030	.850	1.000	1.130	.900	.760	.720	.700
AL2O3	26.740	19.150	17.300	19.000	20.300	18.860	17.300	19.100	18.400	18.700
FE2O3	1.830	1.430	1.300	1.720	2.400	1.560	2.980	1.310	3.950	1.780
FEO	14.580	8.780	7.690	8.460	8.640	9.240	4.900	9.680	6.310	6.870
MNO	.560	.130	.110	.160	.110	.160	.090	.120	.120	.130
MGO	6.090	3.820	4.530	4.980	4.460	4.600	3.400	4.750	4.250	4.170
CAO	.570	2.320	3.120	2.150	2.050	2.970	2.380	1.830	3.870	4.010
NA2O	.060	2.200	2.110	2.330	2.360	2.380	2.900	.760	1.610	1.810
K2O	.690	1.720	1.730	3.070	2.830	2.490	3.120	1.550	1.840	1.850
P2O5	.040	.140	.150	.090	.210	.180	.200	.220	.190	.210
H2O +	.770	1.040	.730	1.380	1.790	1.190	1.130	1.020	.870	1.070
H2O -	.170	.150	.130	.230	.180	.240	.170	.310	.210	.260
CO2	.020	-0.000	-0.000	.030	.090	.010	-0.000	-0.000	-0.000	-0.000
SUM	100.140	100.030	99.030	99.650	99.540	99.750	99.470	99.410	99.590	99.760
LI	-0.000	-0.000	25.000	-0.000	28.000	44.000	-0.000	-0.000	-0.000	-0.000
RB	36.000	41.000	42.000	-0.000	52.000	68.000	-0.000	-0.000	-0.000	-0.000
SR	0.000	169.000	366.000	-0.000	85.000	183.000	-0.000	-0.000	-0.000	-0.000
BA	90.000	448.000	430.000	-0.000	511.000	385.000	-0.000	-0.000	-0.000	-0.000
LA	12.400	-0.000	-0.000	-0.000	-0.000	-0.000	-0.000	-0.000	-0.000	8.500
CE	28.100	-0.000	-0.000	-0.000	-0.000	-0.000	-0.000	-0.000	-0.000	21.800
ND	-0.000	-0.000	-0.000	-0.000	-0.000	-0.000	-0.000	-0.000	-0.000	-0.000
SM	5.100	-0.000	-0.000	-0.000	-0.000	-0.000	-0.000	-0.000	-0.000	3.570
EU	.460	-0.000	-0.000	-0.000	-0.000	-0.000	-0.000	-0.000	-0.000	1.040
GD	-0.000	-0.000	-0.000	-0.000	-0.000	-0.000	-0.000	-0.000	-0.000	-0.000
TB	1.130	-0.000	-0.000	-0.000	-0.000	-0.000	-0.000	-0.000	-0.000	1.180
HO	-0.000	-0.000	-0.000	-0.000	-0.000	-0.000	-0.000	-0.000	-0.000	-0.000
YB	8.990	-0.000	-0.000	-0.000	-0.000	-0.000	-0.000	-0.000	-0.000	6.540
LU	1.540	-0.000	-0.000	-0.000	-0.000	-0.000	-0.000	-0.000	-0.000	1.100

	711-19	712-4	711-2*	712-1*	173*
SIO2	57.500	62.400	62.100	71.600	-0.000
TIO2	.790	.470	.690	.470	-0.000
AL2O3	17.700	18.000	16.200	12.900	-0.000
FE2O3	.860	1.140	2.610	.680	-0.000
FEO	8.630	7.160	4.120	3.050	-0.000
MNO	.250	.120	.090	.100	-0.000
MGO	4.380	4.570	2.850	.900	-0.000
CAO	3.950	2.190	2.050	2.780	-0.000
NA2O	2.740	1.430	3.980	3.630	-0.000
K2O	2.270	.840	3.050	2.570	-0.000
P2O5	.230	.080	.120	.130	-0.000
H2O +	.760	.620	1.030	.620	-0.000
H2O -	.160	.120	.160	.060	-0.000
CO2	.020	-0.000	.020	.830	-0.000
SUM	99.740	99.140	99.070	100.320	-0.000
LI	-0.000	42.000	-0.000	-0.000	-0.000
RB	-0.000	23.000	-0.000	-0.000	-0.000
SR	-0.000	274.000	-0.000	-0.000	-0.000
BA	-0.000	206.000	-0.000	-0.000	-0.000
LA	-0.000	9.200	14.400	17.800	19.500
CE	-0.000	19.400	34.500	40.600	45.300
ND	-0.000	-0.000	21.000	24.500	27.600
SM	-0.000	3.160	5.370	5.850	7.020
EU	-0.000	1.020	1.430	1.450	1.780
GD	-0.000	-0.000	-0.220	-0.000	-0.000
TB	-0.000	1.220	.950	.900	1.100
HO	-0.000	-0.000	1.200	1.400	-0.000
YB	-0.000	6.170	3.060	3.690	4.280
LU	-0.000	1.000	.470	.540	.690

*Apsley biotite gneiss

major elements in wt.%

trace elements in ppm

-0.00 - not determined

Table A.1.10 REE contents of minerals (ppm)

STATEMENT OF DATA

	HB 94*	BIO 94*	K-SPAR 94*	PLAG 94*	BIO 207*	K-SPAR 207*	PLAG 207*	SPHENE 251*	BIO 251*	K-SPAR 251*
LA	83.000	8.030	5.210	6.430	37.100	10.200	14.700	3190.000	59.200	16.400
CE	179.000	14.000	9.670	10.200	63.100	15.900	30.700	9630.000	79.000	32.700
ND	106.000	6.100	-0.000	-0.000	35.600	-0.000	-0.000	6020.000	21.200	-0.000
SM	20.300	1.100	.240	.560	6.930	.760	1.150	993.000	2.140	.820
EU	5.240	.410	1.570	1.400	2.280	4.260	2.790	190.000	.210	.690
GD	14.500	-0.000	-0.000	-0.000	-0.000	-0.000	-0.000	-0.000	-0.000	-0.000
TB	2.370	.140	.025	.110	.600	.150	.170	115.000	.160	.075
HO	-0.000	-0.000	-0.000	-0.000	-0.000	-0.000	-0.000	-0.000	-0.000	-0.000
YB	7.900	.290	.043	.140	.650	.240	.260	212.000	.330	.090
LU	1.500	.047	0.000	0.000	.100	.038	.040	31.600	.040	0.000

	PLAG 251*	BIO 26+	K-SPAR 26+	PLAG 26+	BIO 27+	K-SPAR 27+	PLAG 27+	BIO 115+	K-SPAR 115+	PLAG 115+
LA	19.100	12.400	4.110	6.740	44.300	7.510	12.900	86.700	1.330	2.630
CE	34.400	22.300	6.450	13.500	95.400	10.500	25.400	184.000	3.210	4.220
ND	-0.000	17.500	-0.000	-0.000	-0.000	-0.000	-0.000	109.000	-0.000	-0.000
SM	1.000	1.750	.370	.470	13.600	.830	1.170	19.200	.330	.430
EU	.700	.290	1.450	.900	2.100	.950	1.030	4.620	.380	.420
GD	-0.000	-0.000	-0.000	-0.000	-0.000	-0.000	-0.000	-0.000	-0.000	-0.000
TB	.093	.180	.035	.100	1.390	.150	.210	5.310	.055	.065
HO	-0.000	-0.000	-0.000	-0.000	2.200	-0.000	-0.000	7.500	-0.000	-0.000
YB	.110	.440	.200	.290	6.560	.360	.620	22.800	.190	.190
LU	0.000	.063	.027	.050	1.330	.057	.084	3.810	.031	.032

	HB 70x	BIO 70x	PLAG 70x	CPX 321x	PLAG 321x	GARNET 67#
LA	5.620	3.440	5.140	7.560	13.100	7.550
CE	16.900	13.800	7.510	19.600	21.000	20.300
ND	18.300	11.700	-0.000	-0.000	-0.000	-0.000
SM	2.410	3.160	.220	1.600	.380	5.040
EU	.750	1.120	.380	.340	.860	.600
GD	-0.000	-0.000	-0.000	-0.000	-0.000	-0.000
TB	.430	.500	.039	.330	.069	2.830
HO	-0.000	-0.000	-0.000	-0.000	-0.000	-0.000
YB	1.340	1.210	.031	1.240	.154	13.600
LU	.225	.197	.013	.177	.021	2.850

host rocks - * monzonite
+ quartz monzonite
x diorite
# aluminous hornfels

-0.00 - not determined
0.00 - not detected

A.1.3 Mineral Separation

Minerals were separated by standard magnetic and heavy liquid techniques until an estimated purity of concentrates was better than 99% for mafic minerals, sphene and garnet, and about 98% for plagioclase from basic rocks and K-feldspar. But the purity of plagioclase from felsic rocks was only about 70-80%.

The impurities in plagioclase were mainly quartz and probably also the sodic phase of perthites. The detectable contaminants of K-feldspar concentrates were quartz and plagioclase. Also separated perthitic K-feldspars probably contained a predominance of potassic phases over sodic ones in comparison with the original perthites, as noted earlier.

The impurities in biotites were small composite grains of feldspars, quartz and opaque. Those in hornblende included feldspar, opaque and biotite, while in clinopyroxene, contaminants were hornblende, feldspar and opaque (clinopyroxene, however, was partially altered). Possible contaminants of sphene and garnet were composite grains of felsic minerals and opaque.

A.1.4 Determinative Techniques for Potassium Feldspars

In the course of X-ray work, the Philips wide-range goniometer with filtered copper radiation was used. The scans were made at 1/4° per minute, with a chart speed of 1° 2θ = 1 inch.

In the case of feldspars for which the unit-cell parameters were calculated or "the three reflection method" applied, X-ray diffraction patterns were run over a 2θ range of 15°-60° four to six times for each sample using annealed (48 hours at 700°C - Orville, 1967) reagent grade CaF_2 as an internal standard. The unit-cell parameters were refined on 13-16 reflections by a computer program according to the procedure of Wright and Stewart (1968).

For the determination of obliquity, feldspars were first X-rayed from 2θ 20° to 34° for the identification of the reflection and then scanned over an interval 2θ 29° to 32°. Each determination is the average Δ 2θ value of six oscillations, three in the upscale and three in the downscale directions, measured on the X-ray chart between the 131 and $\bar{1}31$ reflections. Standard errors for the mean obliquity are less than 0.03.

The determination of the bulk composition of perthitic potassium feldspars was done by Orville's method (1960, 1967). The 1-3 mm large chips of K-feldspar were dry heated in a resistance furnace for 48 hours at a temperature of 1050°C. Then K-feldspars were ground and mixed with K Br O_3, which was used

Table A.1.11

Unit-cell parameters of potassic phases of perthites

Sample No.		a(Å)	b(Å)	c(Å)	α	β	γ
58	P	8.576 ±0.002	12.965 ±0.003	7.214 ±0.002	90°36.19' ±2.25'	115°56.82' ±2.08'	87°45.08' ±1.98'
27	QM	8.582 ±0.007	12.964 ±0.007	7.213 ±0.003	90°39.80' ±3.92'	115°55.25' ±3.71'	87°43.42' ±3.27'
44	QM	8.587 ±0.004	12.964 ±0.005	7.216 ±0.003	90°40.05' ±3.41'	115°57.18' ±2.63'	87°45.00' ±2.54'
115	QM	8.576 ±0.004	12.973 ±0.005	7.213 ±0.002	90°38.70' ±3.54'	115°56.82' ±2.72'	87°47.10' ±2.48'
102	M	8.580 ±0.006	12.971 ±0.007	7.212 ±0.003	90°39.25' ±3.67'	116°00.36' ±3.29'	87°47.23' ±3.11'
226	M	8.566 ±0.002	12.981 ±0.003	7.200 ±0.002		116°06.08' ±1.25'	
251	M	8.575 ±0.003	12.968 ±0.003	7.213 ±0.002	90°40.05' ±1.75'	115°57.60' ±1.84'	87°45.15' ±1.96'

1. Host rock: P=pegmatite; QM=quartz monzonite; M=monzonite

as an internal standard. The interval between the ($\bar{2}01$) reflection of potassium feldspars and the (101) reflection of potassium bromate was scanned about 12 times.

The determinations obtained by Orville's method are probably accurate to within ±5 wt.% Or and reproducible for a single sample to within 1% Or.

APPENDIX 2

A.2 The Determination of Rare Earth Elements

A.2.1 Introduction

One of the purposes of the work was to adapt a simple yet sufficiently accurate method to determine enough REE in microgram amounts by neutron activation analysis, to evaluate their fractionation trends. It became evident that not more than three or four rare-earths could be determined by instrumental neutron activation analysis with the available facilities and that radiochemical neutron activation was essential.

In order to eliminate spectral interferences and to increase the signal to the background ratio, the REE were separated as a group from other radionuclides. Then the separated REE were radio-assayed by γ-ray spectrometry with a Ge(Li) detector.

A number of different procedures for the separation of REE as a whole from other radionuclides have been recently published (Tomura et al., 1968; Graber et al., 1970; Denechaud et al., 1970; Barker, 1972, etc.). Since each of these methods has certain advantages, some features from different published procedures were combined. In order to obtain higher precision, a procedure of Denechaud et al. (1970) was accepted as the framework, particularly in two aspects - the addition of a carrier for all REE and the chemical yield determination for each REE. But only several steps of their post-irradiation chemistry were retained (the removal of silica and alumina) and these were combined with conventional hydroxide-fluoride cycles (Schmitt et al., 1963; Tomura et al., 1968; Barker, 1972) for purification from other elements.

Two different procedures for the dissolution of the samples were used in the course of the work - dissolution by acid and by fusion. The fusion procedure was used for common rock samples because of the possible presence of certain minerals (zircon, etc.) which have high contents of REE but are not soluble in acids. On the other hand, the dissolution procedure which was used for some minerals (biotite, feldspars, amphibole) is faster and simpler. This method also allows the separation of any insoluble impurities from analyzed mineral separates, if a filtration step is added (after step 15 in the dissolution procedure - section A.2.12 [illegible]

A.2.2 Sample Preparation and Irradiation

The weighed amount of 0.100 to 0.250 g of the powdered sample (<150 mesh) was heat-sealed in a silica ampoule. About 50-100 mg (weighed) of a standard rare-earth solution was also transferred into another silica ampoule; powdered silica glass was added to about the same height as the samples in the other ampoules. Then the ampoule was encapsulated in a manner similar to that used for the samples. Six samples and two standards were taped together and placed in an Al container for irradiation.

Samples were irradiated in a high flux position in the McMaster Nuclear Reactor (nominal neutron flux of 1.5 x 10^{13} neutron cm^{-2} sec^{-1}; later 5 x 10^{13} neutron cm^{-2} sec^{-1}), followed by 3 days of cooling before chemical processing.

During the initial experiments, the flux inhomogeneities within a group of adjacent samples were monitored. A weighed iron wire flux monitor (50-70 mg of reagent grade iron wire) was taped around the filled part of the ampoule. At any convenient time from about two to several weeks after irradiation the ^{59}Fe activity of the wire was counted on the Na(I) detector for a time sufficient to give about 10^5 counts. This was done twice for each group of samples. After corrections, the specific activities of the wires were calculated as counts/min/mg. The flux received by each sample did not differ more than 5%. Since the variations of flux appeared to be within the ranges of errors, the monitors of flux differential in the reactor were not used afterwards.

A.2.3 Standards and Carriers

Stock solutions of nitrates of each of the rare-earth elements, except Ce, were made from oxides of greater than

99.9% purity ("Specpure" oxides of Johnson Matthey and Company) in order to contain approximately 10 mg of the rare-earth ion per ml. The solutions were standardized by titration with EDTA. Because the commercial cerium oxide, CeO_2 is very difficult to dissolve, the appropriate quantity of cerium ammonium nitrate (primary standard of G.F. Smith Chemical Company) was used to make up the Ce stock solution. The cerium stock solution was also standardized with EDTA. A standard monitor solution was prepared by mixing appropriate dilutions of the stock solutions. The relative abundances of the REE in the standard solution were chosen to be roughly similar to their relative abundances in the samples, so that their composite gamma-ray spectra were similar.

In comparison with the standard monitor solution from the Department of Chemistry, University of Wisconsin, which was included in several irradiations, the writer's solution yielded systematically different results. Since the results of the USGS standard rocks obtained with the Wisconsin monitor solution (Denechaud et al., 1970) were close to the reported values for these standard rocks (c.f. Table A.2.4-6), all results were readjusted according to the Wisconsin standard solution.

The rare-earth ion concentrations in the standard monitor and carrier solutions are given in Table A.2.1.

Table A.2.1 Concentrations of REE in the standard monitor and carrier solutions

Element	Monitor solution (µg REE/g solution)	Carrier solution (mg REE/g solution)
La	22.9	1.08
Ce	55.8	0.462
Pr	8.53	0.501
Nd	31.7	0.241
Sm	7.22	1.04
Eu	4.22	1.15
Gd	7.25	0.346
Tb	2.82	1.20
Dy	13.9	0.158
Ho	2.32	0.423
Er	4.71	0.605
Tm	1.03	0.315
Yb	7.26	1.19
Lu	0.930	1.41
Y	-	0.522

A.2.4 Chemical Separation of the Rare-Earth Element Group

The complete chemical procedures for both samples and standards are given in sections A.2.11-13. Several brief points are noteworthy. The solution of Y^{88} which was used for determination of the chemical yield was made up so that 2 ml of the solution would give about 15,000 counts above the background in the photopeak for Y^{88} at 1.836 MeV in 200 minutes counting time.

Scandium did not have to be removed from the samples analyzed for this work. Its removal before radioassay of the REE, however, considerably improves the precision of the determinations of Nd, Tb, Yb and Lu. Therefore, special efforts were made for its removal. In acid rocks and feldspars, which contain rather low amounts of Sc, it was separated by buffered fluoride precipitation, while in basic rocks and biotites with high Sc contents, a more laborious but more effective solvent-extraction technique was used.

Regarding the buffered fluoride precipitation, Stevenson and Nervik (1961) have pointed out that the behavior of Sc differs very considerably from that of the rare-earths in fluoride solution. They showed that in 1 M acid solution, ScF_3 may be precipitated together with REE essentially quantitatively. But at low acid concentrations with ammonium ions present, the ScF_6^{3-} complex forms (Fischer and Bock, 1942) and in a buffered NH_3 solution at pH 5, REE fluorides may be precipitated quantitatively while most of the Sc remains in solution (Bonner, in

Stevenson and Nervik, 1961).

The solvent-extraction method for removal of Sc which was carried out before the last hydroxide precipitation, is described by Morrison and Freiser (1957). A tracer experiment of P. Helmke (personal communication, 1971) showed that about 85% Sc is removed in the first extraction, while the second extraction (with the solution of 1 mg of Sc ion as holdback carrier added to the aqueous phase) removes an additional 13% of the ^{46}Sc tracer.

Throughout the procedure the glassware for each sample was used repeatedly without special attempts to wash it between steps. The residue from one step does not interfere with the following step and chemical yields can be increased by re-using the glassware. When accurately measured amounts were needed, they were prepared in advance to avoid wasting time during the chemical processing. Six samples and two standards required 8-10 hours for the dissolution procedure and 10-12 hours for the fusion procedure.

A.2.5 Counting Equipment

A Nuclear-Chicago gamma counting system utilizing a 25 cm^3 Ge(Li) diode, an analog digital conventor, a 1600 channel memory and a teletype paper print-out was used during the course of this work. This system permits a resolution of 4.5 KeV (full width at half maximum) for the 320 KeV peak of ^{51}Cr. From undetermined causes, the analyser and amplifiers occasionally drift in energy. Whenever this happened during a count set, the resulting photopeaks were broadened and the area of the peaks had to be calculated differently (see below).

A 3"x3" NaI(Tl) detector, a description of which is given by Chyi (1972) was also used for part of this work to determine the 1.836 MeV photopeak of ^{88}Y and the 1.099 and 1.292 MeV photopeaks of ^{59}Fe from the iron wire flux monitors.

A.2.6 Counting Conditions

The counting procedures for the Ge(Li) detector, including the nuclides used, the energies of the gamma-ray peaks selected for calculations and the starting time of the count following irradiation are summarized in Table A.2.2. The separated REE were counted at three different times - once about 3-4 days after irradiation (I count), one 10 days (II count) and once about 40 days (III count) after the irradiation. The optimum geometries and observation times for these counts were a function of the detection system and the sample activity. With regard to the I count, a set of counts was taken at a great enough distance from the detector so that dead time did not exceed 20%. The observation time needed to achieve satisfactory counting statistics turned out to be usually about 30 minutes and the position of the order of about 10 cm above the detector. For the II and III count sets, the selection of a counting

Table A.2.2 Summary of information pertaining to radioassay

Count set	Days after end of irradiation	Nuclide	Half-life		Energies of γ-rays used, MeV
I	3	^{140}La	40.2	h	0.3288*, 0.4872*
		^{153}Sm	47.0	h	0.0697, 0.1032*
		^{166}Ho	26.9	h	0.0806
		^{177}Lu	6.74	d	0.2084*
II	10	^{140}La	40.2	h	0.3288, 0.4872
		^{147}Nd	11.1	d	0.5310
		^{160}Tb	72.1	d	0.2985*
		^{175}Yb	4.21	d	0.2826*, 0.3961*
		^{177}Lu	6.74	d	0.2084
III	40	^{141}Ce	33.0	d	0.1454
		^{152}Eu	12.7	y	0.1218*, 0.3444*
		^{153}Gd	242.0	d	0.0974
		^{160}Tb	72.1	d	0.2985
		^{169}Yb	32.0	d	0.1772*

*Peaks used in chemical yield determination of irradiated carrier, 8 days after irradiation of carrier position depends on a balancing of the desirability of the accumulation of counts reasonably rapidly and the desirability of obtaining identical counting geometry. The final sets were usually counted at about a centimeter from the detector. In general, 1 KeV:1 channel scale was used for all counts. Due to unexpected problems (e.g. availability of counter), however, all REE listed in Table A.2.2 were not always determined.

Apart from the observed REE, at least two more elements may be determined by this method. They are dysprosium and thulium. The peak of thulium (^{170}Tm 0.0843 MeV), however, is not sufficiently isolated to be measured without careful correction for an overlapping peak of terbium (^{160}Tb 0.0879 MeV). With regard to dysprosium, during the initial experiments, attempts had been made for its determination, but because of a very short half-life (^{165}Dy - 2.3 hours) irradiated samples, which had to be processed after a rather short cooling period, were strongly radioactive and thus both these elements were not determined.

Following the III count set, samples and standards were counted on the Na(I)-detector for a time sufficient to give about 15,000 counts above background for the 1.836 MeV peak of Y^{88}.

A.2.7 Peak Integration

The procedure used for the integration of γ-ray peaks is described in detail by Denechaud (1969) and Denechaud et al. (1970). Briefly, the half-peak area method was used. The spectrum was integrated over the full width of the peak at half maximum height and the average background was subtracted. Regarding the average background, an accurate graph, counts per channel versus the channel number of the pertinent part of the spectrum was drawn in order to determine the baseline. A straight line, which represented the baseline, was drawn between the valleys surrounding the peak. The value of the baseline for the channel which corresponds to the median channel of the energy range to be summed was determined from the graph.

The half peak area method, however, can be used only if the peaks are not broadened (Denechaud, 1969). If the half widths of the peak differed by more than 7%, whole-peak area calculations were used.

The net peaks were corrected for differences in counting time and for decay.

A.2.8 Determination of Chemical Yields

Since the losses for the individual REE are not uniform during the separation, the chemical yield has been determined for each REE. A calculation of individual elemental yields involved a determination of relative yields (i.e. relative differences between recovery of individual REE) and these, along with the absolute field for Y, have been used for the determination of absolute yields for each REE. The tracer of ^{88}Y was chosen because it has REE chemical behaviour, a fairly long half-life of 108 days and an absence of γ-ray in the low energy region, where the peaks to be analyzed occur.

The relative yields were determined by re-irradiation of a portion of the recovered carrier. After all the count sets were completed, the samples and standards were dissolved in 2 M HCl and a small, unweighed amount of the carrier was transferred into a silica ampoule. When this was done for each sample and standard to be re-irradiated, all were taped together and re-irradiated at a total neutron flux equal to the flux samples received in the original irradiation, and thus the residual activity was rendered negligeable. About eight days after the re-irradiation each irradiated carrier was counted on the Ge(Li) detector. Since only relative numbers within the samples were needed, the counting geometry and weights were not important. The γ-ray peaks used for the yield determination are given in Table A.2.2.

Relative chemical yields for La, Sm, Eu, Tb, Yb and Lu were obtained by comparing their corrected activities in the samples to those of the standards. Relative yields for Ce, Nd, Gd and Ho were obtained by interpolation from a graph of relative yield plotted against the REE atomic number. The absolute chemical yield of Dy was assumed to be the same as that of the ^{88}Y tracer since "the ionic radius of Y is similar to that of Dy and its geochemical behaviour is extremely close to that of the heavier lanthanides" (Haskin et al., 1966, p.173).

An absolute chemical yield for each of the REE was then obtained by multiplying the ratio of the relative chemical yield for the element to that for Dy by the absolute chemical yield for Dy.

A.2.9 Calculations

The concentrations for each element were obtained by comparing the activity of samples with that of the standard and correcting for differing weights and the non-quantitative variable chemical yields of the samples, as follows:

$$Cs = (As/Am) \cdot (Gm/Gs) \cdot (Cm/Y)$$

Cs - concentration of the element in the sample in ppm;
Cm - concentration of the element in the standard monitor in ppm;
As - corrected peak area in counts per unit time for the sample;
Am - corrected peak area in counts per unit time for the standard monitor;
Gs - weight of the sample in grams;
Gm - weight of the standard monitor in grams;
Y - absolute chemical yield for the element.

When several values for an element had similar statistical uncertainties, an arithmetic average was taken to get a single value. If the values had significantly different uncertainties, the one with the smallest uncertainty was used to represent the sample.

A.2.10 Evaluation of Results for REE

The precision and accuracy of the analytical procedure were tested by replicate analyses of 10 of the whole-rock and mineral separate samples and 3 of the U.S. Geological Survey standard rocks. The results of replicate analyses for the USGS standard rocks are given in Table A.2.3 together with the average of the coefficient of variations for all replicate analyses.

The data reported in this work were obtained over a period of two years and the analytical precision is significantly better for some analyses than others. In general, the analyses done in the first year have a poorer precision.

The precision for La, Ce, Sm, Eu, Tb, Yb and Lu is generally better than ±10% and for Nd, Gd and Ho better than ±25%. The statistical uncertainties in the calculation of the net peaks appear to be the controlling factor in the precision of the analysis.

The accuracy of analyses can be assessed by comparison with the reported values on the USGS standard rocks BCR-1, W-1 and G-2 (Table A.2.4-6). However, "the accuracy of REE analysis at the present time is not yet such that investigators from different laboratories get the same values for the same samples to within their stated uncertainties. Part of the reason may be sample inhomogeneity, but probably not" (Haskin et al., 1971, p.203). Thus for the comparison, only REE data from some of the laboratories in which extensive REE analyses have been done are given in Tables A.2.4-6. Comparison with these analyses for standard rocks show that the data determined in this work are within the range of reported values. In view of the uncertainties of the real abundances of rare-earths in the standard rocks, it is estimated that the accuracy of this method is expected to be within the limits of precision.

The sensitivity of the method fluctuates, but "because background activity depends on the variable matrix of the sample, it is impossible to define a sensitivity limit to cover all analyses" (Barker, 1972, p.21). The contents of REE in dunite (130) and that of heavy REE in some feldspars, however, appear to be close to the sensitivity limits.

Because of possible inhomogeneity of the standard rocks (c.f. Rey et al., 1970) and for an interlaboratory comparison of the results, the split of standard basalt (BCR-1) analyzed in triplicate at the University of Wisconsin (c.f. Denechaud et al., 1970; Haskin et al., 1970) was also radioanalyzed. The REE abundances obtained agree well both with their data and with the results of replicate analyses of the split of this standard rock provided by D.M. Shaw and are included in the average for BCR-1 in Table A.2.3-4.

Despite the fact that replicate analyses for whole-rocks from the pluton do not indicate significant sample inhomogeneities, it is difficult to evaluate the effect of heterogeneity in general, particularly whether samples are representative since felsic rocks from the pluton are coarse-grained and the bulk of REE is present in accessory minerals in these rocks.

In order to evaluate possible error in radiochemical separation, particularly in the chemical yield determination, an instrumental neutron activation technique similar to that described by Gordon et al. (1968) was used for determination of Eu in standard rocks (Table A.2.3). The results are comparable to those of radiochemical activation analysis.

To graphically illustrate the magnitude of analytical errors on the graphs for the chondrite-normalized REE distribution patterns, Figure A.2.1 shows the REE patterns for standard rocks BCR-1 and G-2 with error bars. The full length of the error bars indicates two "average" standard deviations. "Average" standard deviations were calculated from the averages of coefficients of variation given in Table A.2.3.

As noted above the REE distributions in the rocks and minerals were normalized to the average values for chondrites given by Frey et al. (1968). These values are (in ppm):

Table A.2.3 Precision of REE determinations (ppm)

	1	2	3	4	5	6	7
La	26.1	1.9	94	3.5	7.6		
Ce	53.8	3.1	173	9.2	6.2		
Nd	32.0	4.9	52	6.2	16.2		
Sm	7.23	0.38	7.3	0.	5.5		
Eu	2.04	0.083	1.57	0.05	4.6	1.94	1.48
Gd	7.2	1.5			20.1		
Tb	1.06	0.05	0.56	0.03	5.7		
Ho	1.4	0.23			18.6		
Yb	3.41	0.21	0.80	0.06	7.4		
Lu	0.517	0.033	0.14	0.01	7.1		

1. BCR-1 (average of 7 determinations, except Nd, Gd and Ho which are the average of 3 determinations
2. Standard deviation of BCR-1 determinations
3. G-2 (average of 2 determinations)
4. Standard deviation of the G-2 determinations
5. Average of coefficients of variation - $\bar{V}$ (Ragland et al., 1971) $\bar{V} = \frac{\Sigma V}{n}$, where n = number of all samples (unknowns and standard rocks[1]) analyzed in replicate, and V (coefficient of variation) = $\frac{100\ s}{\bar{x}}$ (s = one standard deviation; $\bar{x}$ = arithmetic mean of replicate analyses).
6. BCR-1 - instrumental neutron activation analysis for Eu
7. G-2 - instrumental neutron activation analysis for Eu

---

[1] For La, Ce, Sm, Eu, Tb, Yb and Lu, "unknowns" represent duplicate analyses of 10 whole-rock and mineral separate samples, while "standard rocks" include 7 replicate analyses of BCR-1 and duplicate analyses of G-2.

The value for Nd is based upon duplicate analyses of 5 unknowns, 3 analyses of BCR-1 and duplicate analyses of G-2, while the values for Gd and Ho are based upon duplicate analyses of 3 unknowns and 3 analyses of BCR-1.

Table A.2.4 Comparison of reported REE abundances (ppm) in standard rock BCR-1

	1	2	3	4	5	6	7
La		26.1	25.2	23.7	23.7	26.0	26.1
Ce	53.9	54.9	54.2	52.0	53.0	51.0	53.8
Nd	32.1	28.8	30.5	26.0	-	29.5	32.0
Sm	7.44	6.74	7.2	6.52	6.2	6.9	7.23
Eu	1.942	1.96	1.97	1.75	1.94	2.0	2.04
Gd	6.47	-	8.0	-	7.5	6.6	7.2
Tb	-	-	1.15	0.95	0.96	0.87	1.06
Ho	-	-	1.34	-	-	1.31	1.4
Yb	3.38	3.68	3.48	2.8	3.2	3.3	3.41
Lu	0.536	0.59	0.526	0.38	0.535	0.57	0.517

1. Philpotts and Schnetzler (1970b) IDMS
2. Gast et al. (1970) IDMS
3. Denechaud et al. (1970); Haskin et al. (1970) RNAA
4. Ragland et al. (1971) RNAA
5. Green et al. (1972) RNAA
6. Rey et al. (1970) RNAA
7. This work (average of 7 determinations, except Nd, Gd, and Ho which are the average of 3 determinations)

Method of analysis:

RNAA - radiochemical neutron activation

IDMS - isotope dilution mass spectroscopy

Table A.2.5 Comparison of reported REE abundances (ppm) in standard rock W-1

	1	2	3	4	5	6	7
La		10.9	11.6	10.2	13.9	11.7	11.1
Ce	23.4	23.6	23.5	22.1	24.0	24.0	24.9
Nd	15.1	13.0	11.0	12.0	21.0	15.0	16.5
Sm	3.76	3.35	3.62	3.40	3.78	3.8	3.52
Eu	1.112	1.082	1.18	0.99	1.04	1.09	1.09
Tb	-	-	0.617	0.58	0.60	0.75	0.62
Yb	2.08	2.21	1.71	2.14	1.90	2.10	1.90
Lu	0.31	0.318	0.322	0.26	0.35	0.33	0.314

1. Philpotts and Schnetzler (1970b) IDMS
2. Shih (1972) IDMS
3. Higuchi et al. (1970) RNAA
4. Ragland et al. (1971) RNAA
5. Tomura et al. (1968) RNAA
6. Haskin and Gehl (1963) RNAA
7. This work (single determination)

Method of analysis:

IDMS - isotope dilution mass spectroscopy

RNAA - radiochemical neutron activation

Table A.2.6 Comparison of reported REE abundances (ppm) in standard rock G-2

	1	2	3	4	5	6
La	85.0	100.0	93.0	91.0	78.0	94.0
Ce	168.5	177.0	170.0	180.0	110.0	173.0
Nd		51.0	50.0	47.0	67.0	52.0
Sm	7.4	7.2	7.2	7.3	7.0	7.3
Eu	1.29	1.51	1.52	1.55	1.3	1.57
Tb	0.40	0.44	0.30	0.50	0.5	0.56
Yb	0.56	0.76	0.72	0.68	0.90	0.80
Lu	0.10	0.11	0.12	0.13	0.13	0.14

1. Buma et al. (1971) INAA
2. Green et al. (1972) RNAA
3. Roy et al. (1970) RNAA
4. Higuchi et al. (1969) RNAA
5. Morrison et al. (1969) RNAA
6. This work (average of 2 determinations)

Method of analysis:

INAA - instrumental neutron activation

RNAA - radiochemical neutron activation

La	0.330	Gd	0.249
Ce	0.880	Tb	0.047
Pr	0.112	Ho	0.070
Nd	0.600	Tm	0.030
Sm	0.181	Yb	0.200
Eu	0.069	Lu	0.034

Figure A.2.1 REE distribution in standard rocks BCR-1 (top) and G-2 (below). Precision is shown by error bars.

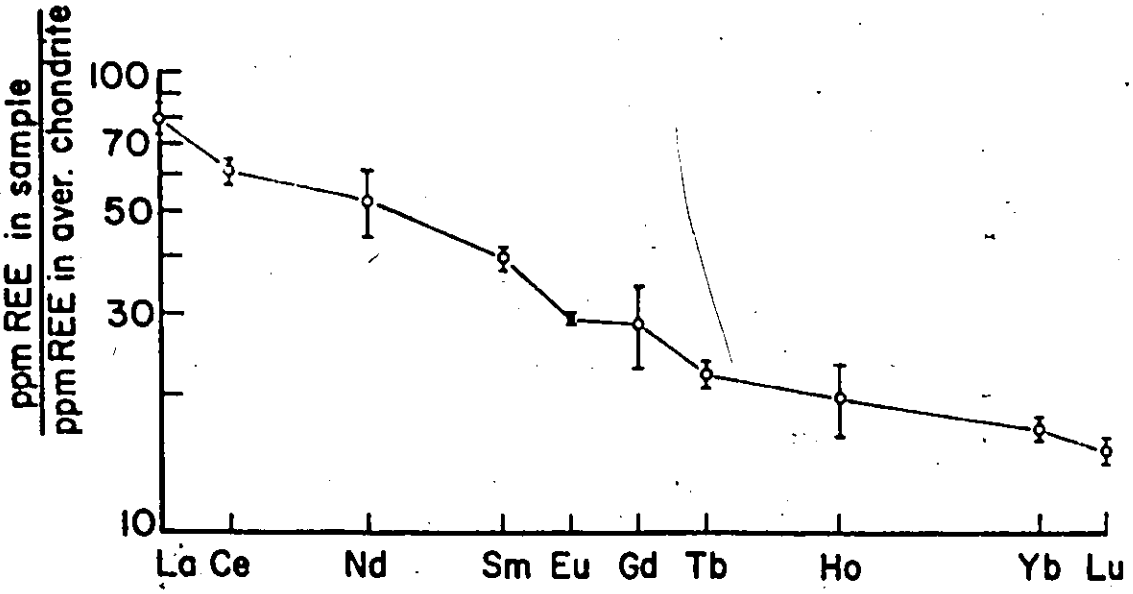
ppm REE in sample / ppm REE in aver. chondrite
100
70
50
30
10
La
Ce
Nd
Sm
Eu
Gd
Tb
Ho
Yb
Lu

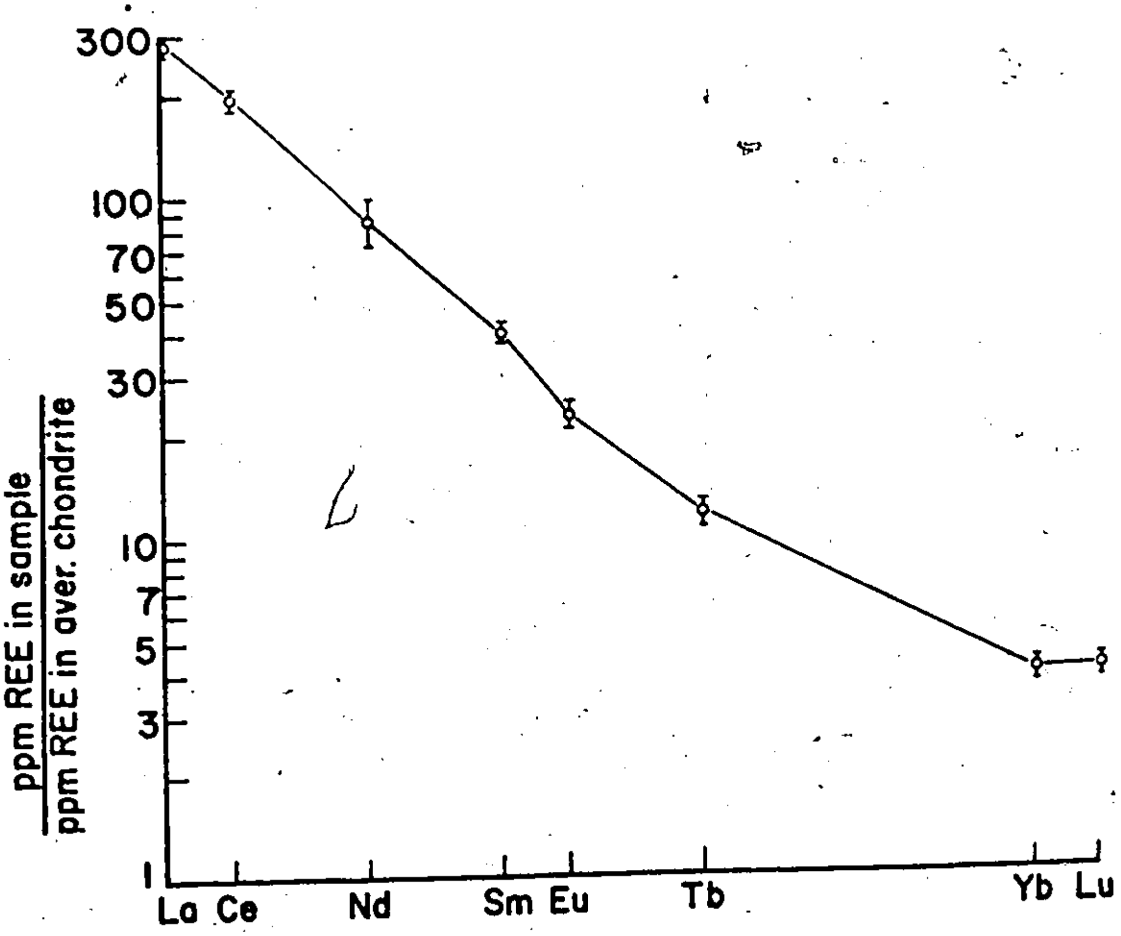
ppm REE in sample / ppm REE in aver. chondrite
300
100
70
50
30
10
7
5
3
1
La
Ce
Nd
Sm
Eu
Tb
Yb
Lu

A.2.11 The Chemical Treatment of Rock Samples

1. Prior to receiving the irradiated samples, 3 ml of the REE carrier solution and 2 ml of a solution containing ^{88}Y tracer are added by pipet to a clean 40 ml zirconium crucible. About 3 ml of 3 M NaOH are added to neutralize the carrier and tracer solutions. Identical amounts of carrier and ^{88}Y tracer are added to a 150 ml beaker, which will receive the standard monitor.

2. The solution in the crucible is evaporated to dryness under a heat lamp. It is then heated to about 150°C on a hot plate and allowed to cool about one hour before the beginning of the chemical processing.

3. The bottom of crucible is covered with about 4 g of sodium peroxide. The ampoule with the sample is cleaned with acetone.

4. The sample is carefully poured into a zirconium crucible and covered with another 5 g of sodium peroxide.

5. The contents of the crucible are melted over a Meeker burner until complete fusion is achieved, mixing as necessary with a nickel spatula.

6. The contents of the crucible are kept completely molten (cherry

red) for about 1 min more with occasional swirling. Longer fusion times shorten the life of the crucible and result in the dissolution of excessive amounts of zirconium, which must be separated from the REE.

7. After the crucible cools to nearly room temperature (on a cool hot plate or in a water bath), it is placed on its side in a 400 ml beaker.

8. About 80 ml H_2O is poured into the beaker with the crucible and its lid. The beaker is covered immediately with a watch glass to contain the vigorous reaction. The spatula is then placed in the beaker to remove any material adhering to it.

9. When the fusion cake is digested, 30-40 ml of conc. HCl is slowly added and the beaker is covered again with the watch glass, swirling gently to facilitate the acid attack.

10. The material adhering to the watch glass is rinsed into the beaker with a stream of conc. HCl.

11. The contents of the beaker are stirred until the precipitate from the fusion cake is dissolved (if necessary additional conc. HCl is slowly added with constant stirring).

12. The crucible and spatula are removed from the beaker and the adhering solution is rinsed into the beaker with a stream of distilled water (it may be necessary to heat and police the crucible with 6 M HCl in order to remove the last traces of the melt; also if any undissolved traces are still present the beaker is placed on the hot plate and heated to decompose them). The total volume of the solution should be around 150 ml.

13. About 10 g of solid NH_4Cl are dissolved in the solution and concentrated ammonia solution is added with continuous stirring to bring the solution to a pH of 9 or greater. This pH can usually be achieved by measuring the volume of the solution when permanent traces of the precipitate first appear and then adding an additional quantity of ammonia equal to 10% of this volume. (The volumes are approximated by using graduated beakers during the procedure).

14. The contents are allowed to age about 2 min and then the precipitate is removed by centrifuging in two centrifuge tubes and the supernate is discarded into the radioactive waste.

15. The beaker is rinsed with a stream of diluted ammonia solution. The washings and the precipitate are stirred together, centrifuged and the supernate discarded.

16. The precipitate is washed with about 50 ml of diluted ammonia solution, breaking up the precipitate with a stirring rod, and centrifuged again and the supernate discarded.

17. The precipitates are dissolved in conc. HCl (each sample is in two tubes - about 5-10 ml of HCl is added to each tube) and the solution is transferred to a 150 ml beaker. The tubes are rinsed with conc.HCl. The final volume of the solution should be about 30-35 ml. Then the volume is increased to 40 ml with H_2O (if the volume previously is about 40 ml, H_2O is not added).

18. The solution is then simmered for 5-10 min. on a hot plate (heated at a 2 o'clock position), cooled to about 60°C in a water bath, and an additional 3 ml (approx.) of conc. HCl are added. The silica is precipitated by adding, dropwise and with stirring, about 1.5 ml of a freshly prepared 1.5% gelatin solution for each 0.25 g of the original rock sample.

19. The contents of the beaker are then transferred to one centrifuge tube, centrifuged and the supernate is transferred to a 400 ml beaker. A 150 ml beaker is rinsed with about 20 ml of 8 M HCl and the rinse is poured into the centrifuge tube. The washings and the precipitate are stirred together with a glass rod, centrifuged, and the supernate transferred to a 400 ml beaker. The rinsing is repeated three times.

20. 16 M NaOH is added slowly with constant stirring into the 400 ml beaker until the pH is 10-11.

21. The contents of the beaker are transferred into two centrifuge tubes. The REE hydroxides are centrifuged out and the supernate, which contains mostly Al, is discarded.

22. The beaker is rinsed once with diluted NaOH, centrifuged and decanted. The precipitate is then washed twice with water.

23. The precipitate is dissolved with 6 M HCl (about 10 ml for each centrifuge tube) and transferred to a 50 ml polycarbonate tube. The glass tubes are rinsed with 6 M HCl and poured again into a polycarbonate tube.

24. The fluorides are precipitated by adding about 5 ml HF and 5 ml saturated ammonium fluoride solution.

25. The contents are centrifuged and the supernate discarded. The precipitate is washed with about 10 ml water, centrifuged again and the supernate is discarded.

26. The fluoride precipitate is dissolved in about 5-10 ml 2 M HCl solution which is saturated with boric acid. The contents of the tube are agitated and heated in a water bath to hasten

dissolution.

27. The hydroxides are precipitated with conc. ammonia solution, which is added in excess in order to bring the solution to a pH of 9 or more. (The volume of the solution is estimated when the first precipitate appears and then additional ammonia solution equal to 10% of this volume is added).

28. The contents are centrifuged, the supernate discarded and the precipitate washed with 10 ml water and centrifuged again. Then the supernate is once again discarded.

29. The precipitate is dissolved in about 15 ml of 6 M HCl. The fluorides are then precipitated with 1 ml HF and 3 ml saturated ammonium fluoride solution (to about pH 5), and centrifuged out. The supernate is discarded.

30. After washing with about 10 ml water, the precipitate is once again centrifuged out and the supernate is discarded.

31. Steps 26-30 are repeated.

32. Step 26 is repeated.

33. The solution is transferred to a glass centrifuge tube and the

polycarbonate tube is rinsed with water into the glass tube.

34. Steps 27 and 28 are repeated.

35. The last hydroxide precipitates are washed twice with water, centrifuged and decanted, then washed with methyl alcohol using a capillary pipet to break the precipitate. The precipitate is centrifuged and the supernate is decanted.

36. 2-3 ml of alcohol are added and the precipitate is broken by pipet and transferred to a vial.

37. The centrifuge tube is washed twice more with alcohol and the washing is added to the vial.

38. The vial is placed in the plastic centrifuge tube in the wool envelope and centrifuged for about 3 min.

39. The supernate is removed by capillary pipet and the precipitate is dried under a heat lamp using an air jet.

A.2.12 The Chemical Treatment of Some Minerals

1. Prior to receiving the irradiated samples, 3 ml of the REE carrier solution and 2 ml of a solution containing ^{88}Y tracer are added by pipet to a teflon crucible. Identical amounts of the carrier and ^{88}Y tracer are added to a 150 ml beaker which will receive the standard monitor.

2. The solution in the crucible is evaporated to about 0.5-1 ml under the heat lamp. The ampoule with the sample is cleaned with acetone.

3. The irradiated sample is transferred carefully to the teflon crucible.

4. The sides of the crucible are washed down with 2 M HCl and the contents of the crucible are swirled to obtain a slurry.

5. About 8 ml of an acid mixture containing three parts of HF and one part of $HClO_4$ are added.

6. The contents of the crucible are swirled and the crucible is then placed on a sand bath on the hot plate behind the lead shielding.

7. The contents of the crucible are heated strongly and evaporated

under a heat lamp to perchloric fumes with occasional stirring.

8. 2-3 ml HF and 1 ml $HClO_4$ are added to the crucible and evaporated to dryness. Most of the $HClO_4$ fumes are driven off, taking care not to convert the perchlorades to oxides (one hour).

9. The crucible is removed from the sand bath, cooled, the external sand is washed off and the outside of the crucible is dried.

10. The sample cake is transferred to a 250 ml glass beaker (containing a 0.5" teflon coated magnetic stirring bar) and the teflon crucible is washed a few times with 0.5 M HCl.

11. 2-3 ml conc.HCl are added to the crucible and covered.

12. The crucible is warmed for 2-3 min. on a sand bath to dissolve the remaining salts.

13. The solution is quantitatively transferred to its respective beaker using minimum amounts of H_2O.

14. The contents of the beaker are stirred, the volume is brought to about 30-40 ml with 2 M HCl, covered with a watch glass and heated to boiling on a hot plate to obtain a clear solution.

15. The contents of the beaker are then cooled on a water bath. The watch glass and the sides of the beaker are washed with H_2O.

16. Enough 16 M NaOH solution is added slowly with constant stirring into the 150 ml beaker, until the pH is 10-11.

17. The contents of the beaker are transferred to a 50 ml polycarbonate centrifuge tube before the precipitate has had a chance to settle. The beaker is washed with diluted NaOH.

18. The precipitate is centrifuged and the supernate is discarded. The precipitate is washed again with water, centrifuged out and the supernate is discarded.

19. The precipitate is dissolved in about 15 ml 6 M HCl. The fluorides are then precipitated with 1 ml HF and 3 ml saturated ammonium fluoride solution (about pH 5), and centrifuged out. The supernate is discarded.

20. After washing with about 10 ml water, the precipitate is once again centrifuged out and the supernate is discarded.

21. The fluoride precipitate is dissolved in about 5-10 ml 2 M HCl solution which is saturated with boric acid. The contents of the tube are agitated and heated in a water bath to hasten

dissolution.

22. The hydroxides are precipitated with concentrated ammonia solution, which is added in excess in order to bring the solution to a pH of 9 or more.

23. The contents are centrifuged, the supernate discarded and the precipitate washed with 10 ml water and centrifuged again. Then the supernate is once again discarded.

24. Steps 19-23 are repeated.

25. Steps 19-21 are repeated.

26. The solution is transferred to a glass centrifuge tube and a polycarbonate tube is rinsed with water into the glass tube.

27. Steps 22 and 23 are repeated.

28. The last hydroxide precipitates are washed twice with water, centrifuged and decanted, then washed with methyl alcohol using a capillary pipet to break the precipitate. The precipitate is centrifuged and the supernate is decanted.

29. 2-3 ml alcohol are added and the precipitate is broken by pipet

and transferred to a vial.

30. The centrifuge tube is washed twice more with alcohol and the washing is added to a vial.

31. The vial is placed in the plastic centrifuge tube in the wool envelope and centrifuged for about 3 min.

32. The supernate is removed by capillary pipet and the precipitate is dried under a heat lamp using an air jet.

A.2.13 The Treatment of Standards

1. The outside of the silica ampoule is carefully cleaned with acetone and then with 0.5 M HCl.

2. The ampoule is opened on a white loading plate and placed into a 150 ml beaker to which the carrier and tracer solutions have been added.

3. The beaker contents are warmed for about 15 min. on a hot plate with occasional washing of the inside of the ampoule with the carrier and tracer solutions.

4. Finally the ampoule is washed with 2 M HCl, monitored to ensure removal of all REE activity and then discarded.

5. About 20 ml of 2 M HCl are added and stirred to equilibrate the carrier and tracer solutions with the standard.

6. The contents of the beaker are filtered through paper in a funnel in order to remove the glass powder and rinsed several times with 2 M HCl into a glass centrifuge tube.

7. Enough conc. ammonia solution is added to precipitate REE hydroxides (adjust to pH 9 or greater), the precipitate is centrifuged out and the supernate is discarded.

8. The hydroxide precipitates are washed twice with water, centrifuged out and the supernate is discarded, then the precipitates are washed with methyl alcohol using a capillary pipet to break the precipitate. The precipitate is centrifuged and the supernate is decanted.

9. 2-3 ml alcohol are added and the precipitate is broken by pipet and transferred to a vial.

10. The centrifuge tube is washed twice more with alochol and the washing is added to the vial.

11. The vial is placed in the plastic centrifuge tube in the wool envelope and centrifuged for about 3 min.

12. The supernate is removed by capillary pipet and the precipitate is dried under a heat lamp using an air jet.

Legend for Map I

Map Unit		Rock Type
1	☐	biotite gneiss s.s.
2	☐	quartzitic biotite gneiss
3	☐	calcareous gneiss
4	☐	amphibolite
5	☐	marble
6 a	⁘	mafic (hornblende) hornfels
6 b	+ + +	mafic (pyroxene) hornfels
7	☐	diorite, syenodiorite
8	☐	monzonite
9	☐	quartz monzonite
10	☐	granodioritic gneiss
11	☐	pegmatite

	Symbol
- - -	slight migmatizatio
× × ×	medium migmatizat
v v	strong migmatizatic
╲	geological boundar
╲ ╲	geological boundar
⋱	geological boundar
╲·╲	fault
⤙10	strike and dip of
⏝	swamp

1 of

Legend for Map I

pe

eiss s.s.

biotite gneiss

gneiss

e

nblende), hornfels

oxene) hornfels

enodiorite

onzonite

tic gneiss

	Symbol
- - -	slight migmatization (amount of leucosome ~10-20%)
x x x	medium migmatization (amount of leucosome ~ 20-40%)
v v	strong migmatization (amount of leucosome ~40-66%)
╲	geological boundary, defined
╲ ╲	geological boundary, approximated
⋱	geological boundary, assumed
-·-·	fault
⅄10	strike and dip of foliation
⋏	swamp

[redacted]

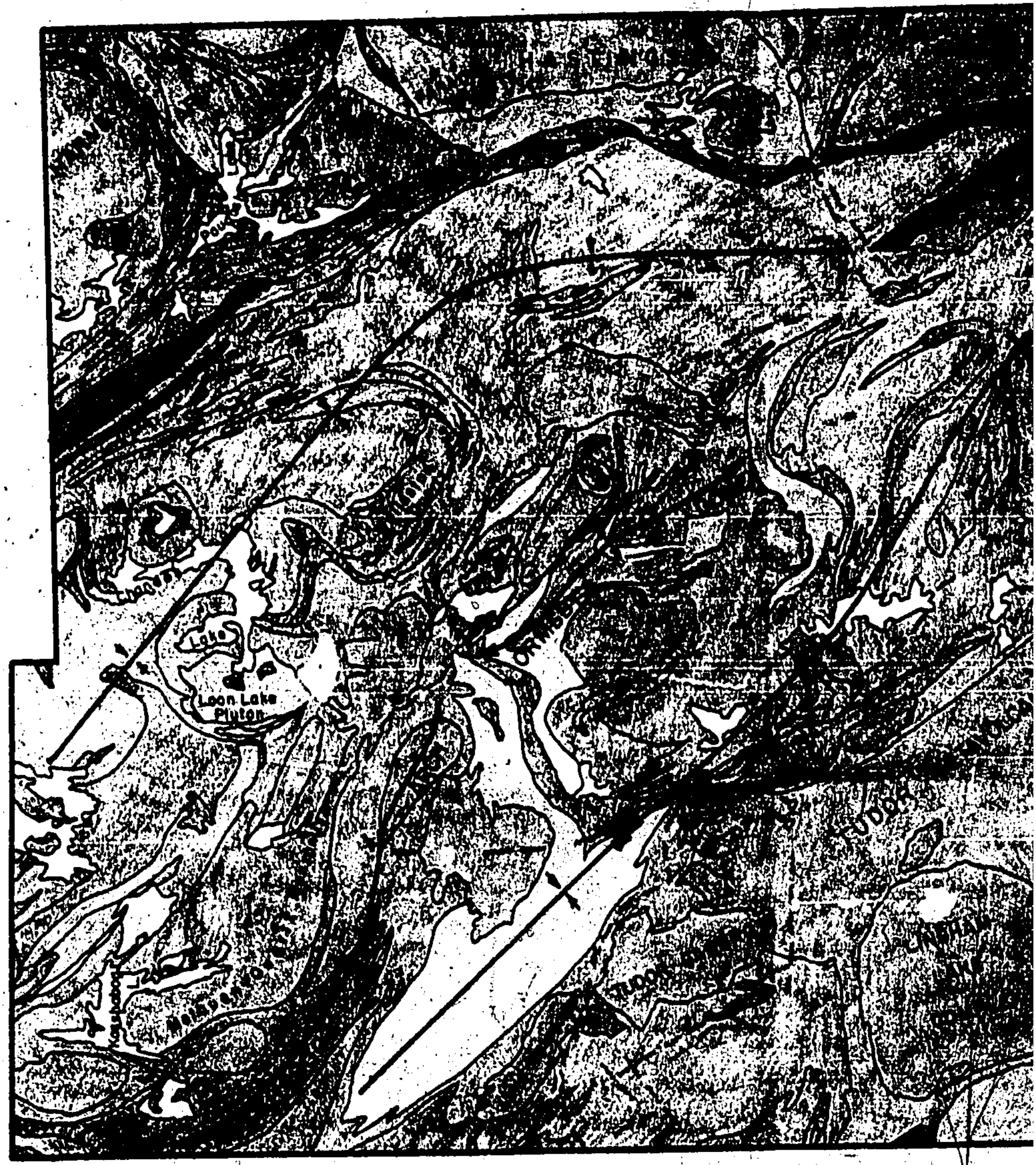
Lake
Loon Lake
Pluton

1 of

EXPLANATION

Paleozoic Rocks

TOWNSHIP INDEX MAP

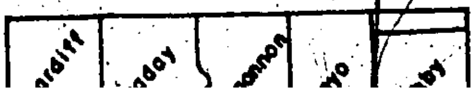
ardiff
aday
annon
yo
aby

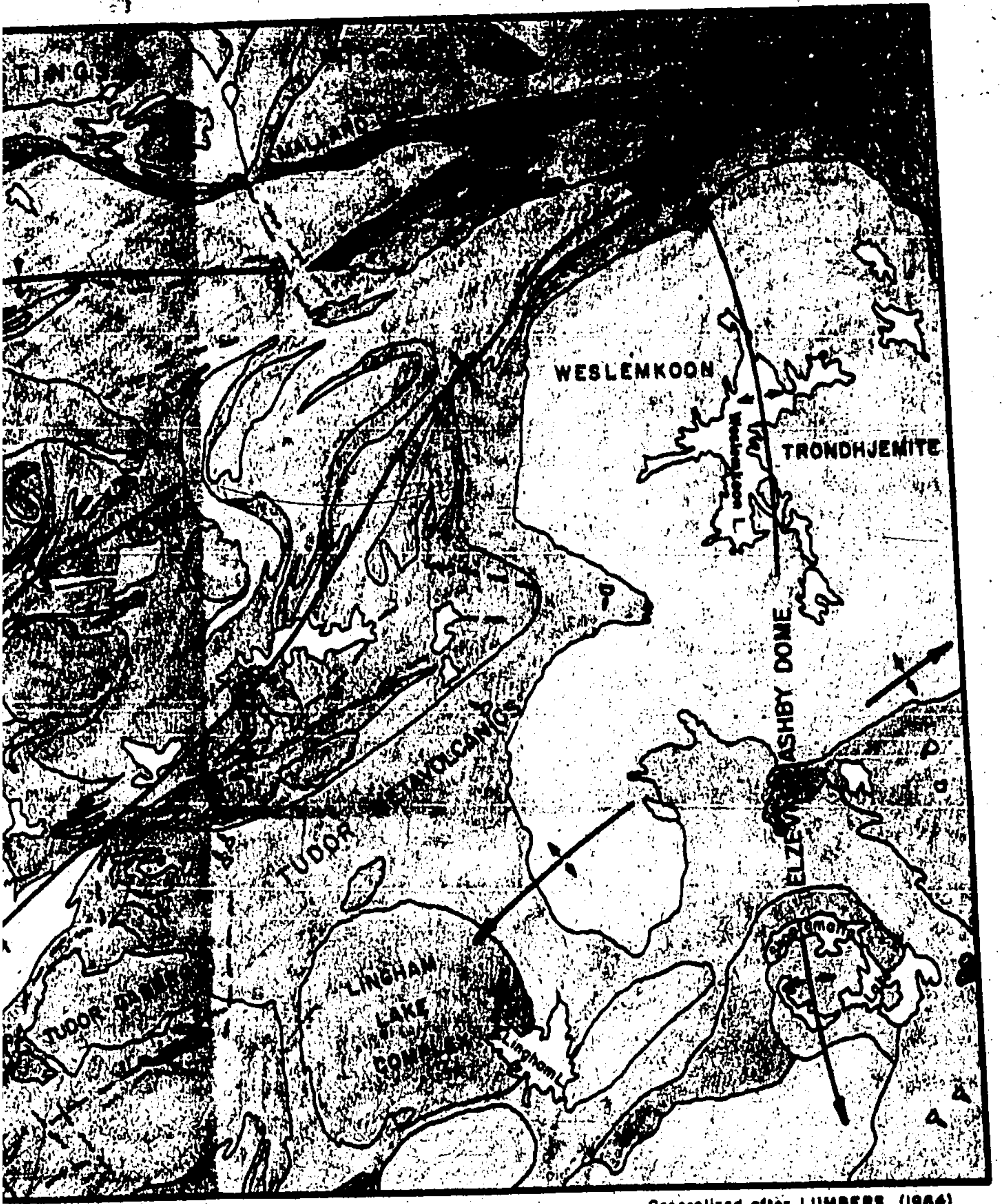
WESLEMKOON
Weslemkoon L.
TRONDHJEMITE
ASHBY DOME
ELZEVIR
TUDOR METAVOLCANICS
TUDOR DOME
LINGHAM LAKE COMPLEX
Lingham L.

Generalized after LUMBERS (1964)

[redacted]

TOWNSHIP INDEX MAP

Cardiff	raday	ngannon	Mayo	shby

SYMBOLS

ᐅ Top Direction in metavolcanics

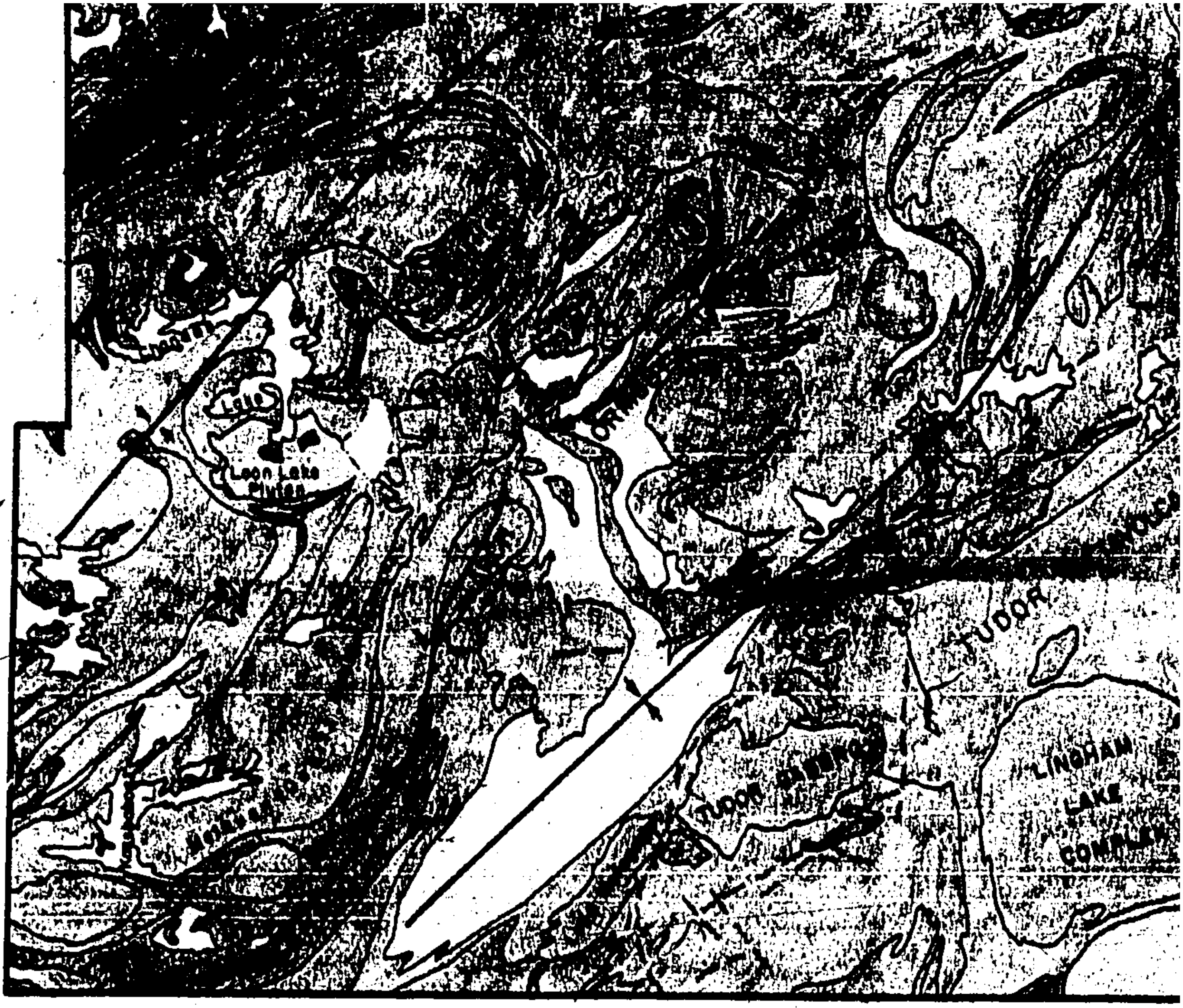
Loon Lake Pluton
TUDOR
TUDOR GABBRO
LINGHAM LAKE COMPLEX

EXPLANATION

Paleozoic Rocks

▨ Middle Ordovician Limestones

Plutonic Rocks

▨ Potassic Granite Group
▨ Syenitic Group
☐ Nepheline Syenite Group
▨ Basic Dikes and Sills
Diorite-Gabbro Group
▨ Sodic Granite Group

Supracrustal Rocks

Hermon Group

☐ Burnt Lake Formation
▨ Turriff Metavolcanics
▨ Vansickle Formation
■ Oak Lake Formation
▨ Tudor Metavolcanics

Mayo Group

▨ Apsley Formation
■ Lasswade Marble
Dungannon Formation

TOWNSHIP INDEX MAP

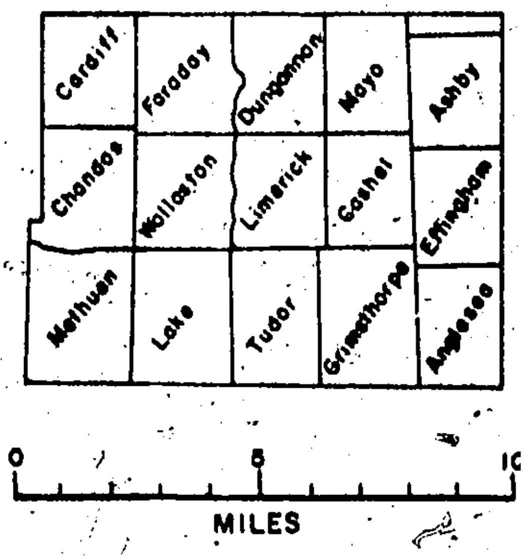
Cardiff
Faraday
Dungannon
Mayo
Ashby
Chandos
Wollaston
Limerick
Cashel
Effingham
Methuen
Lake
Tudor
Grimsthorpe
Anglesea
0
5
10
MILES

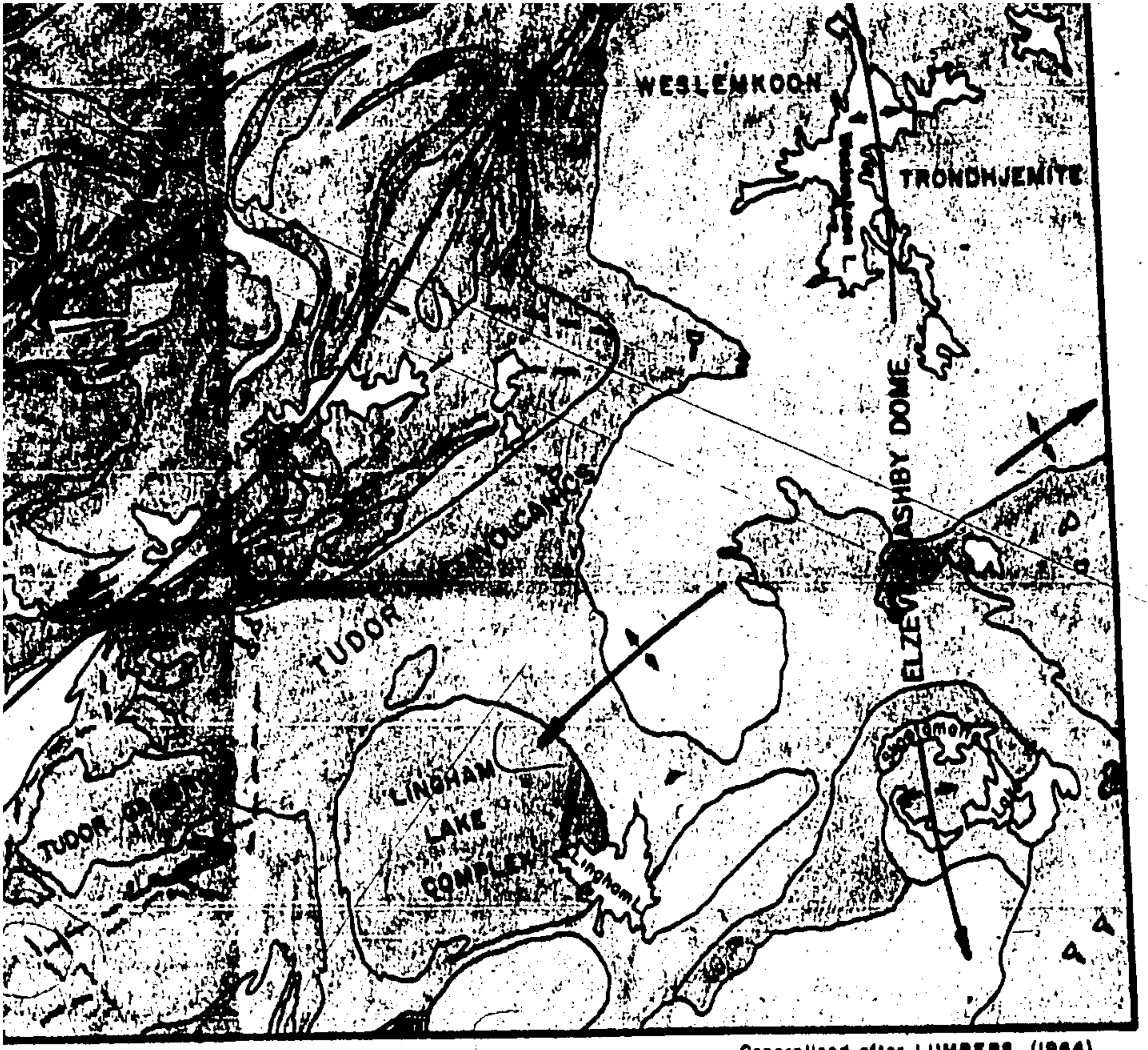
WESLEMKOON
TRONDHJEMITE
ASHBY DOME
ELZEVIR
TUDOR
VOLCANICS
TUDOR
LINGHAM
LAKE
COMPLEX
Lingham L.
P
A
A

Generalized after LUMBERS (1964)

TOWNSHIP INDEX MAP

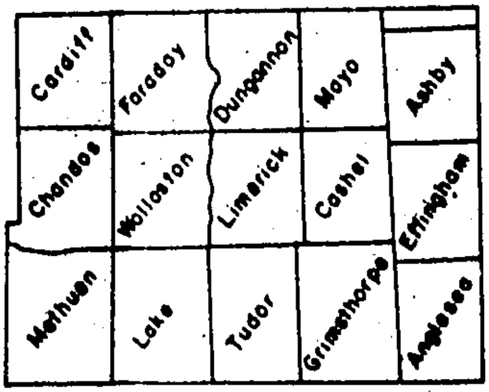
Cardiff
Faraday
Dungannon
Mayo
Ashby
Chandos
Wollaston
Limerick
Cashel
Effingham
Methuen
Lake
Tudor
Grimsthorpe
Anglesea

SYMBOLS

- Top Direction in metavolcanics
- Fault or lineament
- Geologic boundry defined
- Unmapped area or absence of exposure
- Anticlinal fold, plunge in direction of arrow
- Synclinal fold, plunge in direction of arrow

4 of 4

N
1 of

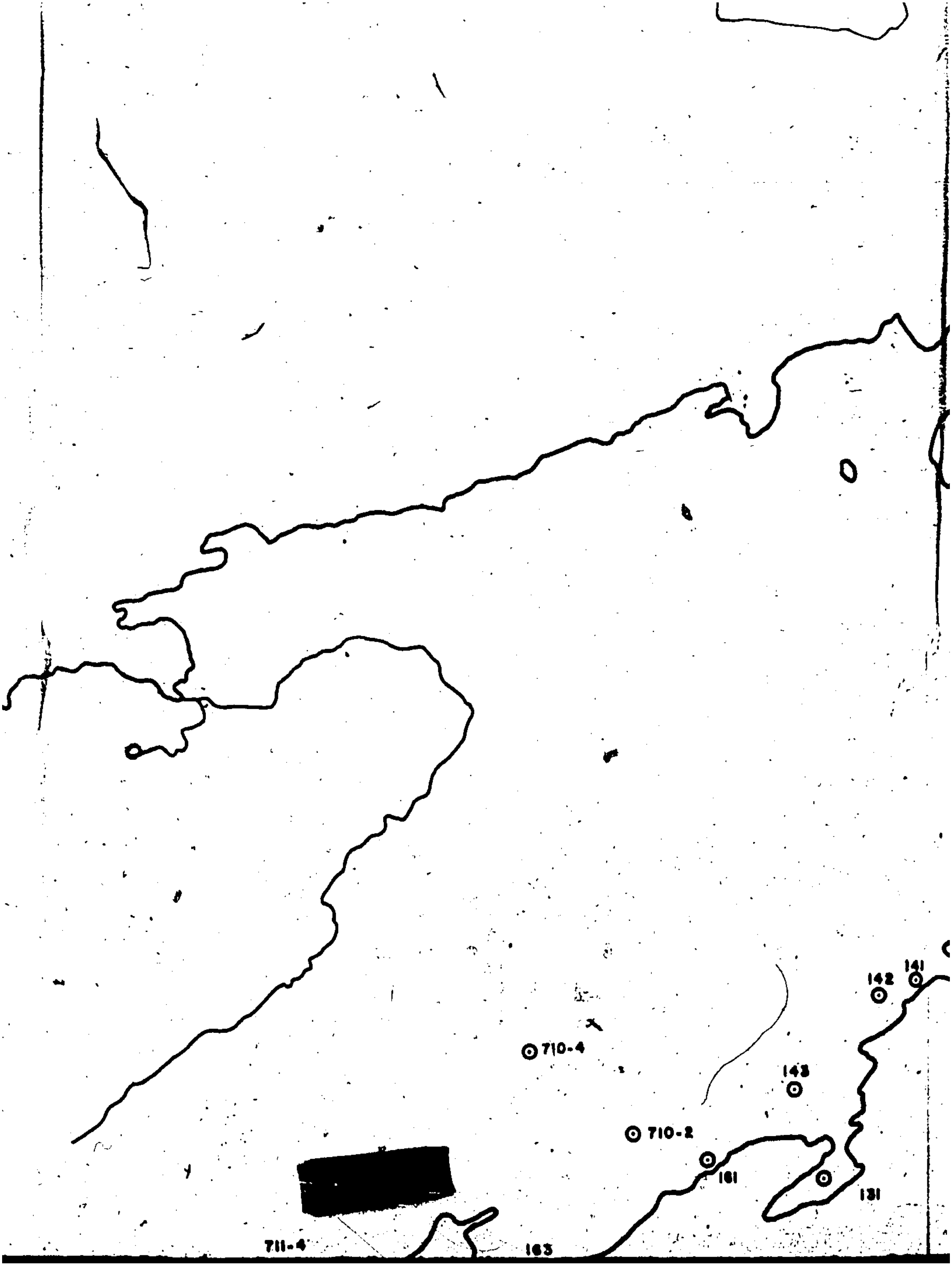
142
141
710-4
143
710-2
161
131
711-4
163

[redacted]

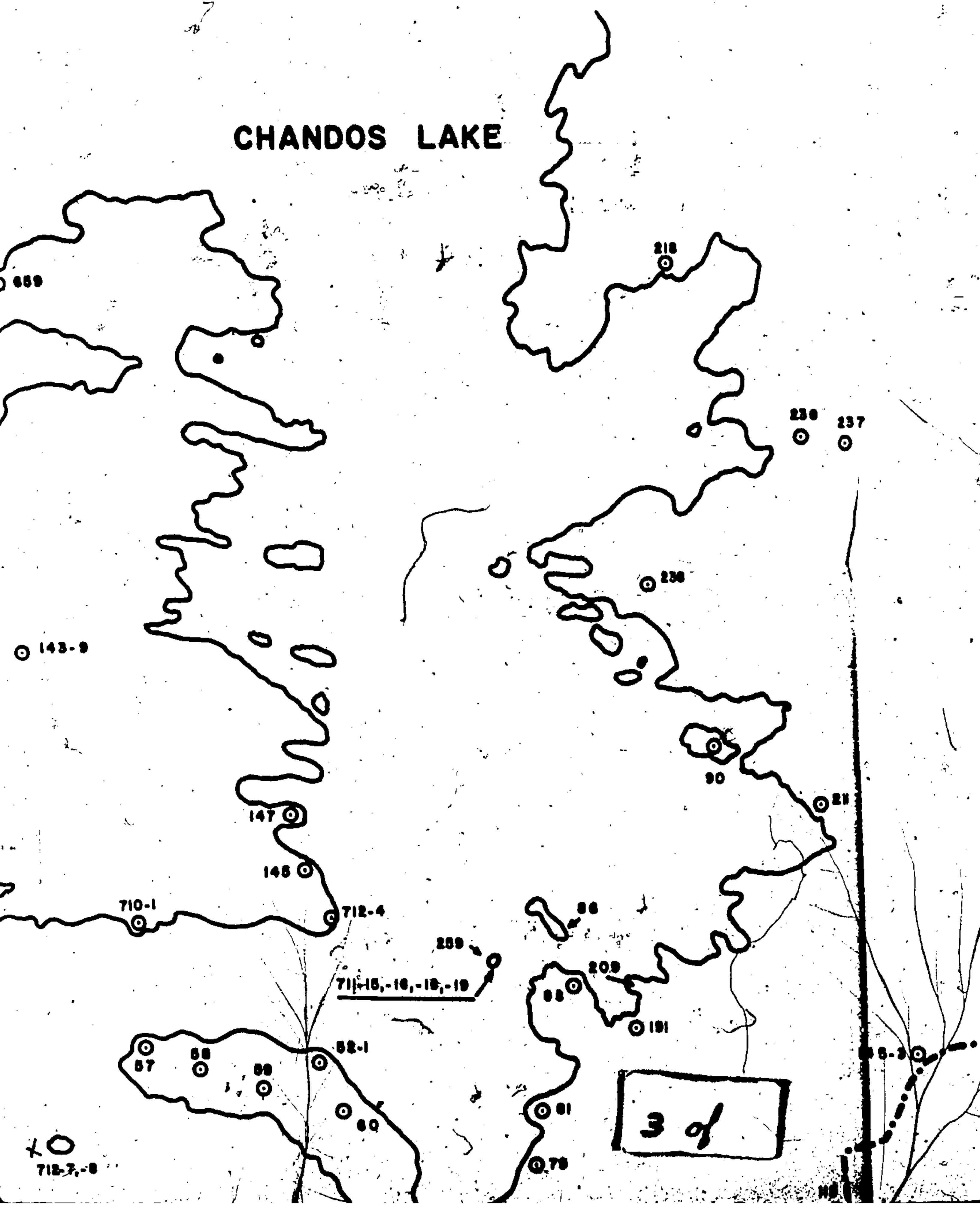
CHANDOS LAKE
659
218
238
237
236
143-9
90
21
147
148
710-1
712-4
86
259
711-15,-16,-18,-19
209
85
191
52-1
57
58
59
60
61
79
712-7,-8
HS-3
HS

3 of

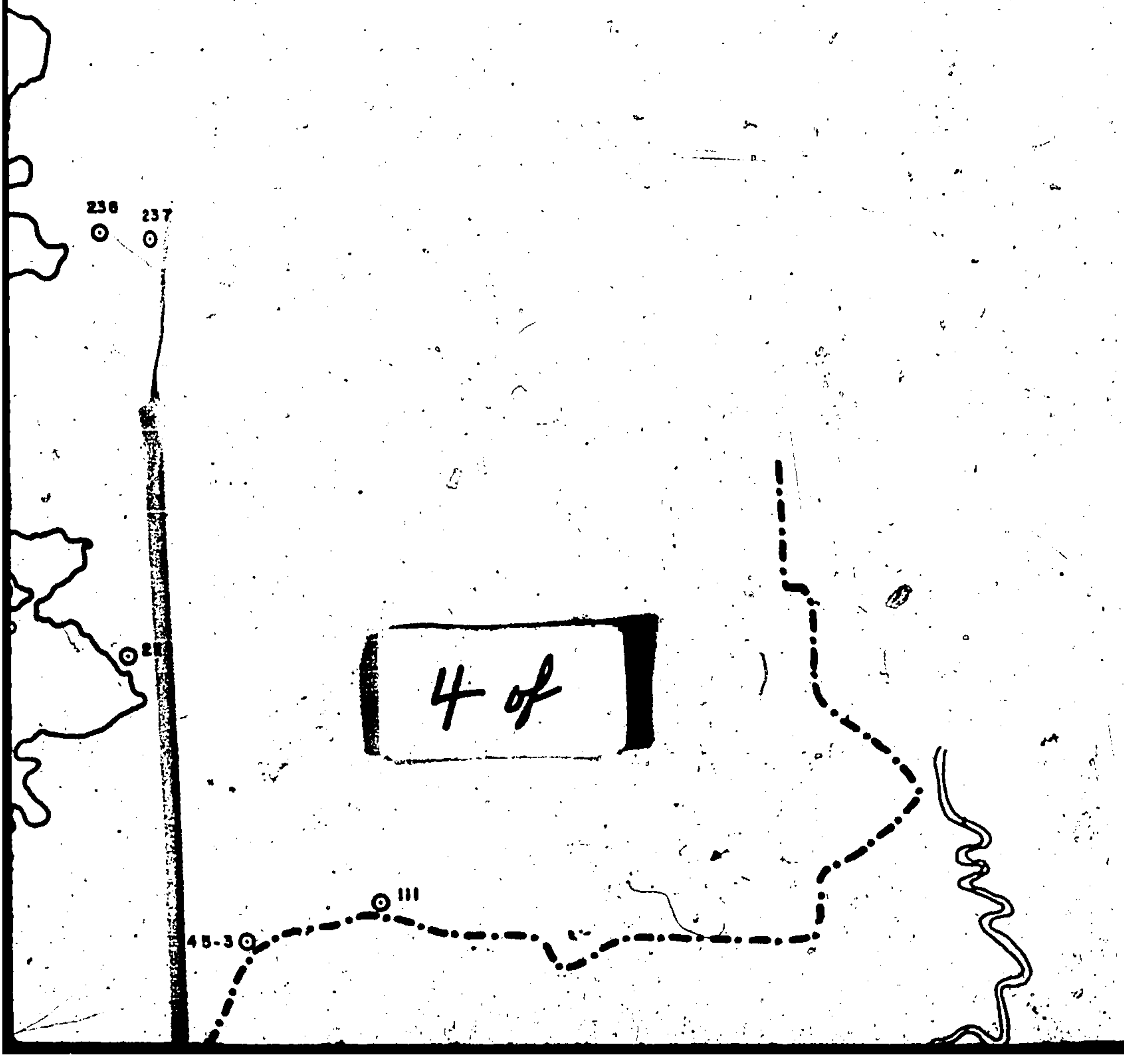
236
237
111
45-3

4 of

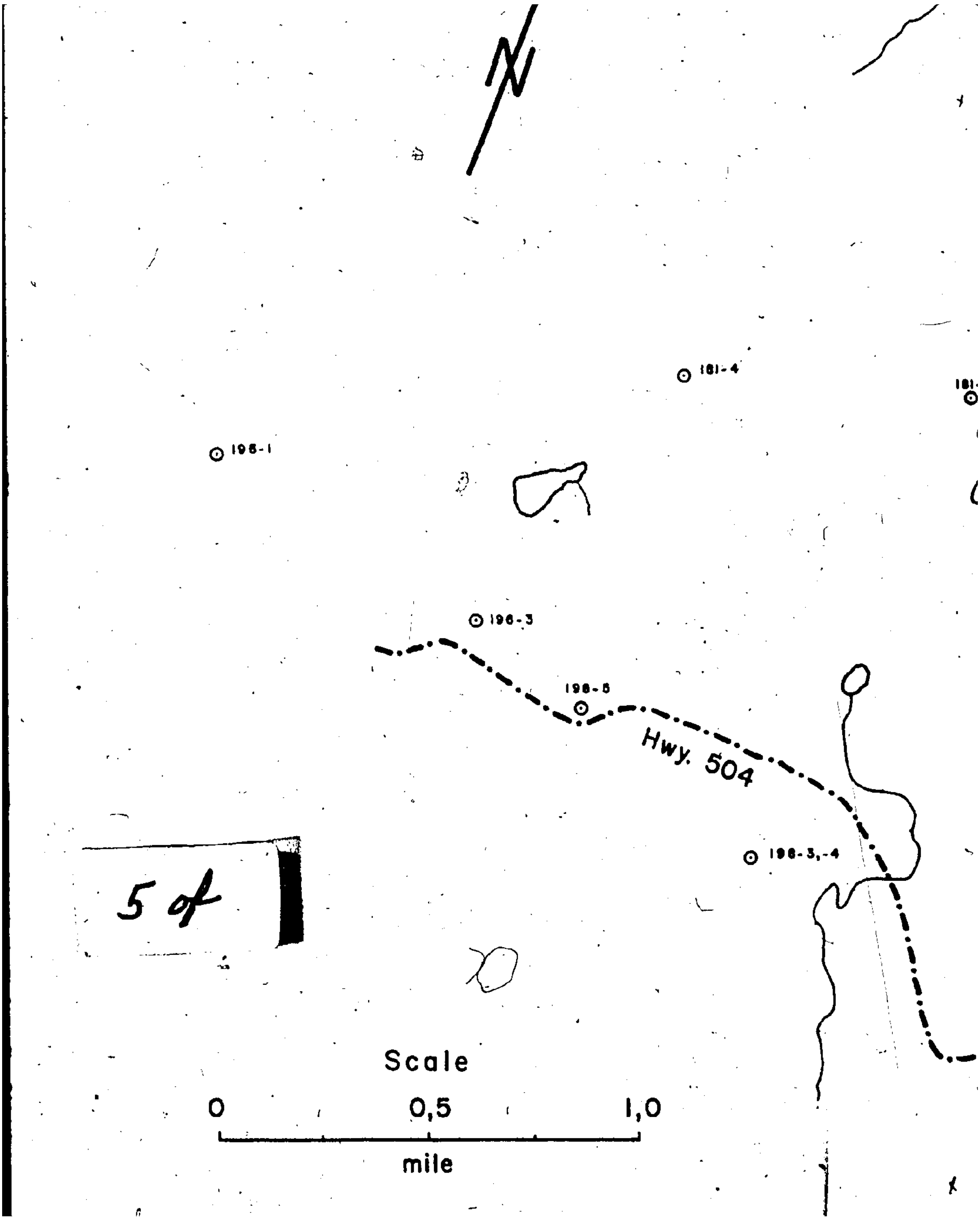
N
181-4
181-
196-1
196-3
196-5
Hwy. 504
196-3,-4
Scale
0
0,5
1,0
mile

5 of

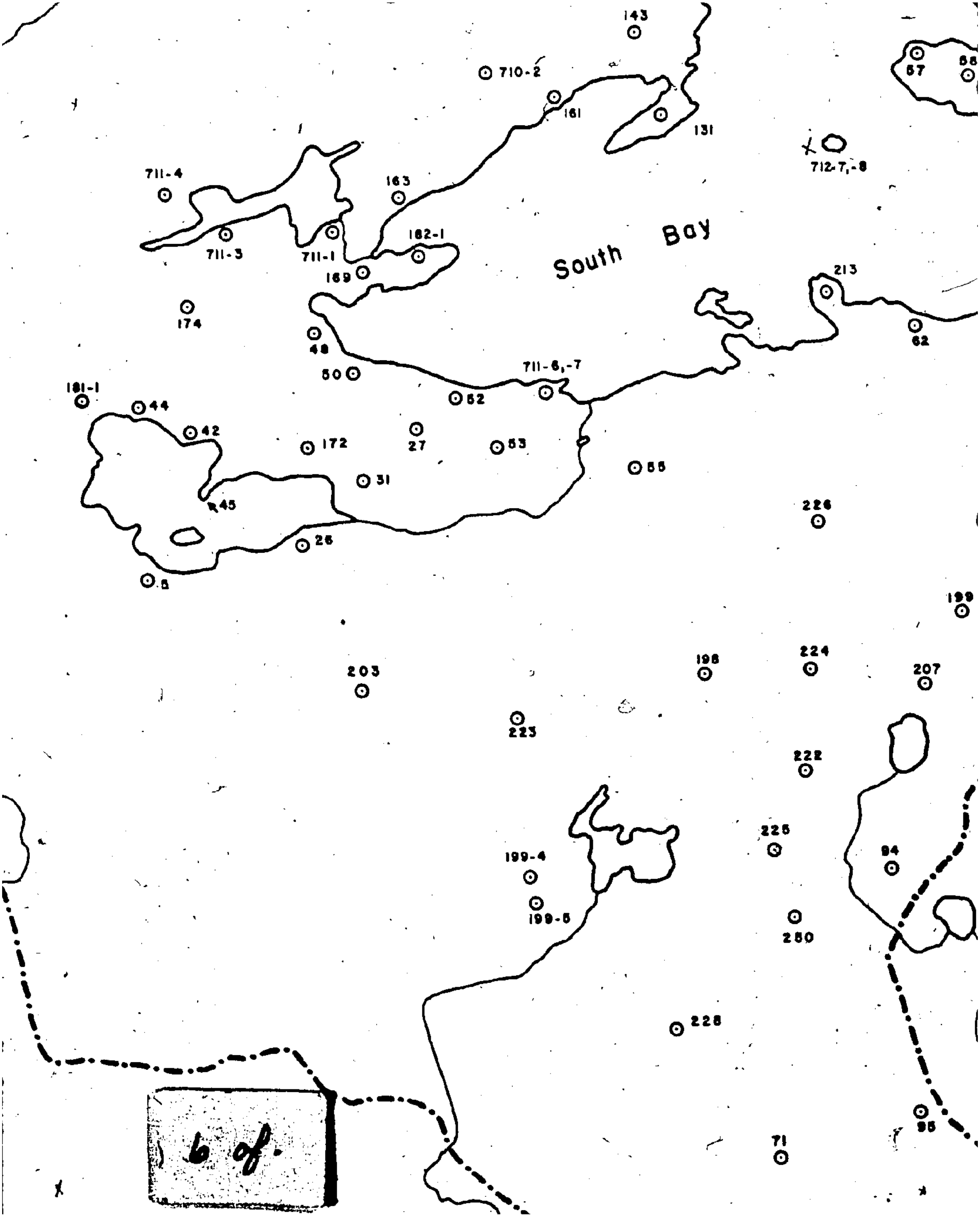
143
710-2
161
131
57
58
712-7,-8
711-4
163
711-3
711-1
162-1
South Bay
169
213
174
48
62
50
711-6,-7
181-1
44
52
42
172
27
53
55
31
45
226
26
5
199
198
224
207
203
223
222
225
199-4
94
199-5
250
228
96
71

6 of.

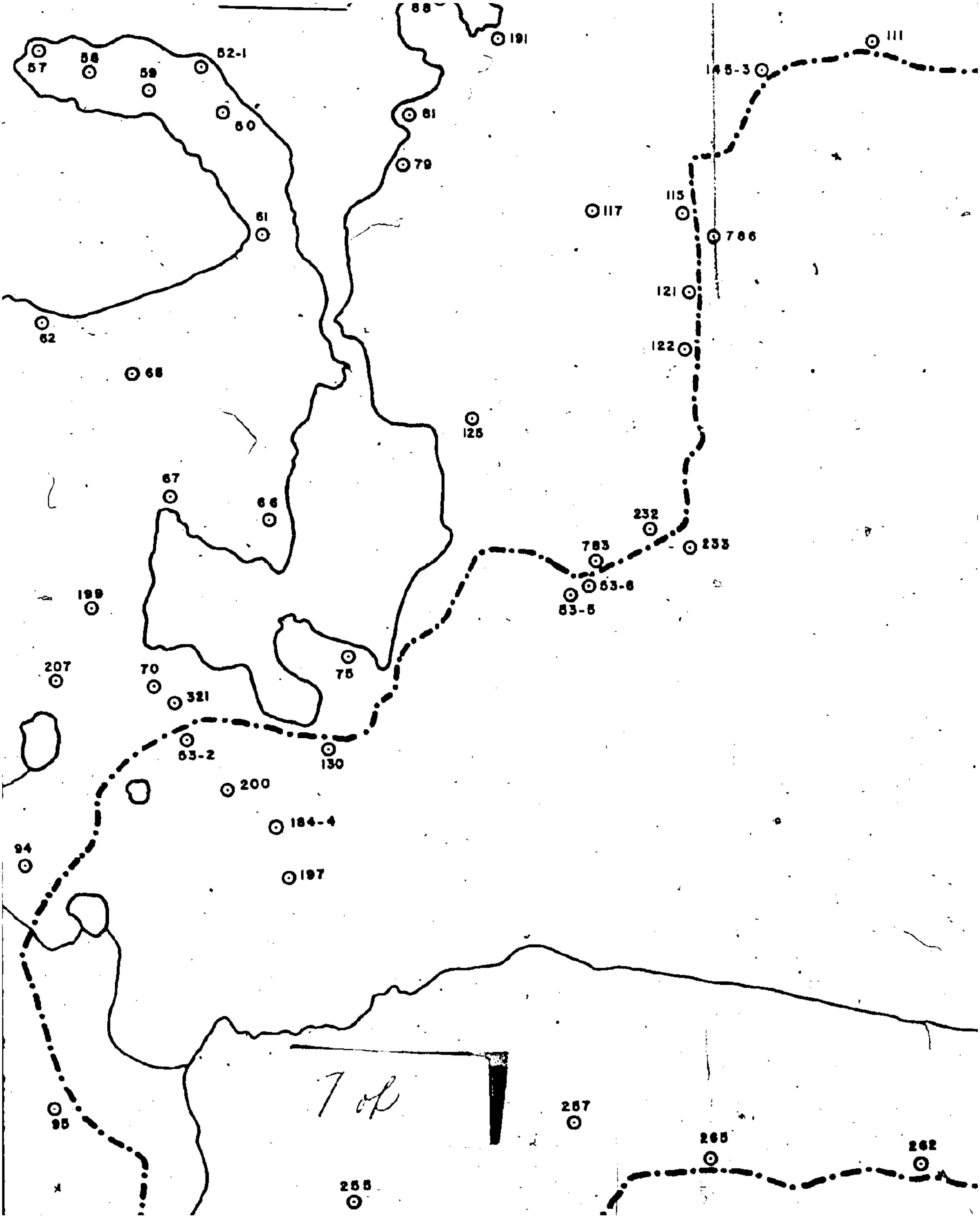
88
191
111
57
58
59
52-1
145-3
60
81
79
117
113
786
61
121
62
122
65
125
67
66
232
783
233
53-6
53-5
199
207
70
75
321
53-2
130
200
184-4
94
197
95
257
265
262
255

7 of

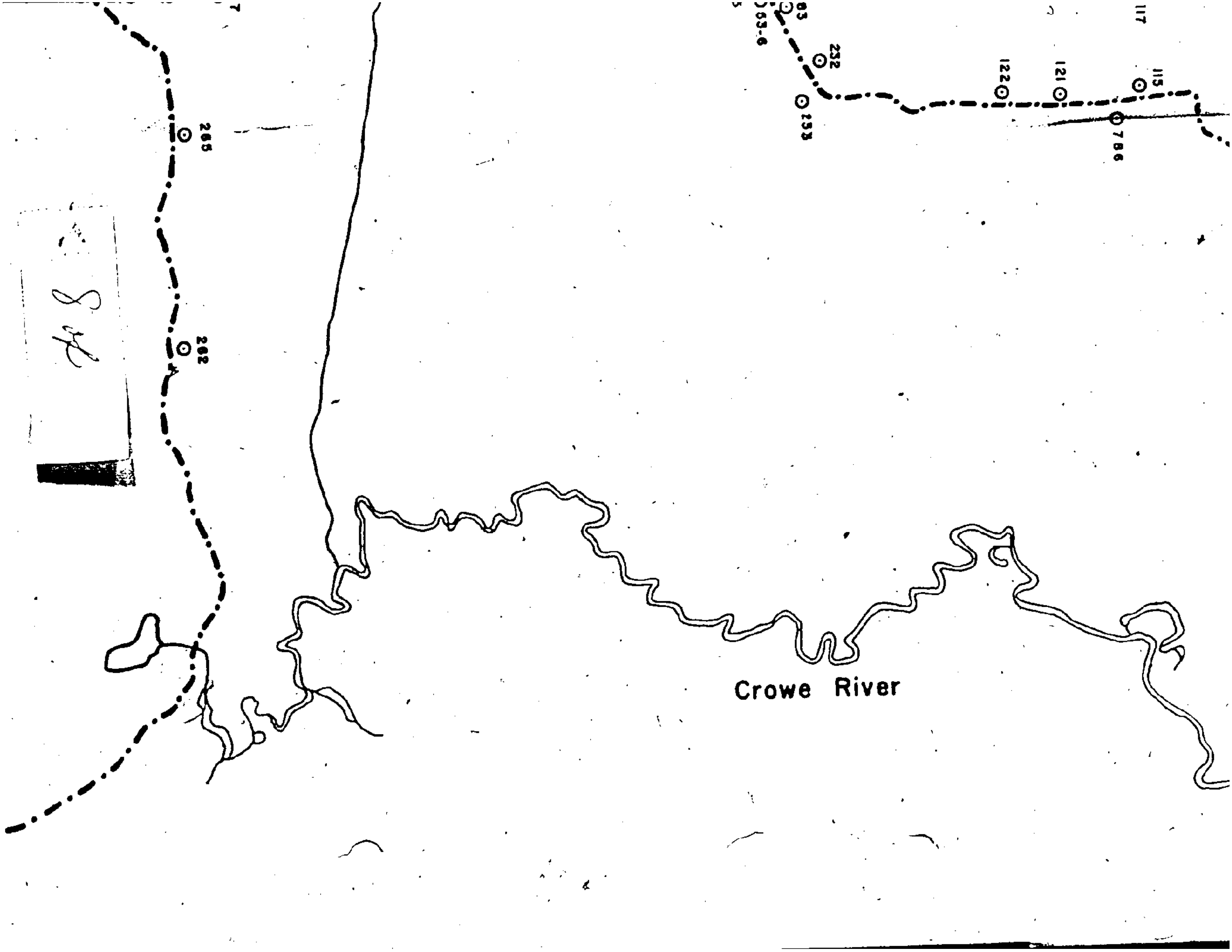
117
115
786
121
122
232
83
233
63-6
Crowe River
7
265
262

8 of

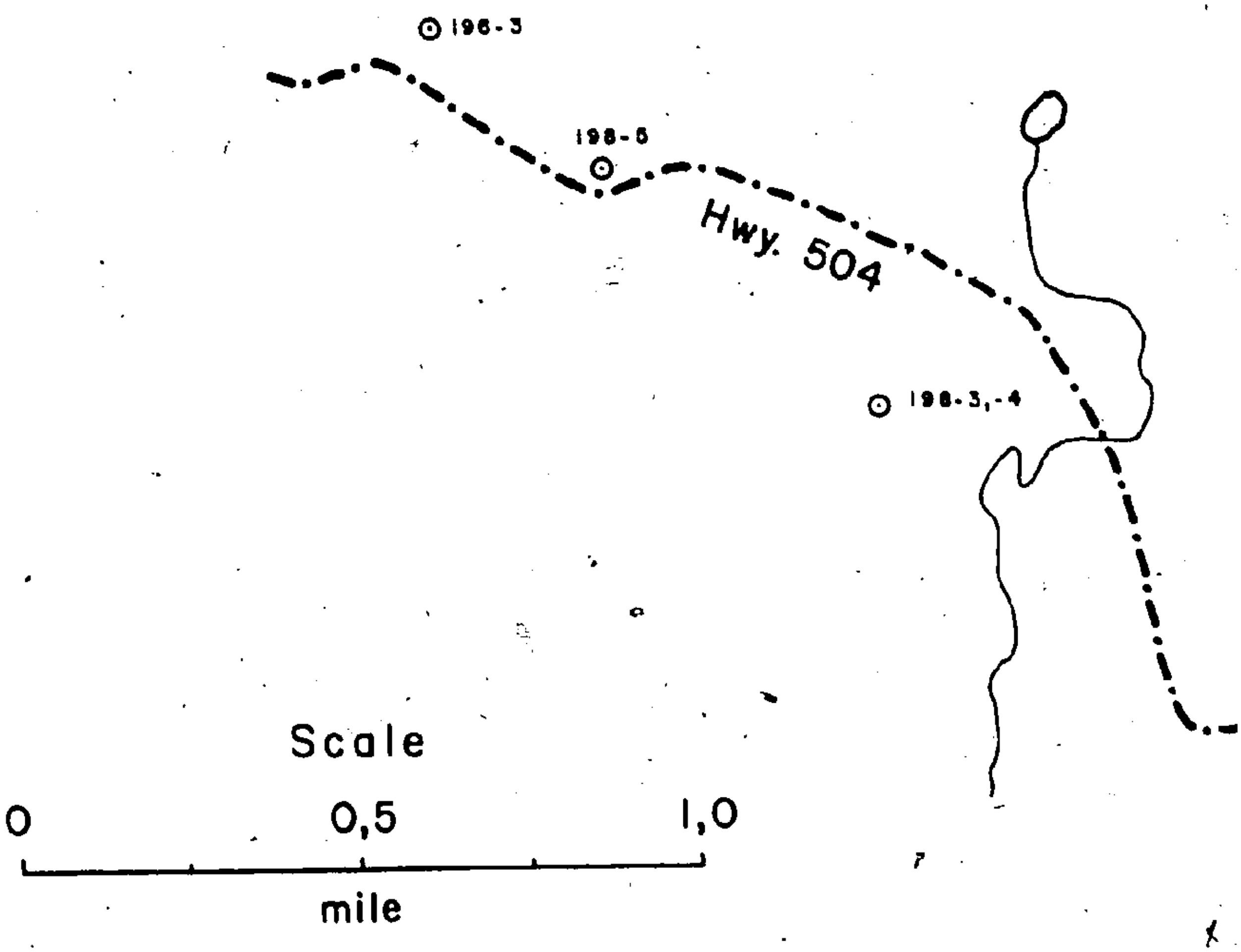
196-3
198-5
Hwy. 504
198-3,-4
Scale
0
0,5
1,0
mile

9 of

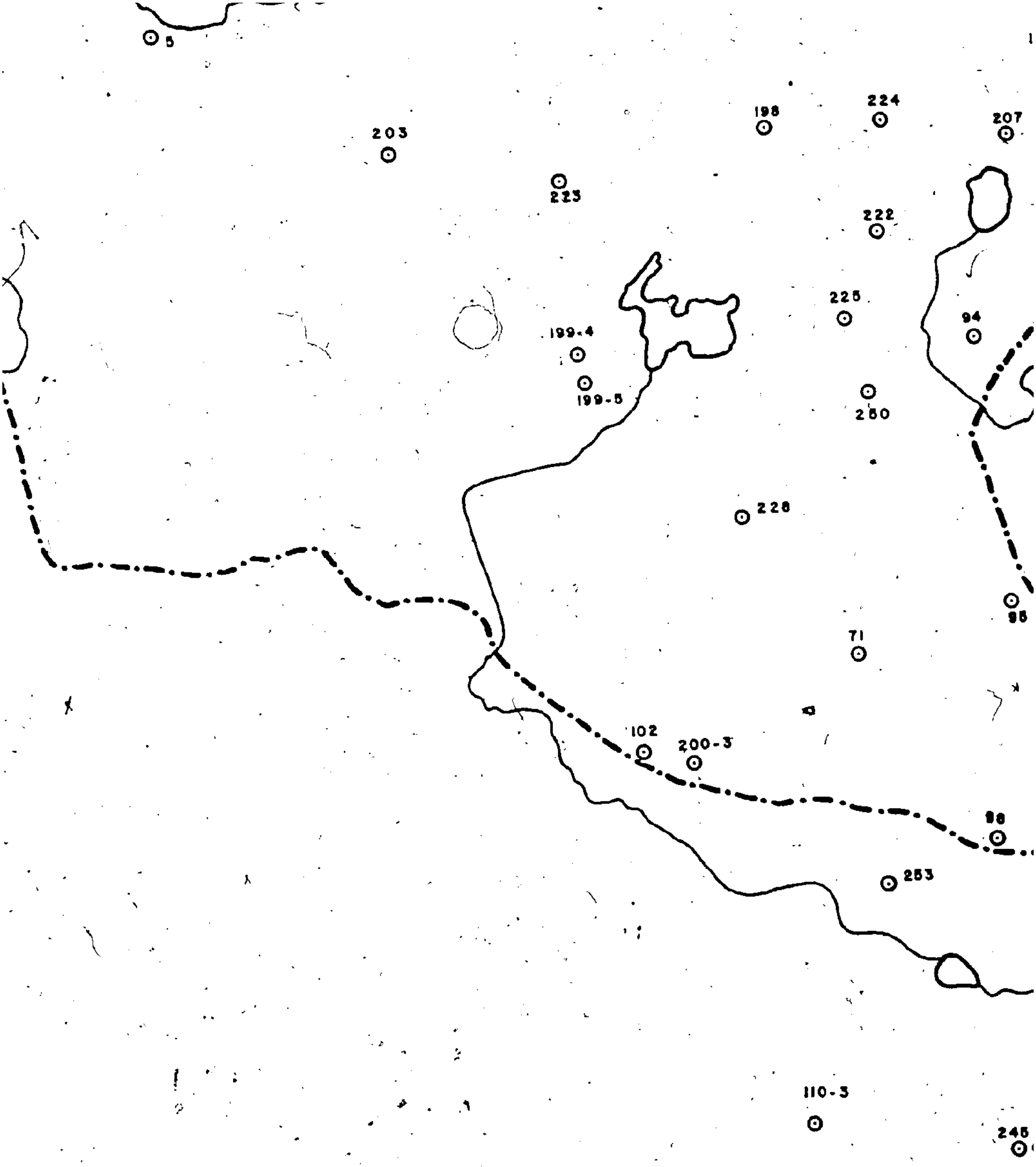
5
203
223
198
224
207
222
225
94
199-4
199-5
250
228
95
71
102
200-3
98
253
110-3
245

10 of

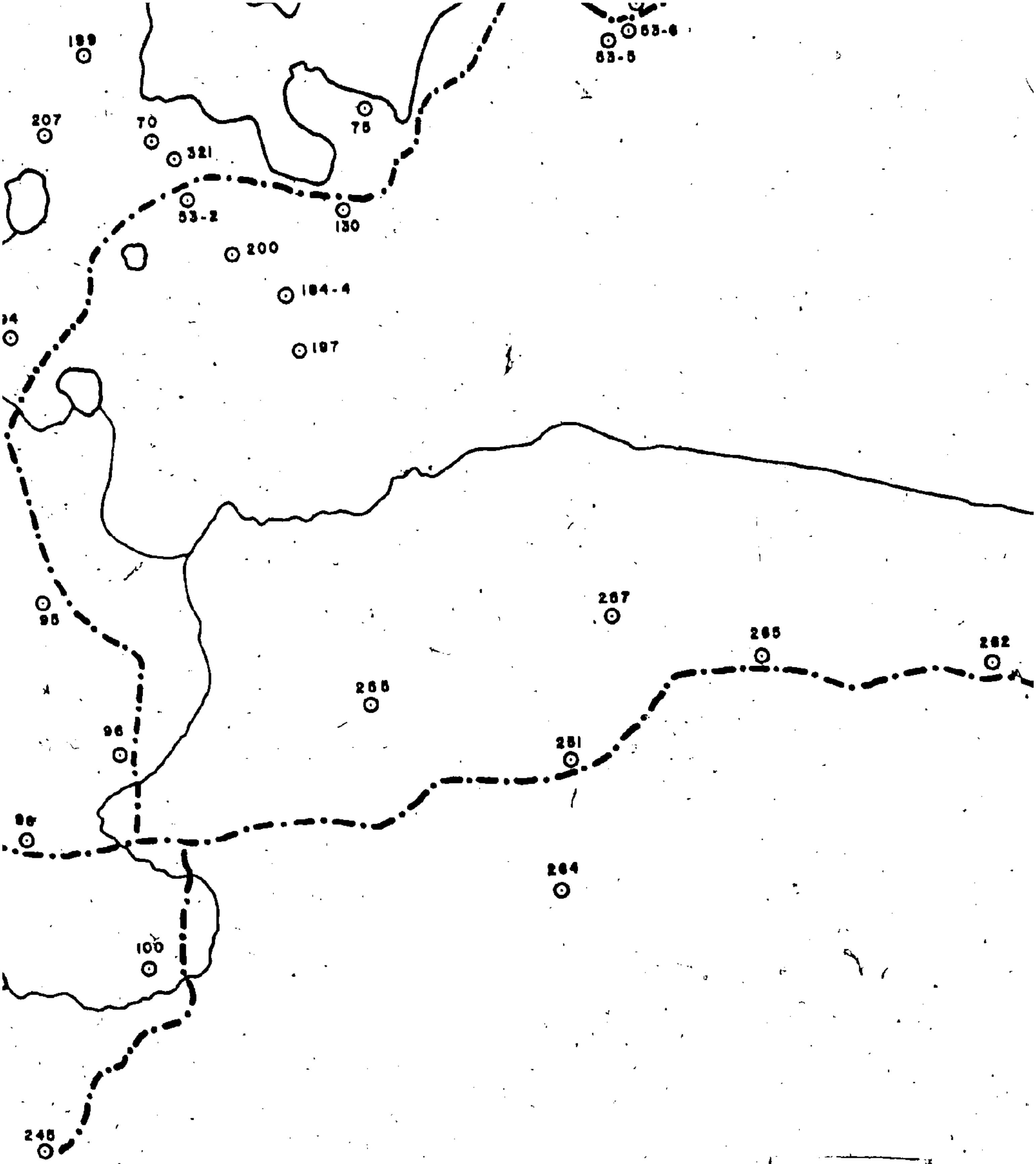
199
207
70
321
75
53-6
53-5
53-2
130
200
184-4
197
267
265
262
95
266
96
251
99
264
100
245

11 of

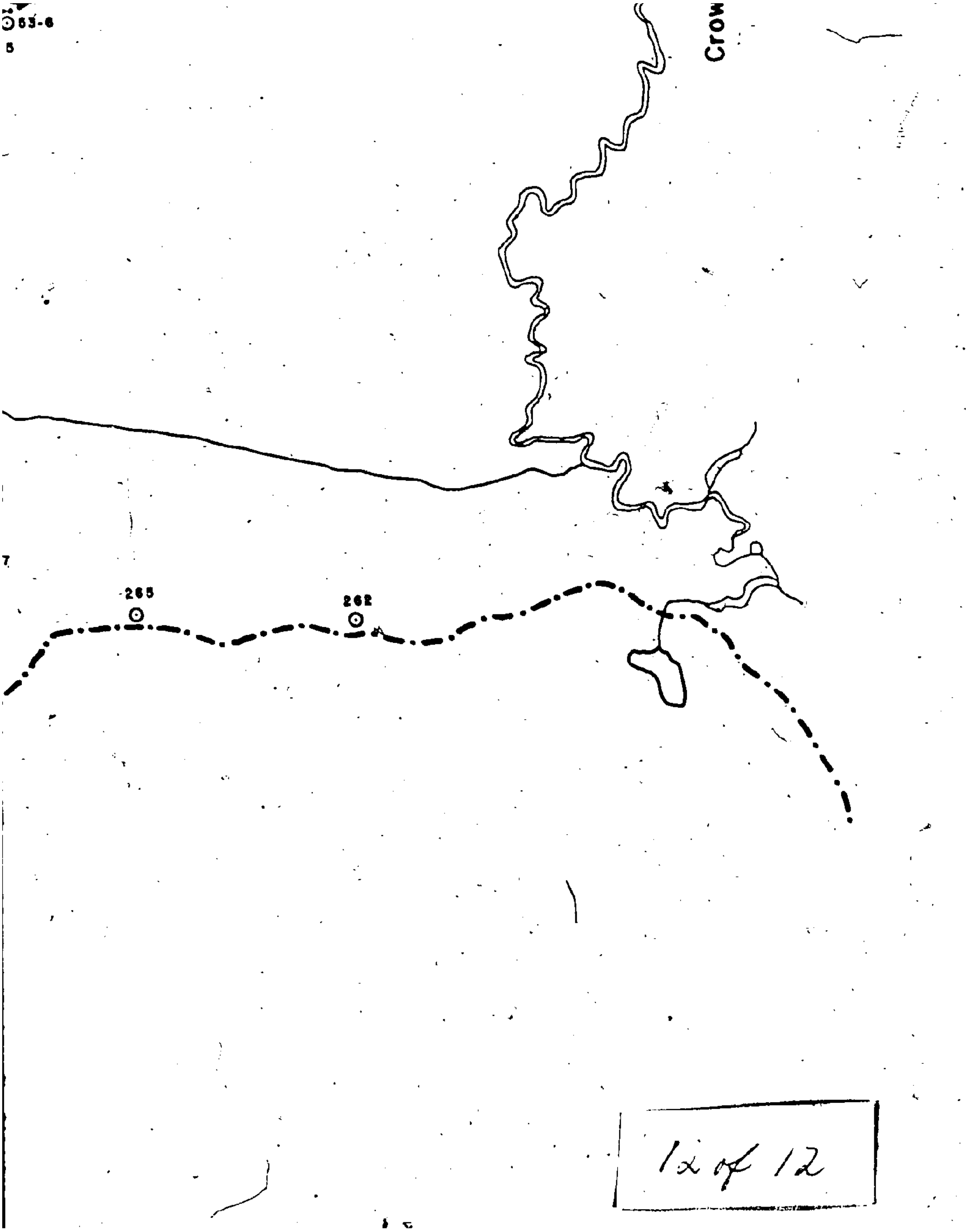
53-6
5
Crow
7
265
262

1x of 12

1 of

CHANDOS (LOON

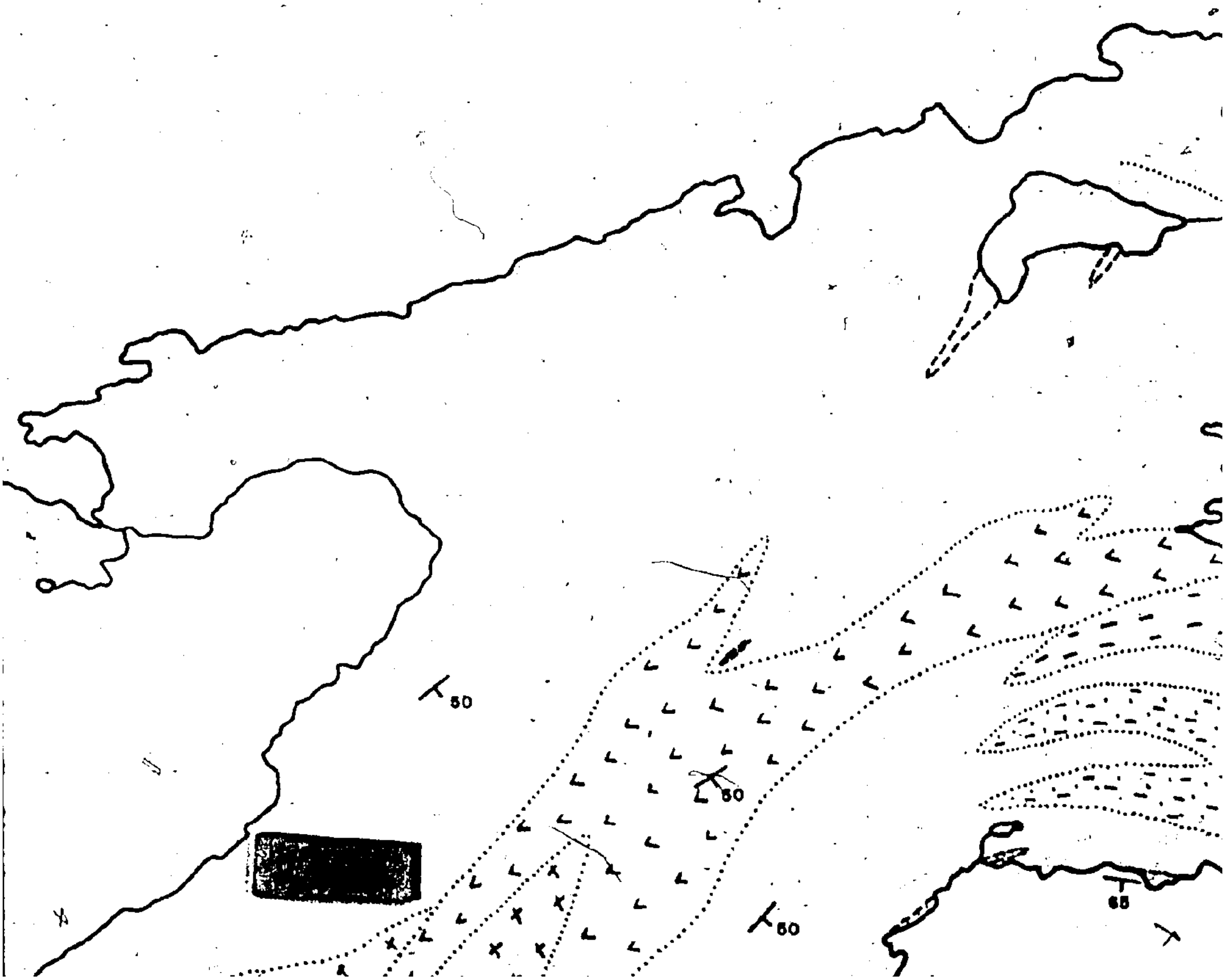

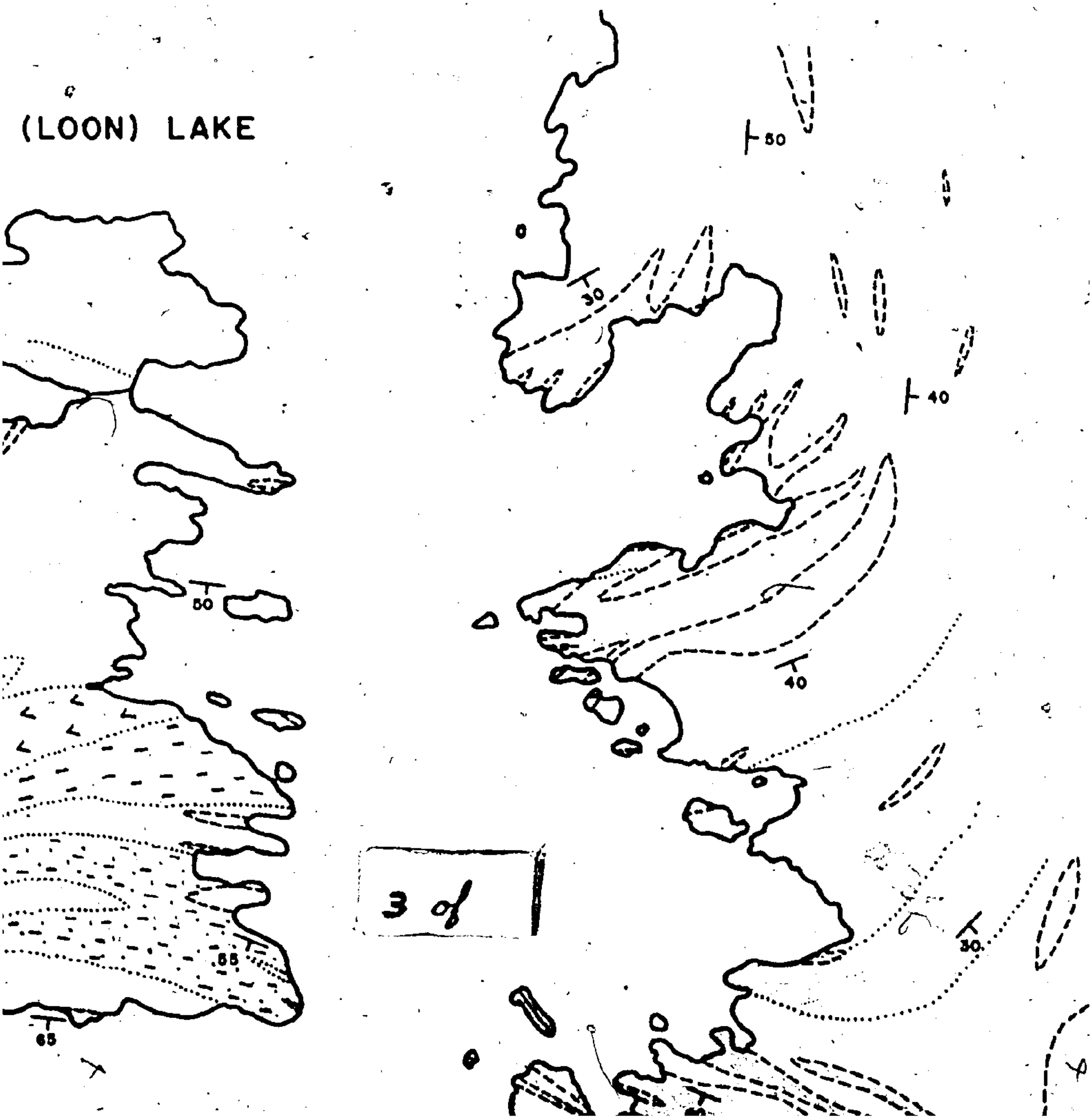
(LOON) LAKE
50
30
40
50
40
55
30
65

3 of

30
40
25
Hwy. 504

4 of

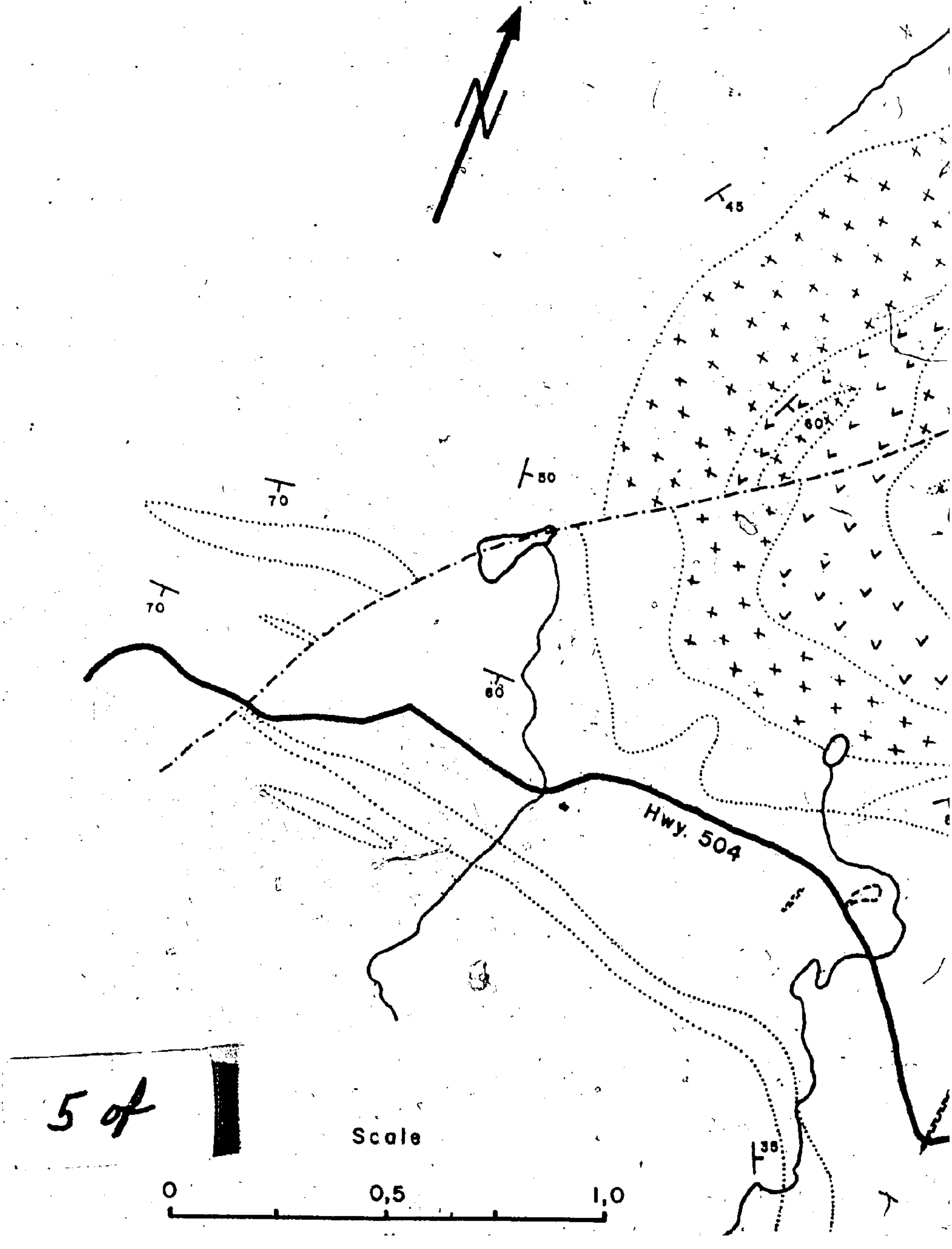
N
45
60
50
70
70
60
Hwy. 504
35
5 of
Scale
0
0,5
1,0

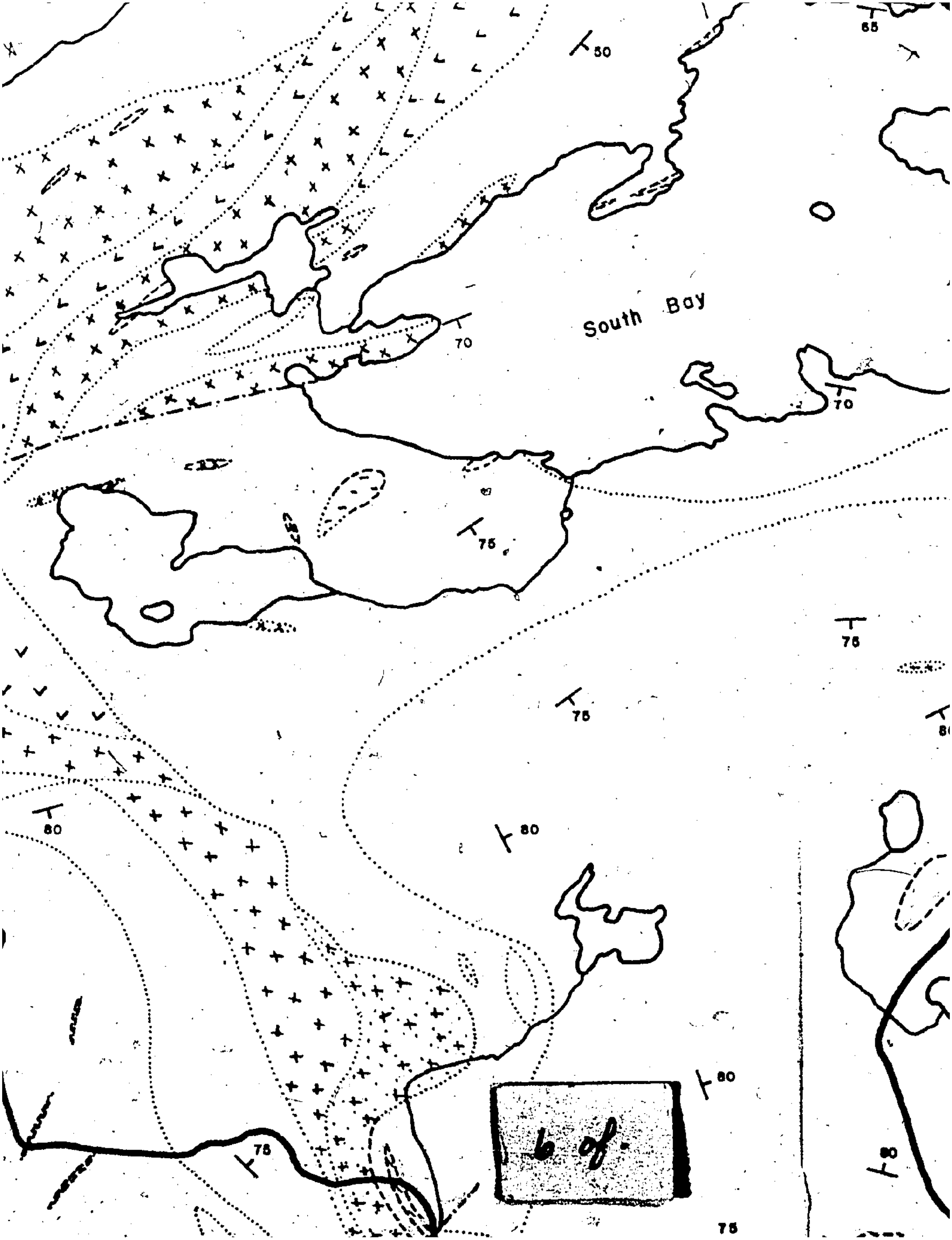
South Bay
50
65
70
70
70
75
75
75
80
80
80
80
75
80
75
6 of

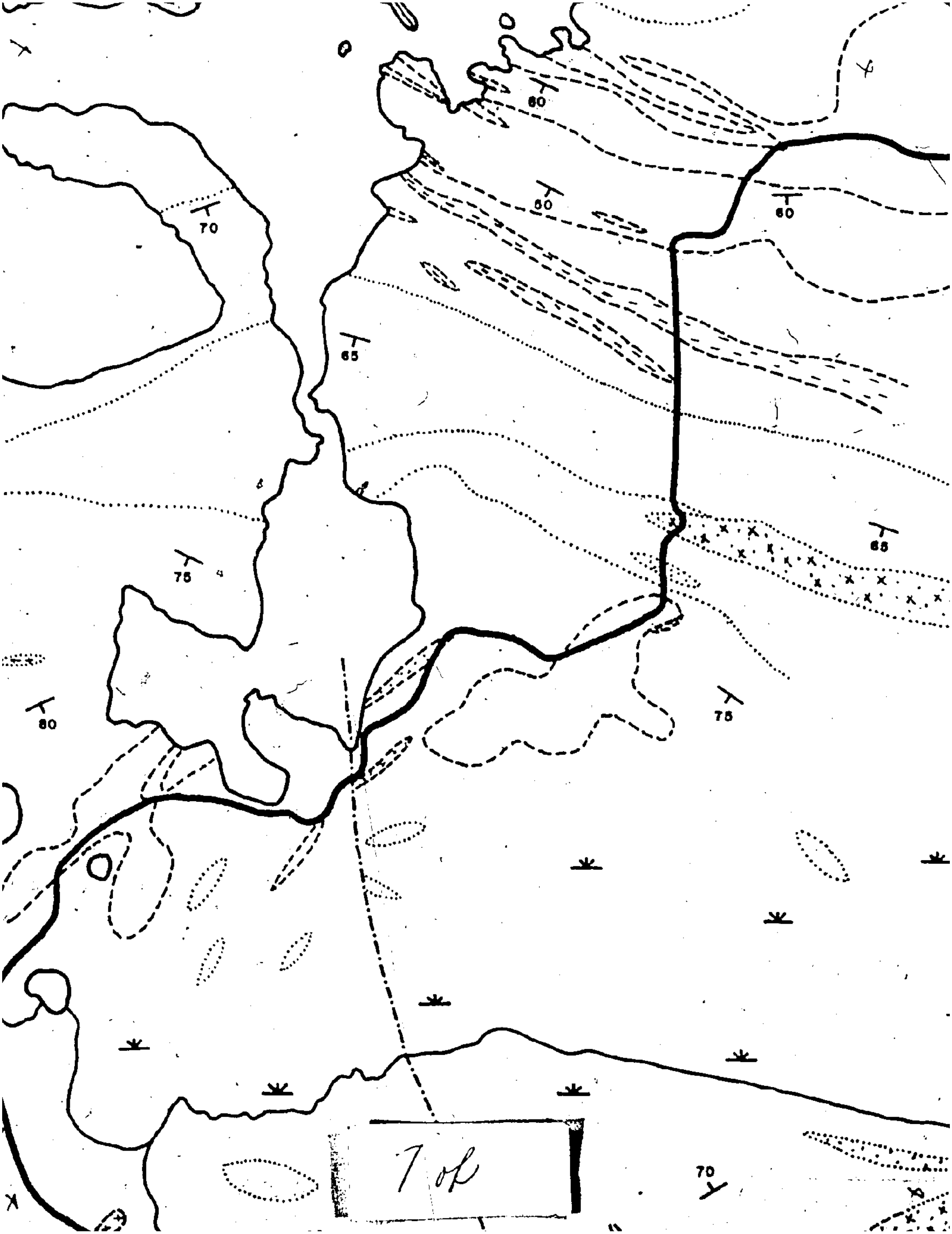
60
60
60
70
65
75
65
80
75
70

7 of

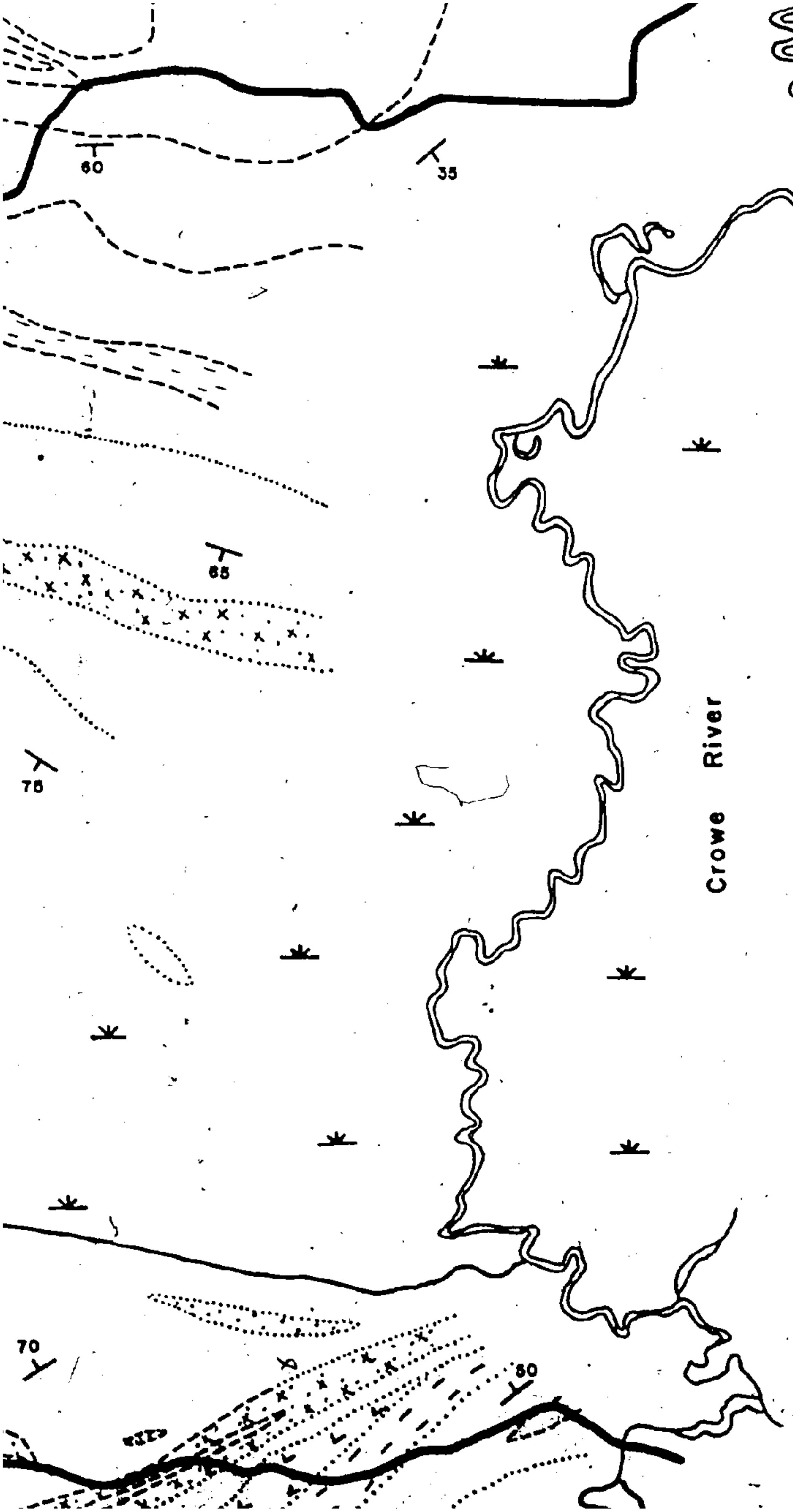
60
35
65
75
Crowe River
70
50

8 of

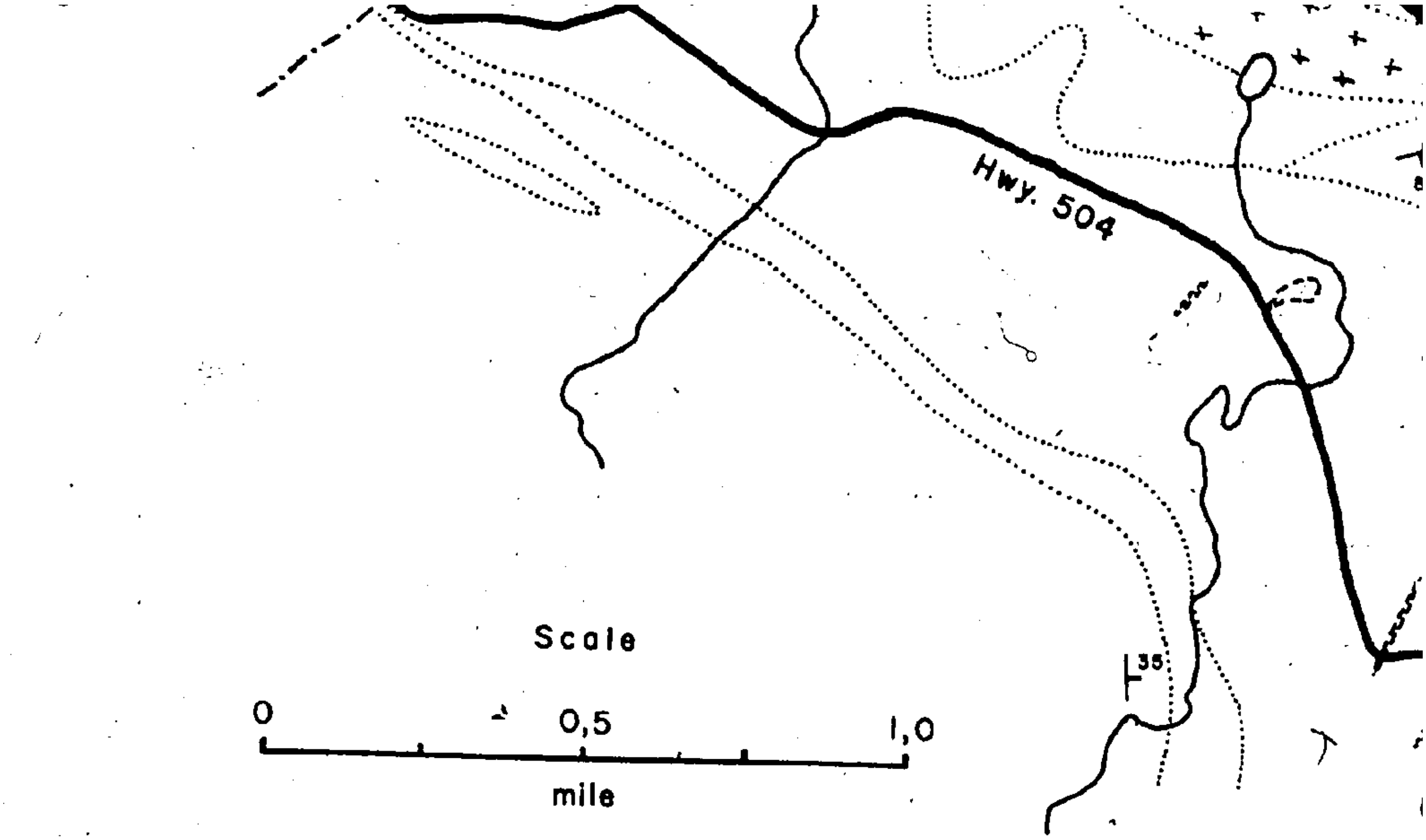
Hwy. 504
35
Scale
0
0,5
1,0
mile

9 of

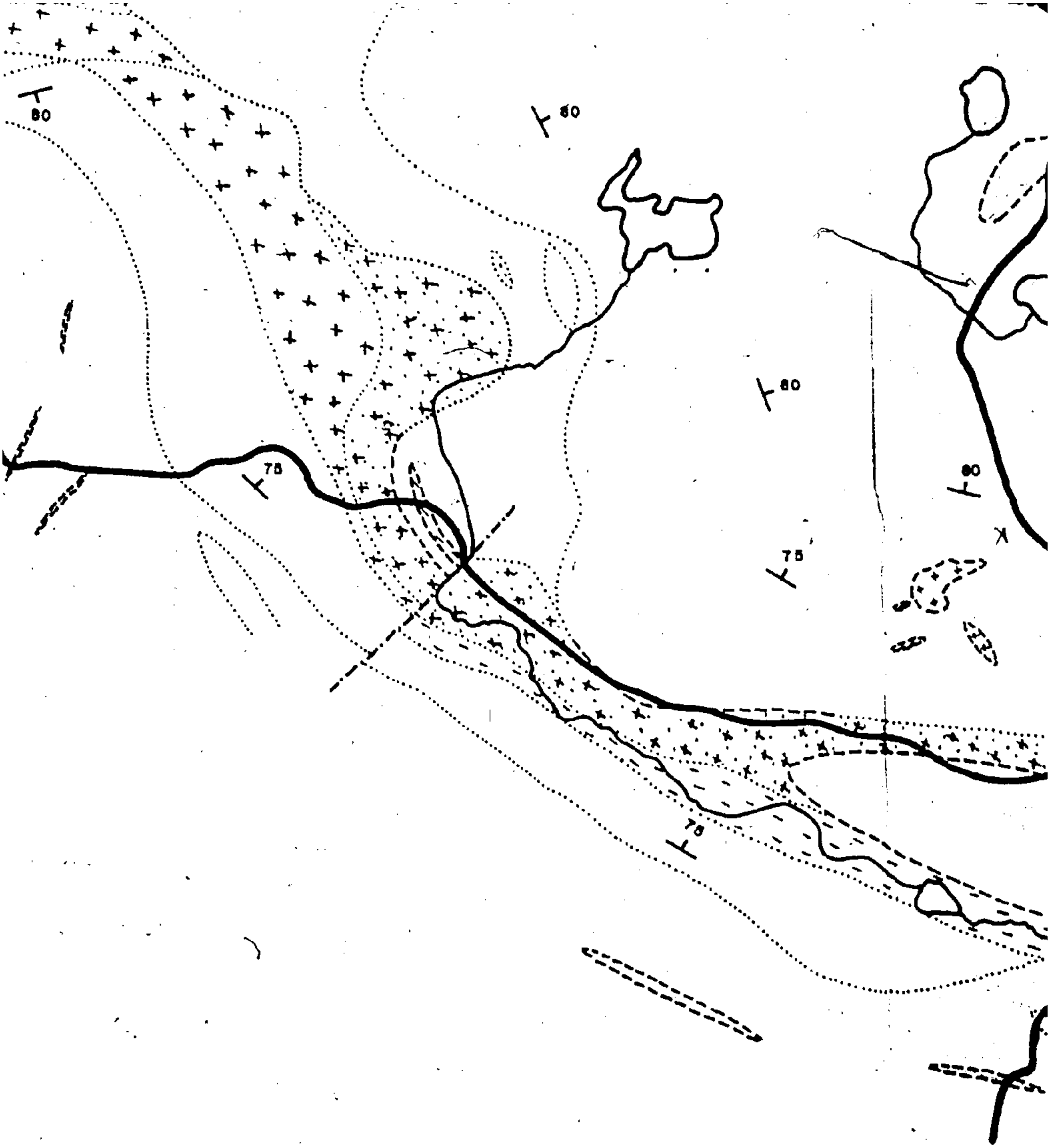
80
60
60
75
80
75
75

10 of

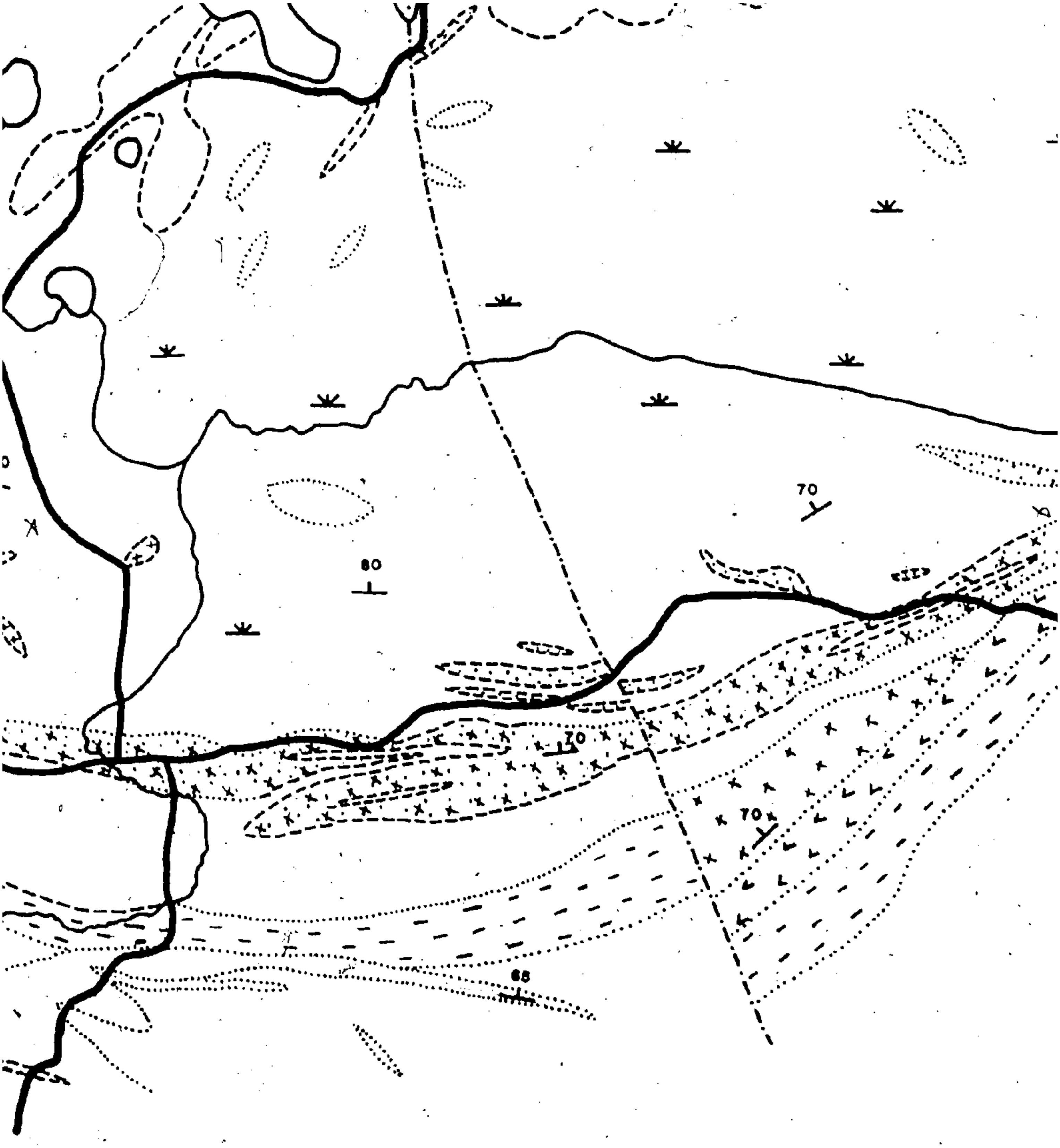
70
80
70
70
68

11 of

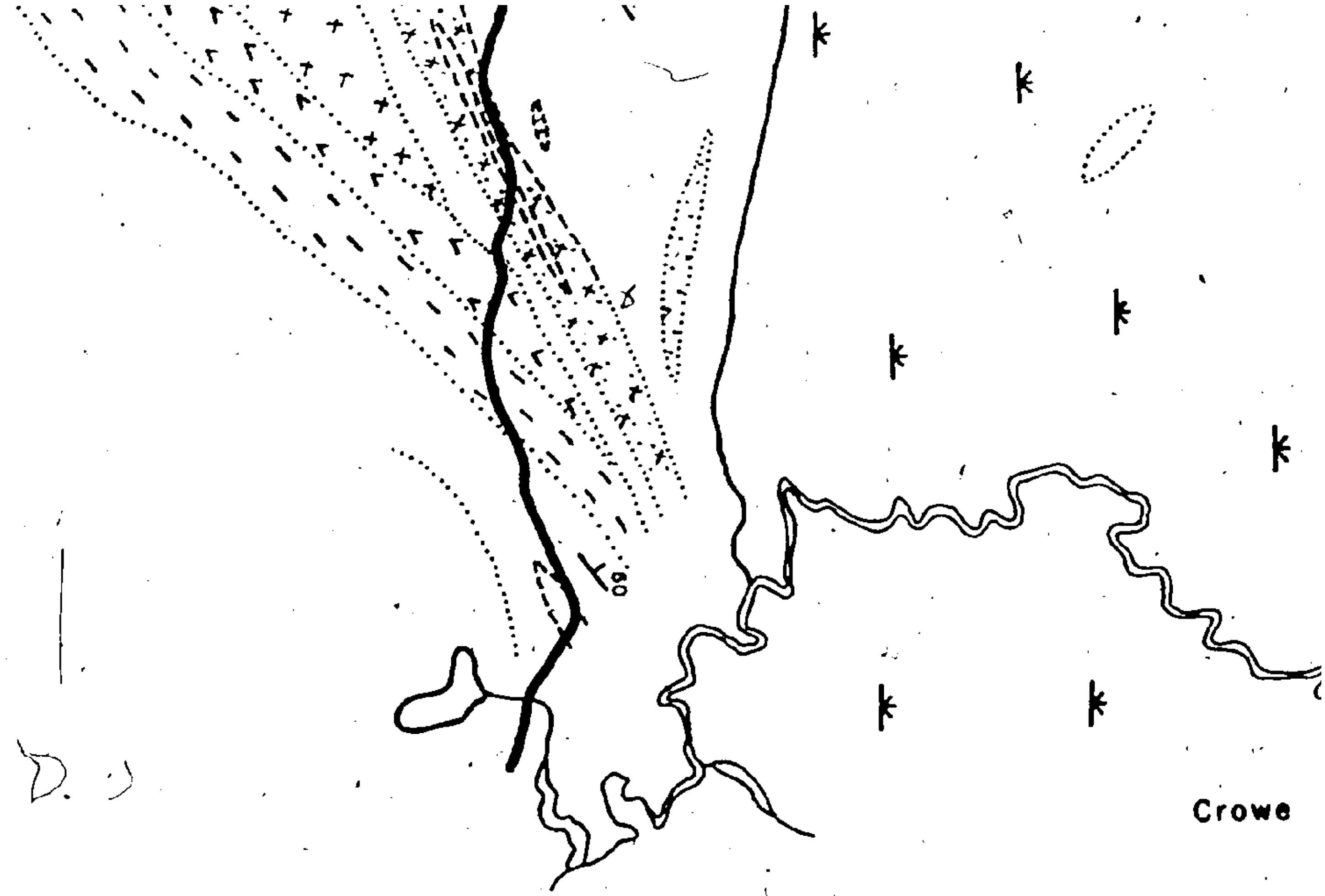

1x of 12